

**SYNTHESIS, CHARACTERIZATION AND
COMPUTATIONAL STUDIES OF
OXOMOLYBDENUM COMPOUNDS WITH
NITROGEN DONOR LIGANDS**

**A Thesis Submitted to
the Graduate School of Engineering and Sciences of
İzmir Institute of Technology
in Partial Fulfillment of the Requirements for the Degree of**

MASTER OF SCIENCE

in Chemistry

**by
Harika KIYAK**

**June 2010
İZMİR**

We approve the thesis of **Harika KIYAK**

Prof. Dr. Işıl TOPALOĞLU SÖZÜER
Supervisor

Assist. Prof. Dr. Armağan KINAL
Co-Supervisor

Assoc. Prof. Dr. Elif SUBAŞI
Committee Member

Assist. Prof. Dr. Nursel ACAR
Committee Member

Assoc. Prof. Dr. Durmuş ÖZDEMİR
Committee Member

17 June 2010

Prof. Dr. Serdar ÖZÇELİK
Head of the Department of Chemistry

Assoc.Prof. Dr. Talat YALÇIN
Dean of the Graduate School of
Engineering and Sciences

ACKNOWLEDGEMENTS

First of all, I would like to express my sincere gratitude to my supervisor Prof. Dr. Hikmet Işıl TOPALOĞLU SÖZÜER for her guidance and endless support throughout the undertaking of this research. Without her guidance, this thesis study could not be completed. I am encouraged with her excellent supervising and endless patience during my academic program and finally able to finish this thesis. During my education at IYTE, I can say faithfully that the best decision was to study with Prof. Dr. Hikmet Işıl TOPALOĞLU SÖZÜER. I feel very privileged and lucky to be part of her project.

I would like to thank my co-supervisor Assist. Prof. Dr. Armağan KINAL for his guidance. He is an excellent scientist, researcher and teacher. It was an honour to study with him.

I would like to thank to Research Council of Izmir Institute of Technology (2007 IYTE 13) and the Scientific and Technological Research Council of Turkey TÜBİTAK (108T614) for financial support for this study, Işın ÖZÇELİK, Pınar BAYDARA and Salih GÜNNAZ for NMR analyses, Hüseyin ÖZGENER for FT-IR and elemental analyses.

My thanks also go to my dear fiance and best friend, Atilla ÖZKAN, for his endless love and encouragement. His endless care and his limitless support were the best motivation for me during my studies. Every time when I needed help, he was there for me to help and he gave me the best support that no one else can give. I want to thank him and his family so much for everything.

I would like to express my thanks to my lovely family for their motivation, continuous support and prayers. My mother always supported me for my educational decisions since I was a child. My father raises me with his endless love.

ABSTRACT

SYNTHESIS, CHARACTERIZATION AND COMPUTATIONAL STUDIES OF OXOMOLYBDENUM COMPOUNDS WITH NITROGEN DONOR LIGANDS

In the first part of the project, the reactions of the solvent-stabilized compound $[\text{MoO}_2\text{Cl}_2(\text{THF})_2]$ with various phenylenediamine and some naphthalenediamine derivatives in THF at room temperature were investigated. These reactions yielded mononuclear and dinuclear compounds of the type $[\text{MoO}_2\text{Cl}_2\text{L}]$ and $[\text{Mo}_2\text{O}_3(\mu_2\text{-O})\text{Cl}_4(\text{L})_2]$ respectively.

In the second part, the reactions of $[\text{Mo}_2\text{O}_3\text{Cl}_4(\text{DMF})_4]$ with phenylenediamine and naphthalenediamine derivatives were studied under similar conditions and Mo-O-Mo bridged dinuclear oxomolybdenum compounds of the type $[\text{Mo}_2\text{O}_3(\mu_2\text{-O})\text{Cl}_4(\text{L})]$ were obtained.

The new compounds were comparatively examined by elemental analysis, FT-IR, $^1\text{H-NMR}$ and $^{13}\text{C-NMR}$ techniques. In addition, quantum chemical calculations including semi empirical PM3 and DFT methods were carried out to discuss the stability and geometry of the compounds.

ÖZET

OKSOMOLİBDEN BİLEŞİKLERİNİN AZOT DONORU LİGANDLARLA OLUŞAN BİLEŞİKLERİNİN SENTEZİ, KARAKTERİZASYONU VE HESAPSAL ÇALIŞMALARI

Projenin birinci kısmında, $[\text{MoO}_2\text{Cl}_2]$ bileşiğinin çözügen bağlanmış kompleksinin, $[\text{MoO}_2\text{Cl}_2(\text{THF})_2]$, fenilendiamin ve naftalendiamin türevleri ile THF içinde oda sıcaklığındaki reaksiyonları, ikinci kısmında ise, $[\text{MoO}_2\text{Cl}_2(\text{DMF})_2]$ bileşiğinin, aynı koşullarda aynı ligandlarla reaksiyonları incelenmiştir.

Bu reaksiyonlar sonucu elde edilen $[\text{MoO}_2\text{Cl}_2\text{L}]$ ve $[\text{Mo}_2\text{O}_3(\mu_2\text{-O})\text{Cl}_4(\text{L})]$ yapısındaki yeni oksomolibden bileşikleri elemental analiz, FT-IR, $^1\text{H-NMR}$, $^{13}\text{C-NMR}$ yöntemleriyle karakterize edilmeye çalışılmış, elde edilen veriler birbirleriyle karşılaştırılmıştır. Buna ilave olarak, bileşiklerin kararlılığını ve geometrisini açıklamak için semi ampirik PM3 ve DFT metotlarını içeren kuantum kimyasal hesapları yapıldı.

TABLE OF CONTENTS

LIST OF FIGURES	xi
LIST OF TABLES	xii
CHAPTER 1. INTRODUCTION	1
CHAPTER 2. OXOMOLYBDENUM CHEMISTRY	3
2.1. Catalytic Applications of Oxomolybdenum Complexes	5
2.1.1. Solvent-Stabilized Oxomolybdenum Complexes	5
2.1.2. N-Ligand Stabilized Oxomolybdenum Complexes	6
2.1.3. Olefin Epoxidation Catalyzed By Oxomolybdenum Complexes	8
2.2. Enzymatic Applications of Oxomolybdenum Complexes.....	10
2.2.1. Molybdenum cofactor (Moco)	10
2.2.2. Mononuclear Molybdenum Enzymes	11
CHAPTER 3. COMPUTATIONAL CHEMISTRY.....	14
3.1. Computational Chemistry Methods	14
3.1.1. Ab Initio Calculations	14
3.1.2. Semiempirical Calculations	15
3.1.3. Molecular Mechanics	16
3.1.4. Density Functional Theory (DFT)	16
3.2. Basis Sets	17
3.2.1. Slater Type Orbital	18
3.2.2. Gaussian Type Orbitals	18
3.2.3. Pople Type Basis Sets	19
CHAPTER 4. EXPERIMENTAL STUDY	21
4.1. Experimental Techniques for Handling Air-Sensitive Compounds.....	21
4.2. The Vacuum-Line Technique	21

4.2.1 The Double Manifold.....	21
4.2.2. The Schlenk Technique.....	22
4.3. Purification of Solvents.....	23
4.4. Materials and Methods.....	24
4.5. Synthesis	25
4.5.1. Reactions of $[\text{MoO}_2\text{Cl}_2(\text{THF})_2]$ with Aromatic Nitrogen Donor Ligands	25
4.5.1.1. Reaction of $[\text{MoO}_2\text{Cl}_2(\text{THF})_2]$ with $[p\text{-H}_2\text{NC}_6\text{H}_4\text{NH}_2]$ (1).....	25
4.5.1.2. Reaction of $[\text{MoO}_2\text{Cl}_2(\text{THF})_2]$ with $[p\text{-H}_2\text{NC}_6\text{H}_2\text{Cl}_2\text{NH}_2]$ (2).....	26
4.5.1.3. Reaction of $[\text{MoO}_2\text{Cl}_2(\text{THF})_2]$ with $[p\text{-H}_2\text{NC}_6(\text{CH}_3)_4\text{NH}_2]$ (3).....	26
4.5.1.4. Reaction of $[\text{MoO}_2\text{Cl}_2(\text{THF})_2]$ with $[p\text{-H}_2\text{NC}_6\text{H}_3\text{NO}_2\text{NH}_2]$ (4).....	26
4.5.1.5. Reaction of $[\text{MoO}_2\text{Cl}_2(\text{THF})_2]$ with $[o\text{-H}_2\text{NC}_6\text{H}_4\text{NH}_2]$ (5)	27
4.5.1.6. Reaction of $[\text{MoO}_2\text{Cl}_2(\text{THF})_2]$ with $[o\text{-H}_2\text{NC}_6\text{H}_3(\text{CH}_3)\text{NH}_2]$ (6).....	27
4.5.1.7. Reaction of $[\text{MoO}_2\text{Cl}_2(\text{THF})_2]$ with $[o\text{-H}_2\text{NC}_6\text{H}_3\text{NO}_2\text{NH}_2]$ (7).....	27
4.5.1.8. Reaction of $[\text{MoO}_2\text{Cl}_2(\text{THF})_2]$ with $[o\text{-H}_2\text{NC}_6\text{H}_3\text{FNH}_2]$ (8).....	27
4.5.1.9. Reaction of $[\text{MoO}_2\text{Cl}_2(\text{THF})_2]$ with $[o\text{-H}_2\text{NC}_6\text{H}_3\text{ClNH}_2]$ (9).....	28
4.5.1.10. Reaction of $[\text{MoO}_2\text{Cl}_2(\text{THF})_2]$ with $[o\text{-H}_2\text{NC}_6\text{H}_3\text{BrNH}_2]$ (10).....	28
4.5.1.11. Reaction of $[\text{MoO}_2\text{Cl}_2(\text{THF})_2]$ with $[o\text{-H}_2\text{NC}_6\text{H}_2\text{Cl}_2\text{NH}_2]$ (11).....	28
4.5.1.12. Reaction of $[\text{MoO}_2\text{Cl}_2(\text{THF})_2]$ with $[m\text{-H}_2\text{NC}_6\text{H}_4\text{NH}_2]$ (12).....	29
4.5.1.13. Reaction of $[\text{MoO}_2\text{Cl}_2(\text{THF})_2]$ with $[m\text{-HNC}_6\text{H}_3(\text{CH}_3)\text{NH}_2]$ (13).....	29

4.5.1.14. Reaction of $[\text{MoO}_2\text{Cl}_2(\text{THF})_2]$ with $[m\text{-H}_2\text{NC}_6\text{H}_3\text{FNH}_2]$ (14)	29
4.5.1.15. Reaction of $[\text{MoO}_2\text{Cl}_2(\text{THF})_2]$ with $[m\text{-H}_2\text{NC}_6\text{H}_3\text{ClNH}_2]$ (15)	29
4.5.1.16. Reaction of $[\text{MoO}_2\text{Cl}_2(\text{THF})_2]$ with $[m\text{-H}_2\text{NC}_6\text{H}(\text{CH}_3)_3\text{NH}_2]$ (16)	30
4.5.1.17. Reaction of $[\text{MoO}_2\text{Cl}_2(\text{THF})_2]$ with $[1,5\text{-H}_2\text{NC}_{10}\text{H}_6\text{NH}_2]$ (17)	30
4.5.1.18. Reaction of $[\text{MoO}_2\text{Cl}_2(\text{THF})_2]$ with $[1,8\text{-H}_2\text{NC}_{10}\text{H}_6\text{NH}_2]$ (18)	30
4.5.1.19. Reaction of $[\text{MoO}_2\text{Cl}_2(\text{THF})_2]$ with $[2,3\text{-H}_2\text{NC}_{10}\text{H}_6\text{NH}_2]$ (19)	31
4.5.2. Reactions of $[\text{Mo}_2\text{O}_3\text{Cl}_4(\text{DMF})_4]$ with Aromatic Nitrogen Donor Ligands	31
4.5.2.1. Reaction of $[\text{Mo}_2\text{O}_3\text{Cl}_4(\text{DMF})_4]$ with $[p\text{-H}_2\text{NC}_6\text{H}_4\text{NH}_2]$ (1)	31
4.5.2.2. Reaction of $[\text{Mo}_2\text{O}_3\text{Cl}_4(\text{DMF})_4]$ with $[p\text{-H}_2\text{NC}_6\text{H}_2\text{Cl}_2\text{NH}_2]$ (20)	31
4.5.2.3. Reaction of $[\text{Mo}_2\text{O}_3\text{Cl}_4(\text{DMF})_4]$ with $[p\text{-H}_2\text{NC}_6(\text{CH}_3)_4\text{NH}_2]$ (3)	32
4.5.2.4. Reaction of $[\text{Mo}_2\text{O}_3\text{Cl}_4(\text{DMF})_4]$ with $[p\text{-H}_2\text{NC}_6\text{H}_3\text{NO}_2\text{NH}_2]$ (4)	32
4.5.2.5. Reaction of $[\text{Mo}_2\text{O}_3\text{Cl}_4(\text{DMF})_4]$ with $[o\text{-H}_2\text{NC}_6\text{H}_4\text{NH}_2]$ (5)	32
4.5.2.6. Reaction of $[\text{Mo}_2\text{O}_3\text{Cl}_4(\text{DMF})_4]$ with $[o\text{-H}_2\text{NC}_6\text{H}_3(\text{CH}_3)\text{NH}_2]$ (6)	32
4.5.2.7. Reaction of $[\text{Mo}_2\text{O}_3\text{Cl}_4(\text{DMF})_4]$ with $[o\text{-H}_2\text{NC}_6\text{H}_3\text{NO}_2\text{NH}_2]$ (21).....	33
4.5.2.8. Reaction of $[\text{Mo}_2\text{O}_3\text{Cl}_4(\text{DMF})_4]$ with $[o\text{-H}_2\text{NC}_6\text{H}_3\text{FNH}_2]$ (8)	33
4.5.2.9. Reaction of $[\text{Mo}_2\text{O}_3\text{Cl}_4(\text{DMF})_4]$ with $[o\text{-H}_2\text{NC}_6\text{H}_3\text{ClNH}_2]$ (22)	33
4.5.2.10. Reaction of $[\text{Mo}_2\text{O}_3\text{Cl}_4(\text{DMF})_4]$ with $[o\text{-H}_2\text{NC}_6\text{H}_3\text{BrNH}_2]$ (10)	34

4.5.2.11. Reaction of $[\text{Mo}_2\text{O}_3\text{Cl}_4(\text{DMF})_4]$ with $[o\text{-H}_2\text{NC}_6\text{H}_2\text{Cl}_2\text{NH}_2]$ (23)	34
4.5.2.12. Reaction of $[\text{Mo}_2\text{O}_3\text{Cl}_4(\text{DMF})_4]$ with $[m\text{-H}_2\text{NC}_6\text{H}_4\text{NH}_2]$ (12)	34
4.5.2.13. Reaction of $[\text{Mo}_2\text{O}_3\text{Cl}_4(\text{DMF})_4]$ with $[m\text{-H}_2\text{NC}_6\text{H}_3(\text{CH}_3)\text{NH}_2]$ (13)	34
4.5.2.14. Reaction of $[\text{Mo}_2\text{O}_3\text{Cl}_4(\text{DMF})_4]$ with $[m\text{-H}_2\text{NC}_6\text{H}_3\text{FNH}_2]$ (24)	35
4.5.2.15. Reaction of $[\text{Mo}_2\text{O}_3\text{Cl}_4(\text{DMF})_4]$ with $[m\text{-H}_2\text{NC}_6\text{H}_3\text{ClNH}_2]$ (15)	35
4.5.2.16. Reaction of $[\text{Mo}_2\text{O}_3\text{Cl}_4(\text{DMF})_4]$ with $[m\text{-H}_2\text{NC}_6\text{H}(\text{CH}_3)_3\text{NH}_2]$ (16)	35
4.5.2.17. Reaction of $[\text{Mo}_2\text{O}_3\text{Cl}_4(\text{DMF})_4]$ with $[1,5\text{-H}_2\text{NC}_{10}\text{H}_6\text{NH}_2]$ (17)	36
4.5.2.18. Reaction of $[\text{Mo}_2\text{O}_3\text{Cl}_4(\text{DMF})_4]$ with $[1,8\text{-H}_2\text{NC}_{10}\text{H}_6\text{NH}_2]$ (18)	36
4.5.2.19. Reaction of $[\text{Mo}_2\text{O}_3\text{Cl}_4(\text{DMF})_4]$ with $[2,3\text{-H}_2\text{NC}_{10}\text{H}_6\text{NH}_2]$ (19)	36
 CHAPTER 5. RESULT AND DISCUSSION	 37
5.1. Synthetic Studies	37
5.2. Spectroscopic Studies	40
5.3. Computational Calculations	45
 CHAPTER 6. CONCLUSIONS	 49
 REFERENCES	 50
 APPENDICES	 58
 APPENDIX A. ^1H NMR AND ^{13}C NMR SPECTRA OF THE PRODUCTS	 58
 APPENDIX B. FT-IR SPECTRA OF THE PRODUCTS	 106

APPENDIX C. STRUCTURES AND CARTESIAN COORDINATES OF OPTIMIZED COMPLEXES	130
--	-----

LIST OF FIGURES

<u>Figure</u>	<u>Page</u>
Figure 2.1 Molybdenum containing oxo groups in the cis and trans orientation.	4
Figure 2.2. The μ -oxido binuclear molybdenum(VI) complex.....	6
Figure 2.3. The synthesis of Solvent-Stabilized Oxomolybdenum Complexes	7
Figure 2.4. The The synthesis of N- ligand stabilized oxomolybdenum complexes.....	8
Figure 2.5. The reaction of solvent substituted complexes with Lewis base ligands	8
Figure 2.6. Similar structures in the literature	9
Figure 2.7. Suggested reaction pathway for cyclohexene epoxidation with TBHP catalyse by dioxo molybdenum complexes.	10
Figure 2.8. Structure of the molybdopterin.....	12
Figure 2.9. Hill classification-mononuclear molybdoenzymes	14
Figure 4.1. The Double Manifold	21
Figure 4.2. Cross section through a double oblique tap.....	22
Figure 4.3. The schlenk tube.....	23
Figure 4.4. Solvent still.....	24

LIST OF TABLES

<u>Table</u>	<u>Page</u>
Table 5.1. The colors,yields and elemental analyses results of compounds 1-24..	40
Table 5.2. Characteristic FT-IR bands (cm^{-1}) for compounds 1-24.....	42
Table 5.3. ^1H -NMR spectroscopic data for compounds 1-24.....	43
Table 5.4. ^{13}C -NMR data for compounds 1-24	45
Table 5.5. Characteristic harmonic vibrational frequencies (cm^{-1}) for compounds 1-24 form DFT calculations	29
Table 5.6. Some selected parameters calculated with DFT for mononuclear compounds 2,7,9,11 and 14.....	47
Table 5.7. Some selected parameters calculated with DFT for dinuclear compounds 1,3-6,8,10,12-13,15-24	48

CHAPTER 1

INTRODUCTION

The chemistry of transition metal-oxo compounds has become an area of permanent interest that has experienced an outstanding renaissance during the last few years (Holm, et al. 1996). Numerous monomeric complexes containing terminal oxo-ligands have been prepared and subjected to intense investigation due to the role they seem to play in many important reactions, such as the oxidation of hydrocarbons and the epoxidation of olefins, either in heterogeneous or homogeneous processes (Teruel, et al. 2001). The oxo-transfer chemistry of molybdenum is the most extensive of any metal in terms of both observed and kinetically defined reactions. Oxo molybdenum complexes have also been studied as models for the active site of oxo-transfer molybdenum enzymes (Hille 1996).

Molybdenum is considered as a trace element, presents several oxidation states, and therefore may change easily its coordination number and to form mono and binuclear oxo complexes which is of great importance from basic as well as applied points of view. The propensity of oxomolybdenum species in higher oxidation states to form di, tri and polynuclear complexes is well known (Garner, et al. 1987). Molybdenum is a relevant element for the synthesis of many homogeneous and heterogeneous catalysts. The element is also essential in several enzymatic systems. One of the characteristics of the molybdenum chemistry is related to the easy conversion between its oxidation states and to the changes of coordination number, observed particularly between Mo(III), Mo(IV), Mo(V) and Mo(VI) (Garner, et al. 1995).

More than 40 years after the birth of modern density functional theory (DFT) the exact exchange-correlation functional remains ever elusive. Therefore DFT currently employs a heuristic approach, spawning an extraordinarily large number of approximate functional being proposed in the literature. As DFT remains reliant upon judicious validation against experiment (i.e., parametrization), accurate experimental data is vital, and the quality of a particular functional is ultimately connected to the quality of experimental data available. A growing body of literature for a posteriori estimates of errors for particular exchange-correlation functional forms the basis for

critical assessment of conclusions drawn from computational results within a DFT framework.

It is particularly important to evaluate the quality of DFT-derived geometries, as their accuracy may be crucial for further computations of energies or properties. For the important class of transition-metal complexes (a stronghold of modern DFT) this validation is hampered by a scarcity of accurate structure determinations in the gas phase, to which the overwhelming majority of DFT applications would refer (Waller, et al. 2007).

In this thesis, we synthesized and characterized monomeric and dimeric dioxomolybdenum compounds using nitrogen donor ligands. The quantum chemical calculations, PM3 and DFT were performed to discuss the geometry and stability of the new complexes.

CHAPTER 2

OXOMOLYBDENUM CHEMISTRY

The chemistry of dioxomolybdenum(VI) complexes is of importance especially in industrial and biochemical catalysis (Sellmann, et al. 1995). The coordination chemistry of molybdenum(VI) has attracted considerable interest due to its biological importance (Enemark, et al. 2004, Holm, et al. 1996) as well as for the importance of molybdenum(VI) complexes as catalysts in various oxidations reactions (Bäckvall 2004, Meunier 2000), such as epoxidation and hydroxylation of olefines (Bregeault 2003, Jorgensen 1989, Rao, et al. 2000, Brito, et al. 2004) oxidation of alcohols (Lorber, et al. 2000) and as catalysts of oxygen atom transfer reactions (Holm, et al. 1990, Dinda, et al. 2002). Moreover, molybdate can catalyze the oxidation of bromide (Meister, et al. 1994) and some peroxo complexes of molybdenum(VI) have been found to oxidize bromide in a stoichiometric reaction (Reynolds, et al. 1997). Molybdenum(VI) chemistry often involves oxo chemistry, that is complexes that have an O^{2-} (oxo) ligand. Octahedral transition metal complexes containing two oxo ligands bonded to the metal can have two orientations, cis-dioxo or trans-dioxo. In general, transition metals having the d^0 electron configuration contain two oxo groups in the cis orientation (at 90 degrees to each other in an octahedral complex). Transition metals having the d^2 electron configuration generally contain two oxo groups in the trans orientation (at 180 degrees to each other in an octahedral complex). These two arrangements are illustrated in Figure 2.1 below.

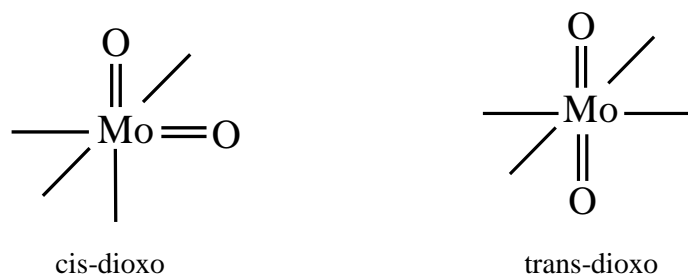


Figure 2.1 Molybdenum containing oxo groups in the cis and trans orientation.
(Source: Jurisson 1997)

Molybdenum(VI) has a d^0 electron configuration so its dioxo complexes usually have a cis-dioxo geometry. Tetrahedral geometries are also known for dioxo complexes. In this geometry there is no cis or trans.

Dichlorodioxomolybdenum(VI), MoO_2Cl_2 , is a useful starting material for preparing a variety of molybdenum compounds. This Mo(VI) compound is tetrahedral in its arrangement of ligands around the molybdenum center. However, MoO_2Cl_2 is moisture sensitive (reacts with water to decompose) and must be prepared just before using it by chlorinating molybdenum(IV) oxide (MoO_2). A related, yet moisture stable molybdenum(VI) compound that is readily prepared and useful as a starting material for preparing a variety of Mo compounds in oxidation state VI as well as lower oxidation states (Jurisson 1997).

Binuclear oxomolybdenum(V) complexes containing the $[\text{Mo}_2\text{O}_3]^{4+}$ core have been reported with a variety of ligands (Garner, et al. 1987). These complexes, which are characterized by possessing an oxygen atom bridging the two molybdenum atoms, shown in Figure 2.2, were known to be formed in oxotransfer processes by comproportion of oxomolybdenum(IV) and dioxomolybdenum(VI) species (Enemark, et al. 1994). Binuclear oxomolybdenum(V) complexes containing the 1,1-dithiobidentate ligands such as dithiocarbamates, xanthates and dithiophosphates (Manwani, et al. 2003), or multidentate ligands such as Schiff bases (Craig, et al. 1985) and a small number of complexes bearing monodentate ligands, $\text{Mo}_2\text{O}_3\text{Cl}_4(\text{C}_5\text{H}_5\text{N})_4$ (El-Essawi, et al. 1986) and $\text{Mo}_2\text{O}_3\text{Cl}_4(\text{OPMe}_3)_2(\text{PMe}_3)_2$ (Cotton, et al. 1999) were previously reported. Binuclear complexes containing the $[\text{Mo}_2\text{O}_4]^{2+}$ unit with N,N-dialkylidithiocarbamates (Zhuang, et al. 1988), oxalate (Modéc, et al. 2004), chloride (Lang, et al. 2004), tropolonate (Takekuma, et al. 2004), 1,10-phenanthroline (Xu, et al. 2001), bipyridine and 4,4-dimethyl-bipyridine (Beck, et al. 1984), ligands were also prepared. Oxomolybdenum complexes containing bridging μ -oxo groups (Mo-O-Mo) have also been studied as catalysts or catalyst precursors for olefin epoxidation (Martins, et al. 2005, Brito, et al. 2004) The oxo-bridged dimer $[\text{Mo}_2\text{O}_4(\mu\text{-O})\text{Cl}_2(\text{pzH})_4]$ (pzH = pyrazole) was reported (Pereira, et al. 2007) to exhibit unusually high activity in the liquid-phase catalytic epoxidation of the cyclic olefins cyclooctene and (R)-(+)-limonene under mild conditions and in the absence of additional organic solvents, using tert-butyl hydroperoxide as the oxidant.

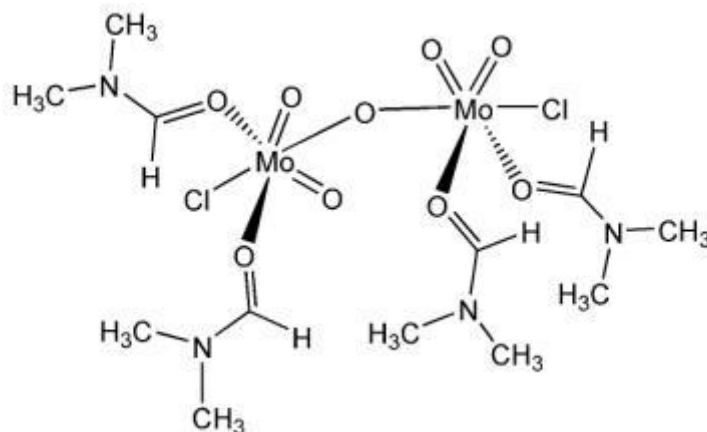


Figure 2.2. The μ -oxido binuclear molybdenum(VI) complex $[\text{Mo}_2\text{O}_4(\mu_2\text{-O})\text{Cl}_2(\text{dmf})_4]$
(Source: Gago, et al. 2009)

2.1. Catalytic Applications of Oxomolybdenum Complexes

Oxomolybdenum complexes are well known oxidation catalysts in chemistry. In particular Mo(VI) derivatives, such as MoO_2X_2 and WO_2X_2 , give rise to molecules of formula $\text{MO}_2\text{X}_2(\text{L-L})$ ($\text{M} = \text{Mo}, \text{W}$) in the presence of Lewis bases or even donor solvents (THF, NCH_3), which exhibit catalytic activity in olefin epoxidation reactions (Veiros, et al. 2006).

2.1.1. Solvent-Stabilized Oxomolybdenum Complexes

Oxomolybdenum complexes with the cis- MoO_2 fragment of the general formula $\text{MoBr}_2\text{O}_2(\text{Solv})_2$ are very important precursors or oxidation catalysts, in chemical and in biological systems (Kumar, et al. 1991, Palanca, et al. 1990, Wilshire, et al. 1979). As starting material for synthesis of oxomolybdenum species with various nitrogen and oxygen donor ligands, it is prepared the complexes of the type $\text{MoX}_2\text{O}_2(\text{Solv})_2$ ($\text{X} = \text{Cl}, \text{Br}$; $(\text{Solv}) = \text{THF}, \text{NCH}_3$) (Kühn, et al. 1999) The synthesis of compounds of general formula $\text{MoX}_2\text{O}_2(\text{Solv})_2$ shown in Figure 2.3, is achieved by dissolving the molybdenumdioxo dichloride or bromide in donor solvent. The product complexes are nearly insoluble in nonpolar nondonor solvents (alkanes or diethyl ether) but are very soluble in most donor solvents (Gonçalves, et al. 2001). These complexes catalyze the epoxidation of olefins with t-butylhydroperoxide. They do not proceed significantly further in the catalytic run. The reason for that observation is the

pronounced water sensitivity of the solvent-stabilized complexes. In contrast to other more strongly coordinating organic ligands, these compounds do not prevent the moisture-induced decomposition of the complexes. The $\text{MoX}_2\text{O}_2(\text{Solv})_2$ complexes are therefore more useful as synthetic precursors for complexes with other, more strongly coordinating ligands than as catalysts themselves.

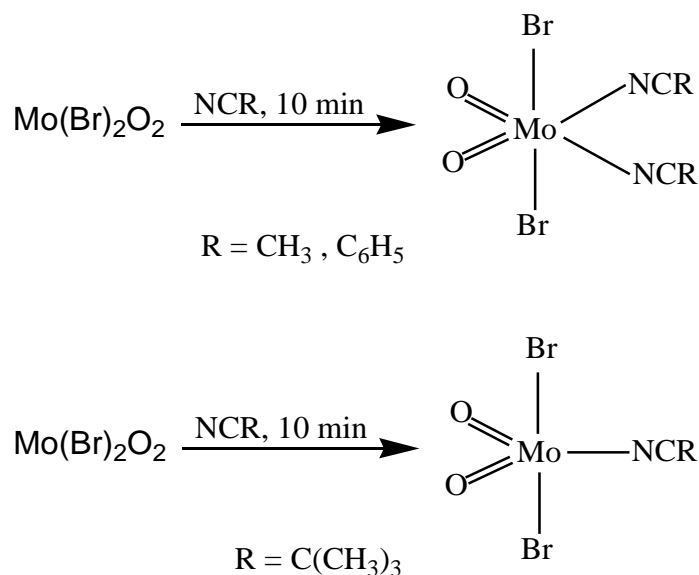


Figure 2.3. The synthesis of Solvent-Stabilized Oxomolybdenum Complexes (Source:Kühn, et al. 1999)

The complex $\text{MoCl}_2\text{O}_2(\text{Solv})_2$ is very electron deficient and readily reacts with electron donor L-L N-ligands to give more stable complexes. (Gonçalves, et al. 2001)

2.1.2. N-Ligand Stabilized Oxomolybdenum Complexes

Organic ligands with donor functionalities such as nitrogen or oxygen atoms react readily with complexes of the type $\text{MoX}_2\text{O}_2(\text{Solv})_2$ forming the octahedrally coordinated complexes which are illustrated in Figure 2.4 (Kühn, et al. 2000).

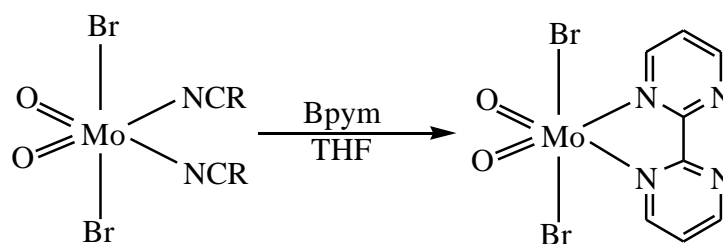


Figure 2.4. The synthesis of N- ligand stabilized oxomolybdenum complexes
(Source:Kühn, et al. 1999)

Reaction of solvent substituted $\text{MoX}_2\text{O}_2(\text{Solv})_2$ complexes with bidentate nitrogen donor ligands leads to complexes of the type $\text{MoX}_2\text{O}_2\text{L}_2$ in nearly quantitative yields at room temperature within few minutes shown in Figure 2.5. $\text{MoX}_2\text{O}_2\text{L}_2$ systems with chelating nitrogen ligands display two important advantages: first, the two different ligand sets X and L can be easily varied in order to fine tune the ligand surrounding of the Mo (VI) center. Secondly, bidentate nitrogen donor ligands offer a great versatility in modifying the electron donor and acceptor properties of the ligands L. (Gonçalves, et al. 2001)

$\text{Mo}=\text{O}$ IR vibrations of $\text{MoX}_2\text{O}_2\text{L}_2$ complexes were used to probe the influence of the ligands on the electronic properties of the metal and the $\text{Mo}=\text{O}$ bond.

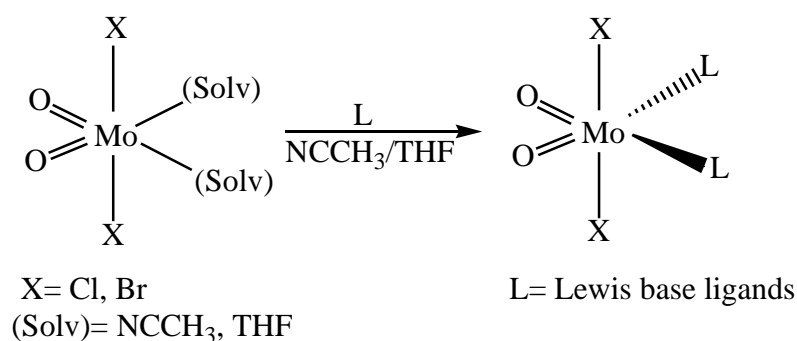


Figure 2.5. The reaction of solvent substituted complexes with Lewis base ligands
(Source: Kühn, et al. 2000)

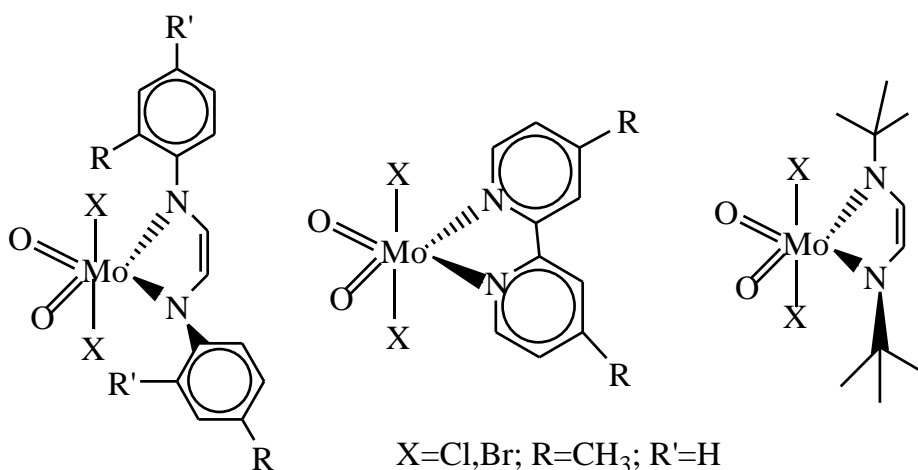
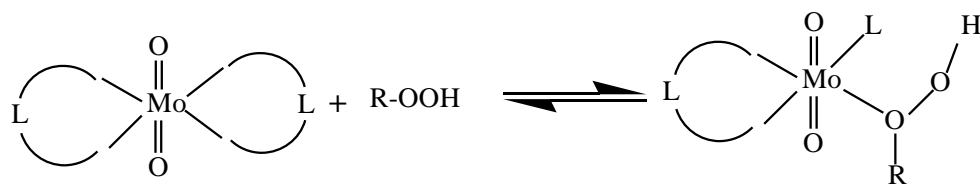


Figure 2.6. Similar structures in the literature
(Source: Kühn, et al. 2000)

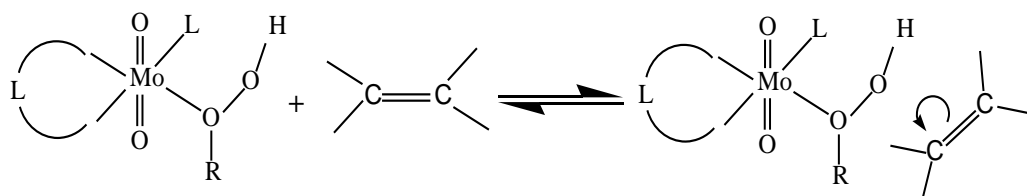
2.1.3 Olefin Epoxidation Catalyzed By Oxomolybdenum Complexes

1,2-Epoxy cyclohexane, one of the most important organic intermediates, represents a rare combination of disparate qualities such as high reactivity and excellent selectivity. It is widely used in the synthesis of products such as enantioselective drugs, the pesticide propargite, epoxy paints, rubber promoters and dyestuff, and the market demand has been steadily increasing over recent years. Transition metal (Mo^{VI} , V^{V} , Ti^{IV} , Re^{VII}) containing catalysts for the epoxidation of cyclohexene have been widely investigated (Wang, et al. 2004). $\text{Mo}(\text{VI})$ is extremely important for epoxidation reactions, because the Lewis acidity of the catalysts has been pointed out as the key function of the catalyst. The major role of $\text{Mo}(\text{VI})$ ion is to withdraw electron from the peroxidic oxygens, making more susceptible to attack by nucleophiles such as olefins. Though significant progress has been made in this field, major problems such as limited catalyst stability and rather difficult, and therefore expensive, synthetic procedures still remain to be solved. Designing a catalyst which gives rapid substrate conversion under mild conditions with high selectivity remains a challenge for these highly reactive systems. The process which is illustrated in Figure 2.7, employs an easily prepared, inexpensive, and stable Mo-containing catalyst together with *tert*-butylhydroperoxide (TBHP).

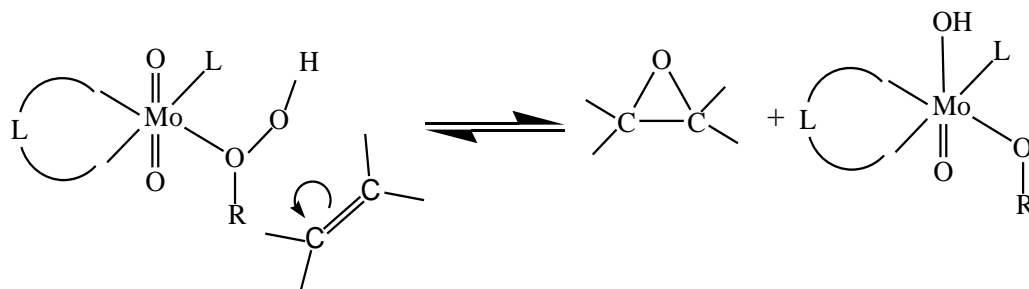
step1



step2



step3



step4

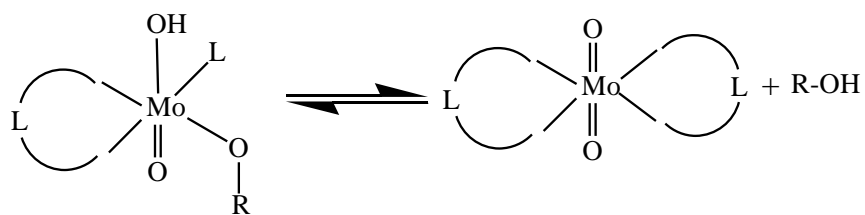


Figure 2.7. Suggested reaction pathway for cyclohexene epoxidation with TBHP catalyzed by dioxo molybdenum complexes. (Source: Gnecco, et al. 2004)

2.2. Enzymatic Applications of Oxomolybdenum Complexes

A variety of transition metals have found applications in biological systems by providing greater catalytic diversity which could not be achieved by the functional groups available in the sidechains of the aminoacids (Holm 1996). Organic forms of molybdenum are found in living matter, from bacteria to animals, including humans. Molybdenum is the only second row transition metal element required in biological reactions. Molybdenum is found in the active sites of so many enzymes due to the extreme solubility of molybdate salts. Molybdenum is the most abundant transition metal in seawater and the ratio of iron to molybdenum in the earth's crust is 3000:1 in favor of iron, but molybdenum is surprisingly 5-fold more abundant in sea water due to the greater solubility of molybdates in comparison to iron oxides. Therefore, it is not surprising that molybdenum has been incorporated widely into biological systems and these aspects of molybdenum chemistry accounts for why it is well suited to participate in the catalysis of certain types of biologically important reactions (Hille, 2002, Sigel, et al. 2002, Hille 1996).

Enzymes containing molybdenum at their active sites are present in all forms of life. A number of well-known enzymes, including xanthine oxidase, nitrate reductase and sulfite oxidase, contain a mononuclear molybdenum center. Mononuclear molybdenum containing enzymes have the general function of catalyzing an oxygen atom transfer (OAT) to or from an acceptor/donor, with the metal oxidation state cycling between the +6 and +4 in the nitrogen, sulfur and carbon cycles and more than 40 enzymes were known. It is a necessary element, apparently for all species and only very small amounts are required. The vast majority of these enzymes possess a Mo=O unit in their active sites are often referred to as oxomolybdenum enzymes (Hille 2002, Kisker, et al. 1997, Basu, et al. 2003 and Enemark, et al. 2004).

2.2.1. Molybdenum Cofactor (Moco)

Molybdenum itself is biologically inactive in biological systems unless it is complexed by a special cofactor. Apart from nitrogenases that contain an iron-molybdenum-sulfur cluster, the biological form of molybdenum present in almost all molybdenum-containing enzymes is an organic molecule known as the molybdenum

cofactor (Moco) shown in Figure 2.8, which contains a mononuclear molybdenum atom coordinated to an organic co-factor named molybdopterin (MPT) (Rajagopalan 1991). MPT contains a pterin, with pyrimidine and pyrazine rings. The pyrazine group is bonded to a pyran ring which carries both $-\text{CH}_2\text{OPO}_3^{2-}$ group and dithiolene group coordinated to molybdenum. Additional ligands that are found in the oxidized Mo(VI) state of the cofactor includes one or two oxo ligands and/or a sulfido ligand and/or an amino acid residue such as serine or cysteine (Kisker, et al. 1997). The polar O, N, NH and NH_2 groups of MPT extensively take part in the formation of hydrogen bonds to complementary groups of the polypeptide chain. When phosphate is bonded to the nucleotide the extent of this hydrogen bonding is greatly increased. This hydrogen bond network would help for appropriate location of the catalytically active center within the polypeptide chain. The task of the cofactor is to position the catalytic metal molybdenum correctly within the active center, to be able to control its redox behaviour, and to take part in its pterin ring system in electron transfer to or from the Mo atom (Kisker, et al. 1997, Basu, et al. 2003 and Enemark, et al. 2004).

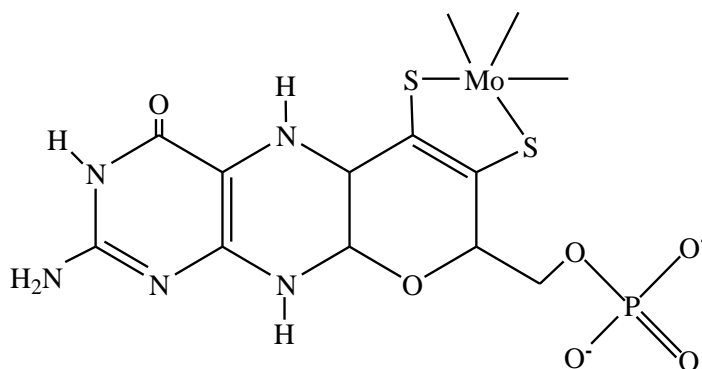


Figure 2.8. Structure of the molybdopterin

2.2.2. Mononuclear Molybdenum Enzymes

The majority of molybdenum enzymes can be classified (Hille 1996,2002 and Sigel, et al. 2002) into three families are illustrated in Figure 2.9, each with a distinct active-site structure and type of reaction catalyzed: (1.1) molybdenum hydroxylases with a monooxo-molybdenum center belong to xanthine oxidase (XO) family, molybdenum oxotransferases with a dioxomolybdenum center belong to the sulphite oxidase (SO) family (George, et al. 1989,1996, Hille 1996 and Kisker, et al. 1997), and

(iii) dimethyl sulfoxide (DMSO) reductase. Sulfite oxidase catalyzes the transformation of sulfite to sulfate, a reaction that is necessary for the metabolism of sulfur-containing amino acids, such as cysteine. Xanthine oxidase catalyzes the breakdown of nucleotides (precursors to DNA and RNA) to form uric acid, which contributes to the antioxidant capacity of the blood (McAlpine, et al. 1997, Bray, et al. 2000, Li, et al. 2000, George, et al. 1996-1999). Of these enzymes, only sulfite oxidase is known to be crucial for human health (Enemark, et al. 2004). Among 40 molybdoenzymes known, only four occur in humans and plants. These enzymes are; sulfite oxidase, nitrate reductase, xanthine oxidase, aldehyde oxidase. The crystal structures of sulphite oxidase (Kisker, et al. 1997), xanthine oxidase and nitrate reductase (Schultz, et al. 1993) have been determined. In humans, the molybdenum enzymes xanthine oxidase, sulfite oxidase and aldehyde oxidase are involved in the human diseases of gout, combined oxidase deficiency and radical damage following cardiac failure. All plants need molybdenum in nitrate reductase for proper nitrogen assimilation. In industrial catalysis, molybdenum is employed by the petroleum refining industry in multiple hydrotreating processes (Hille 2002).

Functionally, molybdoenzymes catalyse a net oxygen atom transfer reaction shown in equation (2.1).



The oxygen atom, either derived from or incorporated into water, to or from a substrate in a two-electron reduction and this net reaction is considered to be a two-electron process. Common to all molybdenum enzymes, the metal centre functions as an electron-transferring unit regardless of the nature of the reaction catalyzed and there is a cycling between the oxidized Mo(VI) and the reduced Mo(IV) states of the enzyme. It is possible to consider the overall reaction mechanism as consisting of a coupled pair of reductive and oxidative half-reactions, determined by the reduction of Mo(VI) and oxidation of Mo(IV), respectively. It is likely that the molybdenum undergoes a direct two-electron change in oxidation state during the half-reaction due to the two-electron redox reaction catalyzed by the enzyme followed by either addition or removal of electrons at the Mo, by means of electron transfer between the Mo and the second redox center (Hille 1996, Kisker, et al. 1997, Basu, et al. 2003 and George, et al. 1989).

Xanthine oxidase (XO) family enzymes contain oxothioMo-center, O-Mo-S. They have been known as the enzymes that catalyze the hydroxylation of substrates in

the presence of an electron acceptor (Hille 1996). Sulphite oxidase (SO) family including DMSO reductase and related enzymes contain dioxoMo-center, O-Mo-O, in contrast to the S-Mo-O unit in the XO family. These types of molybdoenzymes were known to function via an oxygen atom transfer process (Kisker, et al. 1997).

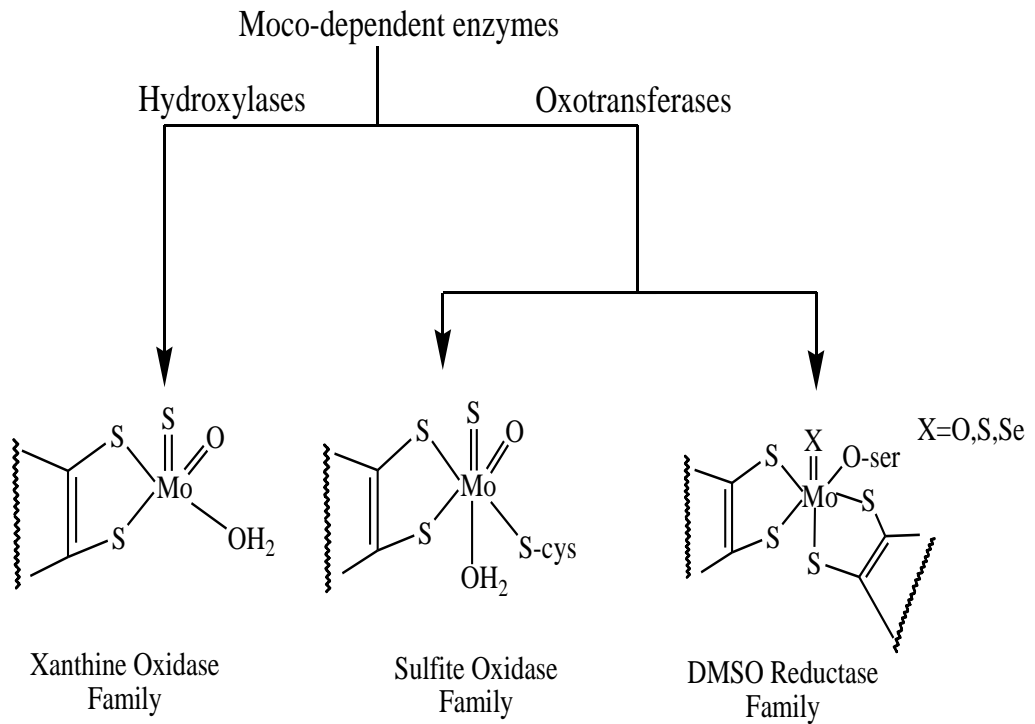


Figure 2.9. Hill classification-mononuclear molybdoenzymes
(Source: Hille 1996)

CHAPTER 3

COMPUTATIONAL CHEMISTRY

Computational chemistry is an exciting and fast-emerging discipline which deals with the modeling and the computer simulation of systems such as biomolecules, polymers, drugs, inorganic and organic molecules, and so on. Since its advent, computational chemistry has grown to the state it is today and it became popular being immensely benefited from the tremendous improvements in computer hardware and software during the last several decades. With high computing power using parallel or grid computing facilities and with faster and efficient numerical algorithms, computational chemistry can be very effectively used to solve complex chemical and biological problems (Ramachandran, et al. 2008).

3.1. Computational Chemistry Methods

Computational chemistry is comprised of a theoretical (or structural) modeling part, known as molecular modeling, and a modeling of processes (or experimentations) known as molecular simulation. Depending upon the level of theory that observed in a computation, the following methods have been identified.

3.1.1. Ab Initio Calculations

The term Ab initio is the Latin term meaning “from the beginning.” This name is given to computations which are derived directly from theoretical principles (such as the Schrödinger equation), with no inclusion of experimental data. This method, in fact, can be seen as an approximate quantum mechanical method. The approximations made are usually mathematical approximations, such as using a simpler functional form for a function, or getting an approximate solution to a differential equation.

The most common type of Ab initio calculation is called a Hartree Fock calculation (HF), in which the primary approximation is called the central field approximation. This method does not include Coulombic electron-electron repulsion in

the calculation. However, its net effect is included in the calculation. This is a variational calculation, meaning that the approximate energies calculated are all equal to or greater than the exact energy. Because of the central field approximation, the energies from HF calculations are always greater than the exact energy and tend to a limiting value called the Hartree Fock limit.

The second approximation in HF calculations is that the wavefunction must be described by some functional form, which is only known exactly for a few one electron systems. The functions used most often are linear combinations of Slater type orbitals (e^{-ax}) or Gaussian type orbitals (e^{-ax^2}), abbreviated as, respectively, STO and GTO. The wavefunction is formed from linear combinations of atomic orbitals, or more often from linear combinations of basis functions. Because of this approximation, most HF calculations give a computed energy greater than the Hartree Fock limit. The exact set of basis functions used is often specified by an abbreviation, such as STO-3G or 6-311++g** (Ramachandran, et al. 2008).

3.1.2. Semiempirical Calculations

Semiempirical calculations are set up with the same general structure as a HF calculation. Within this framework, certain pieces of information, such as two electron integrals, are approximated or completely omitted. In order to correct for the errors introduced by omitting part of the calculation, the method is parameterized, by curve fitting in a few parameters or numbers, in order to give the best possible agreement with experimental data. If the molecule being computed is similar to molecules in the database used to parameterize the method, then the results may be very good. If the molecule being computed is significantly different from anything in the parameterization set, the answers may be very poor.

Semiempirical calculations have been very successful in the description of organic chemistry, where there are only a few elements used extensively and the molecules are of moderate size. However, semiempirical methods have been devised specifically for the description of inorganic chemistry as well (Jensen 2007).

3.1.3. Molecular Mechanics

The methods, referred to as *molecular mechanics*, set up a simple algebraic expression for the total energy of a compound, with no necessity to compute a wavefunction or total electron density (Demmel 1997).

In a molecular mechanics method, the database of compounds used to parameterize the method (a set of parameters and functions is called a force field) is crucial to its success. The molecular mechanics method may be parameterized against a specific class of molecules, such as proteins, organic molecules, organo-metallics, etc. Such a force field would only be expected to have any relevance to describing other proteins.

Molecular mechanics allows the modeling of very large molecules, such as proteins and segments of DNA, making it the primary tool of computational biochemists. The defect of this method is that there are many chemical properties that are not even defined within the method, such as electronic excited states. In order to work with extremely large and complicated systems, often most of the molecular mechanics software packages will have highly powerful and easy to use graphical interfaces (Ramachandran, et al. 2008).

3.1.4. Density Functional Theory (DFT)

An alternative Ab initio method is The Density Functional Theory (DFT) is an alternative ab initio method in which the total energy is expressed in terms of the total electron density, rather than the wavefunction. In this type of calculation, there is an approximate Hamiltonian and an approximate expression for the total electron density. The basis for Density Functional Theory (DFT) is the proof by Hohenberg and Kohn that the ground state electronic energy is determined completely by the electron density ρ . In other words, there exists a one-to-one correspondence between the electron density of a system and the energy. The goal of DFT methods is to design functionals connecting the electron density with the energy (Ramachandran, et al. 2008).

DFT would yield the exact ground state energy and electron density if the exchange-correlation functional was known. In practice, the exact functional is unknown but one may try some approximate form. This has led to an extensive search for

functionals with new variations being published on a regular basis. Because the quality of the results depends critically on the functional, selecting a suitable form will be a vital factor in using the module. DFT methods are broadly classified into two methods: pure DFT and hybrid DFT. They are designated on the basis of type of correlation energy functional, the exchange energy functional, and the potential.

Applications of modern DFT calculations have been extended from small molecules for testing the accuracy to transition metal complexes. For complex molecules, DFT appears to be the method of choice at present. In the last few years, people have begun to apply DFT methods to a variety of systems such as biomolecules, polymers, macromolecules, and so on. Recently, researchers started examining spin densities in bio-inorganic complexes. These are very challenging calculations. involving up to hundreds of electrons. In about 1985, Car and Parrinello introduced a new method whereby one can solve for the electron density for a configuration of nuclei, and then move the nuclei based on the resulting forces, resolve the electronic structure problem, and so on. This means one can do real-time simulations without using any “made up” force fields. This technique has been applied to many problems in chemistry and materials science. Examples are water and ions in water, the proton in water, silicon surfaces, chemical reactions, etc. In the last few years, a lot of work has been done in developing methods which scale linearly with system size (Ramachandran, et al. 2008, Jensen 2007).

3.2. Basis Sets

A basis set is a mathematical description of orbitals of a system, which is used for approximate theoretical calculation or modeling. It is a set of basic functional building blocks that can be stacked or added to have the features that we need. By “stacking” in mathematics, we mean adding things, possibly after multiplying each of them by its own constant illustrated in equation (3.1):

$$\Psi = a_1\varphi_1+a_2\varphi_2+. . .+a_k\varphi_k \quad (3.1)$$



where k is the size of the basis set, $\varphi_1, \varphi_2, . . . , \varphi_k$ are the basis functions and $a_1, a_2, . . . , a_k$ are the normalization constants.

A basis set is a combinations of mathematical functions used to represent atomic orbitals. The employed mathematical functions describe the radial and angular distributions of electron density (Ramachandran, et al. 2008).

3.2.1. Slater Type Orbital

The solution of the Schrödinger equation for the hydrogen atom and other one-electron ions gives atomic orbitals which are a product of a radial function that depend on the distance of the electron from the nucleus and a spherical harmonic. Slater-type orbitals (STOs) represent the real situation for the electron density in the valence region and beyond, but are not so good nearer to the nucleus. Strictly speaking, atomic orbitals (AOs) are the real solutions of the Hartree-Fock (HF) equations for the atom, i.e., wavefunctions for a single electron in the atom. Anything else is not really an atomic orbital function. Hence these functions are named as “basis functions” or “contractions,” which are more appropriate. Earlier, the STOs were used as basis functions due to their similarity to atomic orbitals of the hydrogen atom. Many calculations over the years have been carried out with STOs, particularly for diatomic molecules.

$$\chi_{\zeta,n,l,m}(r,\theta,\varphi) \propto Y_{l,m}(\theta,\varphi) r^{n-1} e^{-\zeta r} \quad (3.2)$$

	
Spherical harmonic function for angular distribution	Exponential function for radial distribution

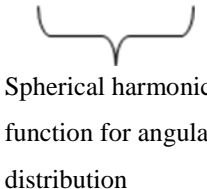
In other words, STO describes fairly well the radial electron distribution. However, STO is difficult to handle because integrations can not be calculated analytically. STO is only used in very special cases (Ramachandran, et al. 2008).

3.2.2. Gaussian Type Orbitals

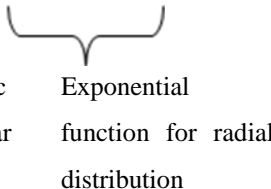
In the 1950s, a modification to the wavefunction was suggested introducing Gaussian type orbitals (GTOs), which contain the exponential $e^{-\beta r^2}$, rather than the e^{-ar}

of the STOs. Such functions are very easy to evaluate. These functions neither represent the electron density of the real situation (the square of a wavefunction is a measure of electron density) nor the STOs. Some early calculations used a large number of individual GTOs. It was then suggested that the GTOs be contracted into separate functions. Each basis function in this approach consists of several GTOs combined together in a linear manner with fixed coefficients (Ramachandran, et al. 2008).

$$\chi_{\zeta,n,l,m}(r,\theta,\phi) \propto Y_{l,m}(\theta,\phi) r^{2n-2} e^{-\zeta r^2} \quad (3.3)$$



Spherical harmonic
function for angular
distribution



Exponential
function for radial
distribution

3.2.3. Pople Type Basis Sets

The basis set notation looks like **k-nlm++G**** or **k-nlm++G(idf,jpd)**.

- ✓ *k* primitive GTOs for core electrons
- n* primitive GTOs for inner valence orbitals
- l* primitive GTOs for medium valence orbitals
- m* primitive GTOs for outer valence orbitals

E.g., 3-21G, 6-31G
and 6-311G

- ✓ + means 1 p diffuse functions added to heavy atoms.
- ++ means 1 p diffuse functions added to heavy atoms and 1 s diffuse functions added to H atom.

E.g., 6-31+G

- ✓ * means 1 d polarization functions added to heavy atoms.
- ** means 1 d polarization functions added to heavy atoms and 1 p polarization functions added to H atom.

E.g., 6-31G*

✓ **idf** means *i* d and 1 f polarization functions added to heavy atoms.

idf,jpd means *i* d and 1 f polarization functions added to heavy atoms and *j* p and 1 d polarization functions added to H atom.

E.g., 6-31+G(d,p)

It was shown in some earlier theoretical studies of molybdenum complexes that DFT method is suitable for geometry optimization and energy calculations of systems with multiple M–L bonds (Zaric, et al. 1997, Webster, et al. 2001, Z'miric', et al. 2002, Kail, et al. 2006). Basis sets for the calculations of molybdenum complexes are given in the literature. Spin-restricted density functional theory (DFT) calculations were carried out for the molybdenum complexes using the DFT method with the hybrid exchange-correlation functional B3LYP (Becke 1993). Of the many available functionals, B3LYP has been chosen because it has provided accurate results for organic molecules in general and for Group 6 metal complexes containing N-donor ligands (Vlc'ek 2002). In the light of this view, B3LYP method was chosen to employ estimating structural parameters and vibrational frequencies for MoN, MoO and NH to provide support for experimentally obtained vibrational assignments.

In the DFT-B3LYP calculations, the LACVP** basis set, which is available in SPARTAN 08, were used. This basis set is combinations of other two basis sets. In LACVP**, molybdenum metal is described with the LANL2DZ basis set and the remaining atoms are described with 6-31+G(d,p) basis sets, respectively.

CHAPTER 4

EXPERIMENTAL STUDY

4.1. Experimental Techniques for Handling Air-Sensitive Compounds

All reactions carried out in this study are air and moisture sensitive therefore Vacuum-Line and Schlenk Technique is used for all experiments.

4.2. The Vacuum-Line Technique

4.2.1 The Double Manifold

If you wish to carry out reactions under dry and inert conditions, a double manifold is an extremely useful piece of apparatus (Figure 4.1) (Leonard, et al. 1995).

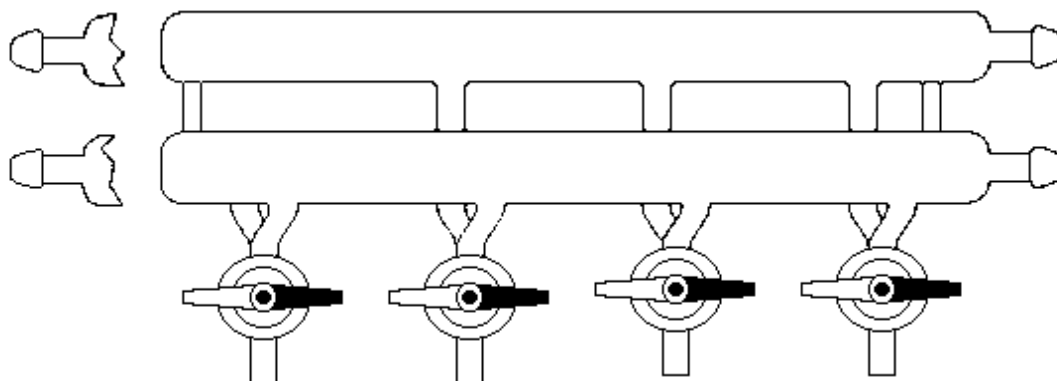


Figure 4.1. The double manifold.

The manifold consists of two glass barrel. One barrel of the manifold is connected to a high vacuum pump another to dry inert gas (Figure 4.2.). Thus, at the turn of the tap, equipment connected to the manifold can be alternately evacuated or filled with inert gas.

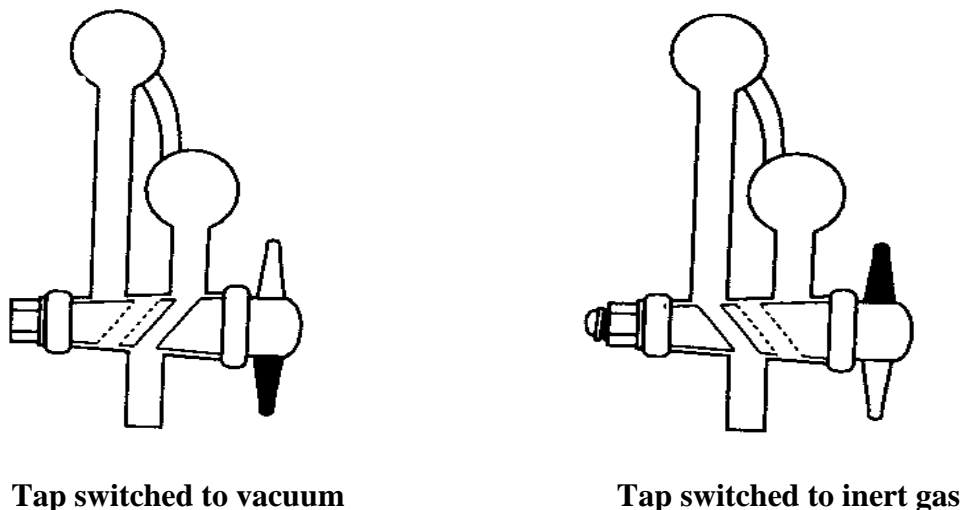


Figure 4.2. Cross section through a double oblique tap.

4.2.2. The Schlenk Technique

To use a schlenk glassware provides facility during the reactions under N_2 , with the schlenk tube one can transfer a solid or liquid in an atmosphere of an inert gas, such as nitrogen or argon (Shriver 1969, Barton 1963).

The inlet is equipped with a stopcock (A) and the main opening has a standard taper (B), which has a small glass ears (C) to hold the stopper or other component with rubber bands or small metal springs.

The basic and simplest schlenk tube is shown in Figure 4.3. The schlenk tube is stoppered and evacuated by pumping through (D). By introducing the inert gas through (A) the tube is filled with the inert gas. The tap is turned through 90° to let gas pass through the tail part and then is turned through 90° to allow gas into the flask.

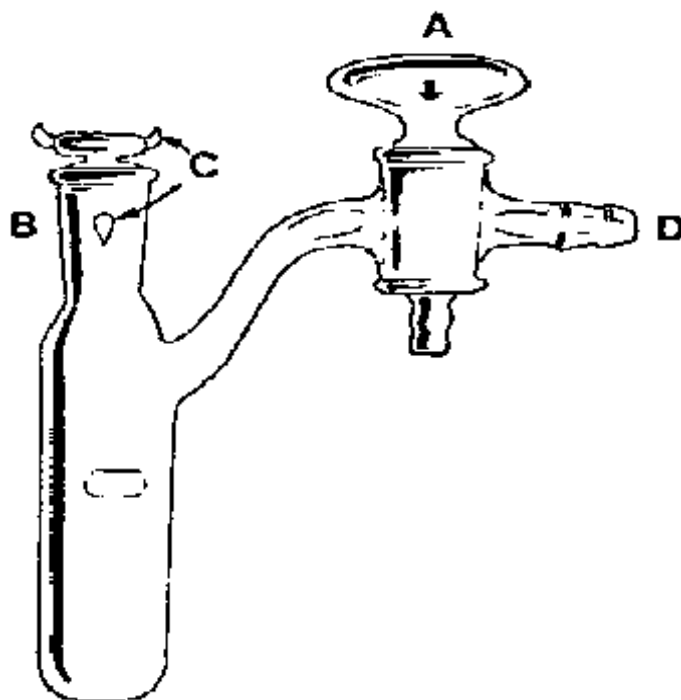


Figure 4.3. The schlenk tube.

4.3. Purification of Solvents

The solvents used are purified, dried under nitrogen by distillation system. A solvent still is used for this purpose (Shriver 1969, Barton, Harwood). This system provides removing the small amount of impurities and any water from the solvent. An example of a solvent still is shown in Figure 4.4.

It consist of a large distillation flask, connected to a reflux condenser via a piece of glassware which can simply be a pressure equalizing funnel modified by the inclusion of a second stopcock. Since the production of very dry solvents usually requires the exclusion of air from the apparatus, the still is fitted so that it can be operated under an inert atmosphere. Firstly, drying agent and solvent are added to the distillation flask under N_2 . With the stopcock A open, the solvent simply refluxes over the drying agent. When the stopcock A is closed, the solvent vapour passes up the narrow tube and dry solvent collects in the central piece of the apparatus. When the required volume of the solvent has been collected, it can be run off through the stopcock B. The solvents were prepared for the use as described below.

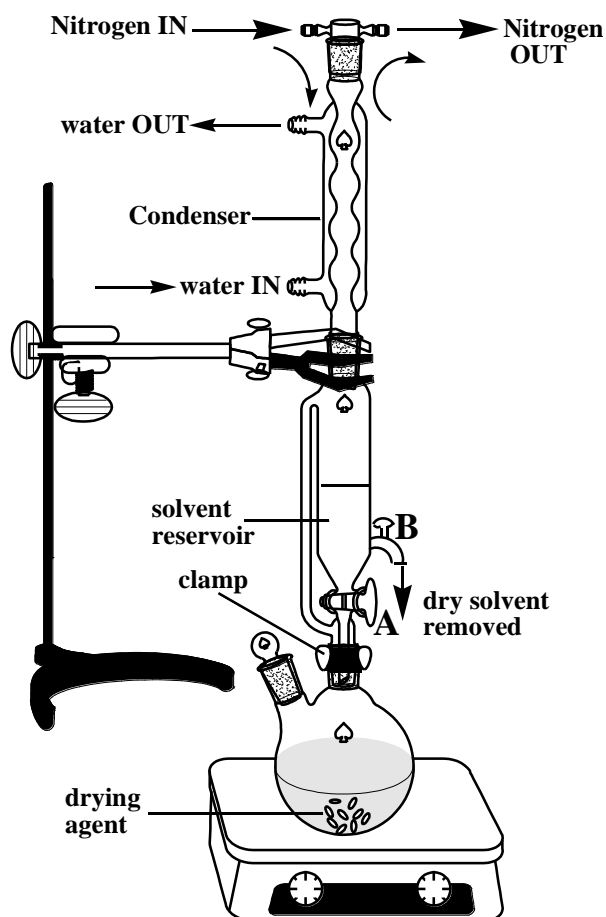


Figure 4.4. Solvent still.

Dichloromethane: The solvent is refluxed over calcium hydride and distilled and then stored onto 4A molecular sieves.

Hexane: The same procedure is performed in purification of dichloromethane.

Tetrahydrofuran: The sodium wire and benzophenone are added to the solvent and it is refluxed under inert atmosphere until the deep blue color persists and then the solvent is distilled and stored onto 4A molecular sieves.

4.4. Materials and Methods

All reactions, synthetic operations, and manipulations were carried out under an oxygen-free and water-free nitrogen atmosphere using standard schlenk techniques, a high-vacuum/gas double line manifold. Reactions were monitored by thin layer chromatography (TLC). Solvents were dried by standard procedures, distilled and kept under nitrogen over 4A molecular sieves. All glassware was oven dried at 120 °C and

schlenk ware was further purged by repeated evacuation and inert gas flushes prior to use. The new compounds were usually purified by CH_2Cl_2 / n-Hexane.

Reagents: Dichloro, Methyl, nitro group functionalized diamines and 1,2-phenylenediamine were obtained from Fluka. Bromo,fluoro,chloro and three/tetra-methyl group substituted diamines were obtained from Aldrich. 1,4-phenylenediamine and naphthalene derivatives were obtained from Acros. Tetrahydrofuran and dimethylformamide were obtained from Merck. Dichloromethane was obtained from Riedel. Hexane was obtained from Carlo Erba. The starting material $[\text{MoO}_2\text{Cl}_2]$ was purchased from Aldrich. $[\text{MoO}_2\text{Cl}_2(\text{THF})_2]$ was prepared according to the literature method (Kuhn, F.E., et al. 2001, Herdtweck, E., et al. 2002). All yields are based on the starting material containing compound.

Instruments: The products were characterized by Fourier Transform Infrared Spectrometry (FT-IR), ^1H -NMR and ^{13}C -NMR spectroscopy and Elemental analysis. Infrared spectra were recorded on as KBr pellet on a Perkin-Elmer model (100) FT-IR spectrometer after grinding the sample with KBr. ^1H -NMR spectra were recorded in DMSO on Varian AS 400 Mercury Plus at Ege University and Varian VnmrJ 400 at İzmir Institute of Technology. Elemental analyses were performed on Leco CHNS 932.

Computational Methods: The geometry optimizations of all complexes were performed at PM3 and B3LYP/LACVP levels of theory. The optimized geometries obtained in the previous step were characterized by utilizing vibrational frequency analyses at PM3 and B3LYP/LACVP levels. All calculations throughout the study have been carried out with SPARTAN08 at Ege University.

4.5. Synthesis

4.5.1. Reactions of $[\text{MoO}_2\text{Cl}_2(\text{THF})_2]$ with Aromatic Nitrogen Donor Ligands

4.5.1.1. Reaction of $[\text{MoO}_2\text{Cl}_2(\text{THF})_2]$ with $[p\text{-H}_2\text{NC}_6\text{H}_4\text{NH}_2]$ (**1**)

A solution of $[\text{MoO}_2\text{Cl}_2(\text{THF})_2]$ (0.40 g, 1.16 mmol) in THF (10 mL) was treated with $p\text{-H}_2\text{NC}_6\text{H}_4\text{NH}_2$ (**1**) (0.13 g, 1.17 mmol). The reaction mixture was stirred further for 30 min. at room temperature. Reaction was monitored by thin layer chromatography (TLC). The mixture was evaporated to dryness and the residue was

crystallized from CH₂Cl₂ /n-hexane (1:4) to afford the compound [Mo₂O₂(μ₂-O)Cl₄(*p*-HNC₆H₄NH₂)₂] (**1**), as light green microcrystals (0.32 g, 80 %).

4.5.1.2. Reaction of [MoO₂Cl₂(THF)₂] with [*p*-H₂NC₆H₂Cl₂NH₂] (**2**)

A solution of [MoO₂Cl₂(THF)₂] (0.45 g, 1.31 mmol) in THF (10 mL) was treated with *p*-H₂NC₆H₂Cl₂NH₂ (**II**) (0.24 g, 1.33 mmol). The reaction mixture was stirred further for 30 min. at room temperature. Reaction was monitored by thin layer chromatography (TLC). The mixture was evaporated to dryness and the residue was crystallized from CH₂Cl₂ /n-hexane (1:4) to afford the compound [MoO₂Cl₂(*p*-HNC₆H₂Cl₂NH₂)] (**2**), as green microcrystals (0.35 g, 78 %).

4.5.1.3. Reaction of [MoO₂Cl₂(THF)₂] with [*p*-H₂NC₆(CH₃)₄NH₂] (**3**)

A solution of [MoO₂Cl₂(THF)₂] (0.36 g, 1.05 mmol) in THF (10 mL) was treated with *p*-H₂NC₆(CH₃)₄NH₂ (**III**) (0.17 g, 1.04 mmol). The reaction mixture was stirred further for 30 min. at room temperature. Reaction was monitored by thin layer chromatography (TLC). The mixture was evaporated to dryness and the residue was crystallized from CH₂Cl₂ /n-hexane (1:4) to afford the compound [Mo₂O₂(μ₂-O)Cl₄(*p*-HNC₆(CH₃)₄NH₂)₂] (**3**), as light orange microcrystals (0.28 g, 77 %).

4.5.1.4. Reaction of [MoO₂Cl₂(THF)₂] with [*p*-H₂NC₆H₃NO₂NH₂] (**4**)

A solution of [MoO₂Cl₂(THF)₂] (0.28 g, 0.80 mmol) in THF (10 mL) was treated with *p*-H₂NC₆H₃NO₂NH₂ (**IV**) (0.12 g, 0.80 mmol). The reaction mixture was stirred further for 30 min. at room temperature. Reaction was monitored by thin layer chromatography (TLC). The mixture was evaporated to dryness and the residue was crystallized from CH₂Cl₂ /n-hexane (1:4) to afford the compound [Mo₂O₂(μ₂-O)Cl₄(*p*-HNC₆H₃NO₂NH₂)₂] (**4**), as green microcrystals (0.21 g, 75 %).

4.5.1.5. Reaction of [MoO₂Cl₂(THF)₂] with [*o*-H₂NC₆H₄NH₂] (5)

A solution of [MoO₂Cl₂(THF)₂] (0.33 g, 0.96 mmol) in THF (10 mL) was treated with *o*-H₂NC₆H₄NH₂ (V) (0.10 g, 0.96 mmol). The reaction mixture was stirred further for 30 min. at room temperature. Reaction was monitored by thin layer chromatography (TLC). The mixture was evaporated to dryness and the residue was crystallized from CH₂Cl₂ /n-hexane (1:4) to afford the compound [Mo₂O₂(μ₂-O)Cl₄(*o*-HNC₆H₄NH₂)₂] (5), as yellow-orange microcrystals (0.25 g, 76 %).

4.5.1.6. Reaction of [MoO₂Cl₂(THF)₂] with [*o*-H₂NC₆H₃(CH₃)NH₂] (6)

A solution of [MoO₂Cl₂(THF)₂] (0.38 g, 1.08 mmol) in THF (10 mL) was treated with *o*-H₂NC₆H₃(CH₃)NH₂ (VI) (0.13 g, 1.08 mmol). The reaction mixture was stirred further for 30 min. at room temperature. Reaction was monitored by thin layer chromatography (TLC). The mixture was evaporated to dryness and the residue was crystallized from CH₂Cl₂ /n-hexane (1:4) to afford the compound [Mo₂O₂(μ₂-O)Cl₄(*o*-HNC₆H₃(CH₃)NH₂)₂] (6), as dark red microcrystals (0.32 g, 84 %).

4.5.1.7. Reaction of [MoO₂Cl₂(THF)₂] with [*o*-H₂NC₆H₃NO₂NH₂] (7)

A solution of [MoO₂Cl₂(THF)₂] (0.43 g, 1.28 mmol) in THF (10 mL) was treated with *o*-H₂NC₆H₃NO₂NH₂ (VII) (0.19 g, 1.28 mmol). The reaction mixture was stirred further for 30 min. at room temperature. Reaction was monitored by thin layer chromatography (TLC). The mixture was evaporated to dryness and the residue was crystallized from CH₂Cl₂ /n-hexane (1:4) to afford the compound [MoO₂Cl₂(*o*-HNC₆H₃NO₂NH)] (7), as pink microcrystals (0.36 g, 84 %).

4.5.1.8. Reaction of [MoO₂Cl₂(THF)₂] with [*o*-H₂NC₆H₃FNH₂] (8)

A solution of [MoO₂Cl₂(THF)₂] (0.48 g, 1.39 mmol) in THF (10 mL) was treated with *o*-H₂NC₆H₃FNH₂ (VIII) (0.18 g, 1.39 mmol). The reaction mixture was stirred further for 30 min. at room temperature. Reaction was monitored by thin layer chromatography (TLC). The mixture was evaporated to dryness and the residue was

crystallized from CH₂Cl₂ /n-hexane (1:4) to afford the compound [Mo₂O₂(μ₂-O)Cl₄(*o*-HNC₆H₃FNH₂)₂] (**8**), as green microcrystals (0.38 g, 79 %).

4.5.1.9. Reaction of [MoO₂Cl₂(THF)₂] with [*o*-H₂NC₆H₃ClNH₂] (**9**)

A solution of [MoO₂Cl₂(THF)₂] (0.46 g, 1.38 mmol) in THF (10 mL) was treated with *o*-H₂NC₆H₃ClNH₂ (**IX**) (0.20 g, 1.38 mmol). The reaction mixture was stirred further for 30 min. at room temperature. Reaction was monitored by thin layer chromatography (TLC). The mixture was evaporated to dryness and the residue was crystallized from CH₂Cl₂ /n-hexane (1:4) to afford the compound [MoO₂Cl₂(*o*-HNC₆H₃ClNH₂)] (**9**), as burgundy microcrystals (0.35 g, 76 %).

4.5.1.10. Reaction of [MoO₂Cl₂(THF)₂] with [*o*-H₂NC₆H₃BrNH₂] (**10**)

A solution of [MoO₂Cl₂(THF)₂] (0.36 g, 1.05 mmol) in THF (10 mL) was treated with *o*-H₂NC₆H₃BrNH₂ (**X**) (0.20 g, 1.05 mmol). The reaction mixture was stirred further for 30 min. at room temperature. Reaction was monitored by thin layer chromatography (TLC). The mixture was evaporated to dryness and the residue was crystallized from CH₂Cl₂ /n-hexane (1:4) to afford the compound [Mo₂O₂(μ₂-O)Cl₄(*o*-HNC₆H₃BrNH₂)₂] (**10**), as burgundy-brown microcrystals (0.28 g, 78 %).

4.5.1.11. Reaction of [MoO₂Cl₂(THF)₂] with [*o*-H₂NC₆H₂Cl₂NH₂] (**11**)

A solution of [MoO₂Cl₂(THF)₂] (0.26 g, 0.75 mmol) in THF (10 mL) was treated with *o*-H₂NC₆H₂Cl₂NH₂ (**XI**) (0.13 g, 0.75 mmol). The reaction mixture was stirred further for 30 min. at room temperature. Reaction was monitored by thin layer chromatography (TLC). The mixture was evaporated to dryness and the residue was crystallized from CH₂Cl₂ /n-hexane (1:4) to afford the compound [MoO₂Cl₂(*o*-HNC₆H₂Cl₂NH₂)] (**11**), as dark burgundy microcrystals (0.19 g, 73 %).

4.5.1.12. Reaction of $[\text{MoO}_2\text{Cl}_2(\text{THF})_2]$ with $[m\text{-H}_2\text{NC}_6\text{H}_4\text{NH}_2]$ (12)

A solution of $[\text{MoO}_2\text{Cl}_2(\text{THF})_2]$ (0.24 g, 0.72 mmol) in THF (10 mL) was treated with $m\text{-H}_2\text{NC}_6\text{H}_4\text{NH}_2$ (XII) (0.08 g, 0.72 mmol). The reaction mixture was stirred further for 30 min. at room temperature. Reaction was monitored by thin layer chromatography (TLC). The mixture was evaporated to dryness and the residue was crystallized from CH_2Cl_2 /n-hexane (1:4) to afford the compound $[\text{Mo}_2\text{O}_2(\mu_2\text{-O})\text{Cl}_4(m\text{-NC}_6\text{H}_4\text{NH}_2)_2]$ (12), as green-grey microcrystals (0.20 g, 83 %).

4.5.1.13. Reaction of $[\text{MoO}_2\text{Cl}_2(\text{THF})_2]$ with $[m\text{-H}_2\text{NC}_6\text{H}_3(\text{CH}_3)\text{NH}_2]$ (13)

A solution of $[\text{MoO}_2\text{Cl}_2(\text{THF})_2]$ (0.34 g, 1.02 mmol) in THF (10 mL) was treated with $m\text{-H}_2\text{NC}_6\text{H}_3(\text{CH}_3)\text{NH}_2$ (XIII) (0.12 g, 1.02 mmol). The reaction mixture was stirred further for 30 min. at room temperature. Reaction was monitored by thin layer chromatography (TLC). The mixture was evaporated to dryness and the residue was crystallized from CH_2Cl_2 /n-hexane (1:4) to afford the compound $[\text{Mo}_2\text{O}_2(\mu_2\text{-O})\text{Cl}_4(m\text{-HNC}_6\text{H}_3(\text{CH}_3)\text{NH}_2)_2]$ (13), as green microcrystals (0.29 g, 85 %).

4.5.1.14. Reaction of $[\text{MoO}_2\text{Cl}_2(\text{THF})_2]$ with $[m\text{-H}_2\text{NC}_6\text{H}_3\text{FNH}_2]$ (14)

A solution of $[\text{MoO}_2\text{Cl}_2(\text{THF})_2]$ (0.29 g, 0.84 mmol) in THF (10 mL) was treated with $m\text{-H}_2\text{NC}_6\text{H}_3\text{FNH}_2$ (XIV) (0.11 g, 0.84 mmol). The reaction mixture was stirred further for 30 min. at room temperature. Reaction was monitored by thin layer chromatography (TLC). The mixture was evaporated to dryness and the residue was crystallized from CH_2Cl_2 /n-hexane (1:4) to afford the compound $[\text{MoO}_2\text{Cl}_2(m\text{-HNC}_6\text{H}_3\text{FNH}_2)_2]$ (14), as grey-green microcrystals (0.21 g, 72 %).

4.5.1.15. Reaction of $[\text{MoO}_2\text{Cl}_2(\text{THF})_2]$ with $[m\text{-H}_2\text{NC}_6\text{H}_3\text{ClNH}_2]$ (15)

A solution of $[\text{MoO}_2\text{Cl}_2(\text{THF})_2]$ (0.31 g, 0.89 mmol) in THF (10 mL) was treated with $m\text{-H}_2\text{NC}_6\text{H}_3\text{ClNH}_2$ (XV) (0.13 g, 0.89 mmol). The reaction mixture was

stirred further for 30 min. at room temperature. Reaction was monitored by thin layer chromatography (TLC). The mixture was evaporated to dryness and the residue was crystallized from CH₂Cl₂ /n-hexane (1:4) to afford the compound [Mo₂O₂(μ₂-O)Cl₄(*m*-HNC₆H₃ClNH₂)₂] (**15**), as grey-black microcrystals (0.23 g, 47 %).

4.5.1.16. Reaction of [MoO₂Cl₂(THF)₂] with [*m*-H₂NC₆H(CH₃)₃NH₂] (**16**)

A solution of [MoO₂Cl₂(THF)₂] (0.45 g, 1.32 mmol) in THF (10 mL) was treated with *m*-H₂NC₆H(CH₃)₃NH₂ (**XVI**) (0.19 g, 1.32 mmol). The reaction mixture was stirred further for 30 min. at room temperature. Reaction was monitored by thin layer chromatography (TLC). The mixture was evaporated to dryness and the residue was crystallized from CH₂Cl₂ /n-hexane (1:4) to afford the compound [Mo₂O₂(μ₂-O)Cl₄(*m*-HNC₆H(CH₃)₃NH₂)₂] (**16**), as light orange microcrystals (0.39 g, 87 %).

4.5.1.17. Reaction of [MoO₂Cl₂(THF)₂] with [*l*,5-H₂NC₁₀H₆NH₂] (**17**)

A solution of [MoO₂Cl₂(THF)₂] (0.43 g, 1.26 mmol) in THF (10 mL) was treated with *l*,5-H₂NC₁₀H₆NH₂ (**XVII**) (0.20 g, 1.26 mmol). The reaction mixture was stirred further for 30 min. at room temperature. Reaction was monitored by thin layer chromatography (TLC). The mixture was evaporated to dryness and the residue was crystallized from CH₂Cl₂ /n-hexane (1:4) to afford the compound [Mo₂O₂(μ₂-O)Cl₄(*l*,5-HNC₁₀H₆NH₂)₂] (**17**), as dark grey microcrystals (0.35 g, 81 %).

4.5.1.18. Reaction of [MoO₂Cl₂(THF)₂] with [*l*,8-H₂NC₁₀H₆NH₂] (**18**)

A solution of [MoO₂Cl₂(THF)₂] (0.72 g, 2.13 mmol) in THF (10 mL) was treated with *l*,8-H₂NC₁₀H₆NH₂ (**XVIII**) (0.34 g, 2.13 mmol). The reaction mixture was stirred further for 30 min. at room temperature. Reaction was monitored by thin layer chromatography (TLC). The mixture was evaporated to dryness and the residue was crystallized from CH₂Cl₂ /n-hexane (1:4) to afford the compound [Mo₂O₂(μ₂-O)Cl₄(*l*,8-HNC₁₀H₆NH₂)₂] (**18**), as green microcrystals (0.60 g, 83 %).

4.5.1.19. Reaction of $[\text{MoO}_2\text{Cl}_2(\text{THF})_2]$ with $[2,3\text{-H}_2\text{NC}_{10}\text{H}_6\text{NH}_2]$ (**19**)

A solution of $[\text{MoO}_2\text{Cl}_2(\text{THF})_2]$ (0.72 g, 2.13 mmol) in THF (10 mL) was treated with $2,3\text{-H}_2\text{NC}_{10}\text{H}_6\text{NH}_2$ (**XIX**) (0.34 g, 2.13 mmol). The reaction mixture was stirred further for 30 min. at room temperature. Reaction was monitored by thin layer chromatography (TLC). The mixture was evaporated to dryness and the residue was crystallized from CH_2Cl_2 /n-hexane (1:4) to afford the compound $[\text{Mo}_2\text{O}_2(\mu_2\text{-O})\text{Cl}_4(2,3\text{-HNC}_{10}\text{H}_6\text{NH}_2)_2]$ (**19**), as lavender-grey microcrystals (0.56 g, 78 %).

4.5.2. Reactions of $[\text{Mo}_2\text{O}_3\text{Cl}_4(\text{DMF})_4]$ with Aromatic Nitrogen Donor Ligands

4.5.2.1. Reaction of $[\text{Mo}_2\text{O}_3\text{Cl}_4(\text{DMF})_4]$ with $[p\text{-H}_2\text{NC}_6\text{H}_4\text{NH}_2]$ (**1**)

A solution of $[\text{Mo}_2\text{O}_3\text{Cl}_4(\text{DMF})_4]$ (0.23 g, 0.37 mmol) in THF (10 mL) was treated with $p\text{-H}_2\text{NC}_6\text{H}_4\text{NH}_2$ (**I**) (0.08 g, 0.74 mmol). The reaction mixture was stirred further for 30 min. at room temperature. Reaction was monitored by thin layer chromatography (TLC). The mixture was evaporated to dryness and the residue was crystallized from CH_2Cl_2 /n-hexane (1:4) to afford the compound $[\text{Mo}_2\text{O}_2(\mu_2\text{-O})\text{Cl}_4(p\text{-HNC}_6\text{H}_4\text{NH}_2)_2]$ (**1**), as light green microcrystals (0.15 g, 65 %).

4.5.2.2. Reaction of $[\text{Mo}_2\text{O}_3\text{Cl}_4(\text{DMF})_4]$ with $[p\text{-H}_2\text{NC}_6\text{H}_2\text{Cl}_2\text{NH}_2]$ (**20**)

A solution of $[\text{Mo}_2\text{O}_3\text{Cl}_4(\text{DMF})_4]$ (0.25 g, 0.40 mmol) in THF (10 mL) was treated with $p\text{-H}_2\text{NC}_6\text{H}_2\text{Cl}_2\text{NH}_2$ (**II**) (0.14 g, 0.80 mmol). The reaction mixture was stirred further for 30 min. at room temperature. Reaction was monitored by thin layer chromatography (TLC). The mixture was evaporated to dryness and the residue was crystallized from CH_2Cl_2 /n-hexane (1:4) to afford the compound $[\text{Mo}_2\text{O}_2(\mu_2\text{-O})\text{Cl}_4(p\text{-HNC}_6\text{H}_2\text{Cl}_2\text{NH}_2)_2]$ (**20**), as green-brown microcrystals (0.29 g, 72 %).

4.5.2.3. Reaction of [Mo₂O₃Cl₄(DMF)₄] with [*p*-H₂NC₆(CH₃)₄NH₂] (3)

A solution of [Mo₂O₃Cl₄(DMF)₄] (0.37 g, 0.37 mmol) in THF (10 mL) was treated with *p*-H₂NC₆(CH₃)₄NH₂ (**III**) (0.12 g, 0.74 mmol). The reaction mixture was stirred further for 30 min. at room temperature. Reaction was monitored by thin layer chromatography (TLC). The mixture was evaporated to dryness and the residue was crystallized from CH₂Cl₂ /n-hexane (1:4) to afford the compound [Mo₂O₂(μ₂-O)Cl₄(*p*-HNC₆(CH₃)₄NH₂)₂] (**3**), as light orange microcrystals (0.26 g, 70 %).

4.5.2.4. Reaction of [Mo₂O₃Cl₄(DMF)₄] with [*p*-H₂NC₆H₃NO₂NH₂] (4)

A solution of [Mo₂O₃Cl₄(DMF)₄] (0.13 g, 0.21 mmol) in THF (10 mL) was treated with *p*-H₂NC₆H₃NO₂NH₂ (**IV**) (0.06 g, 0.42 mmol). The reaction mixture was stirred further for 30 min. at room temperature. Reaction was monitored by thin layer chromatography (TLC). The mixture was evaporated to dryness and the residue was crystallized from CH₂Cl₂ /n-hexane (1:4) to afford the compound [Mo₂O₂(μ₂-O)Cl₄(*p*-HNC₆H₃NO₂NH₂)₂] (**4**), as green microcrystals (0.08 g, 61 %).

4.5.2.5. Reaction of [Mo₂O₃Cl₄(DMF)₄] with [*o*-H₂NC₆H₄NH₂] (5)

A solution of [Mo₂O₃Cl₄(DMF)₄] (0.11 g, 0.18 mmol) in THF (10 mL) was treated with *o*-H₂NC₆H₄NH₂ (**V**) (0.04 g, 0.36 mmol). The reaction mixture was stirred further for 30 min. at room temperature. Reaction was monitored by thin layer chromatography (TLC). The mixture was evaporated to dryness and the residue was crystallized from CH₂Cl₂ /n-hexane (1:4) to afford the compound [Mo₂O₂(μ₂-O)Cl₄(*o*-HNC₆H₄NH₂)₂] (**5**), as yellow-orange microcrystals (0.07 g, 64 %).

4.5.2.6. Reaction of [Mo₂O₃Cl₄(DMF)₄] with [*o*-H₂NC₆H₃(CH₃)NH₂] (6)

A solution of [Mo₂O₃Cl₄(DMF)₄] (0.22 g, 0.36 mmol) in THF (10 mL) was treated with *o*-H₂NC₆H₃(CH₃)NH₂ (**VI**) (0.08 g, 0.72 mmol). The reaction mixture was stirred further for 30 min. at room temperature. Reaction was monitored by thin layer

chromatography (TLC). The mixture was evaporated to dryness and the residue was crystallized from CH₂Cl₂ /n-hexane (1:4) to afford the compound [Mo₂O₂(μ₂-O)Cl₄(*o*-HNC₆H₃(CH₃)NH₂)₂] (**6**), as dark red microcrystals (0.14 g, 64 %).

4.5.2.7. Reaction of [Mo₂O₃Cl₄(DMF)₄] with [*o*-H₂NC₆H₃NO₂NH₂] (**21**)

A solution of [Mo₂O₃Cl₄(DMF)₄] (0.20 g, 0.32 mmol) in THF (10 mL) was treated with *o*-H₂NC₆H₃NO₂NH₂ (**VII**) (0.10 g, 0.64 mmol). The reaction mixture was stirred further for 30 min. at room temperature. Reaction was monitored by thin layer chromatography (TLC). The mixture was evaporated to dryness and the residue was crystallized from CH₂Cl₂ /n-hexane (1:4) to afford the compound [Mo₂O₂(μ₂-O)Cl₄(*o*-HNC₆H₃NO₂NH₂)₂] (**21**), as light green microcrystals (0.15 g, 75 %).

4.5.2.8. Reaction of [Mo₂O₃Cl₄(DMF)₄] with [*o*-H₂NC₆H₃FNH₂] (**8**)

A solution of [Mo₂O₃Cl₄(DMF)₄] (0.13 g, 0.21 mmol) in THF (10 mL) was treated with *o*-H₂NC₆H₃FNH₂ (**VIII**) (0.05 g, 0.42 mmol). The reaction mixture was stirred further for 30 min. at room temperature. Reaction was monitored by thin layer chromatography (TLC). The mixture was evaporated to dryness and the residue was crystallized from CH₂Cl₂ /n-hexane (1:4) to afford the compound [Mo₂O₂(μ₂-O)Cl₄(*o*-HNC₆H₃FNH₂)₂] (**8**), as green microcrystals (0.07 g, 53 %).

4.5.2.9. Reaction of [Mo₂O₃Cl₄(DMF)₄] with [*o*-H₂NC₆H₃ClNH₂] (**22**)

A solution of [Mo₂O₃Cl₄(DMF)₄] (0.13 g, 0.21 mmol) in THF (10 mL) was treated with *o*-H₂NC₆H₃ClNH₂ (**IX**) (0.06 g, 0.42 mmol). The reaction mixture was stirred further for 30 min. at room temperature. Reaction was monitored by thin layer chromatography (TLC). The mixture was evaporated to dryness and the residue was crystallized from CH₂Cl₂ /n-hexane (1:4) to afford the compound [Mo₂O₂(μ₂-O)Cl₄(*o*-HNC₆H₃ClNH₂)₂] (**22**), as light lavender microcrystals (0.08 g, 61 %).

4.5.2.10. Reaction of $[\text{Mo}_2\text{O}_3\text{Cl}_4(\text{DMF})_4]$ with $[o\text{-H}_2\text{NC}_6\text{H}_3\text{BrNH}_2]$ (**10**)

A solution of $[\text{Mo}_2\text{O}_3\text{Cl}_4(\text{DMF})_4]$ (0.13 g, 0.21 mmol) in THF (10 mL) was treated with $o\text{-H}_2\text{NC}_6\text{H}_3\text{BrNH}_2$ (**X**) (0.08 g, 0.42 mmol). The reaction mixture was stirred further for 30 min. at room temperature. Reaction was monitored by thin layer chromatography (TLC). The mixture was evaporated to dryness and the residue was crystallized from CH_2Cl_2 /n-hexane (1:4) to afford the compound $[\text{Mo}_2\text{O}_2(\mu_2\text{-O})\text{Cl}_4(o\text{-HNC}_6\text{H}_3\text{BrNH}_2)_2]$ (**10**), as burgundy-brown microcrystals (0.07 g, 53 %).

4.5.2.11. Reaction of $[\text{Mo}_2\text{O}_3\text{Cl}_4(\text{DMF})_4]$ with $[o\text{-H}_2\text{NC}_6\text{H}_2\text{Cl}_2\text{NH}_2]$ (**23**)

A solution of $[\text{Mo}_2\text{O}_3\text{Cl}_4(\text{DMF})_4]$ (0.12 g, 0.19 mmol) in THF (10 mL) was treated with $o\text{-H}_2\text{NC}_6\text{H}_2\text{Cl}_2\text{NH}_2$ (**XI**) (0.07 g, 0.38 mmol). The reaction mixture was stirred further for 30 min. at room temperature. Reaction was monitored by thin layer chromatography (TLC). The mixture was evaporated to dryness and the residue was crystallized from CH_2Cl_2 /n-hexane (1:4) to afford the compound $[\text{Mo}_2\text{O}_2(\mu_2\text{-O})\text{Cl}_4(o\text{-HNC}_6\text{H}_2\text{Cl}_2\text{NH}_2)_2]$ (**23**), as green-grey microcrystals (0.07 g, 67 %).

4.5.2.12. Reaction of $[\text{Mo}_2\text{O}_3\text{Cl}_4(\text{DMF})_4]$ with $[m\text{-H}_2\text{NC}_6\text{H}_4\text{NH}_2]$ (**12**)

A solution of $[\text{Mo}_2\text{O}_3\text{Cl}_4(\text{DMF})_4]$ (0.11 g, 0.18 mmol) in THF (10 mL) was treated with $m\text{-H}_2\text{NC}_6\text{H}_4\text{NH}_2$ (**XII**) (0.04 g, 0.36 mmol). The reaction mixture was stirred further for 30 min. at room temperature. Reaction was monitored by thin layer chromatography (TLC). The mixture was evaporated to dryness and the residue was crystallized from CH_2Cl_2 /n-hexane (1:4) to afford the compound $[\text{Mo}_2\text{O}_2(\mu_2\text{-O})\text{Cl}_4(m\text{-NC}_6\text{H}_4\text{NH}_2)_2]$ (**12**), as green-grey microcrystals (0.08 g, 73 %).

4.5.2.13. Reaction of $[\text{Mo}_2\text{O}_3\text{Cl}_4(\text{DMF})_4]$ with $[m\text{-H}_2\text{NC}_6\text{H}_3(\text{CH}_3)\text{NH}_2]$ (**13**)

A solution of $[\text{Mo}_2\text{O}_3\text{Cl}_4(\text{DMF})_4]$ (0.12 g, 0.19 mmol) in THF (10 mL) was treated with $m\text{-H}_2\text{NC}_6\text{H}_3(\text{CH}_3)\text{NH}_2$ (**XIII**) (0.05 g, 1.38 mmol). The reaction mixture

was stirred further for 30 min. at room temperature. Reaction was monitored by thin layer chromatography (TLC). The mixture was evaporated to dryness and the residue was crystallized from CH₂Cl₂ /n-hexane (1:4) to afford the compound [Mo₂O₂(μ₂-O)Cl₄(*m*-HNC₆H₃(CH₃)NH₂)₂] (**13**), as green microcrystals (0.07 g, 58 %).

4.5.2.14. Reaction of [Mo₂O₃Cl₄(DMF)₄] with [*m*-H₂NC₆H₃FNH₂] (**24**)

A solution of [Mo₂O₃Cl₄(DMF)₄] (0.11 g, 0.18 mmol) in THF (10 mL) was treated with *m*-H₂NC₆H₃FNH₂ (**XIV**) (0.04 g, 0.36 mmol). The reaction mixture was stirred further for 30 min. at room temperature. Reaction was monitored by thin layer chromatography (TLC). The mixture was evaporated to dryness and the residue was crystallized from CH₂Cl₂ /n-hexane (1:4) to afford the compound [Mo₂O₂(μ₂-O)Cl₄(*m*-HNC₆H₃FNH₂)₂] (**24**), as grey microcrystals (0.06 g, 55 %).

4.5.2.15. Reaction of [Mo₂O₃Cl₄(DMF)₄] with [*m*-H₂NC₆H₃CINH₂] (**15**)

A solution of [Mo₂O₃Cl₄(DMF)₄] (0.13 g, 0.21 mmol) in THF (10 mL) was treated with *m*-H₂NC₆H₃CINH₂ (**XV**) (0.06 g, 0.84 mmol). The reaction mixture was stirred further for 30 min. at room temperature. Reaction was monitored by thin layer chromatography (TLC). The mixture was evaporated to dryness and the residue was crystallized from CH₂Cl₂ /n-hexane (1:4) to afford the compound [Mo₂O₂(μ₂-O)Cl₄(*m*-HNC₆H₃CINH₂)₂] (**15**), as grey-black microcrystals (0.07 g, 54 %).

4.5.2.16. Reaction of [Mo₂O₃Cl₄(DMF)₄] with [*m*-H₂NC₆H(CH₃)₃NH₂] (**16**)

A solution of [Mo₂O₃Cl₄(DMF)₄] (0.11 g, 0.18 mmol) in THF (10 mL) was treated with *m*-H₂NC₆H(CH₃)₃NH₂ (**XVI**) (0.05 g, 0.36 mmol). The reaction mixture was stirred further for 30 min. at room temperature. Reaction was monitored by thin layer chromatography (TLC). The mixture was evaporated to dryness and the residue was crystallized from CH₂Cl₂ /n-hexane (1:4) to afford the compound [Mo₂O₂(μ₂-O)Cl₄(*m*-HNC₆H(CH₃)₃NH₂)₂] (**16**), as light orange microcrystals (0.08 g, 73 %).

4.5.2.17. Reaction of $[\text{Mo}_2\text{O}_3\text{Cl}_4(\text{DMF})_4]$ with $[1,5\text{-H}_2\text{NC}_{10}\text{H}_6\text{NH}_2]$ (17)

A solution of $[\text{Mo}_2\text{O}_3\text{Cl}_4(\text{DMF})_4]$ (0.12 g, 0.19 mmol) in THF (10 mL) was treated with $1,5\text{-H}_2\text{NC}_{10}\text{H}_6\text{NH}_2$ (**XVII**) (0.06 g, 0.38 mmol). The reaction mixture was stirred further for 30 min. at room temperature. Reaction was monitored by thin layer chromatography (TLC). The mixture was evaporated to dryness and the residue was crystallized from CH_2Cl_2 /n-hexane (1:4) to afford the compound $[\text{Mo}_2\text{O}_2(\mu_2\text{-O})\text{Cl}_4(1,5\text{-HNC}_{10}\text{H}_6\text{NH}_2)_2]$ (**17**), as dark grey microcrystals (0.09 g, 75 %).

4.5.2.18. Reaction of $[\text{Mo}_2\text{O}_3\text{Cl}_4(\text{DMF})_4]$ with $[1,8\text{-H}_2\text{NC}_{10}\text{H}_6\text{NH}_2]$ (18)

A solution of $[\text{Mo}_2\text{O}_3\text{Cl}_4(\text{DMF})_4]$ (0.12 g, 0.19 mmol) in THF (10 mL) was treated with $1,8\text{-H}_2\text{NC}_{10}\text{H}_6\text{NH}_2$ (**XVIII**) (0.06 g, 0.38 mmol). The reaction mixture was stirred further for 30 min. at room temperature. Reaction was monitored by thin layer chromatography (TLC). The mixture was evaporated to dryness and the residue was crystallized from CH_2Cl_2 /n-hexane (1:4) to afford the compound $[\text{Mo}_2\text{O}_2(\mu_2\text{-O})\text{Cl}_4(1,8\text{-HNC}_{10}\text{H}_6\text{NH}_2)_2]$ (**18**), as green microcrystals (0.08 g, 67 %).

4.5.2.19. Reaction of $[\text{Mo}_2\text{O}_3\text{Cl}_4(\text{DMF})_4]$ with $[2,3\text{-H}_2\text{NC}_{10}\text{H}_6\text{NH}_2]$ (19)

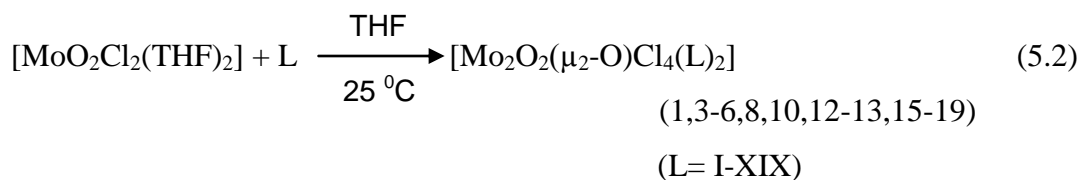
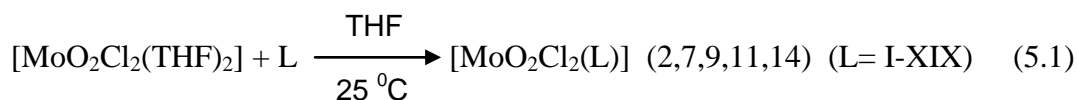
A solution of $[\text{Mo}_2\text{O}_3\text{Cl}_4(\text{DMF})_4]$ (0.13 g, 0.21 mmol) in THF (10 mL) was treated with $2,3\text{-H}_2\text{NC}_{10}\text{H}_6\text{NH}_2$ (**XIX**) (0.07 g, 0.42 mmol). The reaction mixture was stirred further for 30 min. at room temperature. Reaction was monitored by thin layer chromatography (TLC). The mixture was evaporated to dryness and the residue was crystallized from CH_2Cl_2 /n-hexane (1:4) to afford the compound $[\text{Mo}_2\text{O}_2(\mu_2\text{-O})\text{Cl}_4(2,3\text{-HNC}_{10}\text{H}_6\text{NH}_2)_2]$ (**19**), as lavender-grey microcrystals (0.08 g, 62 %).

CHAPTER 5

RESULT AND DISCUSSION

5.1. Synthetic Studies

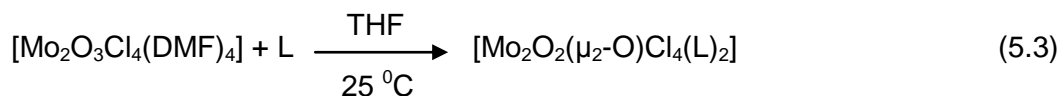
The first part of the thesis, the reactions of the solvent-stabilized compound $[\text{MoO}_2\text{Cl}_2(\text{THF})_2]$ with substituted phenylenediamines and naphthalenediamine derivatives (I-XIX) were investigated shown in equations 5.1 and 5.2. The solvent-stabilized compound $[\text{MoO}_2\text{Cl}_2(\text{THF})_2]$ was obtained according to the literature method (Kuhn, et al. 2001, Herdtweck, et al. 1999). The reactions were performed under nitrogen gas atmosphere and at room temperature.



The reactions of $[\text{MoO}_2\text{Cl}_2(\text{THF})_2]$ with $p\text{-H}_2\text{NC}_6\text{H}_2\text{Cl}_2\text{NH}_2$ (II), $o\text{-H}_2\text{NC}_6\text{H}_3\text{NO}_2\text{NH}_2$ (VII), $o\text{-H}_2\text{NC}_6\text{H}_3\text{ClNH}_2$ (IX), $o\text{-H}_2\text{NC}_6\text{H}_2\text{Cl}_2\text{NH}_2$ (XI) and $m\text{-H}_2\text{NC}_6\text{H}_3\text{FNH}_2$ (XIV) yielded the mononuclear compounds $[\text{MoO}_2\text{Cl}_2(p\text{-NC}_6\text{H}_2\text{Cl}_2\text{NH}_2)]$ (2), $[\text{MoO}_2\text{Cl}_2(o\text{-HNC}_6\text{H}_3\text{NO}_2\text{NH})]$ (7), $[\text{MoO}_2\text{Cl}_2(o\text{-HNC}_6\text{H}_3\text{ClNH})]$ (9), $[\text{MoO}_2\text{Cl}_2(o\text{-HNC}_6\text{H}_2\text{Cl}_2\text{NH}_2)]$ (11) and $[\text{MoO}_2\text{Cl}_2(m\text{-HNC}_6\text{H}_3\text{FNH}_2)]$ (14) respectively whereas the reactions of $[\text{MoO}_2\text{Cl}_2(\text{THF})_2]$ with $p\text{-H}_2\text{NC}_6\text{H}_4\text{NH}_2$ (I), $p\text{-H}_2\text{NC}_6(\text{CH}_3)_4\text{NH}_2$ (III), $p\text{-H}_2\text{NC}_6\text{H}_3\text{NO}_2\text{NH}_2$ (IV), $o\text{-H}_2\text{NC}_6\text{H}_4\text{NH}_2$ (V), $o\text{-H}_2\text{NC}_6\text{H}_3(\text{CH}_3)\text{NH}_2$ (VI), $o\text{-H}_2\text{NC}_6\text{H}_3\text{FNH}_2$ (VIII), $o\text{-H}_2\text{NC}_6\text{H}_3\text{BrNH}_2$ (X), $m\text{-H}_2\text{NC}_6\text{H}_4\text{NH}_2$ (XII), $m\text{-H}_2\text{NC}_6\text{H}_3(\text{CH}_3)\text{NH}_2$ (XIII), $m\text{-H}_2\text{NC}_6\text{H}_3\text{ClNH}_2$ (XV), $m\text{-H}_2\text{NC}_6\text{H}(\text{CH}_3)_3\text{NH}_2$ (XVI), $1,5\text{-H}_2\text{NC}_{10}\text{H}_6\text{NH}_2$ (XVII), $1,8\text{-H}_2\text{NC}_{10}\text{H}_6\text{NH}_2$ (XVIII) and $2,3\text{-H}_2\text{NC}_{10}\text{H}_6\text{NH}_2$ (XIX) yielded dinuclear compounds $[\text{Mo}_2\text{O}_2(\mu_2\text{-O})\text{Cl}_4(p\text{-$

HNC₆H₄NH₂)₂] (1), [Mo₂O₂(μ₂-O)Cl₄(*p*-HNC₆(CH₃)₄NH₂)₂] (3), [Mo₂O₂(μ₂-O)Cl₄(*p*-HNC₆H₃NO₂NH₂)₂] (4), [Mo₂O₂(μ₂-O)Cl₄(*o*-HNC₆H₄NH₂)₂] (5), [Mo₂O₂(μ₂-O)Cl₄(*o*-HNC₆H₃(CH₃)NH₂)₂] (6), [Mo₂O₂(μ₂-O)Cl₄(*o*-HNC₆H₃FNH₂)₂] (8), [Mo₂O₂(μ₂-O)Cl₄(*o*-HNC₆H₃BrNH₂)₂] (10), [Mo₂O₂(μ₂-O)Cl₄(*m*-NC₆H₄NH₂)₂] (12), [Mo₂O₂(μ₂-O)Cl₄(*m*-HNC₆H₃(CH₃)NH₂)₂] (13), [Mo₂O₂(μ₂-O)Cl₄(*m*-HNC₆H₃ClNH₂)₂] (15), [Mo₂O₂(μ₂-O)Cl₄(*m*-HNC₆H(CH₃)₃NH₂)₂] (16), [Mo₂O₂(μ₂-O)Cl₄(*l*,5-HNC₁₀H₆NH₂)₂] (17), [Mo₂O₂(μ₂-O)Cl₄(*l*,8-HNC₁₀H₆NH₂)₂] (18) and [Mo₂O₂(μ₂-O)Cl₄(2,3-HNC₁₀H₆NH₂)₂] (19) respectively.

The second part of the thesis, the starting compound [Mo₂O₃Cl₄(DMF)₄] was prepared from the reaction of [MoO₂Cl₂(DMF)₂] with PPh₃ in DMF solvent (Aguado, et al. 2007). The reactions of the solvent-stabilized compound [Mo₂O₃Cl₄(DMF)₄] with substituted phenylenediamines and naphthalenediamine derivatives (I-XIX) were investigated under similar conditions which is illustrated in equation 5.3 and Mo-O-Mo bridged dinuclear oxomolybdenum compounds of the type [Mo₂O₂(μ₂-O)Cl₄(L)₂] were obtained.



(1,3-6,8,10,12-13,15-19,20-24)

(L= I-XIX)

The reactions of [Mo₂O₃Cl₄(DMF)₄] with *p*-H₂NC₆H₄NH₂ (I), *p*-H₂NC₆H₂Cl₂NH₂ (II), *p*-H₂NC₆(CH₃)₄NH₂ (III), *p*-H₂NC₆H₃NO₂NH₂ (IV), *o*-H₂NC₆H₄NH₂ (V), *o*-H₂NC₆H₃(CH₃)NH₂ (VI), *o*-H₂NC₆H₃NO₂NH₂ (VII), *o*-H₂NC₆H₃FNH₂ (VIII), *o*-H₂NC₆H₃ClNH₂ (IX), *o*-H₂NC₆H₃BrNH₂ (X), *o*-H₂NC₆H₂Cl₂NH₂ (XI), *m*-H₂NC₆H₄NH₂ (XII), *m*-H₂NC₆H₃(CH₃)NH₂ (XIII), *m*-H₂NC₆H₃FNH₂ (XIV), *m*-H₂NC₆H₃ClNH₂ (XV), *m*-H₂NC₆H(CH₃)₃NH₂ (XVI), *l*,5-H₂NC₁₀H₆NH₂ (XVII), *l*,8-H₂NC₁₀H₆NH₂ (XVIII) and 2,3-H₂NC₁₀H₆NH₂ (XIX) yielded the dinuclear compounds [Mo₂O₂(μ₂-O)Cl₄(*p*-HNC₆H₄NH₂)₂] (1), [Mo₂O₂(μ₂-O)Cl₄(HNC₆H₂Cl₂NH₂)₂] (20), [Mo₂O₂(μ₂-O)Cl₄(*p*-HNC₆(CH₃)₄NH₂)₂] (3), [Mo₂O₂(μ₂-O)Cl₄(*p*-HNC₆H₃NO₂NH₂)₂] (4), [Mo₂O₂(μ₂-O)Cl₄(*o*-HNC₆H₄NH₂)₂] (5), [Mo₂O₂(μ₂-O)Cl₄(*o*-HNC₆H₃(CH₃)NH₂)₂] (6), [Mo₂O₂(μ₂-O)Cl₄(*o*-HNC₆H₃NO₂NH₂)₂] (21), [Mo₂O₂(μ₂-O)Cl₄(*o*-HNC₆H₃FNH₂)₂] (8), [Mo₂O₂(μ₂-O)Cl₄(HNC₆H₃ClNH₂)₂] (22), [Mo₂O₂(μ₂-O)Cl₄(*o*-HNC₆H₃BrNH₂)₂] (10), [Mo₂O₂(μ₂-O)Cl₄(*o*-HNC₆H₂Cl₂NH₂)₂]

(23), $[\text{Mo}_2\text{O}_2(\mu_2\text{-O})\text{Cl}_4(m\text{-NC}_6\text{H}_4\text{NH}_2)_2]$ (12), $[\text{Mo}_2\text{O}_2(\mu_2\text{-O})\text{Cl}_4(m\text{-HNC}_6\text{H}_3(\text{CH}_3)\text{NH}_2)_2]$ (13), $[\text{Mo}_2\text{O}_2(\mu_2\text{-O})\text{Cl}_4(m\text{-HNC}_6\text{H}_3\text{FNH}_2)_2]$ (24), $[\text{Mo}_2\text{O}_2(\mu_2\text{-O})\text{Cl}_4(m\text{-HNC}_6\text{H}_3\text{CINH}_2)_2]$ (15), $[\text{Mo}_2\text{O}_2(\mu_2\text{-O})\text{Cl}_4(m\text{-HNC}_6\text{H}(\text{CH}_3)_3\text{NH}_2)_2]$ (16), $[\text{Mo}_2\text{O}_2(\mu_2\text{-O})\text{Cl}_4(I,5\text{-HNC}_{10}\text{H}_6\text{NH}_2)_2]$ (17), $[\text{Mo}_2\text{O}_2(\mu_2\text{-O})\text{Cl}_4(I,8\text{-HNC}_{10}\text{H}_6\text{NH}_2)_2]$ (18) and $[\text{Mo}_2\text{O}_2(\mu_2\text{-O})\text{Cl}_4(2,3\text{-HNC}_{10}\text{H}_6\text{NH}_2)_2]$ (19) respectively.

In literature, the complexes of Mo(V) compounds containing the Mo_2O_3 unit were previously prepared via reduction of the corresponding dioxomolybdenum(VI) compounds with P oxo-acceptors followed by comproportionation reaction and reported to possess a Mo–O–Mo bridge and two terminal oxygen atoms in either cis or trans configuration with respect to the Mo centers (Kamenar, et al. 1982, Perera, et al. 1995). This is a well known fact that, in absence of serious steric restrictions, oxomolybdenum(IV) and dioxomolybdenum(VI) species have a strong tendency to associate leading to stable comproportionation products of oxomolybdenum(V), which are considerably more resistant to reduction. $[\text{Mo}_2\text{O}_3\text{Cl}_4(\text{L})_4]$ (L = pyridine, bipyridine, 1,10-phenroline and diphenylphosphinomethane) type compounds were also reported in the literature. These species were obtained by the reaction of the binuclear species $[\text{Mo}_2\text{O}_3\text{Cl}_4(\text{DMF})_4]$ with four mole of the related ligand (Aguado, et al. 2007).

All the new compounds are air and moisture stable, whereas the starting materials $[\text{MoO}_2\text{Cl}_2(\text{THF})_2]$ and $[\text{Mo}_2\text{O}_3\text{Cl}_4(\text{DMF})_4]$, could only be handled and stored under an inert gas atmosphere. The new compounds 1-24 were obtained in high yields by crystallization method. The compounds 1-24 are hardly soluble in common organic solvents apart from DMSO and DMF. They are all stable under air and they can be stored for months, at room temperature and in a dry atmosphere, without noticeable decomposition. The new compounds were treated with either one, two or excess equivalents of the related phenylenediamine derivative which they were originally obtained at both room and elevated temperatures. The fact that no reactions were observed in any of these cases further supports the stability of the new compounds 1-24. The elemental analyses results, yields, and colors of complexes 1-24 are given in Table 5.1. The elemental analyses of the new compounds are in good agreement with the suggested formulations.

Table 5.1. The colors, yields and elemental analyses results of compounds 1-24.

Compound No	Color (decomp. at)	Yield (%)		Found (Calcd) (%)		
		1*	2**	C	H	N
1	Light green	80	65	23.76(24.18)	3.40(2.37)	8.90(9.40)
2	Green	78		20.22(19.28)	2.12(1.08)	8.51(7.49)
3	Light orange	77	70	33.03(33.92)	5.26(4.27)	8.23(7.91)
4	Green	75	61	21.75(21.01)	3.04(1.76)	12.32(12.25)
5	Yellow-orange	76	64	23.79(24.18)	3.85(2.37)	10.02(9.40)
6	Dark red	84	64	27.68(26.95)	3.38(2.91)	8.69(8.98)
7	Pink	84		21.36(20.71)	1.62(0.87)	11.79(12.08)
8	Green	79	53	23.21(22.81)	3.40(1.91)	8.11(8.87)
9	Burgundy	76		21.18(21.36)	2.89(1.90)	7.86(8.30)
10	Burgundy-brown	78	53	19.47(19.12)	2.96(1.60)	7.87(7.43)
11	Dark burgundy	73		20.95(19.22)	2.21(1.34)	7.34(7.47)
12	Grey-green	83	73	24.97(24.27)	3.38(2.04)	9.35(9.43)
13	Green	85	58	27.83(27.03)	3.93(2.59)	9.35(9.02)
14	Grey-green	72		22.63(22.24)	3.45(1.87)	7.42(8.65)
15	Grey-black	74	54	22.34(21.74)	3.06(1.52)	8.94(8.45)
16	Light orange	87	73	31.48(30.75)	4.11(3.34)	7.68(8.44)
17	Dark grey	81	75	35.27(34.51)	3.44(2.61)	7.63(8.05)
18	Green	83	67	35.09(34.51)	3.70(2.61)	7.68(8.05)
19	Grey-lavender	78	62	35.14(31.51)	3.53(2.61)	7.57(8.05)
20	Brown-green		72	20.11(19.64)	3.10(1.37)	7.08(7.64)
21	Light green		75	20.97(21.01)	2.45(1.76)	12.68(12.25)
22	Light lavender		61	20.98(21.68)	3.12(1.82)	8.96(8.43)
23	Grey-green		67	20.49(19.70)	3.02(1.10)	8.45(7.66)
24	Grey		55	23.79(22.88)	2.99(1.60)	9.65(8.89)

* The yields consist of the new compounds obtained from the first part reactions.

** The yields consist of the new compounds obtained from the second part reactions.

5.2. Spectroscopic Studies

IR spectra data for the complexes 1-24 are given in Table 5.2. and their spectra are shown in Figures B.1.- B.24. The compounds 1-24 are characterized by two strong bands in the region $939-1183\text{ cm}^{-1}$ that has been assigned to $\nu(\text{Mo}=\text{O})$. It is well known that in IR spectra, the symmetric and asymmetric stretching vibrations are observed near 900 cm^{-1} attributed to a *cis*- MoO_2^{+2} core (Doonan, et al. 2005). The symmetric and asymmetric IR stretching vibrations for both mononuclear and dinuclear dioxo molybdenum complexes 1-24 were found in the expected range and were assignable to Mo=O moiety.

One of the most important vibrations observed in the region between $684-822\text{ cm}^{-1}$ is suggested the presence of Mo-O-Mo bridging the structures. For compounds 1,3-6,8,10,12-13,15-24; the Mo-O-Mo bridging peaks observed which means that these

compounds have dinuclear feature. The lack of Mo-O-Mo bridging vibrations refer to the mononuclear compounds which were observed for compounds 2,7,9,11 and 14.

The range between 3021-3748 cm^{-1} were assigned as a NH group and the symmetric and asymmetric stretching modes of a NH_2 group for compounds 1-24. The lack of peaks due to the symmetric and antisymmetric modes of a NH_2 and a NH group suggest double deprotonation reaction results in the formation of a Mo=N linkage for compound 2. The peak observed at 1319 cm^{-1} in the IR spectra of compound 2 was ascribed to $\nu(\text{Mo}=\text{N})$ stretching vibration. In contrast to the metal-oxo stretching bands, identification of metal-imido stretching bands are problematic due to the metal-nitrogen vibrational mode being coupled with metal-ligand or N-R modes and commonly obscured by other vibrations. In general, identifying a $\nu(\text{Mo}=\text{N})$ or $\nu(\text{M}\equiv\text{N})$ vibration is difficult because of (i) the variability in the Mo-N bond order, and (ii) coupling of the Mo=N vibration to other vibrations in the molecule, in particular the adjacent N-C vibration of the imido group (Grupta, et al. 2007). A value of 1100-1300 cm^{-1} for the $\nu(\text{Mo}=\text{N})$ has been suggested by Dehnicke (Dehnicke, et al. 1981). McCleverty et al. (Lee, et al. 1998) reported values in the range 1200-1250 cm^{-1} for the compounds $[\text{MoTp}^*(\text{O})\text{Cl}(=\text{NR})]$ (R=4-tolyl, and $\text{C}_6\text{H}_4\text{NMe}_2$ -4). The dinuclear compounds of the type $[\text{MoTp}^*(\text{O})\text{Cl}](\mu\text{-O})[\text{MoTp}^*(\text{Cl})(\equiv\text{NC}_6\text{H}_4\text{Y})]$ (Y = *p*-F, *p*-Br, *m*-I, *m*-Cl, *p*-OMe, *p*-OEt, *p*-OPr, *p*-OBu, *p*-NO₂) also exhibited peaks at ca. 1200-1300 cm^{-1} , which were ascribed to $\nu(\text{Mo}=\text{N})$ (Topaloglu-Sozuer, et al. 2004, Topaloglu-Sozuer, et al. 2005, Topaloglu-Sozuer, et al. 2005, Topaloglu-Sozuer, et al. 2005). Similarly the mononuclear compounds $[\text{MoOCl}_2(=\text{NC}_6\text{H}_4\text{NH}_2)]$, $[\text{MoOCl}_2(=\text{NC}_6\text{H}_4\text{CN})]$, $[\text{MoOCl}_2(=\text{NC}_6\text{H}_4\text{CH}_3)]$ exhibited peaks in the range between 1206-1259 cm^{-1} attributed to $\nu(\text{Mo}=\text{N})$ (Kılıçkaya, et al. 2009).

Table 5.2. Characteristic FT-IR bands (cm^{-1}) for compounds 1-24.

Compound No	$\nu\text{N-H}$	νNH_2	$\nu\text{Mo=O}$	$\nu\text{Mo=N}$	$\nu\text{Mo-O-Mo}$	$\nu\text{Mo-N}$
1	3327	3411	963-1111		822	467-508
2		3316-3336	958-1081	1319		
3	3383		972-1106		739	470
4	3198	3362-3471	972-1098		729	475-534
5	3060	3350	970-1118		759	490-583
6	3412		967-1118		720	495-565
7	3331-3430		1104-1163			550
8	3361		974-1122		728	504
9	3352	3647-3671	1096-1183			554
10	3354		972-1121		730	499-548
11	3185	3346	965-1119			568
12	3419	3748	946-1112		774	518-596
13	3430		947-1106		725	496-563
14	3350		957-1048			559
15	3420		940-973		684	539-566
16	3021-3061	3409	972-1080		735	486-511
17	3028	3423	973-1066		787	514-532
18	3060	3414	947-1132		751	572
19	3399		968-1107		747	479-554
20	3326		966-1099		729	487-561
21	3230	3337-3429	939-1102		745	549-566
22	3353		971-1119		732	494-559
23	3418		965-1119		727	543-582
24	3216	3321-3416	959-1130		773	505-582

The $^1\text{H-NMR}$ spectra data for the complexes are given in Table 5.3 and their spectra are shown in Figures A.1-A.24. For compounds 1,3-24; the signals observed between 7.63-10.58 ppm revealed the presence of NH protons which result from deprotonation of NH_2 groups attached to the aromatic rings. However, no such signal was observed for the compound 2. Moreover, the two vibrations at *ca.* 3370 and 3450 cm^{-1} from the symmetric and asymmetric stretching modes of the NH_2 groups of the free ligands have completely disappeared in 2.

The $^1\text{H-NMR}$ spectra of compounds 1-6,8,10-24 revealed broad bands in the region between 3.29-3.98 ppm that could be attributed to the NH_2 protons. According to these observations, it can be said that only a single amine functionality reacted to produce an imido ligand, the second one remaining unreacted.

Table 5.3. $^1\text{H-NMR}$ spectroscopic data for compounds 1-24.

Compound No	$\delta_{\text{H}}^{\text{b}}$	Assignment
1	3.29 6.74 7.65	br, 4H, NH_2 s, 8H, C_6H_4 br, 2H, NH
2	3.60 7.14	s, 2H, NH_2 s, 2H, C_6H_2
3	3.35 2.09 7.93	br, 4H, NH_2 s, 24H, $(\text{CH}_3)_4$ s, 2H, NH
4	3.45 7.01 7.32 7.87 7.96	br, 4H, NH_2 d, 2H, C_6H_3 d, 2H, C_6H_3 s, 2H, C_6H_3 s, 2H, NH
5	3.44 6.82-6.98 7.93	br, 4H, NH_2 m, 8H, C_6H_4 s, 2H, NH
6	3.35 2.18 6.58 6.73 6.97 7.95	br, 4H, NH_2 s, 6H, CH_3 d, 2H, C_6H_3 s, 2H, C_6H_3 d, 2H, C_6H_3 s, 2H, NH
7	6.64-6.66 7.63	m, 3H, C_6H_3 s, 1H, NH
8	3.37 6.41-7.12 7.93	br, 4H, NH_2 m, 6H, C_6H_3 s, 2H, NH
9	6.67-7.01 7.77	m, 2H, C_6H_3 s, 2H, NH
10	3.46 6.82-7.04 7.93	br, 4H, NH_2 m, 6H, C_6H_3 s, 2H, NH
11	3.38 6.88 7.62 10.58	s, 2H, NH_2 s, 1H, C_6H_2 s, 1H, C_6H_2 br, 1H, NH

(cont. on next page)

Table 5.3. (cont.)

12	3.33 6.47-7.04 7.93	br, 4H, NH_2 m, 8H, C_6H_4 s, 2H, NH
13	3.30 2.04 6.36 6.50 6.92 8.41	s, 4H, NH_2 s, 6H, CH_3 d, 2H, C_6H_3 s, 2H, C_6H_3 d, 2H, C_6H_3 s, 2H, NH
14	3.57 6.47-7.02 8.53	br, 2H, NH_2 m, 3H, C_6H_3 s, 1H, NH
15	3.32 6.81-6.93 7.73	s, 4H, NH_2 m, 6H, C_6H_3 br, 2H, NH
16	3.31 2.10 6.72 7.93	s, 4H, NH_2 s, 18H, $(\text{CH}_3)_3$ s, 2H, C_6H s, 2H, NH
17	3.39 7.04-7.54 7.95	br, 4H, NH_2 m, 12H, C_{10}H_6 s, 2H, NH
18	3.53 7.06 7.29 7.44 7.94	br, 4H, NH_2 d, 4H, C_{10}H_6 t, 4H, C_{10}H_6 d, 4H, C_{10}H_6 s, 2H, NH
19	3.42 7.22-7.93 8.30	m, 4H, NH_2 m, 12H, C_{10}H_6 s, 2H, NH
20	3.37 6.78 8.01	br, 4H, NH_2 s, 4H, C_6H_2 s, 2H, NH
21	3.98 6.63-7.58 7.95	br, 4H, NH_2 m, 6H, C_6H_3 s, 2H, NH
22	3.47 6.67-7.03 7.93	br, 4H, NH_2 m, 6H, C_6H_3 s, 2H, NH
23	6.98 7.96	s, 4H, C_6H_2 s, 2H, NH
24	3.42 6.41-7.00 8.56	br, 4H, NH_2 m, 6H, C_6H_3 s, 2H, NH

¹³C-NMR spectra of the novel complexes showed changes the chemical shifts between the free and bonded ligands are shown in Table 5.4. This behavior can be explained by electron deficient of Mo center in the starting compound and coordination of N donor ligands. It demonstrated that phenylenediamine ligands influence the electron density at the metal center of these complexes. Carbons attached via N-Mo in the complexes displayed the shifted signals consistent with an increased electron density at the metal center.

Table 5.4. ¹³C-NMR data for compounds 1-24.

Compound No	δ_c^b
1	145.38, 121.08
2	138.91, 126.77, 121.16, 118.99
3	146.28, 128.67, 123.92, 122.02, 14.99
4	144.88, 130.71, 129.61, 123.29, 120.94, 117.61
5	162.81, 123.06, 120.72, 109.99
6	162.99, 139.48, 121.31, 118.96, 31.47
7	145.48, 137.27, 129.75, 118.84, 113.21, 112.32
8	162.81, 149.05, 144.25, 127.75, 115.34, 113.11
9	162.56, 141.29, 136.82, 122.45, 118.66, 117.14
10	162.81, 133.92, 123.71, 121.17, 113.54, 105.77
11	144.12, 133.23, 121.33, 118.68
12	141.00, 130.69, 128.87, 125.97, 113.22, 109.42
13	143.84, 133.68, 131.57, 122.02, 112.39, 109.56, 17.50
14	144.79, 138.82, 131.89, 126.58, 116.60
15	147.82, 145.41, 138.09, 118.30, 117.76, 114.17
16	146.28, 129.56, 128.87, 128.41, 123.92, 122.02, 15.29, 14.99, 13.59
17	144.27, 132.43, 126.62, 122.59, 119.04, 116.94
18	138.92, 136.69, 131.87, 126.60, 122.97, 116.65
19	162.79, 131.09, 130.03, 126.47, 124.58
20	162.99, 134.99, 119.80, 119.64, 117.55
21	162.99, 142.76, 140.53, 137.36, 122.73, 112.94
22	162.79, 138.81, 128.94, 123.12, 117.53, 114.47
23	162.99, 152.66, 147.32, 118.95
24	153.62, 147.96, 137.93, 116.15, 110.00, 108.89

(400 MHz, 293 K, DMSO)

5.3. Computational Calculations

The characteristic harmonic vibrational frequencies of the complexes (1-24) were calculated at the B3LYP/LACVP** level of theory. Initial geometries of all

structures suggested by the experimental findings were fully optimized to their equilibrium geometries. Harmonic vibrational frequency calculations result in no imaginary frequencies, indicating that all structures are minima in the potential energy surface. The calculated frequencies of the complexes (1-24) are given in Table 5.5. The FT-IR frequencies result from experimental study are generally in good agreement with the calculated ones.

Table 5.5. Characteristic harmonic vibrational frequencies (cm^{-1}) for compounds 1-24 from DFT calculations.

Compound No	$\nu\text{N-H}$	νNH_2	$\nu\text{Mo=O}$	$\nu\text{Mo=N}$	$\nu\text{Mo-O-Mo}$	$\nu\text{Mo-N}$
1	3439-3516	3608-3729	1019-1026		712	472
2		3569-3698	979-994	1315		
3	3535	3627-3745	1024-1026		760	523-529
4	3453-3521	3556-3721	1019-1028		707	514-518
5	3330-3446	3496-3657	1019-1036		767	485
6	3350-3509	3419-3678	1011-1030		768	460-467
7	3524-3528		980-999			466-485
8	3360-3462	3507-3637	1019-1038		790	561-563
9	3527-3532		978-997			487
10	3332-3450	3479-3638	1017-1037		768	505-530
11	3523	3574-3684	981-1001			447
12	3532-3536	3583-3591	1023-1032		756	558-563
13	3442-3517	3579-3687	1013-1027		705	530-531
14	3521	3602-3720	979-1003			500
15	3446-3519	3590-3705	1017-1027		697	546-554

(cont. on next page)

Table 5.5. (cont.)

16	3514- 3527	3588- 3691	1022- 1035		746	475- 478
17	3424- 3521	3603- 3721	1021- 1026		700	584- 589
18	3291- 3334	3494- 3601	1020- 1029		716	491- 502
19	3557- 3526	3434- 3586	1011- 1015		704	561- 601
20	3463- 3520	3613- 3745	1015- 1026		691	571- 577
21	3331- 3448	3494- 3638	1019- 1029		770	537- 566
22	3332- 3457	3475- 3637	1015- 1027		772	514- 529
23	3333- 3453	3496- 3636	1017- 1028		782	514- 588
24	3471- 3517	3589- 3704	1013- 1025		702	543- 552

Existing of the bending vibration of the Mo-O-Mo bridge points out that the structure is dinuclear. So, this property is important for separating dinuclear structures from mononuclear ones. For compounds 2-24 expect for 1, the agreement in experimental and theoretical data for the bending vibration of the Mo-O-Mo bridge is almost perfect. Although the calculated frequency value for compound 1 is significantly lower than the one obtained from FT-IR spectroscopy, it still characterizes that this frequency belong to the bending vibration of the Mo-O-Mo bridge. In addition, despite all of the stretching vibrations of Mo=O bonds are slightly overestimated by DFT calculations as expected, they have rather good accordance with experimental data.

Some selected geometrical parameters calculated at the B3LYP/LACVP** level of theory are summarized in Tables 5.6 and 5.7.

Table 5.6. Some selected parameters calculated with DFT for mononuclear compounds 2,7,9,11 and 14.

Compounds	Parameter				
	Mo-N	Mo-Cl	Mo-O	O-Mo-O	Cl-Mo-Cl
2	2.10	2.41	1.71	111.19	147.56
7	2.41	2.40	1.71	107.01	151.60
9	2.41	2.41	1.71	107.07	152.48
11	2.37	2.35	1.71	105.30	132.40
14	2.33	2.36	1.71	105.96	137.50

Table 5.7. Some selected parameters calculated with DFT for dinuclear compounds 1,3-6,8,10,12-13,15-24.

Compounds	Parameter		
	Mo-N	Mo=O	Mo-O-Mo
1	1.99	1.68	138.23
3	1.82	1.66	104.39
4	1.99	1.68	109.39
5	1.97	1.68	155.27
6	2.00	1.69	153.66
8	1.96	1.68	165.91
10	1.96	1.68	155.87
12	2.01	1.67	162.90
13	1.98	1.68	138.61
15	1.98	1.68	138.11
16	1.98	1.68	153.53
17	1.99	1.68	141.29
18	1.99	1.68	143.95
19	1.99	1.68	143.13
20	1.99	1.68	134.45
21	1.96	1.68	156.96
22	1.96	1.68	159.75
23	1.96	1.68	158.12
24	1.98	1.68	137.52

CHAPTER 6

CONCLUSIONS

In the first part of this study, the reactions of the solvent-sustituted complex $[\text{MoO}_2\text{Cl}_2(\text{THF})_2]$ with various phenylenediamine and some naphthalenediamine ligands bearing different functional groups at para, meta and ortho positions of the phenyl rings leads to mononuclear and dinuclear compounds of the type $[\text{MoO}_2\text{Cl}_2\text{L}]$ and $[\text{Mo}_2\text{O}_3(\mu_2\text{-O})\text{Cl}_4(\text{L})_2]$, respectively. In the second part, the reactions of $[\text{Mo}_2\text{O}_3\text{Cl}_4(\text{DMF})_4]$, prepared from the reaction of $[\text{MoO}_2\text{Cl}_2(\text{DMF})_2]$ with PPh_3 in DMF solvent, with phenylenediamine and naphthalenediamine derivatives were studied under similar conditions and Mo-O-Mo bridged dinuclear oxomolybdenum compounds of the type $[\text{Mo}_2\text{O}_3(\mu_2\text{-O})\text{Cl}_4(\text{L})_2]$ were obtained.

The products are less soluble in organic solvents than the starting material and easily precipitated from the reaction mixture in a short while after their formation. All the new compounds are air and moisture stable, whereas the starting material $[\text{MoO}_2\text{Cl}_2(\text{THF})_2]$, could only be handled and stored under an inert gas atmosphere.

It was shown that harmonic vibrational frequency values of complexes were in good agreement with the experimental results as expected. The computational calculations, agreement in experiment and theory point out that DFT method at B3LYP/LACVP** level of theory is suitable method for geometry optimization and energy calculations of molybdenum complexes.

REFERENCES

- Aguado, R., Escribano, J., Pedrosa, M.R., De Cian, A., Sanz, R., Arna'iz, F.J. 2007. *Polyhedron*. 26: 3842–3848.
- Astashkin, A. V., Mader, M. L., Pacheco, A., Enemark, J. H., Raitsimring, A. M. 2000. Direct Detection of the proton-containing group coordinated to Mo(V) in the high pH form of chicken liver sulfite oxidase by refocused primary Esem spectroscopy: structural and mechanistic implications. *J. Am. Chem. Soc.* 122: 529–5302.
- Bäckvall, J.-E. 2004. *Modern Oxidation Methods*. Wiley-VCH Ed.
- Barton, C.J., 1963. "In Techniques of Chemistry". 3: H.B. Jonassen and A. Weissberger, eds., *Wiley-Interscience*, New York.
- Beck, J., Hiller, W., Schweda, E., Strahle, J., *Naturforsch. Z.* 1984. *B: Chem. Sci.* 39: 1110.
- Becke, A.D. 1993. *J. Chem. Phys.* 98: 5648
- Berg, J. M., Holm, R. H. 1985. Model for the active site of oxo-transfer molybdoenzymes: synthesis, structure, and properties. *J. Am. Chem. Soc.* 107: 917-925.
- Boyd, D.B., Lipkowitz, K.B. 2000. *Reviews in Computational Chemistry, History of the Gordon Conferences on Computational Chemistry*. Wiley-VCH, New York, p399–439.
- Bray, R. C., Adams, B., Smith, A.T., Bennett, B., Bailey, S. 2000. Reversible dissociation of thiolate ligands from molybdenum in an enzyme of the dimethyl sulfoxide reductase family. *Biochemistry*. 39: 11258-11269.
- Bregeault, J.-M. 2003. *Dalton Trans.* 3289–3302
- Brito, J.A., Gomez, M., Muller, G., Teruel, H., Clinet, J.-C., Dunach, E. and Maestro, M.A. 2004. *Eur. J. Inorg. Chem.* 4278–4285.
- Chaudhury, P. K., Das S. K., Sarkar, S. 1996. Inhibition patterns of a model complex mimicking the reductive half-reaction of sulphite oxides. *Biochem. J.* 319: 953-959.
- Pereira, C.C.L., Balula, S.S., Almeida Paz, F.A., Valente, A.A., Pillinger, M., Klinowski, J., Goncalves, I.S. 2007. *Inorg. Chem.* 46 (21): 8508-8510.
- Cotton, F.A., Daniels, L.M., Herrero, S. 1999. *Acta Crystallogr., Sec. C: Cryst. Struct. Commun.* 55: IUC9900018.

- Craig, J.A., Harlan, E.W., Snyder, B.S., Whitener, M.A., Holm, R.H. 1985. *Inorg. Chem.* 28: 2082
- Das, S. K., Chaudhury, P. K., Biswas, D., Sarkar, S. 1994. Modeling for the active site of sulfite oxidase, *J. Am. Chem. Soc.* 116: 9061-9070.
- Dehnicke K., Strahle J. 1981. *Angew. Chem., Int. Ed. Engl.* 20, 413
- Didarul A. Chowdhury, Mohammad N. Uddin and Abul K.M. L. Rahman Chiang Mai. 2006. Synthesis and Characterization of Dioxo-molybdenum (VI) Complexes of Some Dithiocarbamates. *Chiang Mai J. Sci.* 33(3) : 357 – 362
- Dinda R., Sengupta, P., Mayer-Figge, H. and Sheldrick, W.S. 2002. *J. Chem. Soc. Dalton Trans.* : 4434–4439.
- Doonan, C. J., Millar, A. J., Nielsen, D. J., Young, C. G. *Inorg. Chem.* 2005, 44: 4506-4514.
- Dowerah, D.; Spence, J. T., Singh, R., Wedd, A. G., Wilson, G. L., Farchione, F., Enemark, J.H., Kristofzski, J., Bruck, M. 1987. Molybdenum(VI) and molybdenum(V) complexes with N,N'-dimethyl-N,N'-bis(2-mercaptophenyl)ethylenediamine, *J. Am. Chem. Soc.* 109: 5655- 5665.
- El-Essawi, M.M., Weller, F., Stahl, K., Kersting, M., Dehnicke, Q., *Anorg. Z.* 1986. *Allg.Chem.* 542: 175.
- Ellis, P. J., Conrads, T., Hille, R., Kuhn, P. 2001. Crystal structure of the 100 kDa arsenite oxidase from *alcaligenes faecalis* in two crystal forms at 1.64 Å and 2.03 Å, structure 9:125-132.
- Enemark, J.H., Young, C.G. 1994 *Adv. Inorg. Chem.* 40: 2.
- Enemark, J. H., Cooney, J. A, Wang, J-J., Holm, R.H. 2004. Synthetic analogues and reaction systems relevant to the molybdenum and tungsten oxotransferases, *Chem. Rev.* 104: 1175-1200.
- Enemark, J.H., Cooney, J.J.A., Wang, J.-J. and Holm, R.H. 2004. *Chem. Rev.* 104: 1175–1200.
- Gago, S., Neves, P., Monteiro, B., Pessêgo, M., Lopes, A.D., Valente, A.A., Almeida Paz, F.A., Pillinger, M., Moreira, J., Silva, C.M., Gonçalves*, I.S. 2009. *Eur. J. Inorg. Chem.* 4528–4537.
- Garner, C.D., Charnock, C.M. in: G. Wilkinson, R.D. Gilliard and J.A. McCleverty. 1987. "Comprehensive Coordination Chemistry". Pergamon Pres .Oxford. 1323.
- Garton, S. D., Temple, C. A., Dhawan, I. K., Barber, M. J., Rajagopalan, K. V., Johnson, M.K. 2000. resonance raman characterization of biotin sulfoxide reductase. comparing oxomolybdenum enzymes in the Me₂SO reductase family, *J. Biol. Chem.* 275: 6798 – 6805.

- Ge Wang, Gang Chen, Rudy L. Luck, Zhiqiang Wang', Zhongcheng Mu, David G. Evans and Xue Duan. 2004. New molybdenum(VI) catalysts for the epoxidation of cyclohexene: synthesis, reactivity and crystal structures. *Inorganica Chimica Acta*. 357:3223-3229
- George, G. N., Garrett, R. M., Prince, R.C., Rajagopalan, K. V. 1996. The molybdenum site of sulfite oxidase. *J. Am. Chem. Soc.* 118: 8588-8592.
- George, G. N., Hilton, J., Rajagopalan, K.V. 1996. X-ray absorption spectroscopy of dimethyl sulfoxide reductase from *rhodobacter sphaeroides*. *J. Am. Chem. Soc.* 118:1113-1117.
- George, G. N., Hilton, J., Temple, C., Prince, R. C., Rajagopalan, K. V. 1999. Structure of the molybdenum site of dimethyl sulfoxide reductase. *J. Am. Chem. Soc.* 121: 1256-1266.
- George, G. N., Kipke, C. A., Prince, R. C., Suede, R. A., Enemark, J. H., Cramer, S. P. 1989. Structure of the active site of sulfite oxidase. x-ray absorption spectroscopy of the molybdenum (IV), molybdenum(V), and molybdenum(VI) oxidation states, *Biochemistry* 28: 5075- 5080.
- Gnecco, J.A., Borda, G. and Reyes, P. 2004. Catalytic epoxidation of cyclohexene using Molybdenum complexes. *Journal of the Chilean Chemical Society*. 49:179-184
- Gonçalves, I.S., Santos, M.A, Romão, C.C., Lopes, A.D., Rodríguez-Borges, J.E, Pillinger, M., Ferreira, P., Rocha, J. and Kühn, F.E. 2001. Chiral dioxomolybdenum(VI) complexes for enantioselective alkene epoxidation. *Journal of Organometallic Chemistry*. 626: 1-10
- Gupta, S., Barik, A. K., Pal, S., Hazra, A., Roy, S., Butcher, R. J., Kar, S. K. 2007. *Polyhedron*. 26: 133-141.
- Hall, P. Basu. 2006. *Chem. Eur. J.* 12: 7501.
- Harwood, L.M., Moody, C.J. "Experimental Organic Chemistry" University of Oxford.
- Hay, P.J., Wadt, W.R. 1985. *J. Chem. Phys.* 82: 270-284-299.
- Hille, R. 1996. Structure and function of mononuclear molybdenum enzymes, *J. Biol. Inorg. Chem.* 1: 397-404.
- Hille, R. 1996. The mononuclear molybdenum enzymes, *Chem. Rev.* 96: 2757-2816.
- Hille, R. 2002. Molybdenum and tungsten in biology. *Trends in Biochemical Science*. 27: 360-367.
- Holm, R. H. 1987. Metal-centered oxygen atom transfer reactions. *Chem. Rev.* 87: 1401- 1449.

- Holm, R. H. 1990. The biologically relevant oxygen atom transfer chemistry of molybdenum: from synthetic analogue systems to enzyme. *Coord. Chem. Rev.* 100 : 183-221.
- Holm, R. H. 1996. Structural and functional aspects of metal sites in biology. *Chem. Rev.* 96 : 2239-2314.
- Holm, R.H. 1990. *Coord. Chem. Rev.* 100 : 183–221.
- Holm, R.H., Kennepohl, P. and Solomon, E.I. 1996. *Chem. Rev.* 96: 2239–2314.
- Jensen, F. 2007. *Introduction to Computational Chemistry*, Denmark: Wiley.
- Jorgensen, K.A. 1989. *Chem. Rev.* 89 : 431–458.
- Jurisson, S. 1997. *Inorganic Synthesis.* 31: 246-247
- Kail, B.W, Pe´rez, L.M, Zarić, S.D., Millar, A.J., Young, C.G., Basu, M.B., Stolz, P., Smith, M. T. 2003. A coordination chemist’s view of the active sites of mononuclear molybdenum enzymes. *Current Science.* 84: 1412-1418.
- Kamenar, B., Penavic, M., Korpar-Colig, B., Markovic, B. 1982. *Inorg. Chim. Acta* 65: L245.
- Kılıçkaya, G., Doğan, B., Acar, N., Topaloğlu-Sözüer, I. 2009. *Turkish Journal of chemistry.* 33: 693-708.
- Kisker, C., Schindelin, H., Pacheco, A., Wehbi, W. A., Garrett, R. M., Rajagopalan, K. V., Enemark, J. H., Rees, D. C. 1997. Molecular basis of sulfite oxidase deficiency from the structure Of sulfite oxidase. *Cell.* 91: 973-983.
- Kisker, C., Schindelin, H., Rees, D. C. 1997. Molybdenum-cofactor-containing enzymes: structure and mechanism, *Annu. Rev. Biochem.* 66: 233-267.
- Krishnan, R., Binkley, J.S., Seeger, R., Pople, J.A. 1980. *J. Chem. Phys.* 72:650.
- Kühn, F.E, Lopes, A.D, Santos, A., Herdtweck, E., Haider, J.J., Romão C.C. and Santos, A.G. 2000. Lewis base adducts of bis-(halogeno)dioxomolybdenum(VI): syntheses, structures, and catalytic applications *Journal of Molecular Catalysis.* 151:147-160.
- Kühn, F.E., Herdtweck, E., Haider, J.J, Herrmann, W.A, Goncalves, I.S, Lopes, A.D. and Romão, C.C. 1993. *J. Organomet. Chem.* 583: 3.
- Kühn, F.E., Herdtweck, E., Haider, J.J, Herrmann, W.A., Gonçalves, I.S, Lopes, A.D. and Romão, C.C. 1999. Bis-acetonitrile(dibromo)dioxomolybdenum(VI) and derivatives: synthesis, reactivity, structures and catalytic applications. *Journal of Organometallic Chemistry* 583: 3-10

- Kühn, F.E., Santos, M.A, Gonçalves, I.S., Romao, C.C, Lopes, A.D. 2001. *Appl. Organomet Chem.* 43: 15.
- Kumar S.B., Chaudhury, M. 1991. *J. Chem. Soc. Dalton Trans.* 2169.
- Lang, H., Fanwick, P.E., Walton, R.A. 2002. *Inorg. Chim. Acta* 328: 232
- Laughlin, L. J., Young, C. G. 1996. Oxygen atom transfer, coupled electron-proton transfer, and correlated electron-nucleophile transfer reactions of oxomolybdenum(IV) and dioxomolybdenum(VI) complexes. *Inorg. Chem.* 35: 1050-1958.
- Lee, S. M., Kowallick, R., Marcaccio, M., McCleverty, J. A., Ward, M. D. *J. 1998. Chem. Soc., Dalton Trans.* 3443-3450.
- Leonard, J., Lygo, B., Procter, G. 1995. *Advanced Practical Organic Chemistry. published by Blackie Academic and Professional, an imprint of Chapman and Hall.*
- Li, H.-K., Temple, C., Rajagopalan, K.V., Schindelin, H. 2000; The 1.3 Å crystal structure of rhodobacter sphaeroides dimethyl sulfoxide reductase reveals two distinct molybdenum coordination environments *J. Am. Chem. Soc.* 122:7673-7680.
- Lim, B. S., Holm, R. H. 2001. Bis(dithiolene)molybdenum analogues relevant to the DMSO reductase enzyme family: synthesis, structures, and oxygen atom transfer reactions and kinetics, *J. Am. Chem. Soc.* 123: 1920-1930.
- Lorber, C., Plutino, M. R., Elding, L. I., Nordlander, E. 1997. Kinetics of oxygen-atom transfer reactions involving molybdenum dithiolene complexes. *J. Chem. Soc., Dalton Trans*, 3997-4003.
- Lorber, C.Y, Smidt S.P, and Osborn, J.A. 2000. *Eur. J. Inorg. Chem.* 655–658
- Luís F. Veiros, Ângela Prazeres, Paulo J. Costa, Carlos C. Romão, Fritz E. Kühn and Maria José Calhorda. 2006. *Dalton Trans.* Olefin epoxidation with tert-butyl hydroperoxide catalyzed by MoO₂X₂L complexes: a DFT mechanistic study. *Dalton Trans.* 1383–1389.
- Manwani, N., Ratnani, R., Prasad, R.N., Drake, J.E., Hurthouse, M.B., Light, M.E. 2003. *Inorg. Chim. Acta.* 351: 49.
- McAlpine, A. S., McEwan, A. G., Bailey, S. 1998. The high resolution crystal structure of DMSO reductase in complex with DMSO, *J. Mol. Biol.* 275: 613-623.
- McAlpine, A. S., McEwan, A. G., Shaw, A. L., Bailey, S. 1997. Molybdenum active centre of DMSO reductase from rhodobacter capsulatus, *J. Biol. Inorg. Chem.* 2: 690-701
- McCleverty, J.A., Denti, G. and Reynolds, S. 1983. *J. Chem. Soc., Dalton Trans.* 81-89.

- McLean, A.D., Chandler, G.S. 1980. *J. Chem. Phys.* 72: 5639.
- Meister, G.E. and Butler, A. 1994. *Inorg. Chem.* 33 : 3269–3275
- Meunier, B. 2000. *Metal-Oxo and Metal-Peroxo Species in Catalytic Oxidations*, Springer, Berlin
- Modéc, B. , Brencic, J.V., Koller, J. 2004. *Eur. J. Inorg. Chem.* 1611.
- Palanca P., Picher T., Sanz V., Go'mez P., Romero, Llopis E., Domenech A., Cervilla, A. 1990. *J. Chem. Soc. Chem. Comm.* 531.
- Perera, S.D., Shaw, B.L., Thornton-Pett, M. 1995. *Inorg. Chim. Acta* 234: 185.
- Rajagopalan, K. V. 1991. The pterin molybdenum cofactors. *Adv. Enzymol.* 64: 215–290.
- Ramachandran, K.I., Deepa, G., Namboori, K. 2008. *Computational Chemistry and Molecular Modelling*, Berlin: Springer.
- Rao, S.N., Munshi K.N. and Rao, N.N. 2000. *J. Mol. Cat. A: Chem.* 156 : 205–211.
Reactivity of -Benzoin Oxime with Molybdenum(VI). *Synthesis and Reactivity in Inorganic, Metal-Organic, and Nano-Metal Chemistry.* 30:2009 — 2028
- Reynolds, M.S., Babinski, K.J., Bouteneff, M.C., Brown, J.L., Campbell, R.E., Cowan, M.A., Durwin, M.R., Foss, T., O'Brien P. and Penn, H.R. 1997. *Inorg. Chim. Acta.* 263: 225–230
- Schultz, B. E., Gheller, S. F., Muetterties M. C., Scott, M. C., Holm, R. H. 1993. Molybdenum mediated oxygen-atom transfer: an improved analog reaction system of the molybdenum oxotransferases. *J. Am. Chem. Soc.* 115: 2714-2722.
- Schultz, B. E., Gheller, S. F., Muetterties, M. C., Scott, M. C., Holm, R. H. 1993. Molybdenum mediated oxygen-atom transfer: an improved analog reaction system of the molybdenum oxotransferases, *J. Am. Chem. Soc.* 115: 2714-2722.
- Schultz, B. E., Hille, R., Holm, R. H. 1995. Direct OAT in the mechanism of action of rhodobacter sphaeroides dimethyl sulfoxide reductase, *J. Am. Chem. Soc.* 117: 827-828.
- Sellmann, D., Hadawi, B., Knoch F., and Mool, M. 1995. Transition-Metal Complexes with Sulfur Ligands. 113. Syntheses, X-ray Crystal Structures, and Reactivity of Molybdenum(II) Complexes with Thioetherthiolate Ligands Having XS₄ Donor Atom Sets (X=S, O, NH). *Inorg. Chem.* 34: 5963
- Shriver, D.F. 1969. "The Manipulation of Air Sensitive Compounds" *McGraw-Hill, New York*
- Sigel, A., Sigel, H. 2002 Molybdenum and tungsten -their roles in biological processes, *Marcell Decker, New York*

- Sugimoto, H., Harihara, M., Shiro, M., Sugimoto, K., Tanaka, K., Miyake, H., Tsukube, H. 2005. Dioxo-molybdenum(VI) and mono-oxo-molybdenum(IV) complexes supported by new aliphatic dithiolene ligands: new models with weakened M-O bond characters for the arsenite oxidase active site. *Inorg. Chem.* 44: 6386-6392.
- Takekuma, S., Tomoda, K., Sasaki, M., Minematsu, T., Takekuma, H. 2004. *Bull. Chem. Soc. Jpn.* 77: 1935.
- Thapper, A., Deeth, R. J., Nordlander, E., 2002. A Density functional study of oxygen atom transfer reactions between biological oxygen atom donors and molybdenum(IV) bis(dithiolene) complexes. *Inorg. Chem.* 42: 6695-6702.
- Tong, Y.-L., Ma, J.-F., Law, W.-F., Yan, Y., Wong, W.-T., Zhang, Z.-Y., Mak, T. C. W., Ng, D. K. P. 1999. Synthesis, electrochemistry, and oxygen-atom transfer reactions of dioxotungsten(VI) and -molybdenum(VI) complexes with N₂O₂ and N₂S₂ tetradentate ligands, *Eur. J. Inorg. Chem.* 313-321.
- Tong, Y.-L., Yan, Y., Chan, E. S. H., Yang, Q., Mak, T. C. W., Ng, D. K. P. 1998. Cis-dioxo-tungsten(VI) and -molybdenum(VI) complexes with N₂O₂ tetradentate ligands: synthesis, structure, electrochemistry and oxo-transfer properties *J. Chem. Soc., Dalton Trans.* 3057-3064.
- Topaloglu-Sozuer, I., Gunyar, A., Jeffery, J. C., Hamidov, H. 2004. *Trans. Met. Chem.* 29: 780-785.
- Topaloglu-Sozuer, I., Irdem, S. D., Jeffery, J. C., Hamidov, H., Senturk, O.S. 2005. *Z. Naturforsch.* 60b: 15-21.
- Topaloglu-Sozuer, I., Irdem, S. D., Jeffery, J. C., Hamidov, H. 2005. *J. Coord. Chem.* 58: 175-187.
- Topaloglu-Sozuer, I., Gunyar, A., Dulger-Irdem, S., Baya, M., Poli, R. 2005. *Inorg. Chim. Acta.* 358: 3303-3310.
- Tucci, G. C., Donahue, J. P., Holm, R. H. 1998. Comparative kinetics of oxo transfer to substrate mediated by bis(dithiolene)dioxomolybdenum and -tungsten complexes. *Inorg. Chem.* 37: 1602-1608
- Tuczek, F., Horn, K.H., Lehnert, N. 2003. Vibrational spectroscopic properties of molybdenum and tungsten N₂ and N₂H_x complexes with depe coligands: comparison to dppe systems and influence of H-bridges. *Coordination Chemistry Reviews.* 245: 107-120
- Ueyama, N., Oku, H., Kondo, M., Okamura, T., Yoshinaga, N., Nakamura, A. 1996. Trans influence of oxo and dithiolene coordination in oxidized models of molybdenum oxido- reductase. *Inorg. Chem.* 35: 643-650.
- Vlc̃ek A.Jr. 2002. *Coord. Chem. Rev.* 230 : 225

- Waller, M.P., Braun, H., Hojdis, N. and Bühl, M. 2007. *J. Chem. Theory Comput.* 3: 2234-2242
- Warren J.H. 2003 “A Guide to Molecular Mechanics and Quantum Chemical Calculations” *Wavefunction Inc.*
- Webster, C.E, Hall, M.B. 2001. *J. Am. Chem. Soc.* 123: 5820
- Wilshire, J.P., Leon, L., Bosserman, P., Sawyer, D.T. 1979. *J. Am. Chem. Soc.* 101
- Xu, L., Wang, E., Hu, C., Huang, R. 2001. *Transition Met. Chem.* 26: 563.
- Young, C. G., Laughlin, L. J.; Colmane, S., Scrofani, S. D. B. 1996. Oxygen atom transfer, sulfur atom transfer, and correlated electron-nucleophile transfer reactions of oxo- and thiomolybdenum(IV) complexe. *Inorg. Chem.* 35: 5368-5377.
- Z'miric', A., Zanic', S.D. 2002, *Inorg. Chem. Commun.* 5: 446.
- Zanic, S., Hall, M.B. 1997. “Molecular Modeling and Dynamics of Bioinorganic Systems”. *Kluwer Academic Publishers.* 255.
- Zekri O., Boutamine, S., Hank, Z., Slaouti, H., Meklati M. and Vittori, O. 2000.
- Zhuang, B., Zuang, L., He, L., Yang, Y., Lu, J. 1988. *Inorg. Chim. Acta* 145: 225

APPENDIX A

^1H NMR AND ^{13}C NMR SPECTRA OF THE PRODUCTS

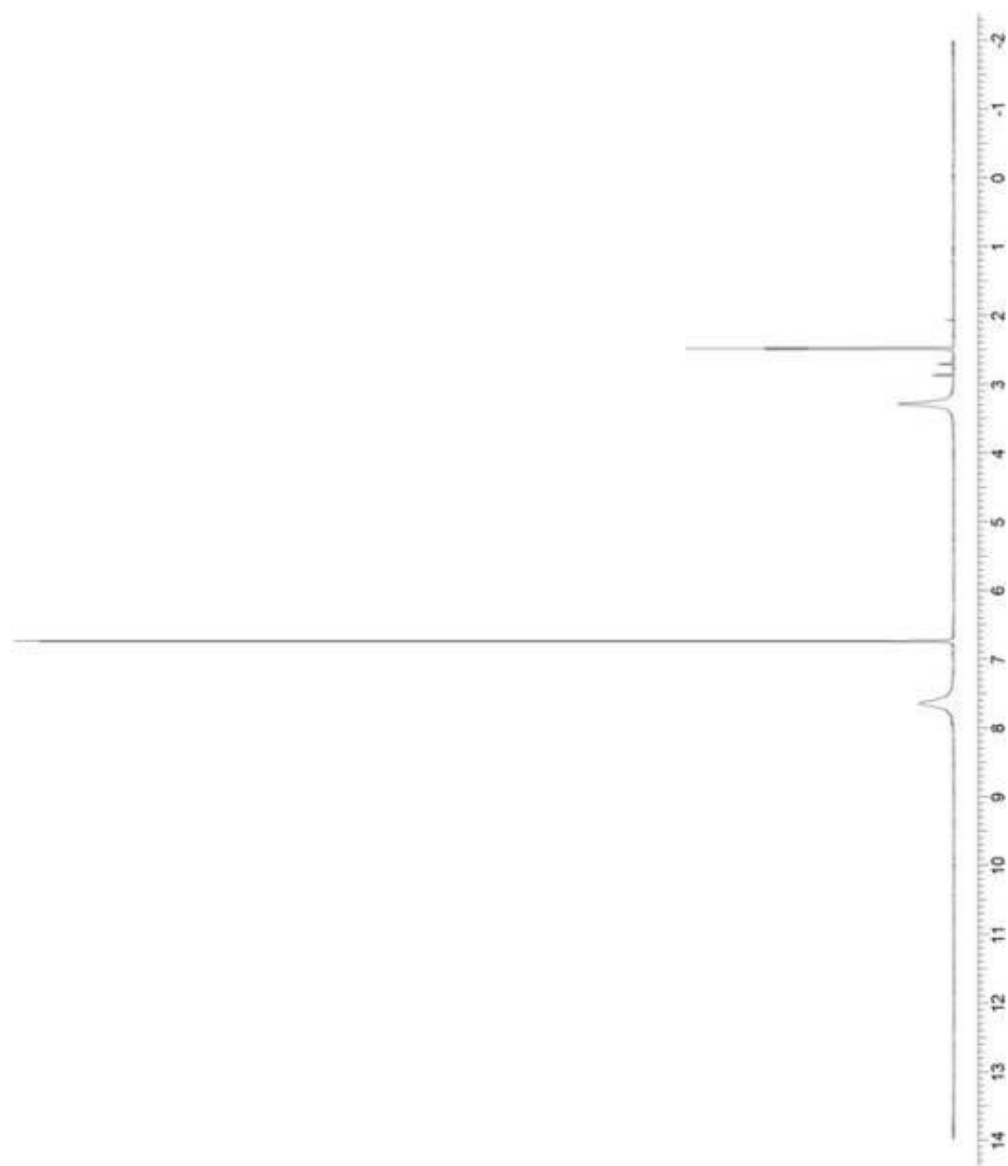


Figure A.1. ^1H -NMR spectrum of $[\text{Mo}_2\text{O}_2(\mu_2\text{-O})\text{Cl}_4(\text{NH}_2\text{C}_6\text{H}_4\text{NH})_2]$ (**1**)

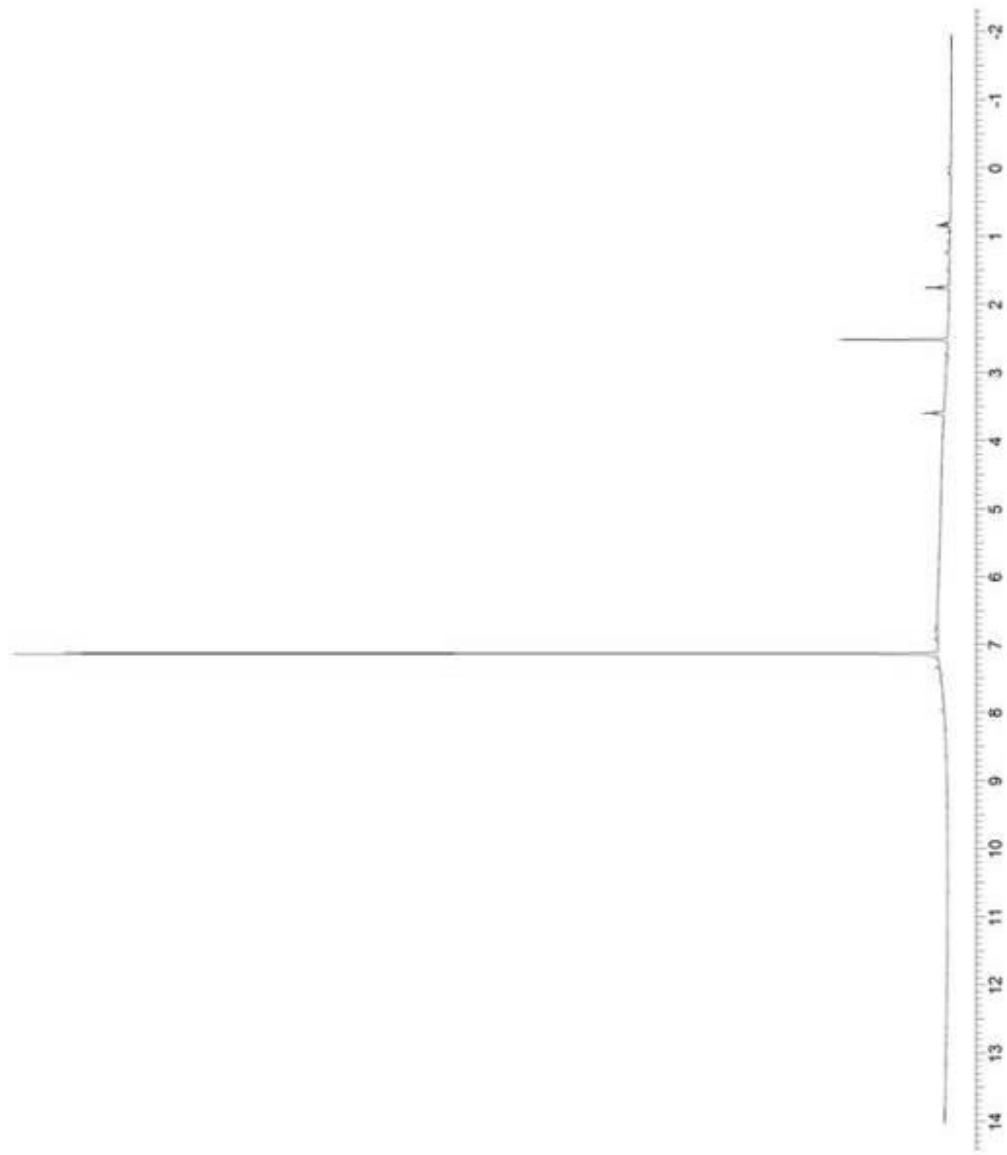


Figure A.2. ^1H NMR spectrum of $[\text{MoO}_2\text{Cl}_2(\text{NH}_2\text{C}_6\text{H}_4\text{Cl}_2\text{NH})]$ (**2**)



Figure A.3. $^1\text{H-NMR}$ spectrum of $[\text{Mo}_2\text{O}_2(\mu_2\text{-O})\text{Cl}_4(\text{NH}_2\text{C}_6(\text{CH}_3)_4\text{NH}_2)_2]$ (**3**)

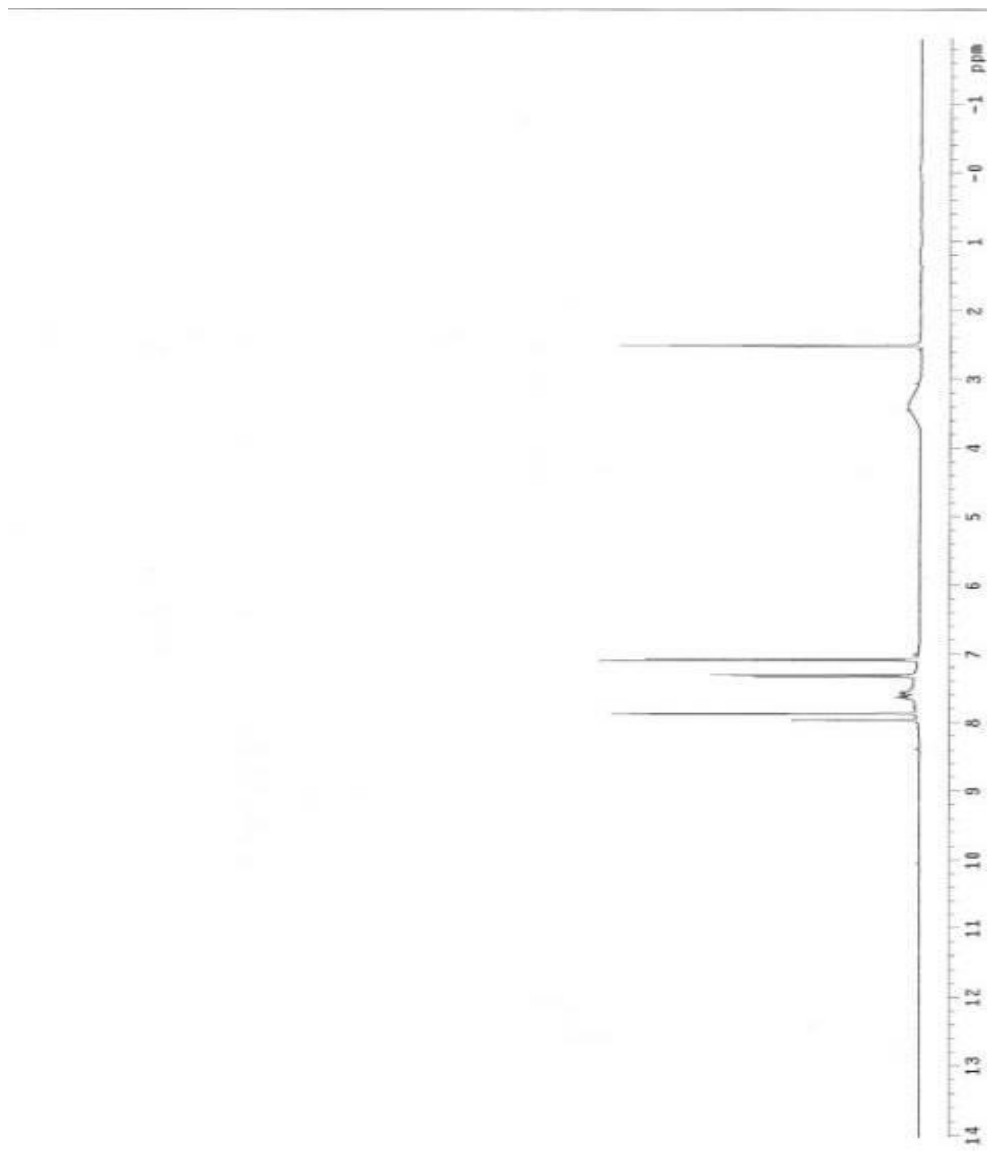


Figure A.4. ¹H-NMR spectrum of $[\text{Mo}_2\text{O}_2(\mu_2\text{-O})\text{Cl}_4(\text{NH}_2\text{C}_6\text{H}_3\text{NO}_2\text{NH})_2]$ (**4**)

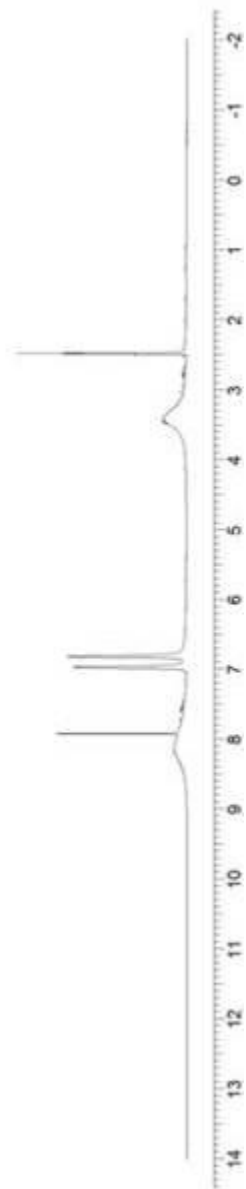


Figure A.5. $^1\text{H-NMR}$ spectrum of $[\text{Mo}_2\text{O}_2(\mu_2\text{-O})\text{Cl}_4(\text{NH}_2\text{C}_6\text{H}_4\text{NH}_2)_2]$ (**5**)

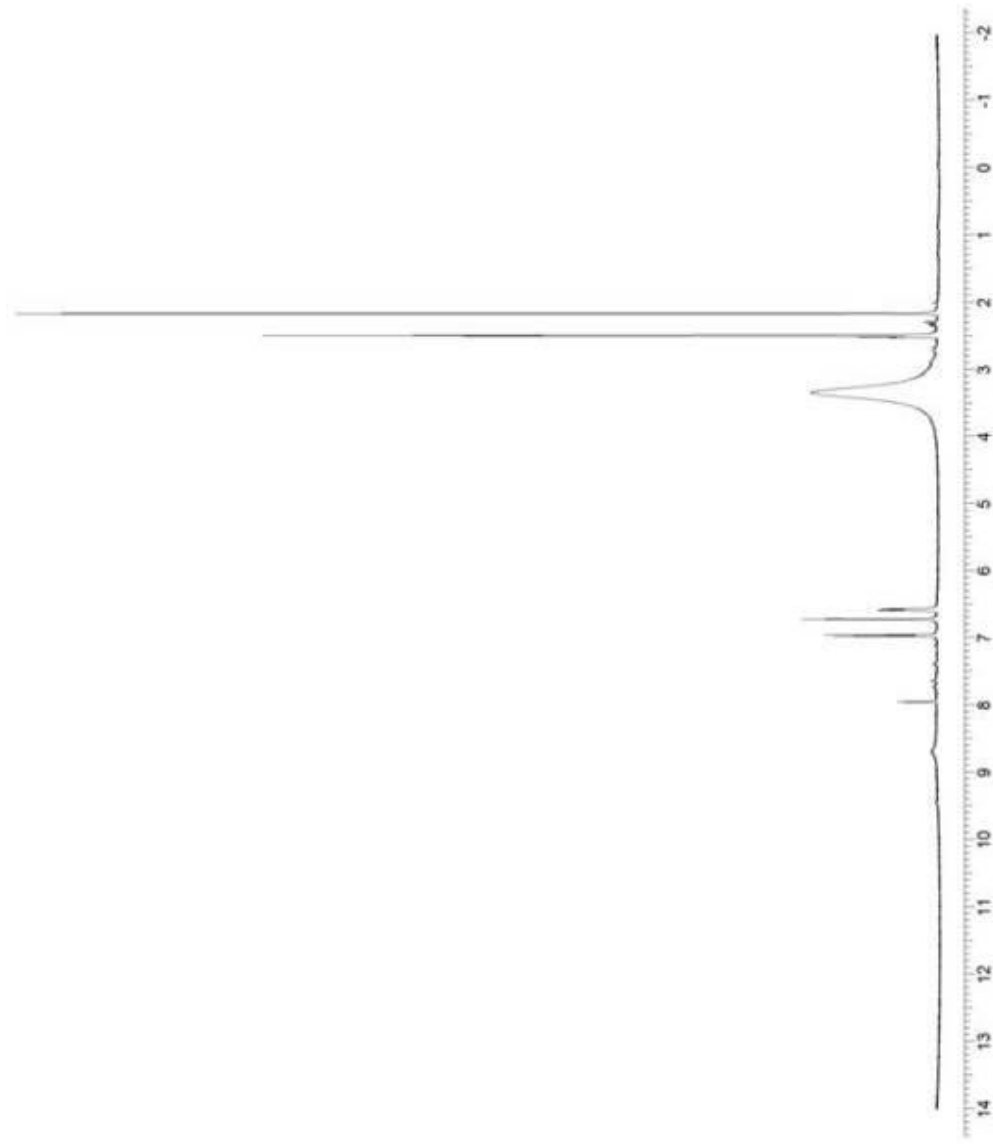


Figure A.6. ¹H-NMR spectrum of $\text{Mo}_2\text{O}_2(\mu_2\text{-O})\text{Cl}_4(\text{NH}_2\text{C}_6\text{H}_3(\text{CH}_3)\text{NH})_2$ (**6**)

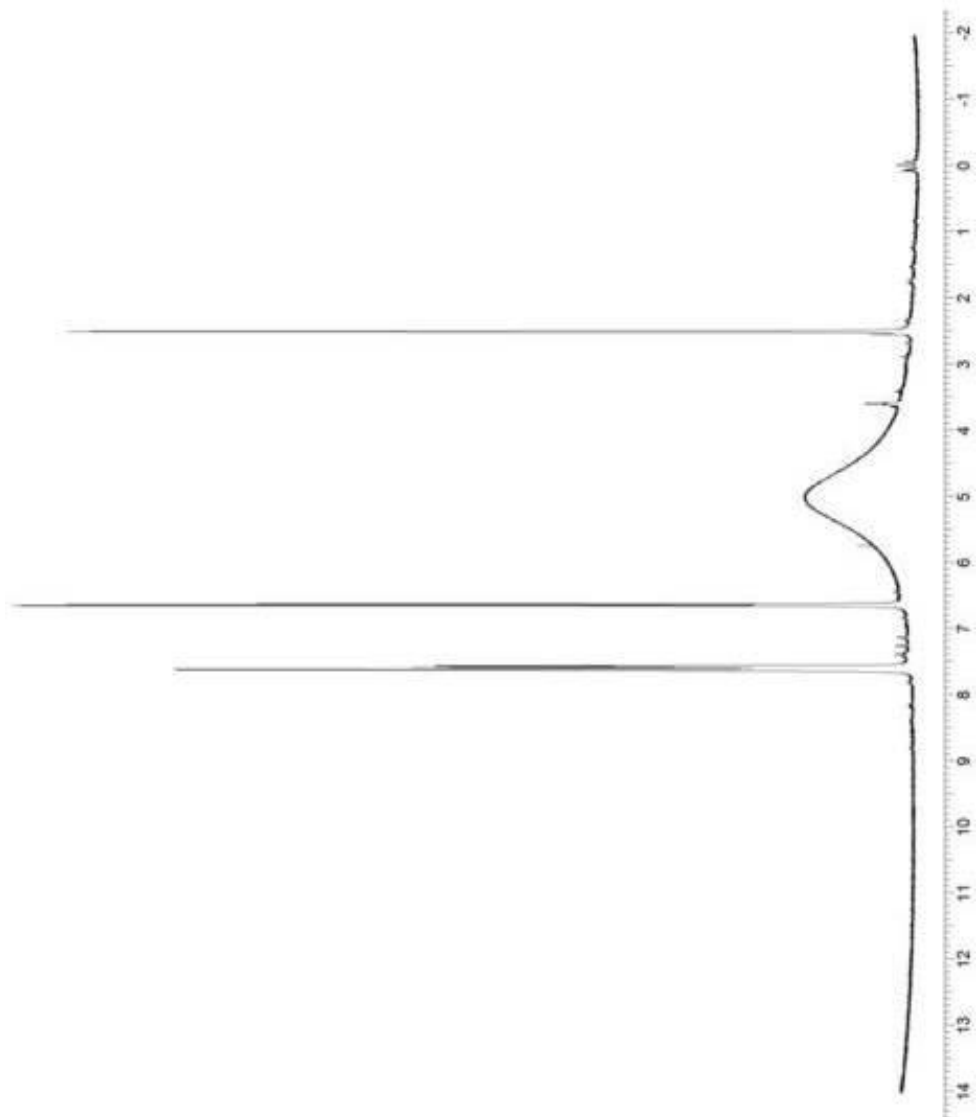


Figure A.7. ¹H-NMR spectrum of [MoO₂Cl₂(NHC₆H₃NO₂NH)] (7)



Figure A.8. $^1\text{H-NMR}$ spectrum of $[\text{Mo}_2\text{O}_2(\mu_2\text{-O})\text{Cl}_4(\text{NH}_2\text{C}_6\text{H}_3\text{FNH})_2]$ (**8**)

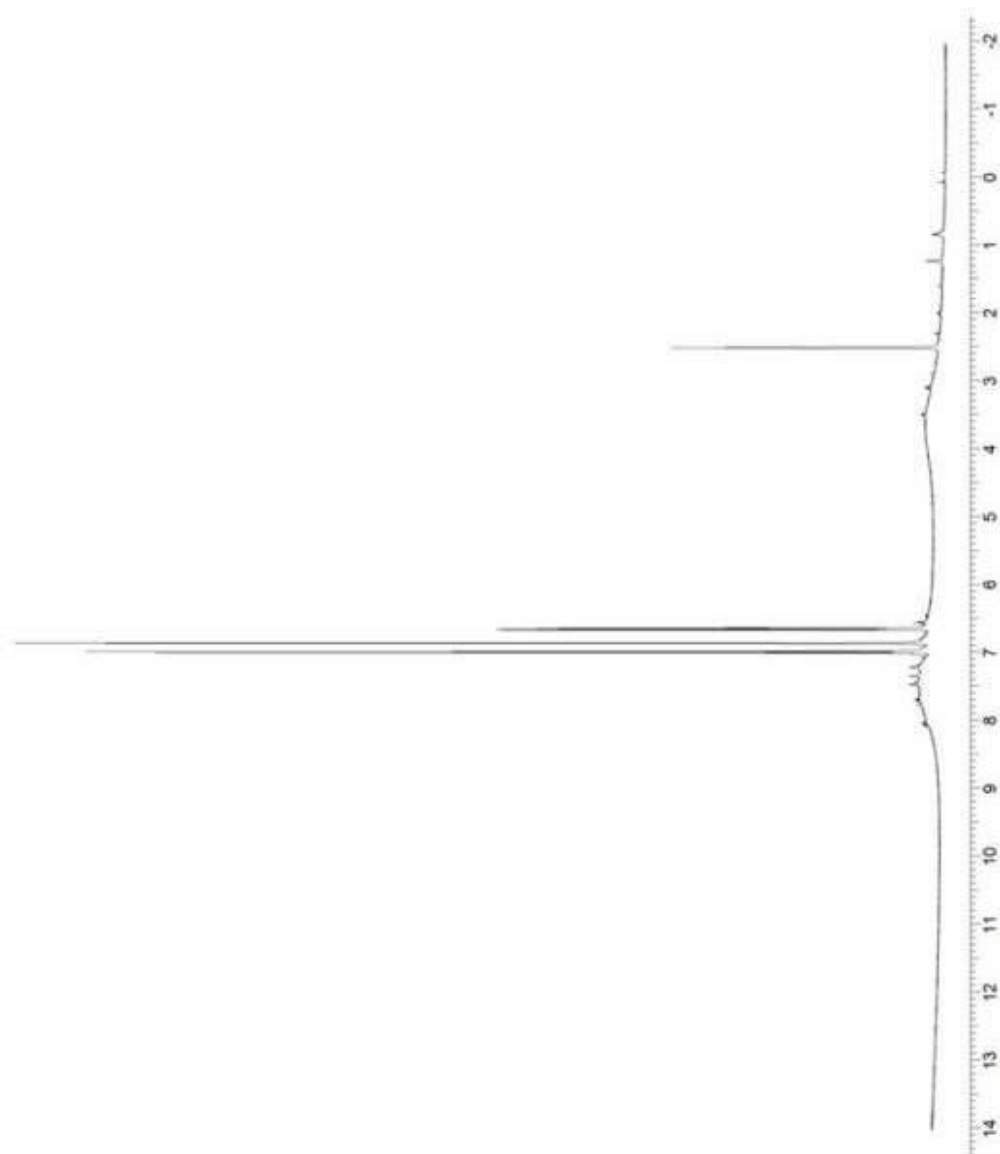


Figure A.9. ¹H-NMR spectrum of [MoO₂Cl₂(NHC₆H₃CINH)] (9)

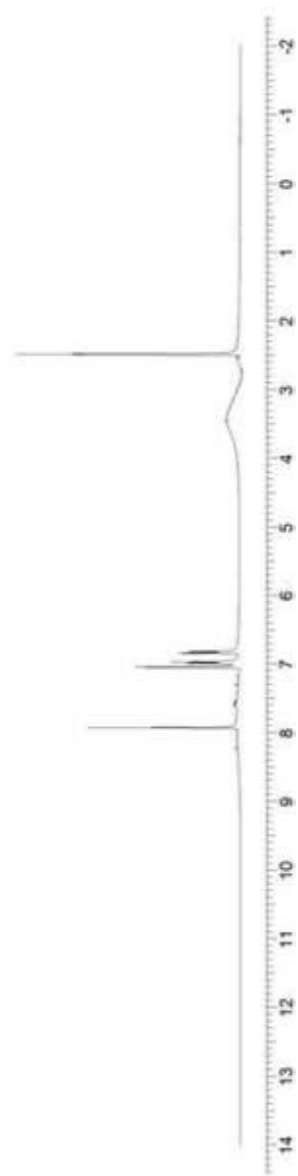


Figure A.10. $^1\text{H-NMR}$ spectrum of $[\text{Mo}_2\text{O}_2(\mu_2\text{-O})\text{Cl}_4(\text{NH}_2\text{C}_6\text{H}_3\text{BrNH}_2)_2]$ (**10**)

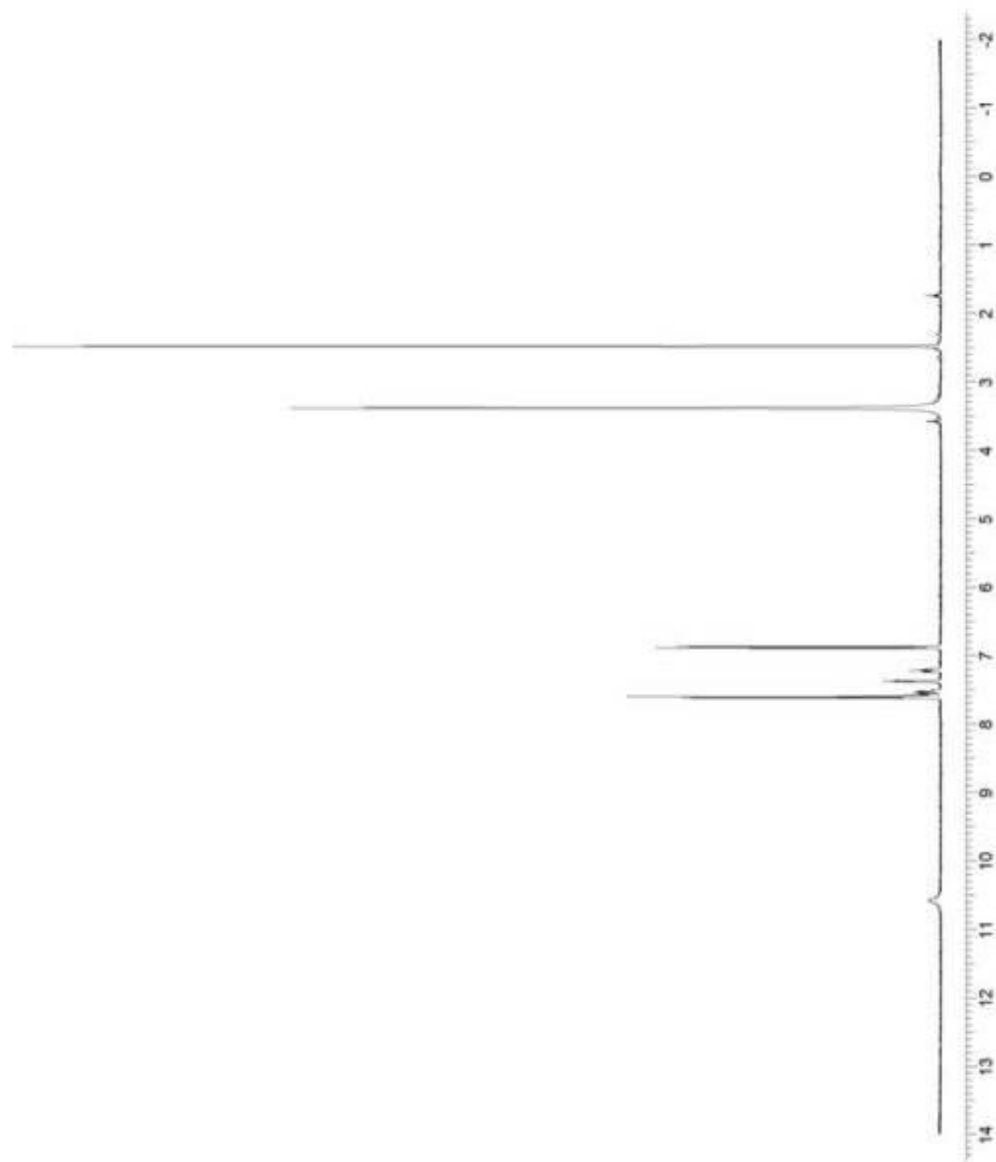


Figure A.11. ¹H-NMR spectrum of [MoO₂Cl₂(NH₂C₆H₂Cl₂N)] (**11**)

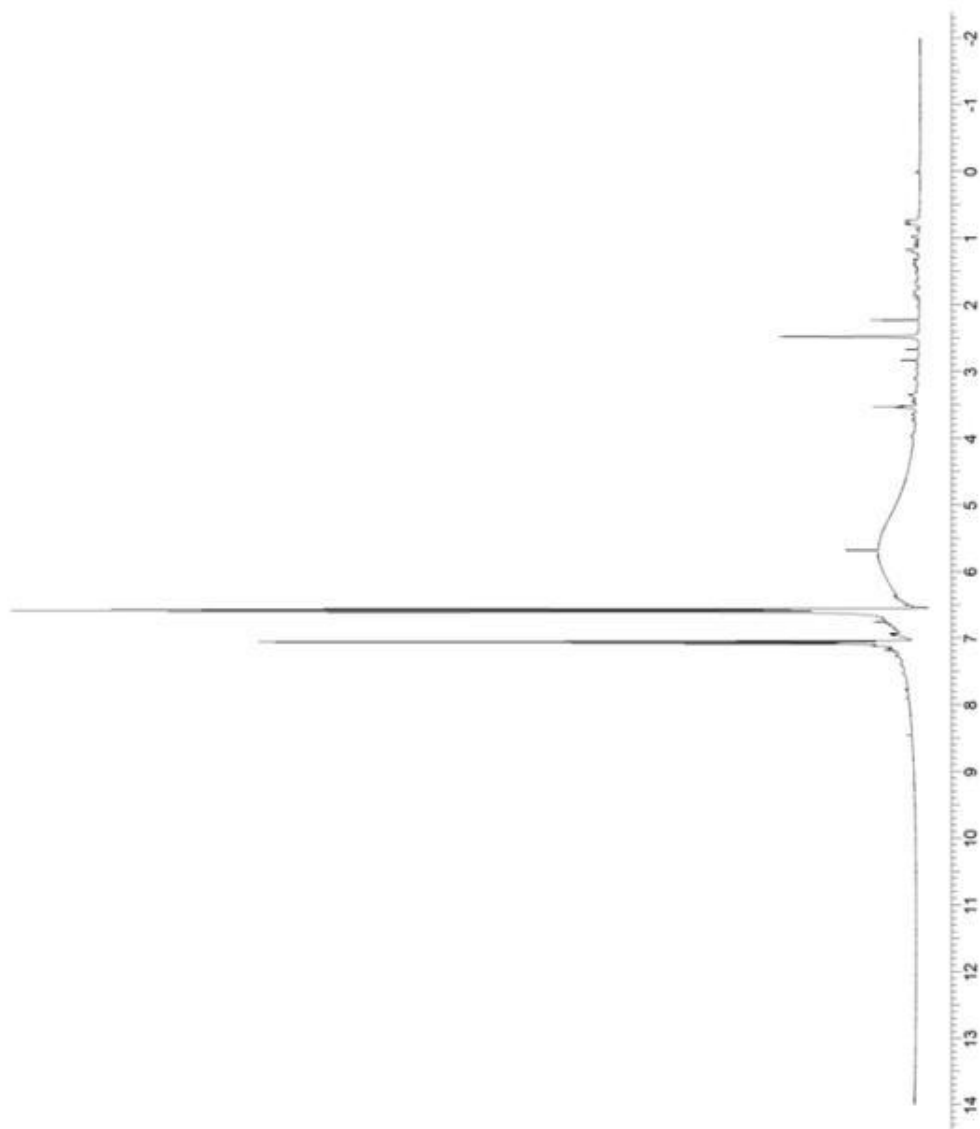


Figure A.12. $^1\text{H-NMR}$ spectrum of $[\text{Mo}_2\text{O}_2(\mu_2\text{-O})\text{Cl}_4(\text{NH}_2\text{C}_6\text{H}_4\text{N})_2]$ (**12**)

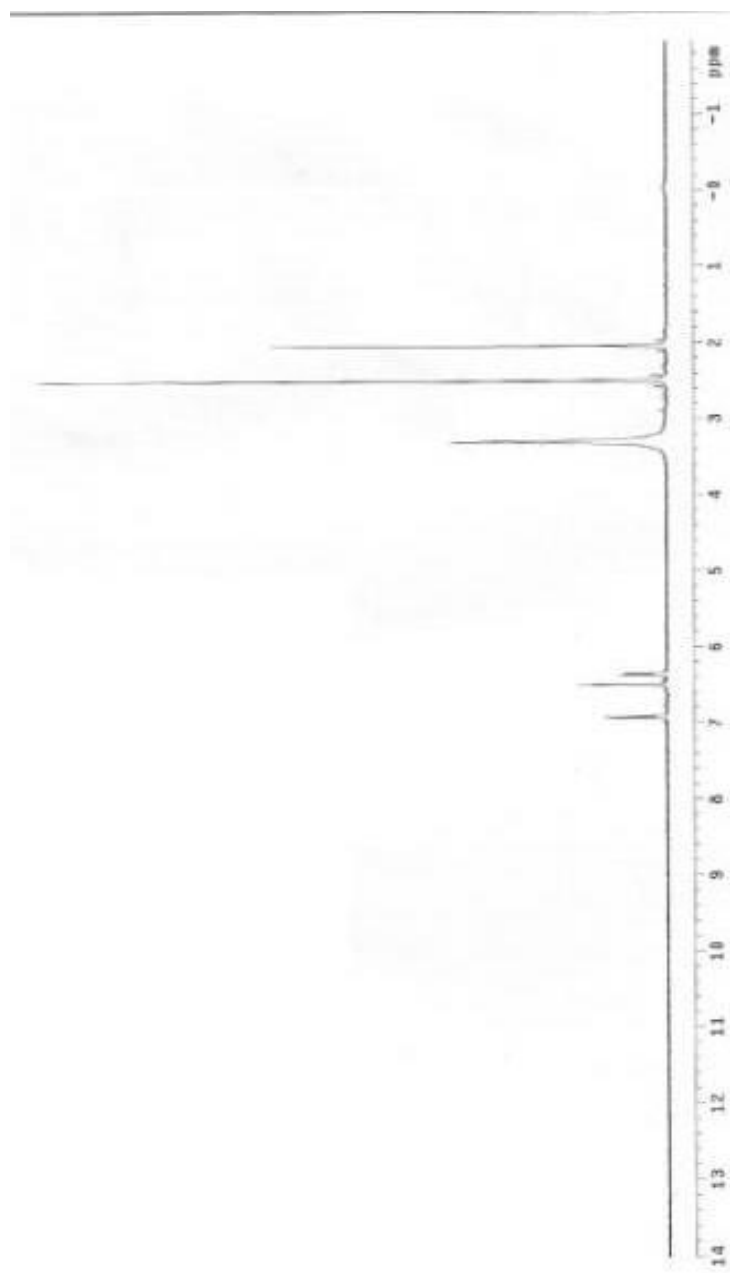


Figure A.13. $^1\text{H-NMR}$ spectrum of $[\text{Mo}_2\text{O}_2(\mu_2\text{-O})\text{Cl}_4(\text{NH}_2\text{C}_6\text{H}_3(\text{CH}_3)\text{N})_2]$

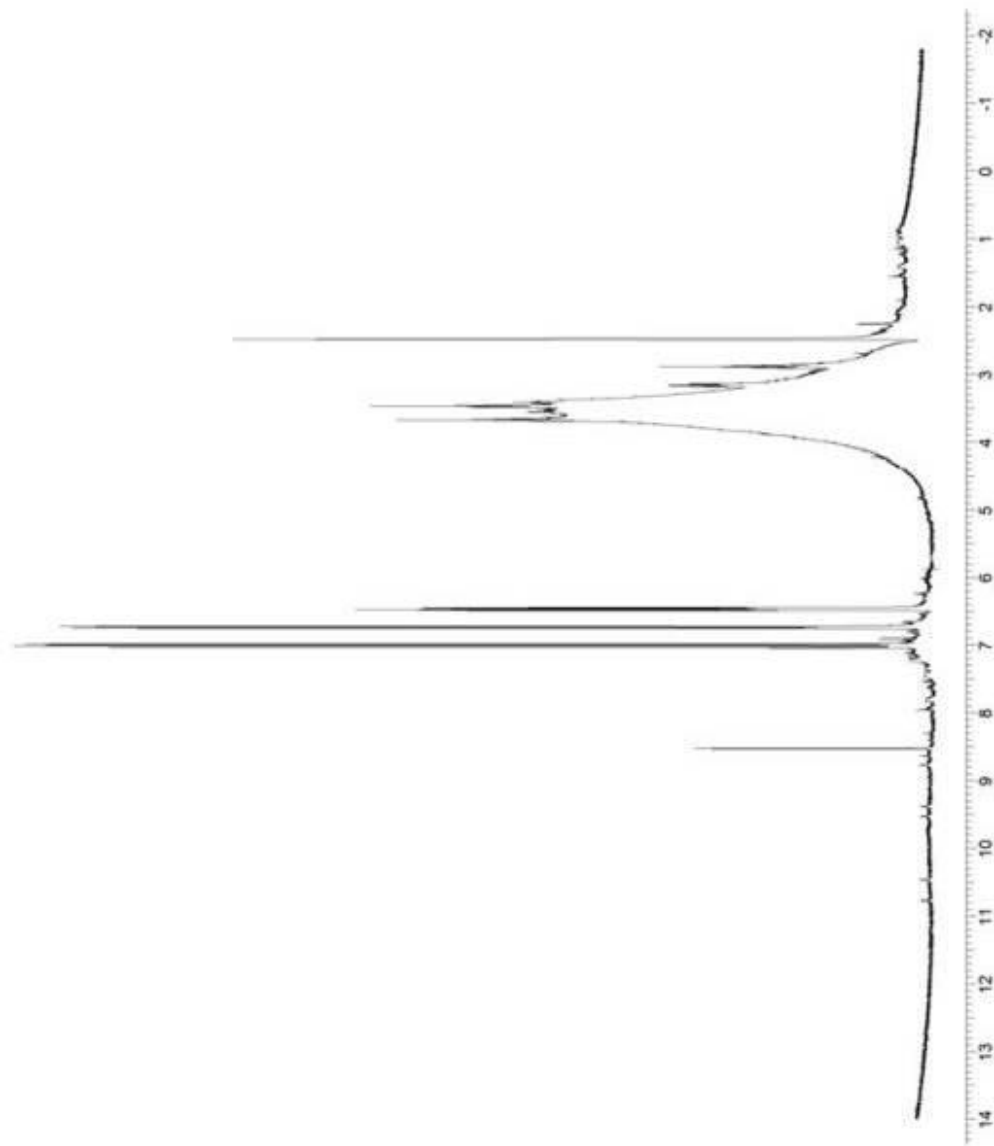


Figure A.14. $^1\text{H-NMR}$ spectrum of $[\text{MoO}_2\text{Cl}_2(\text{NH}_2\text{C}_6\text{H}_3\text{FNH})]$ (**14**)

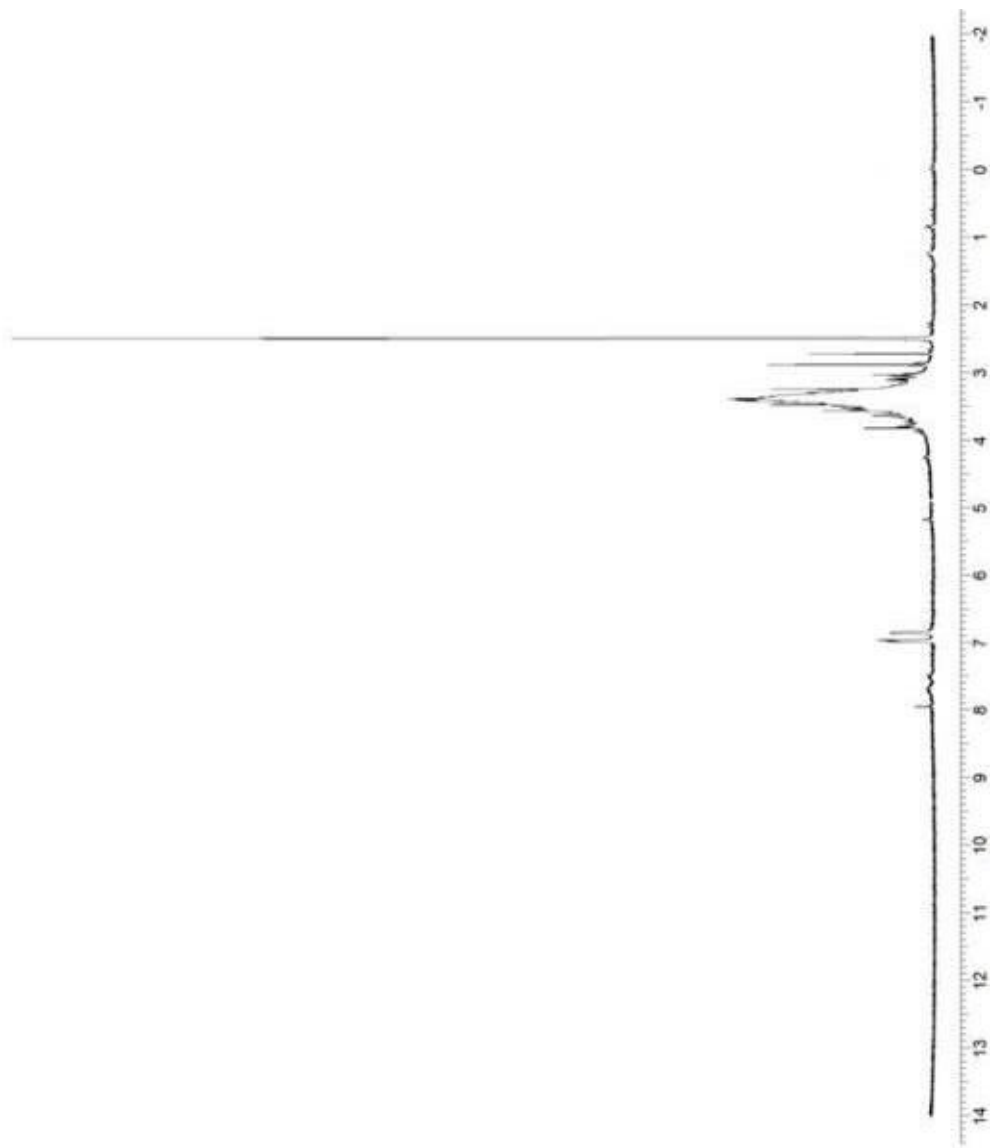


Figure A.15. ¹H-NMR spectrum of [Mo₂O₂(μ₂-O)Cl₄(NH₂C₆H₃ClN)₂] (**15**)



Figure A.16. $^1\text{H-NMR}$ spectrum of $[\text{Mo}_2\text{O}_2(\mu_2\text{-O})\text{Cl}_4(\text{NH}_2\text{C}_6\text{H}(\text{CH}_3)_3\text{N})_2]$ (**16**)

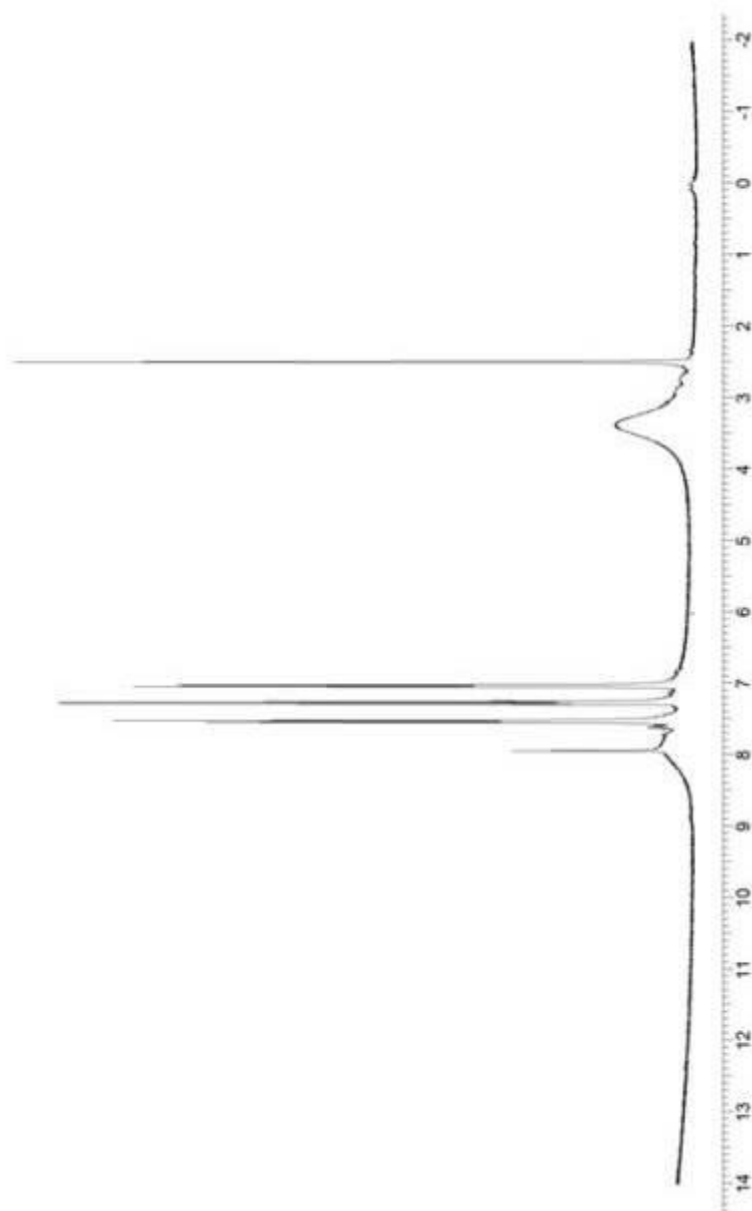


Figure A.17. $^1\text{H-NMR}$ spectrum of $[\text{Mo}_2\text{O}_2(\mu_2\text{-O})\text{Cl}_4(\text{NH}_2\text{C}_{10}\text{H}_6\text{NH})_2]$ (**17**)

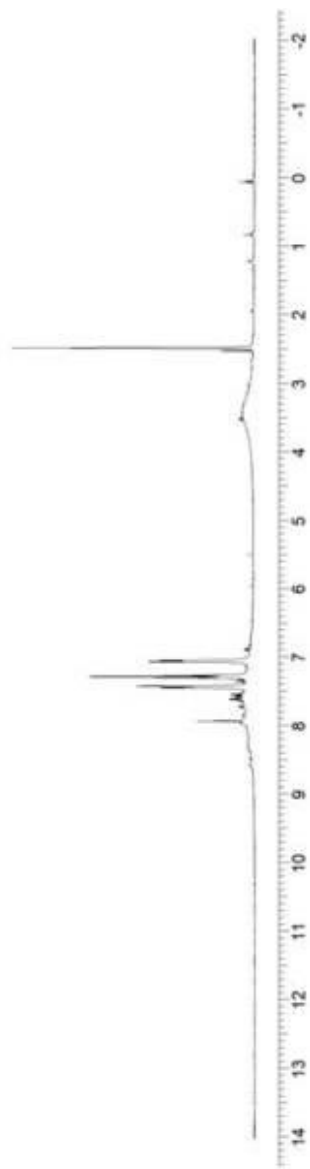


Figure A.18. $^1\text{H-NMR}$ spectrum of $[\text{Mo}_2\text{O}_2(\mu_2\text{-O})\text{Cl}_4(\text{NH}_2\text{C}_{10}\text{H}_6\text{NH})_2]$ (**18**)

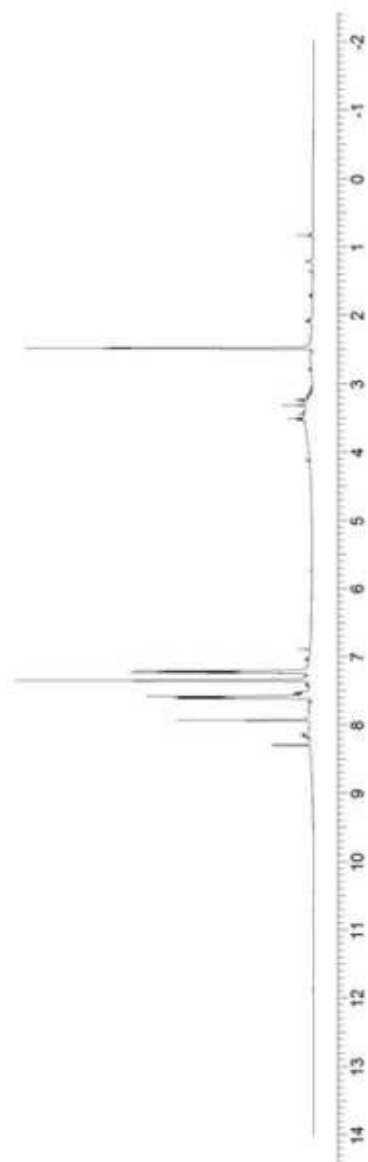


Figure A.19. $^1\text{H-NMR}$ spectrum of $[\text{Mo}_2\text{O}_2(\mu_2\text{-O})\text{Cl}_4(\text{NH}_2\text{C}_{10}\text{H}_6\text{NH})_2]$ (**19**)

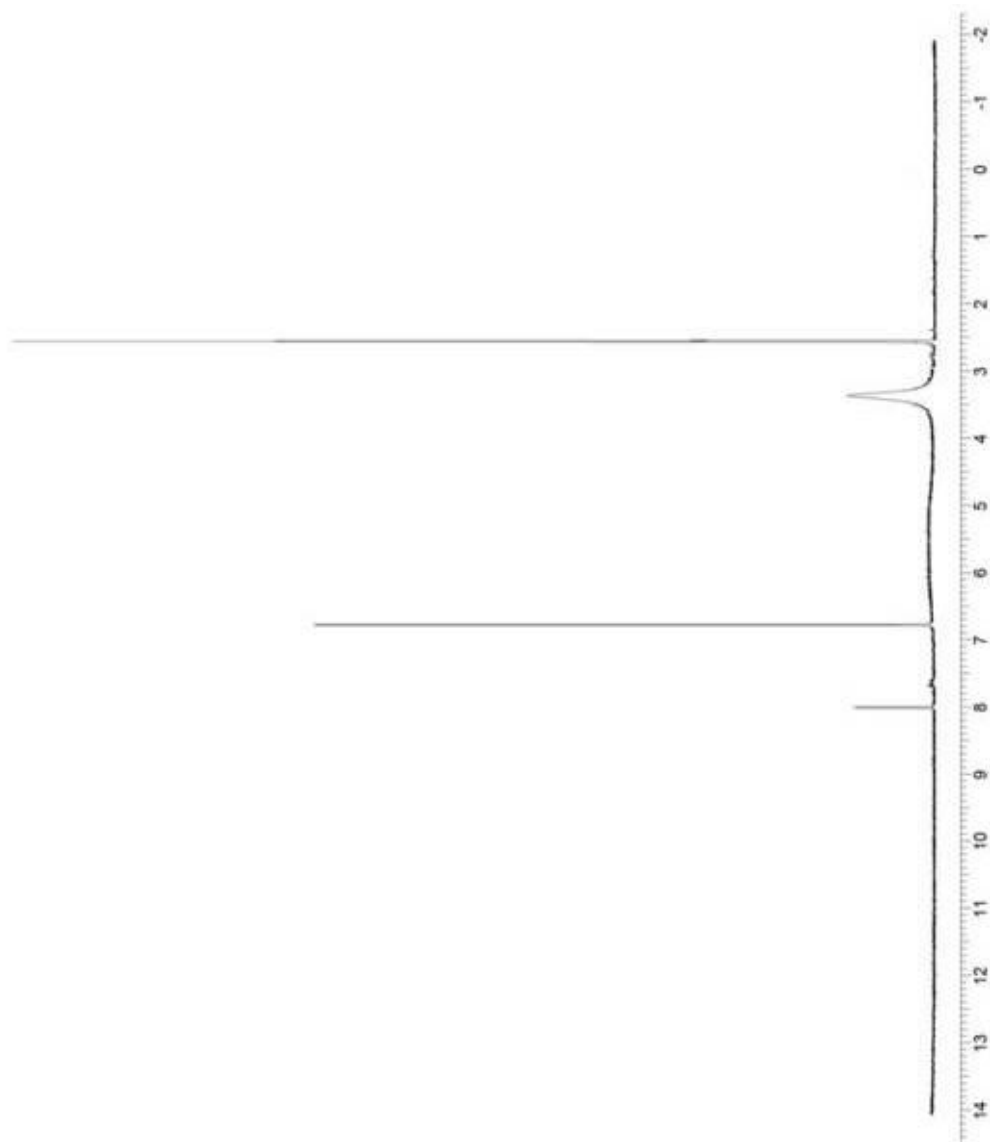


Figure A.20. $^1\text{H-NMR}$ spectrum of $[\text{Mo}_2\text{O}_2(\mu_2\text{-O})(\text{NH}_2\text{C}_6\text{H}_2\text{Cl}_2\text{NH})_2]$

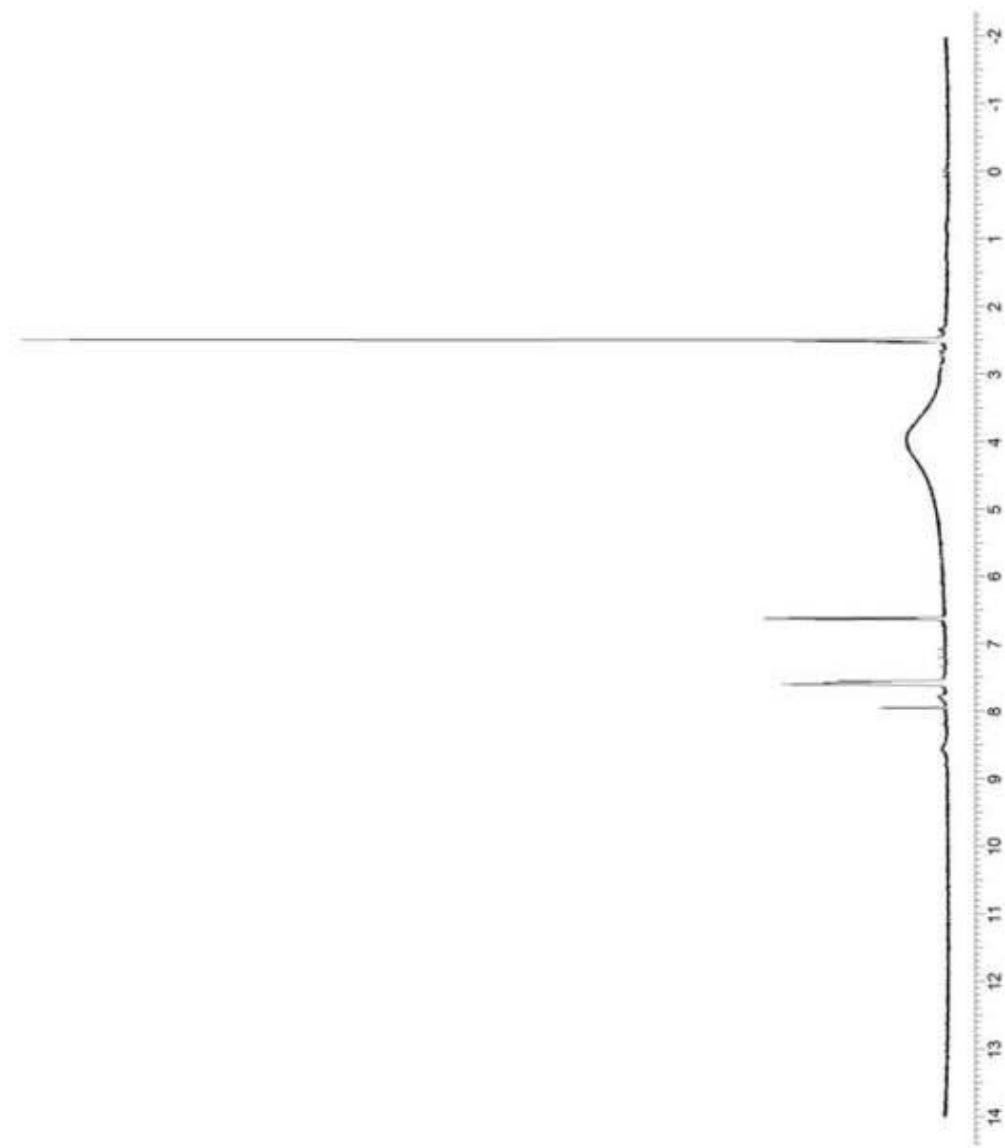


Figure A.21. $^1\text{H-NMR}$ spectrum of $[\text{Mo}_2\text{O}_2(\mu_2\text{-O})\text{Cl}_4(\text{NH}_2\text{C}_6\text{H}_3\text{NO}_2\text{NH}_2)_2]$ (**21**)

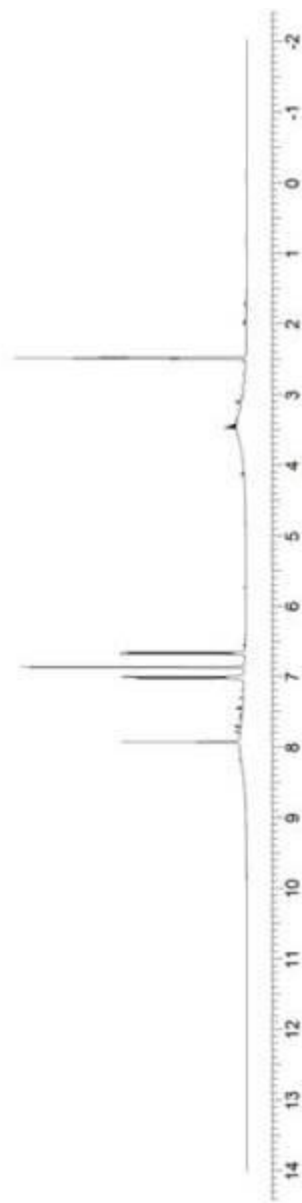


Figure A.22. $^1\text{H-NMR}$ spectrum of $[\text{Mo}_2\text{O}_2(\mu_2\text{-O})\text{Cl}_4(\text{NH}_2\text{C}_6\text{H}_3\text{CINH})_2]$ (**22**)

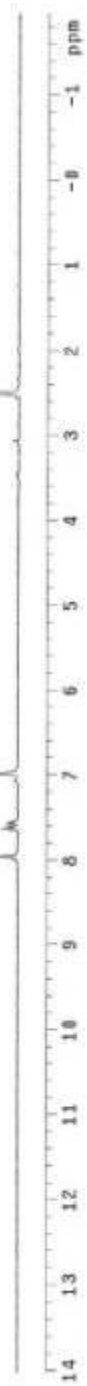


Figure A.23. $^1\text{H-NMR}$ spectrum of $[\text{Mo}_2\text{O}_2(\mu_2\text{-O})\text{Cl}_4(\text{NHC}_6\text{H}_2\text{Cl}_2\text{NH})_2]$ (**23**)

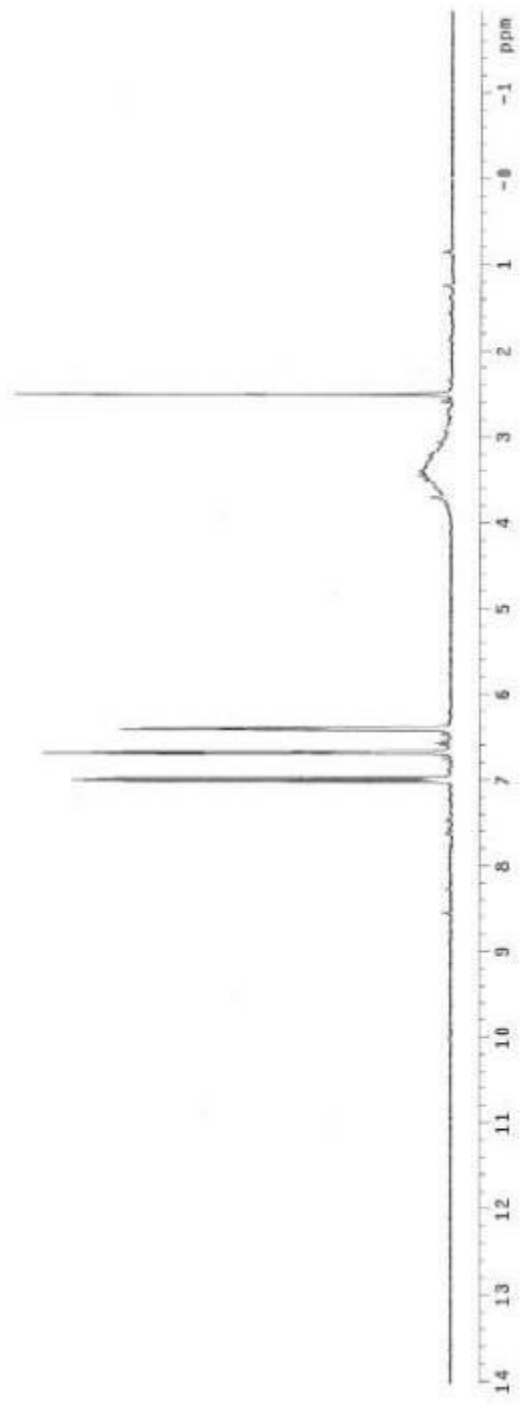


Figure A.24. ¹H-NMR spectrum of [Mo₂O₂(μ₂-O)Cl₄(NH₂C₆H₃FN)₂] (**24**)

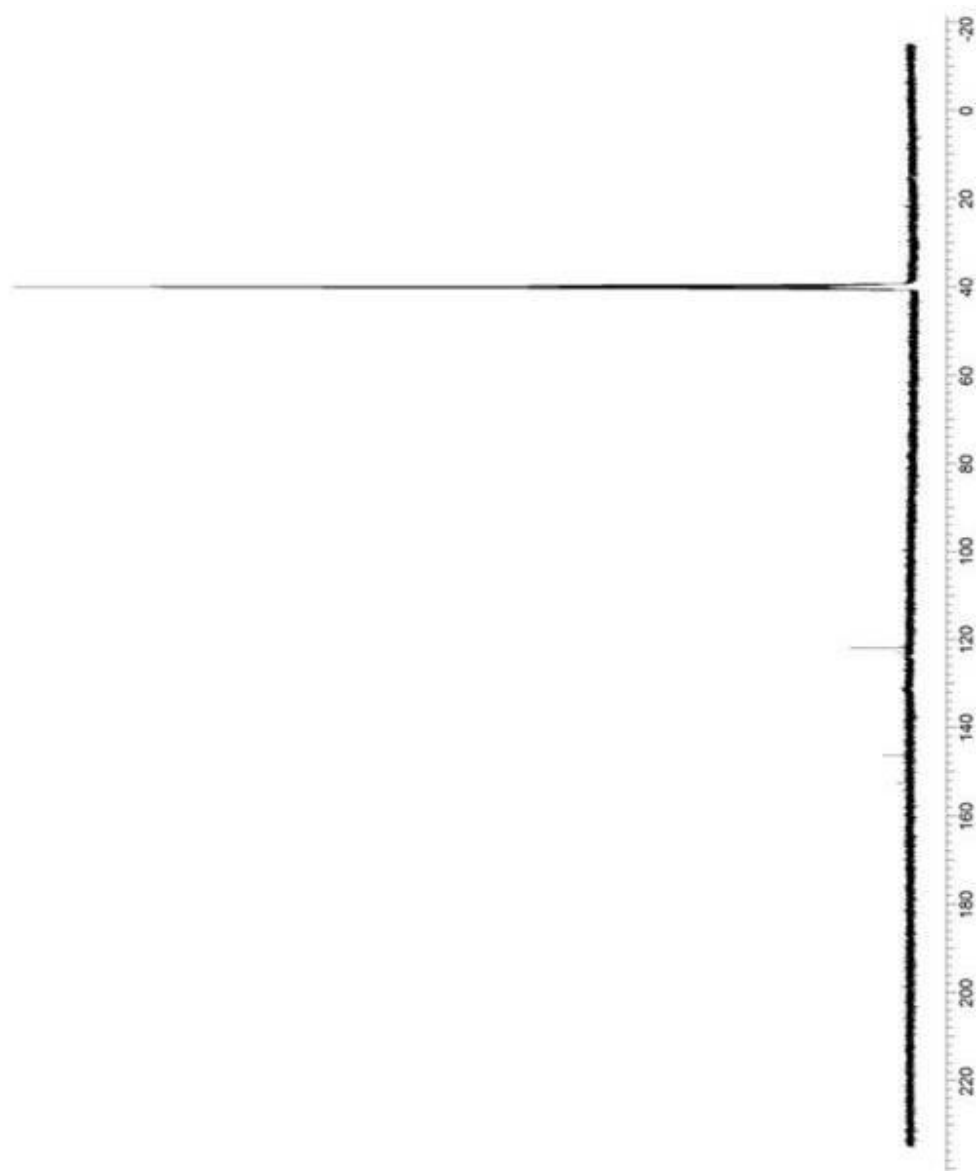


Figure A.25. ^{13}C NMR spectrum of $[\text{Mo}_2\text{O}_2(\mu_2\text{-O})(\text{NH}_2\text{C}_6\text{H}_4\text{NH})_2]$ (**1**)

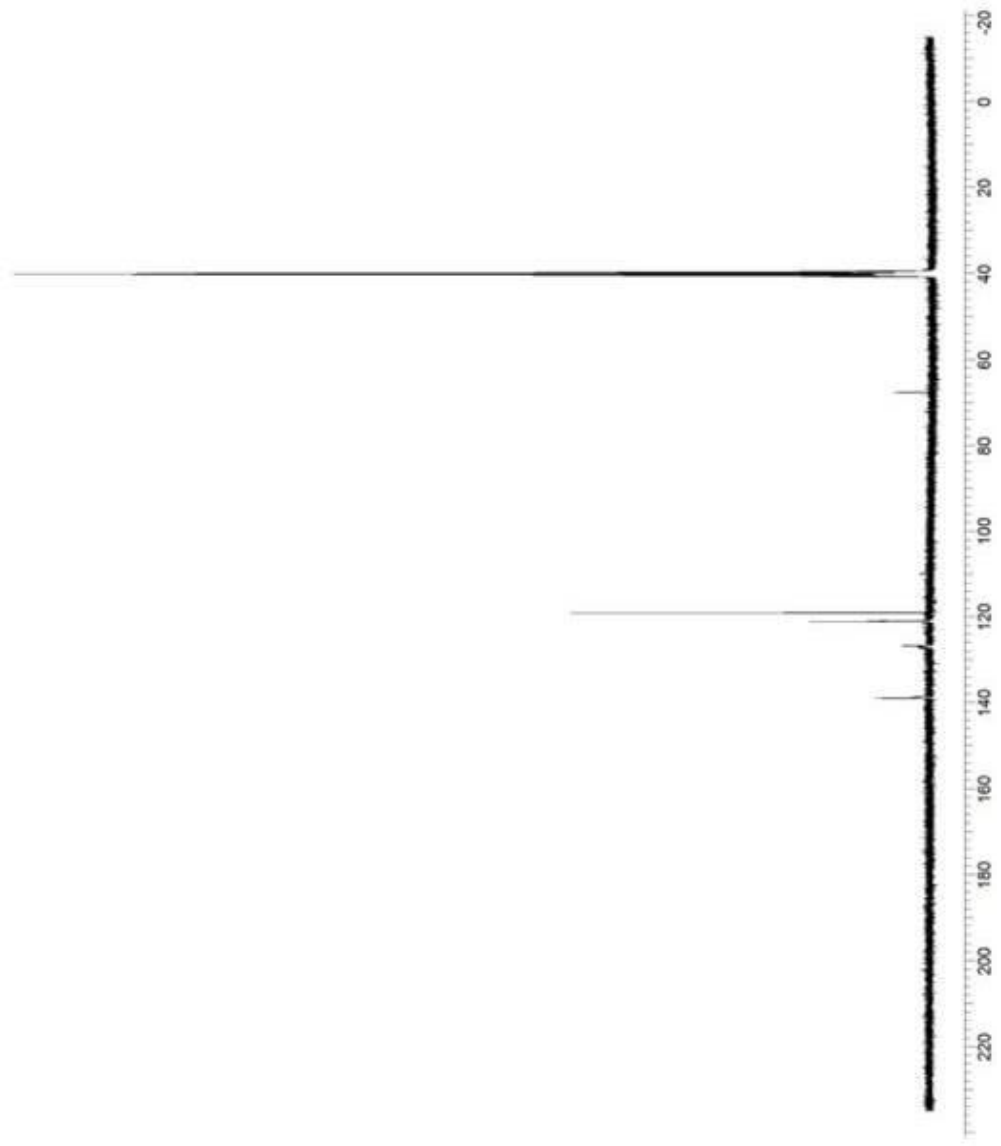


Figure A.26. ^{13}C NMR spectrum of $[\text{MoO}_2\text{Cl}_2(\text{NH}_2\text{C}_6\text{H}_4\text{Cl}_2\text{NH})]$ (2)

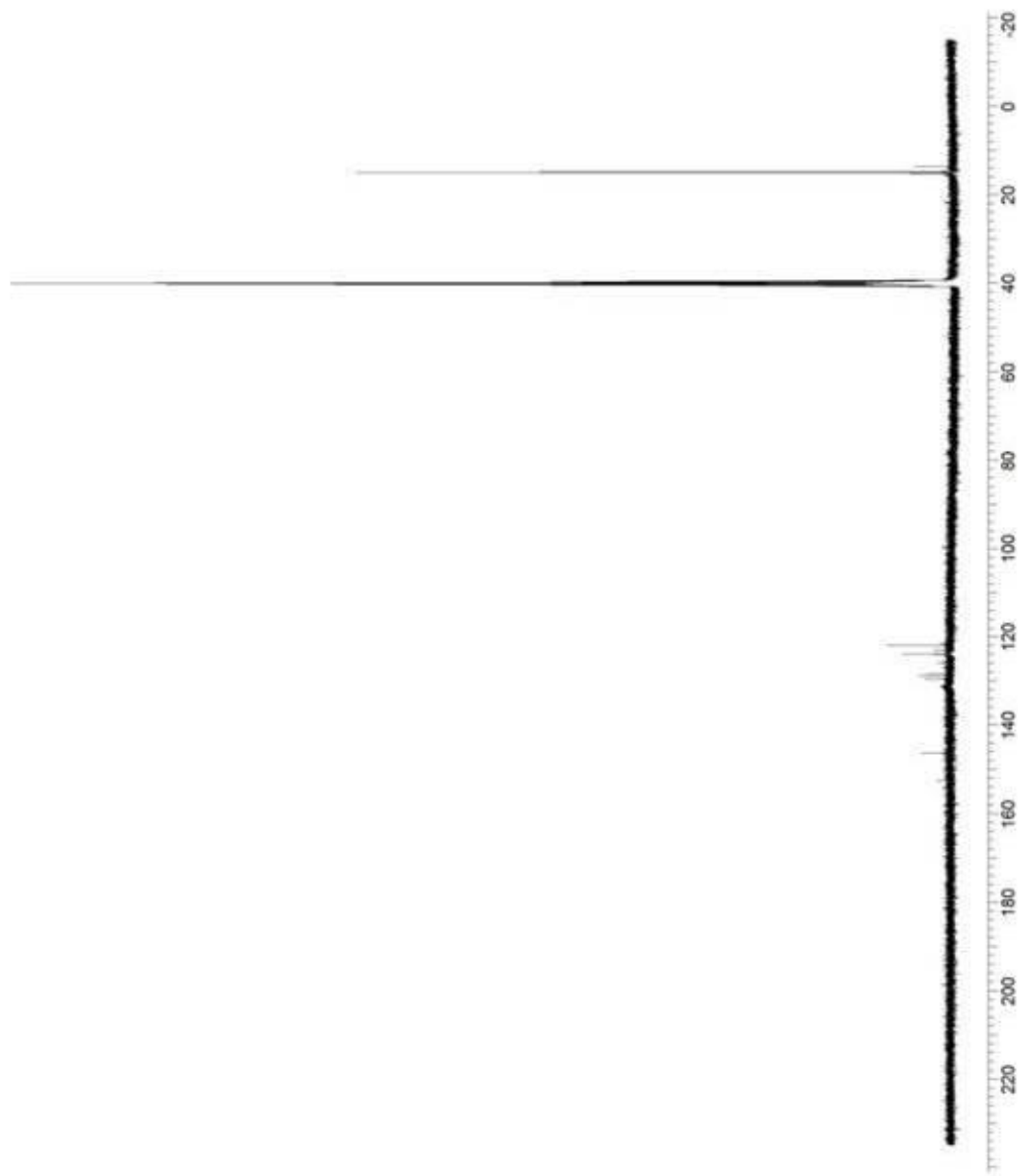


Figure A.27. ^{13}C NMR spectrum of $[\text{Mo}_2\text{O}_2(\mu_2\text{-O})\text{Cl}_4(\text{NH}_2\text{C}_6(\text{CH}_3)_4\text{NH})_2]$ (**3**)

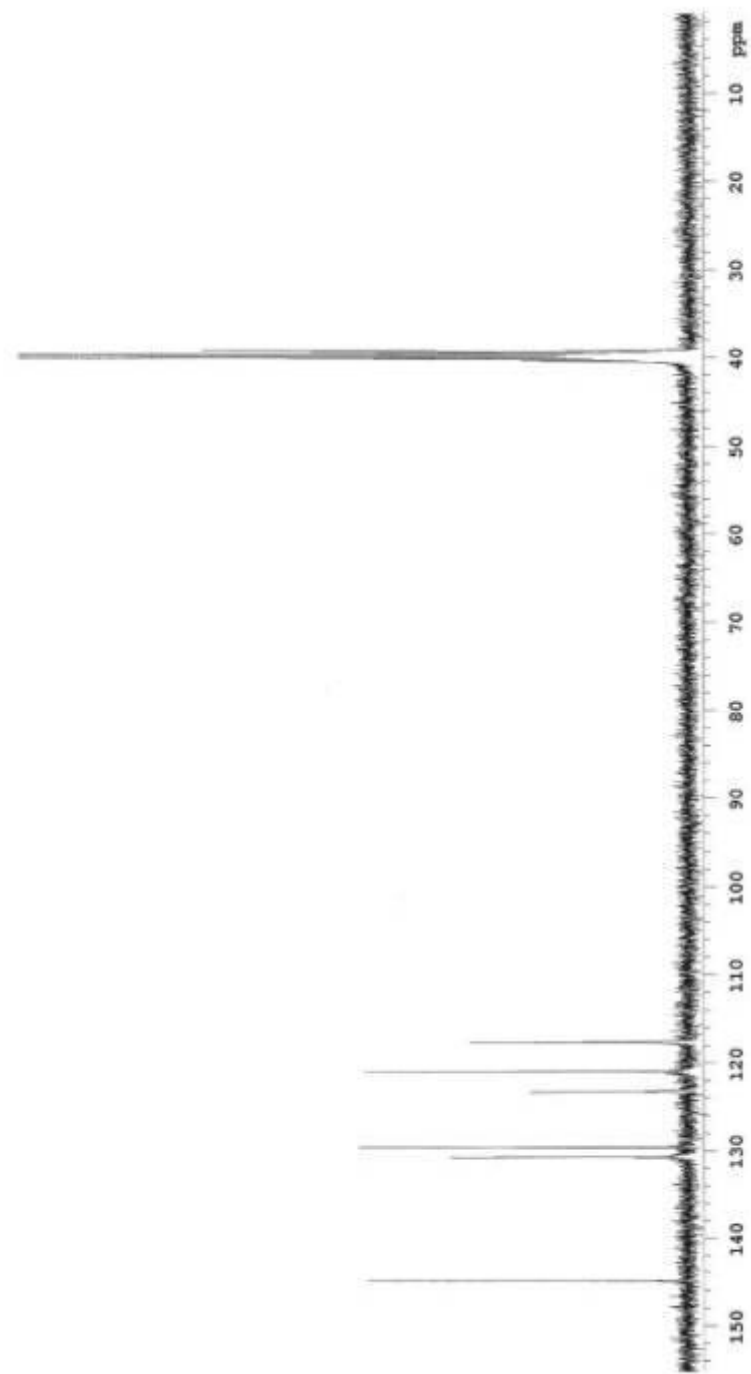


Figure A.28. ^{13}C NMR spectrum of $[[\text{Mo}_2\text{O}_2(\mu_2\text{-O})\text{Cl}_4(\text{NH}_2\text{C}_6\text{H}_3\text{NO}_2\text{NH}_2)_2]$ (**4**)

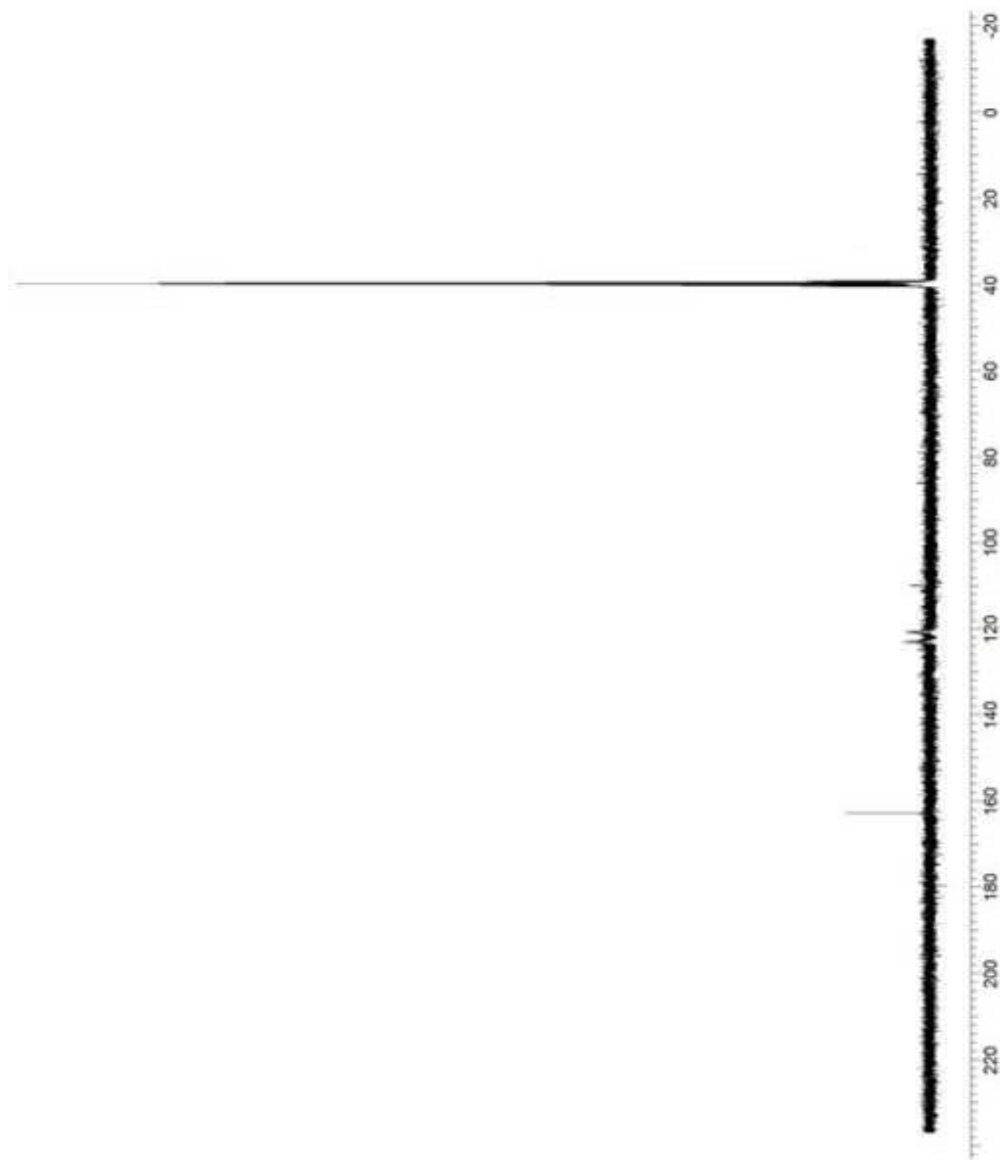


Figure A.29. ^{13}C NMR spectrum of $[\text{Mo}_2\text{O}_2(\mu_2\text{-O})\text{Cl}_4(\text{NH}_2\text{C}_6\text{H}_4\text{NH}_2)_2]$ (**5**)

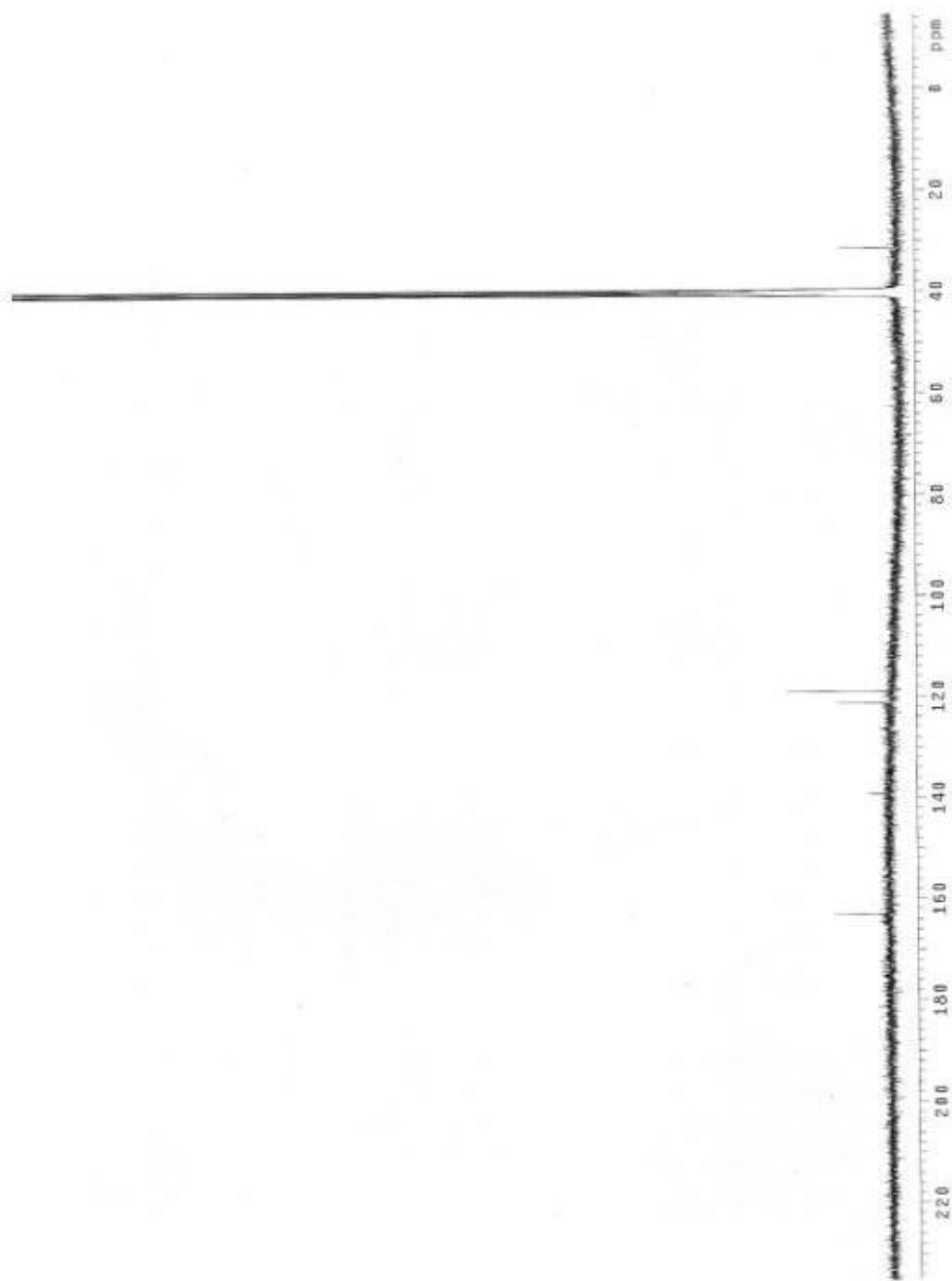


Figure A.30. ^{13}C NMR spectrum of $[\text{Mo}_2\text{O}_2(\mu_2\text{-O})\text{Cl}_4(\text{NH}_2\text{C}_6\text{H}_3(\text{CH}_3)\text{NH})_2]$ (**6**)

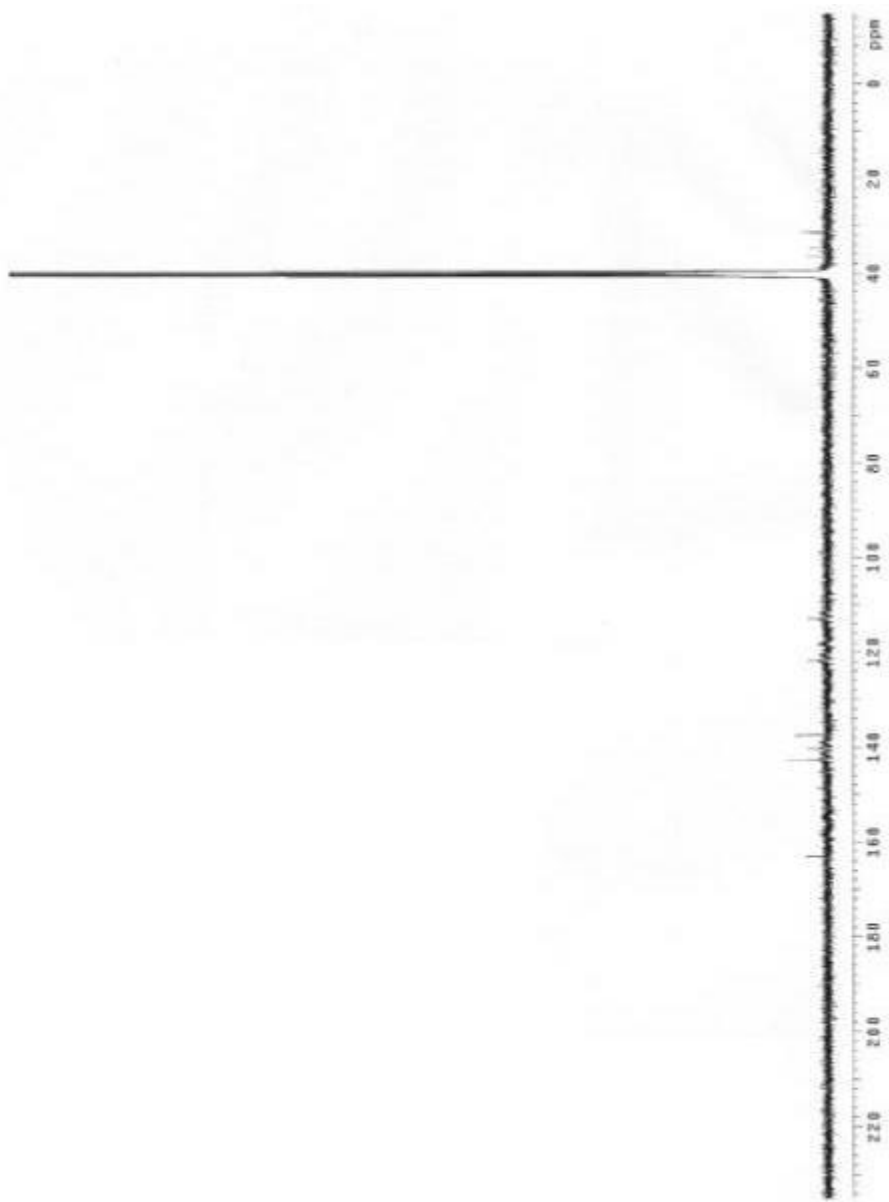


Figure A.31. ^{13}C NMR spectrum of $[\text{MoO}_2\text{Cl}_2(\text{NHC}_6\text{H}_3\text{NO}_2\text{NH})]$ (7)

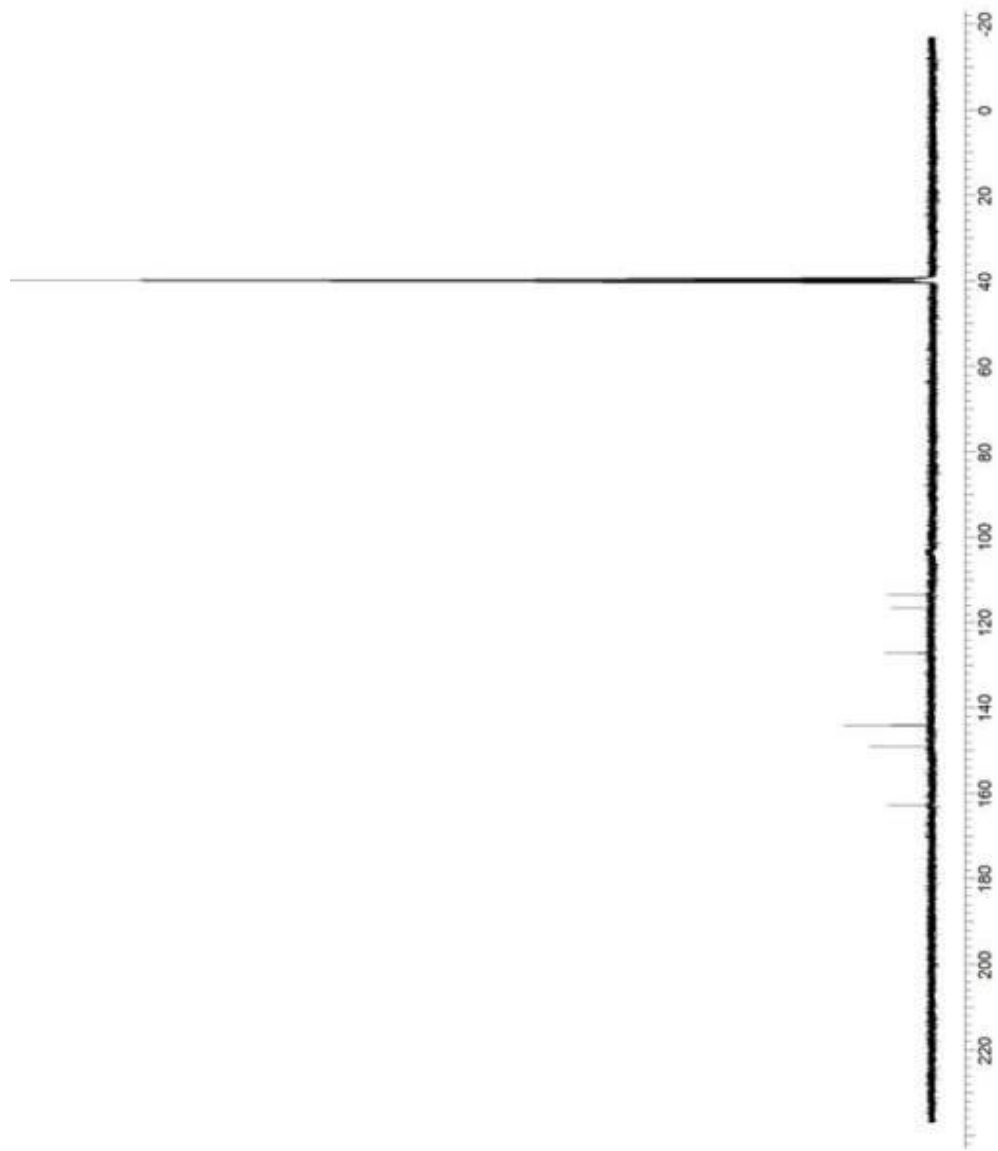


Figure A.32. ^{13}C NMR spectrum of $[\text{Mo}_2\text{O}_2(\mu_2\text{-O})\text{Cl}_4(\text{NH}_2\text{C}_6\text{H}_3\text{FNH})_2]$ (**8**)

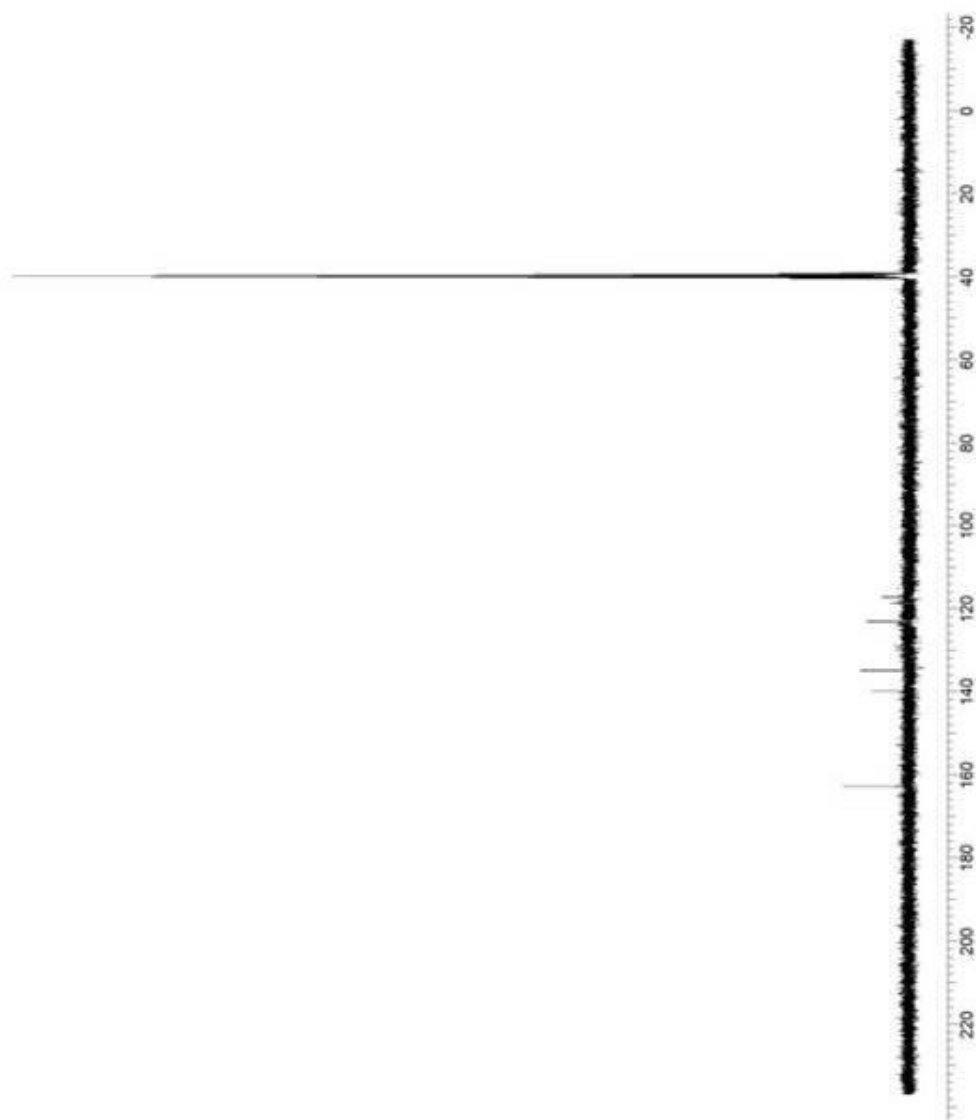


Figure A.33. ^{13}C NMR spectrum of $[\text{MoO}_2\text{Cl}_2(\text{NHC}_6\text{H}_3\text{ClNH})]$ (**9**)

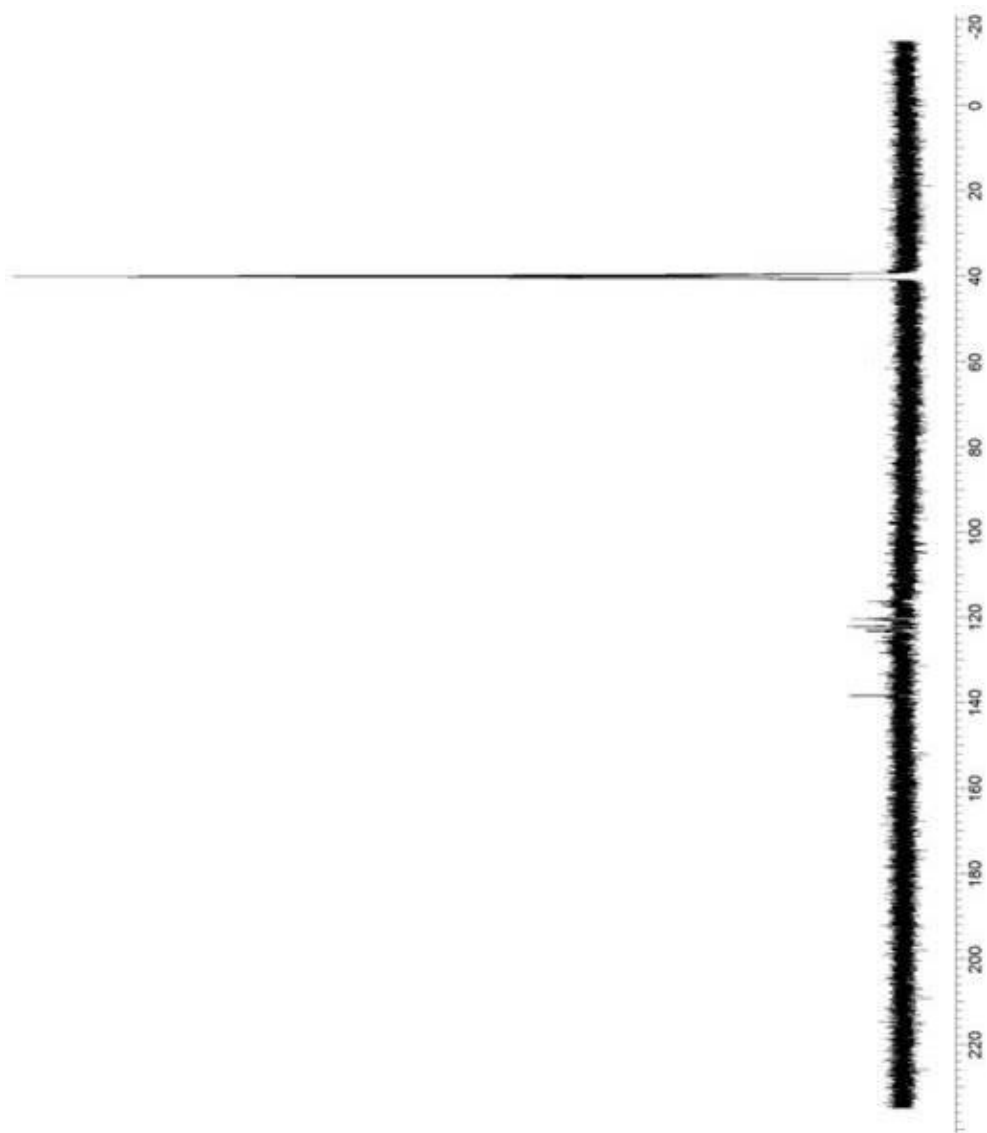


Figure A.34. ^{13}C NMR spectrum of $[\text{Mo}_2\text{O}_2(\mu_2\text{-O})\text{Cl}_4(\text{NH}_2\text{C}_6\text{H}_3\text{BrNH})_2]$ (**10**)

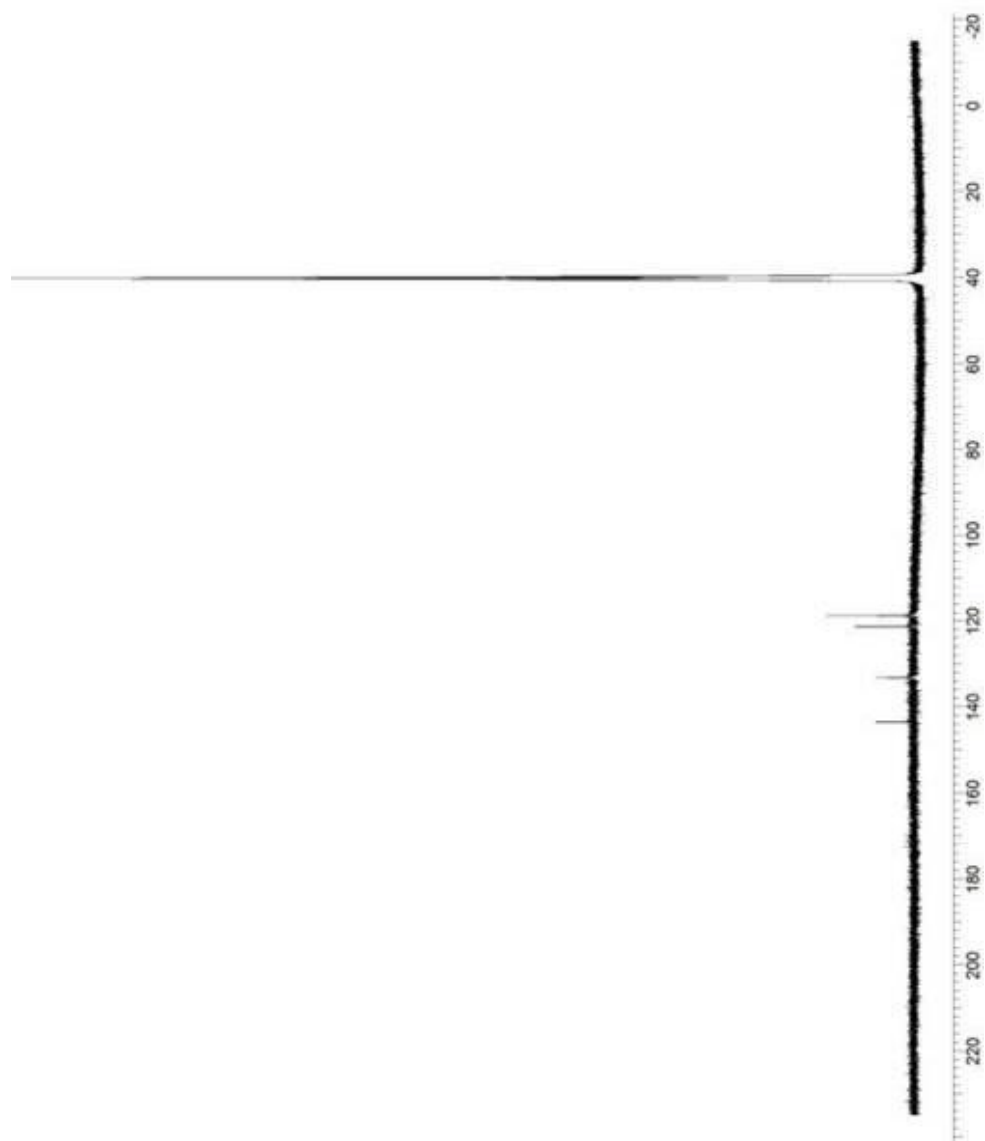


Figure A.35. ^{13}C NMR spectrum of $[\text{MoO}_2\text{Cl}_2(\text{NH}_2\text{C}_6\text{H}_4\text{Cl}_2\text{N})]$ (**11**)

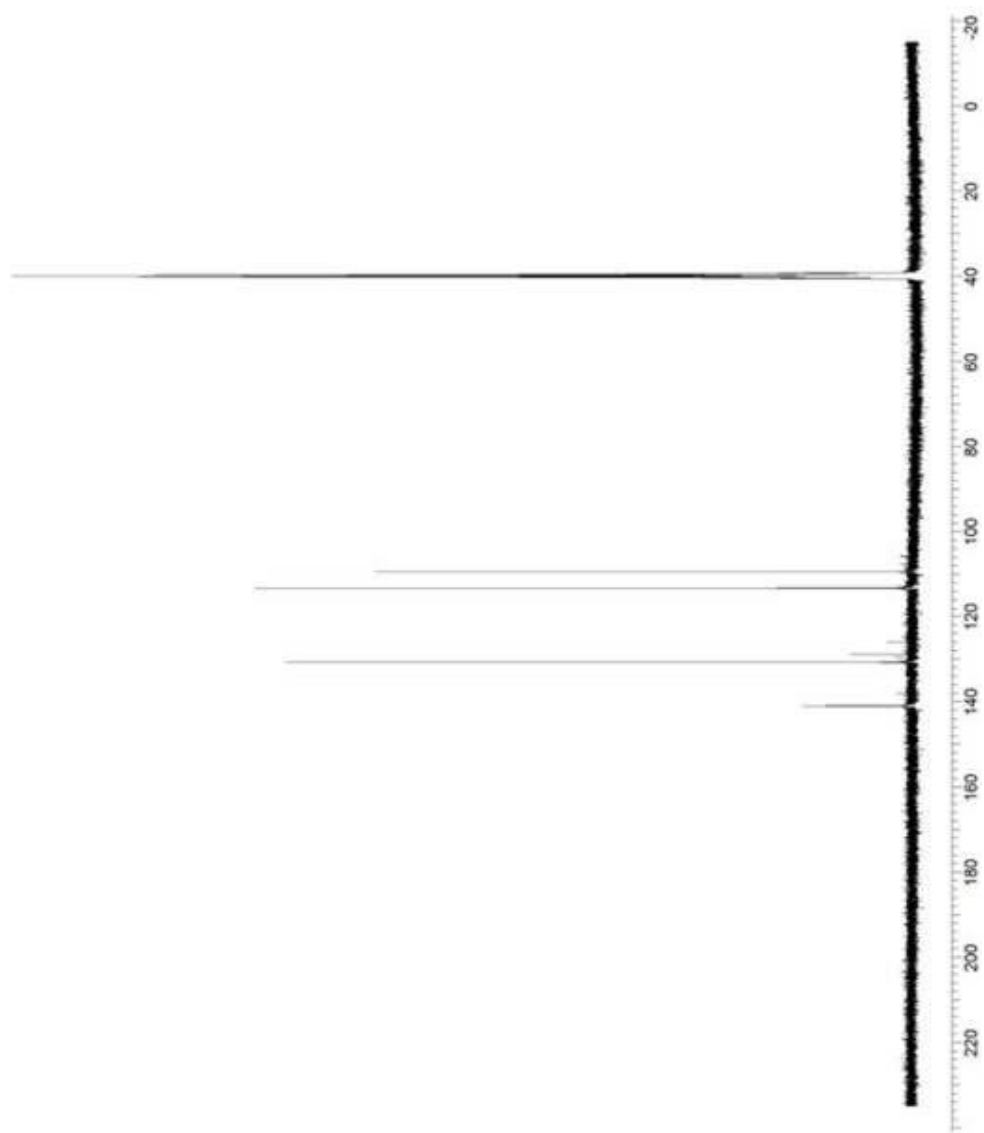


Figure A.36. ^{13}C NMR spectrum of $[\text{Mo}_2\text{O}_2(\mu_2\text{-O})\text{Cl}_4(\text{NH}_2\text{C}_6\text{H}_4\text{N})_2]$ (**12**)

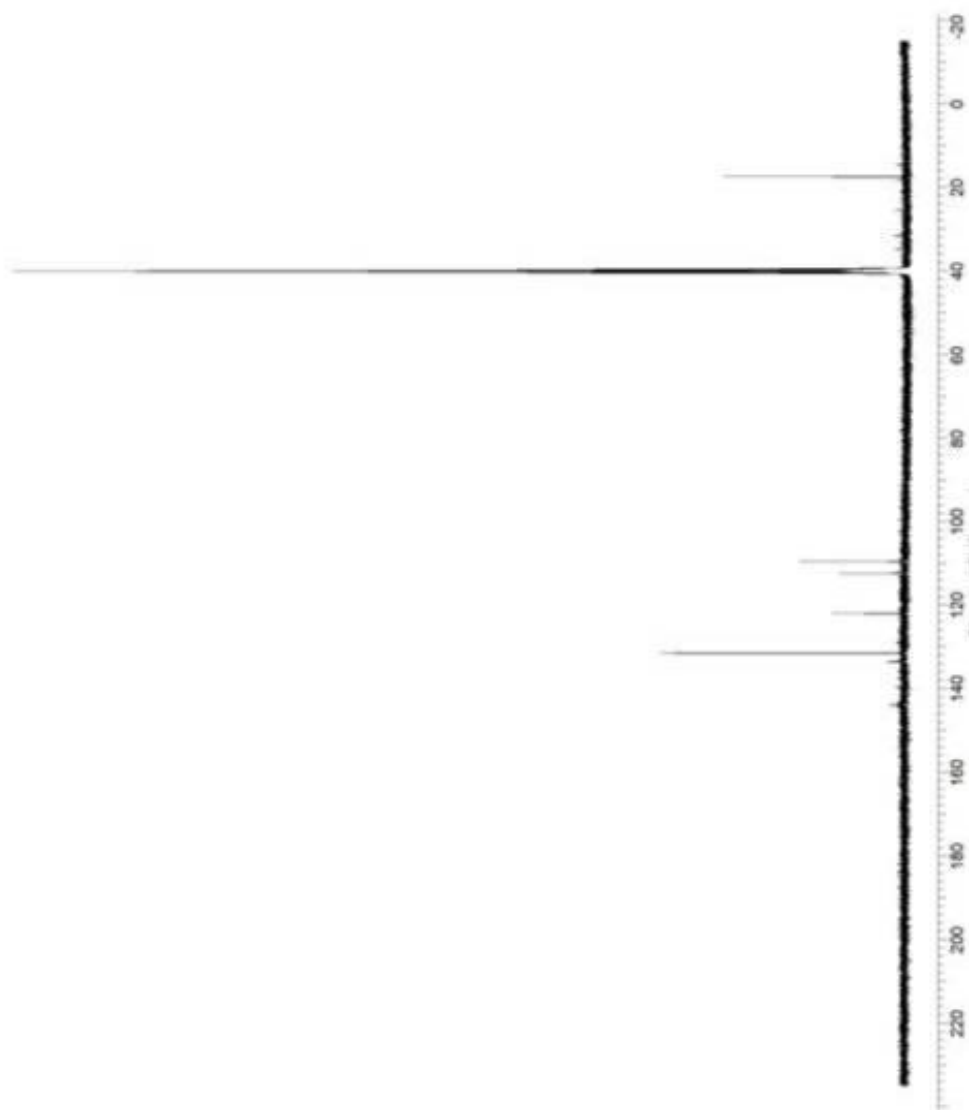


Figure A.37. ^{13}C NMR spectrum of $[\text{Mo}_2\text{O}_2(\mu_2\text{-O})\text{Cl}_4(\text{NH}_2\text{C}_6\text{H}_3(\text{CH}_3)\text{N})_2]$ (**13**)

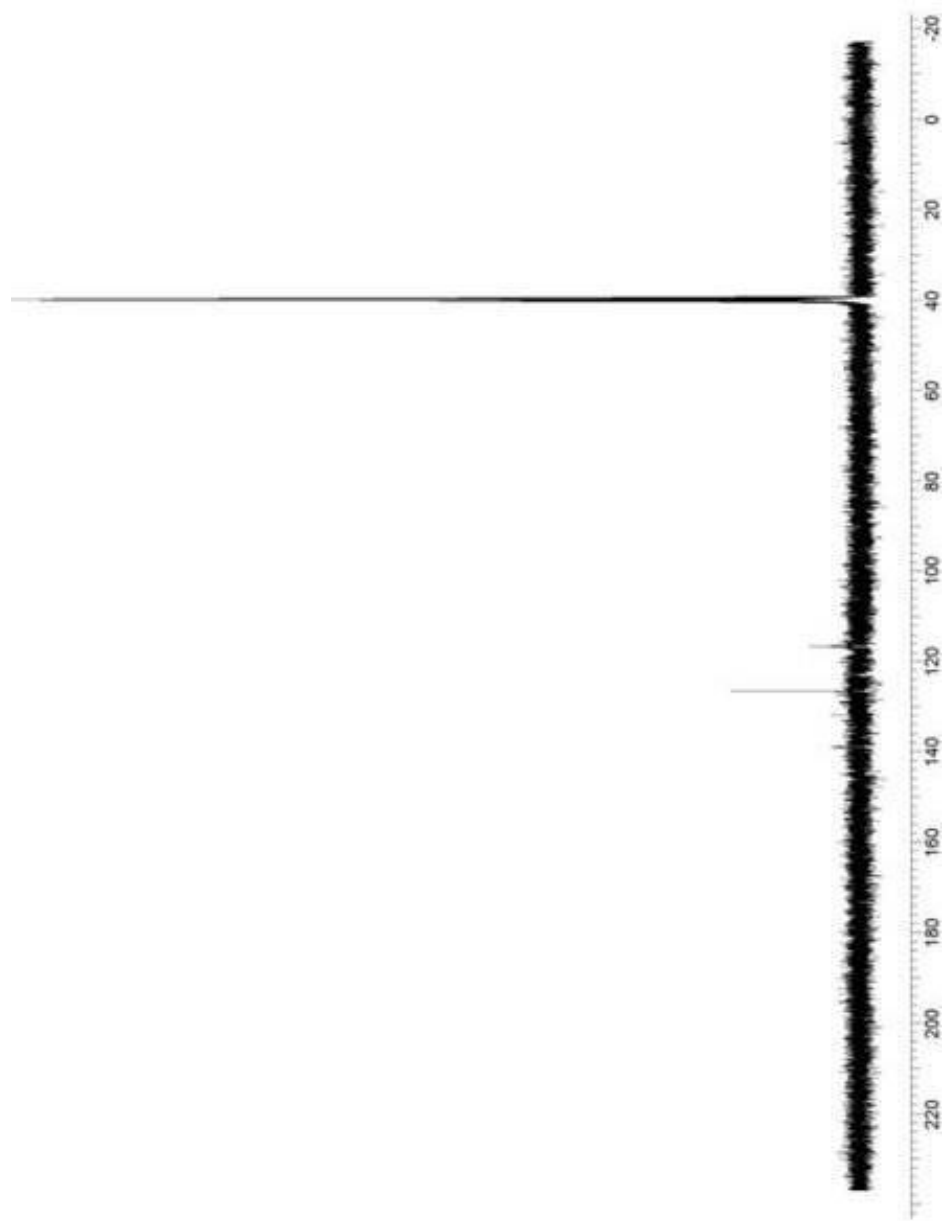


Figure A.38. ^{13}C NMR spectrum of $[\text{MoO}_2\text{Cl}_2(\text{NH}_2\text{C}_6\text{H}_3\text{FNH})]$ (**14**)

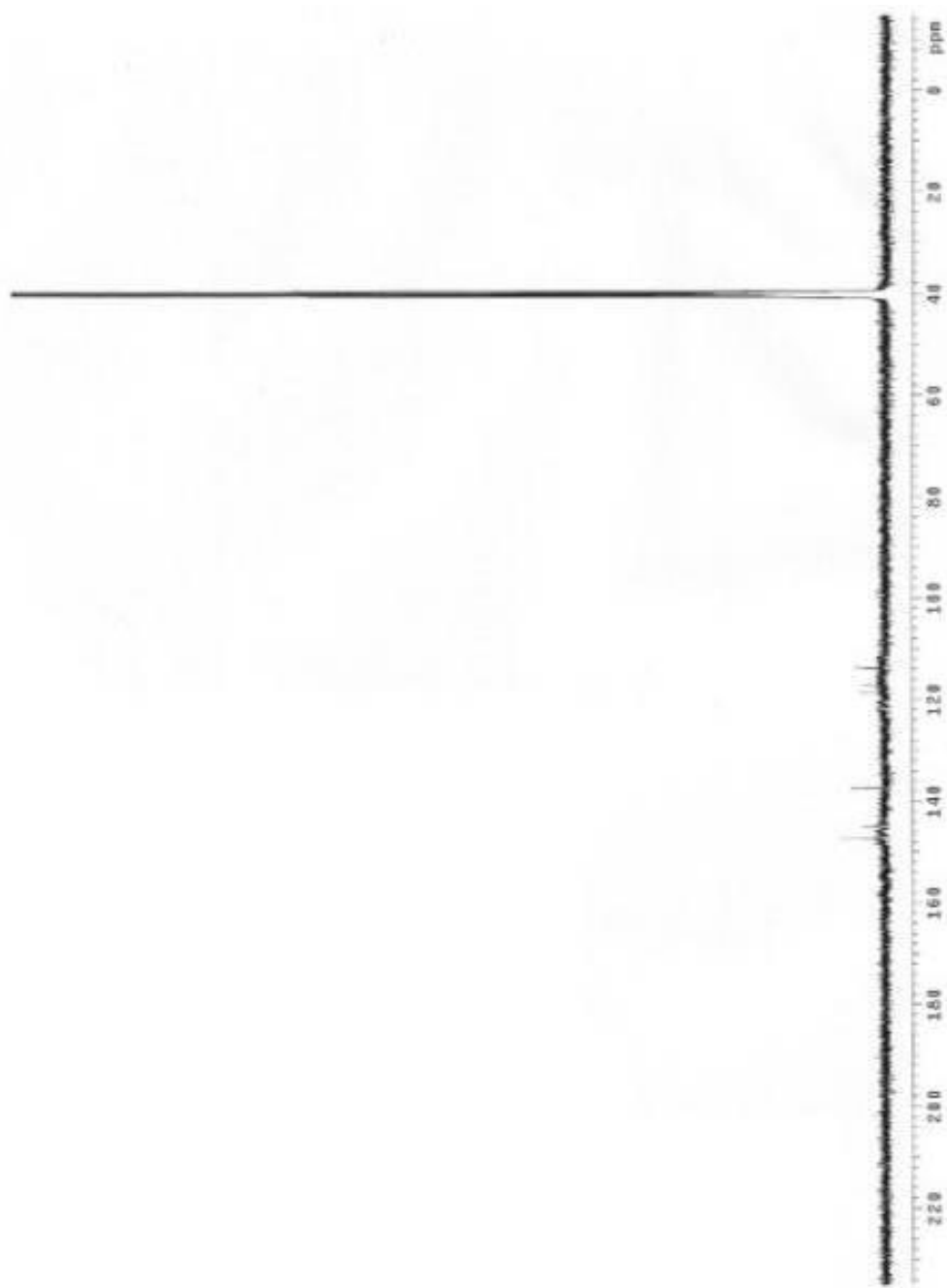


Figure A.39. ^{13}C NMR spectrum of $[\text{Mo}_2\text{O}_2(\mu_2\text{-O})\text{Cl}_4(\text{NH}_2\text{C}_6\text{H}_3\text{ClN})_2]$ (**15**)

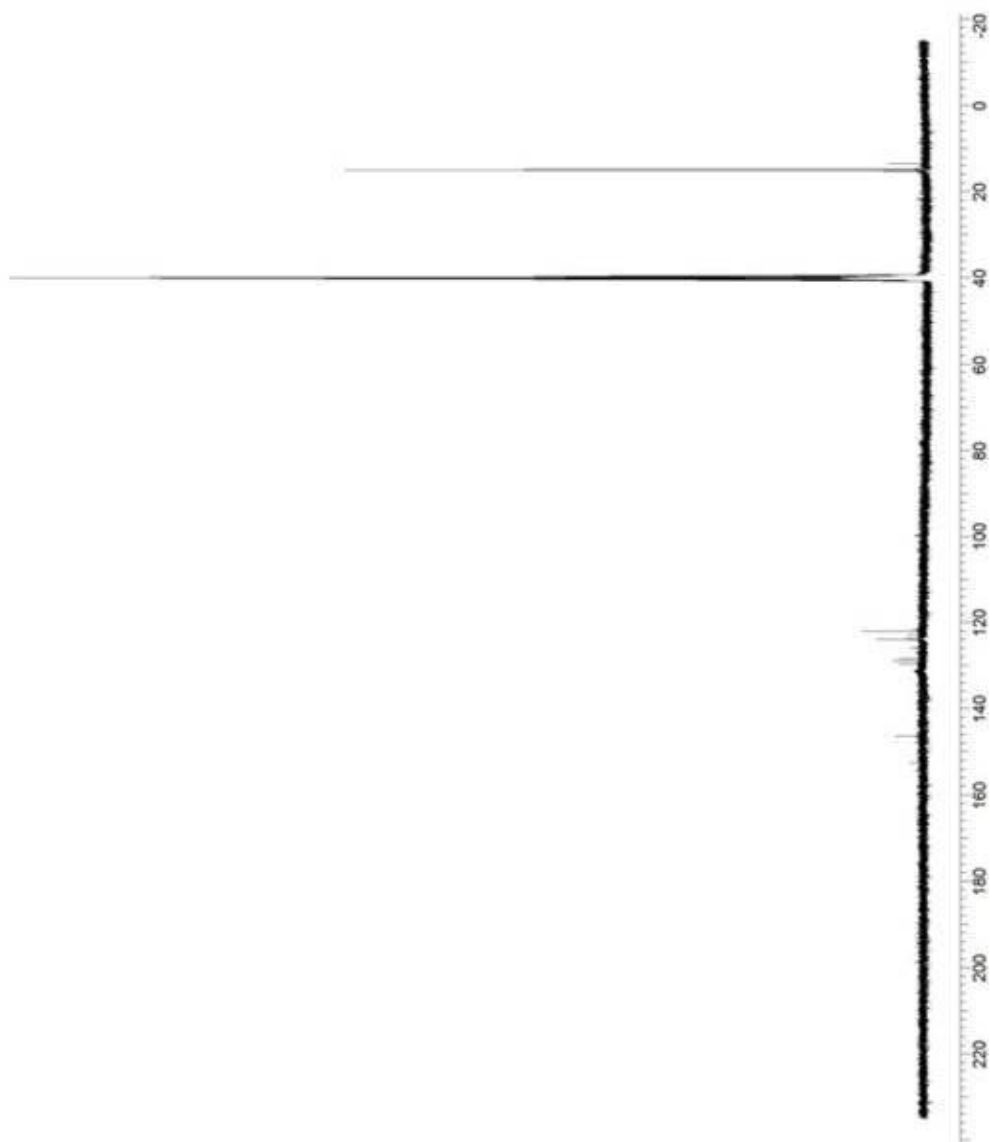


Figure A.40. ^{13}C NMR spectrum of $[\text{Mo}_2\text{O}_2(\mu_2\text{-O})\text{Cl}_4(\text{NH}_2\text{C}_6\text{H}(\text{CH}_3)_3\text{N})_2]$ (**16**)

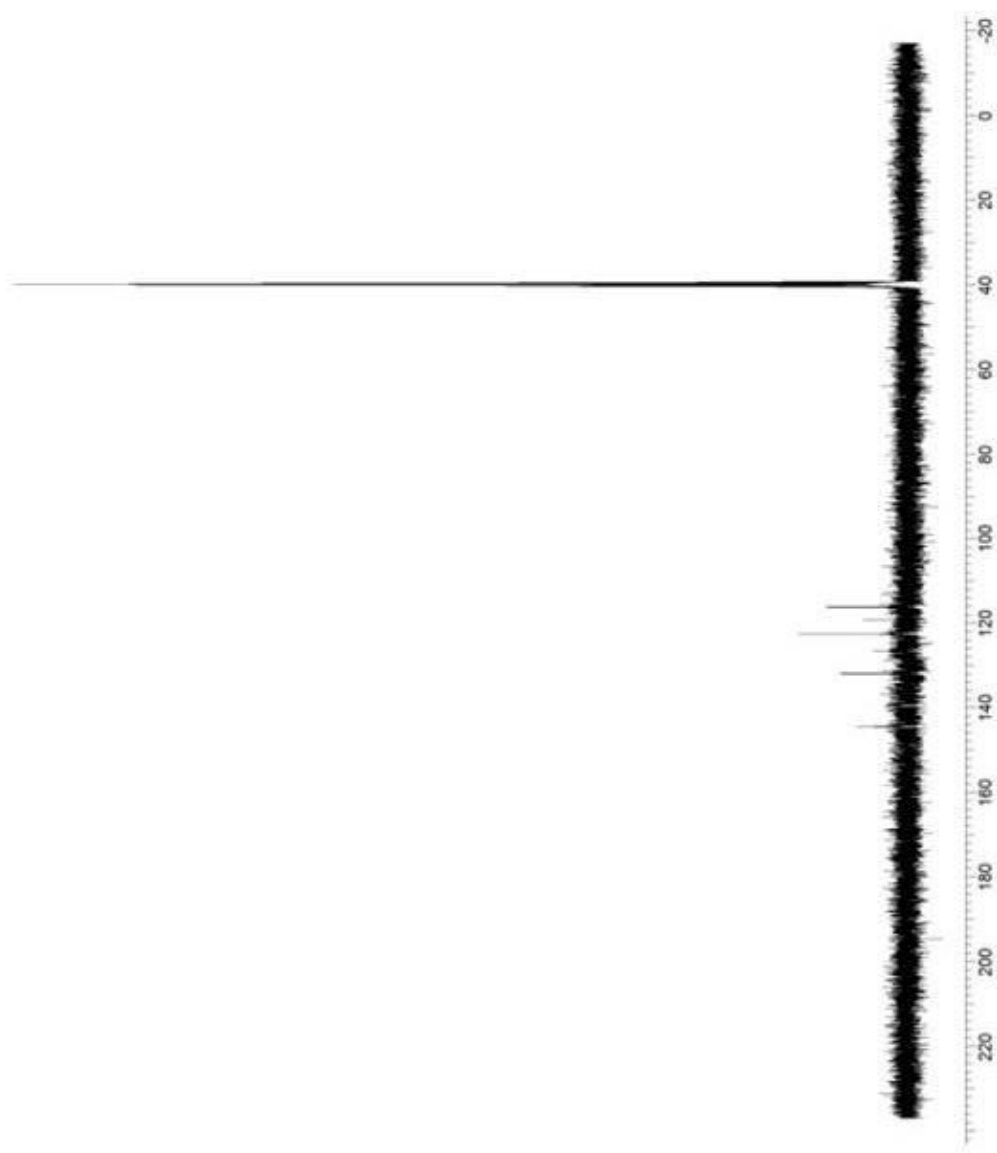


Figure A.41. ^{13}C NMR spectrum of $[\text{Mo}_2\text{O}_2(\mu_2\text{-O})\text{Cl}_4(\text{NH}_2\text{C}_{10}\text{H}_6\text{NH})_2]$ (17)

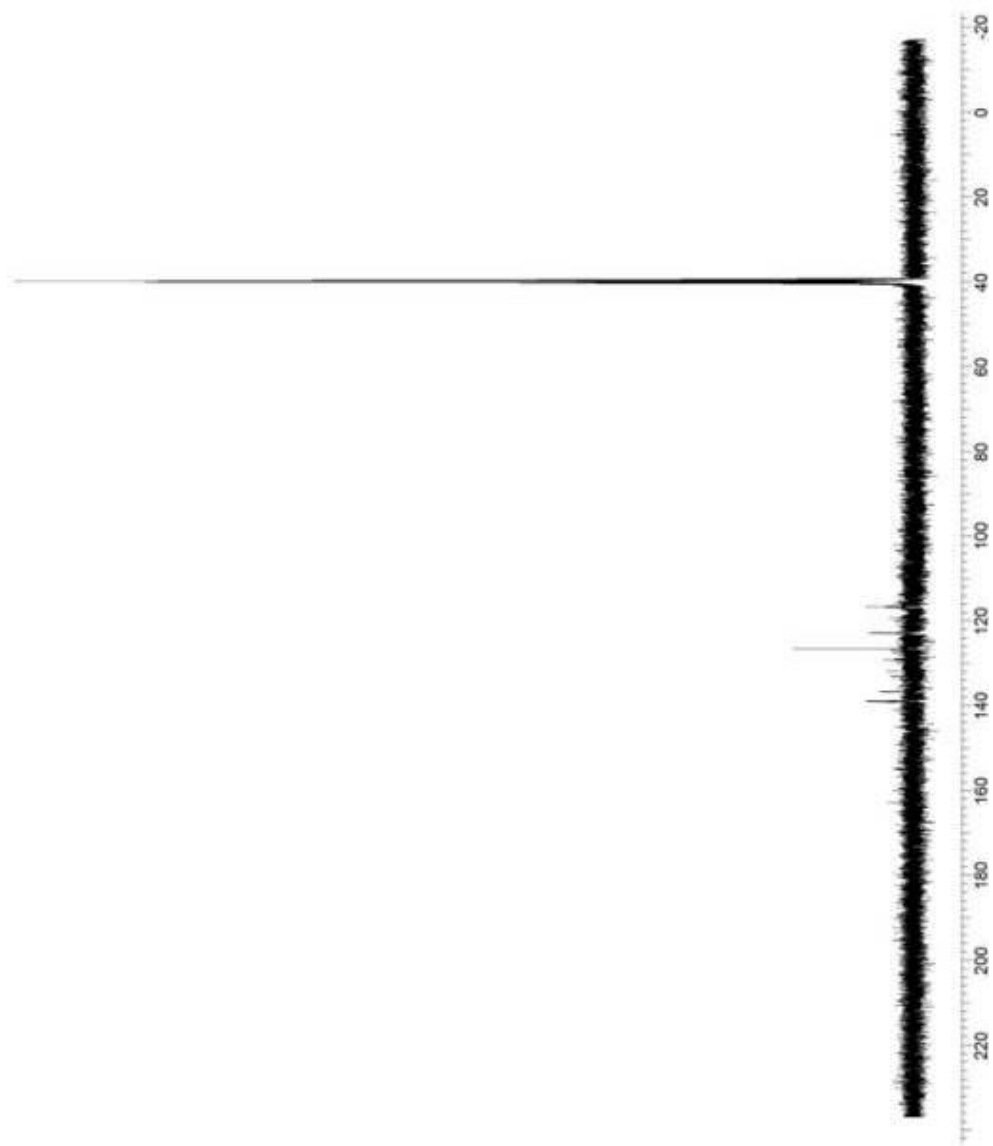


Figure A.42. ^{13}C NMR spectrum of $[\text{Mo}_2\text{O}_2(\mu_2\text{-O})\text{Cl}_4(\text{NH}_2\text{C}_{10}\text{H}_6\text{NH})_2]$ (**18**)

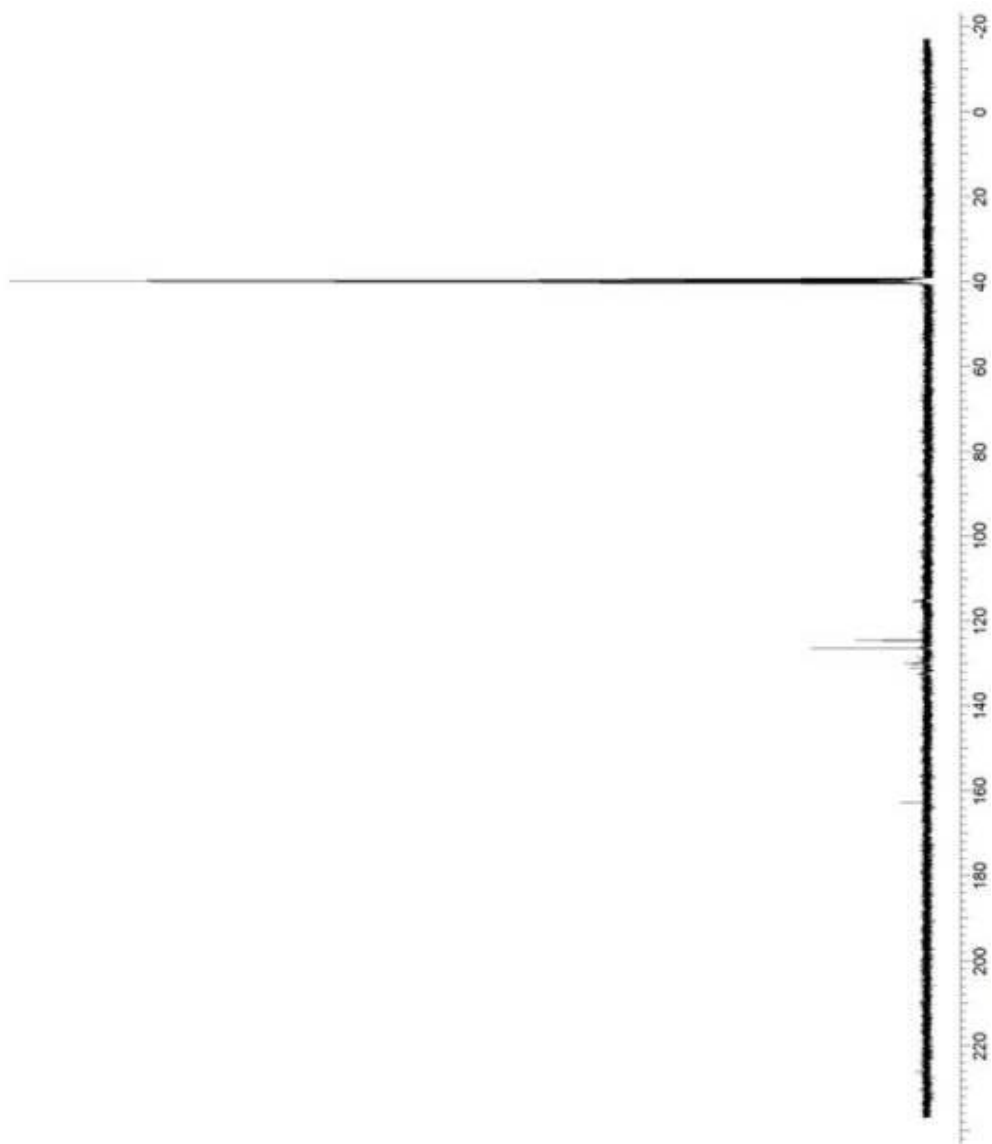


Figure A.43. ^{13}C NMR spectrum of $[\text{Mo}_2\text{O}_2(\mu_2\text{-O})\text{Cl}_4(\text{NH}_2\text{C}_{10}\text{H}_6\text{NH})_2]$ (**19**)

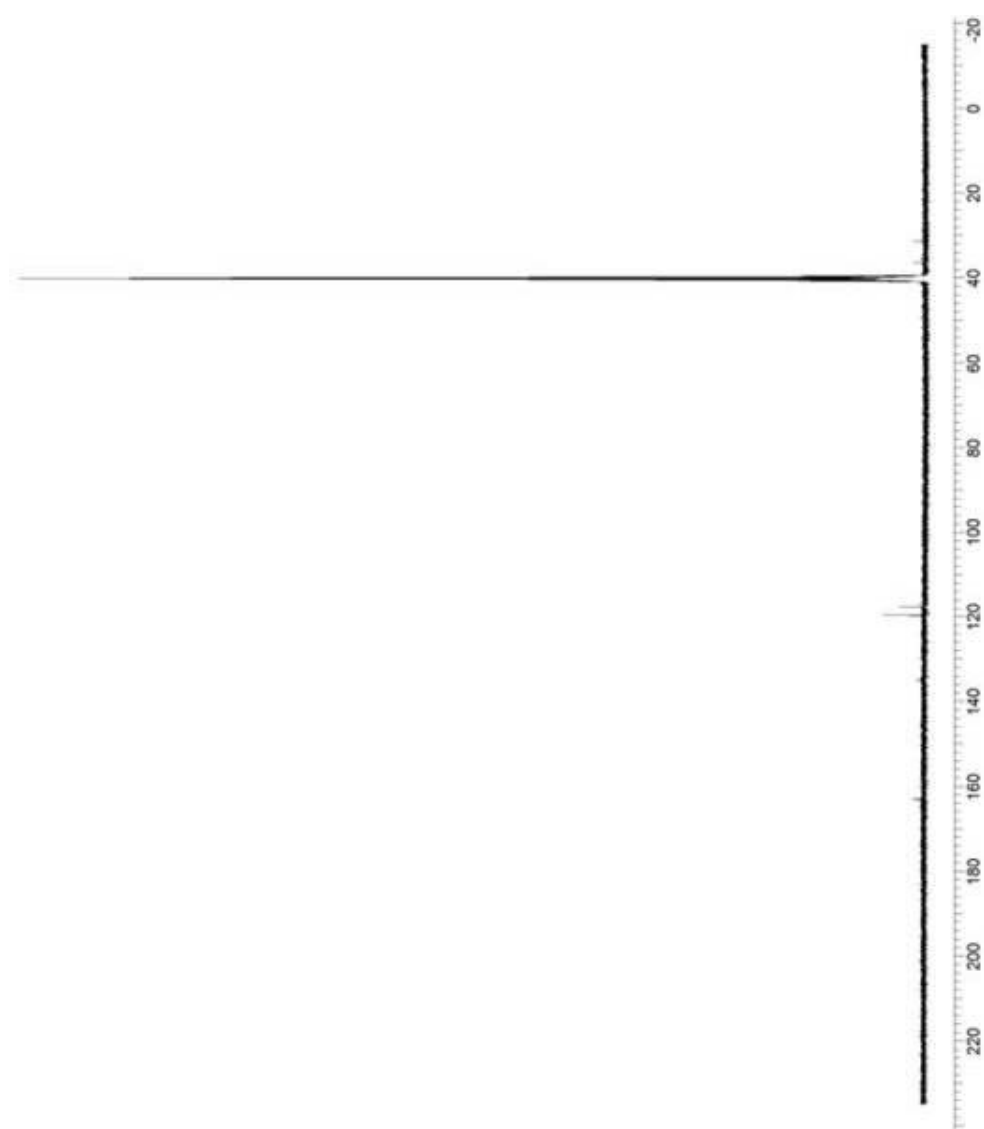


Figure A.44. ^{13}C NMR spectrum of $[\text{Mo}_2\text{O}_2(\mu_2\text{-O})\text{Cl}_4(\text{NH}_2\text{C}_6\text{H}_4\text{Cl}_2\text{NH})_2]$ (**20**)

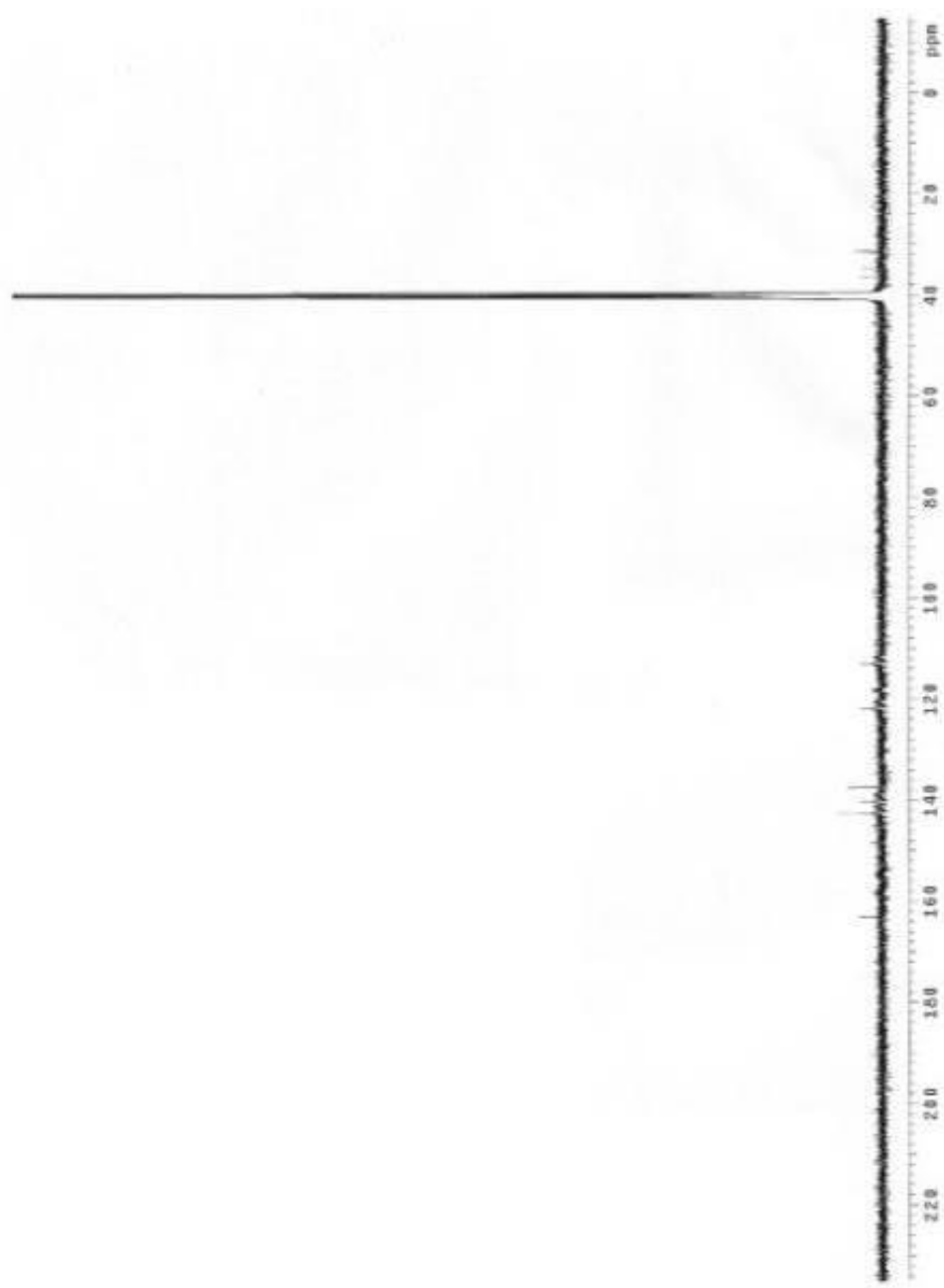


Figure A.45. ^{13}C NMR spectrum of $[\text{Mo}_2\text{O}_2(\mu_2\text{-O})\text{Cl}_4(\text{NH}_2\text{C}_6\text{H}_3\text{NO}_2\text{NH}_2)_2]$ (**21**)

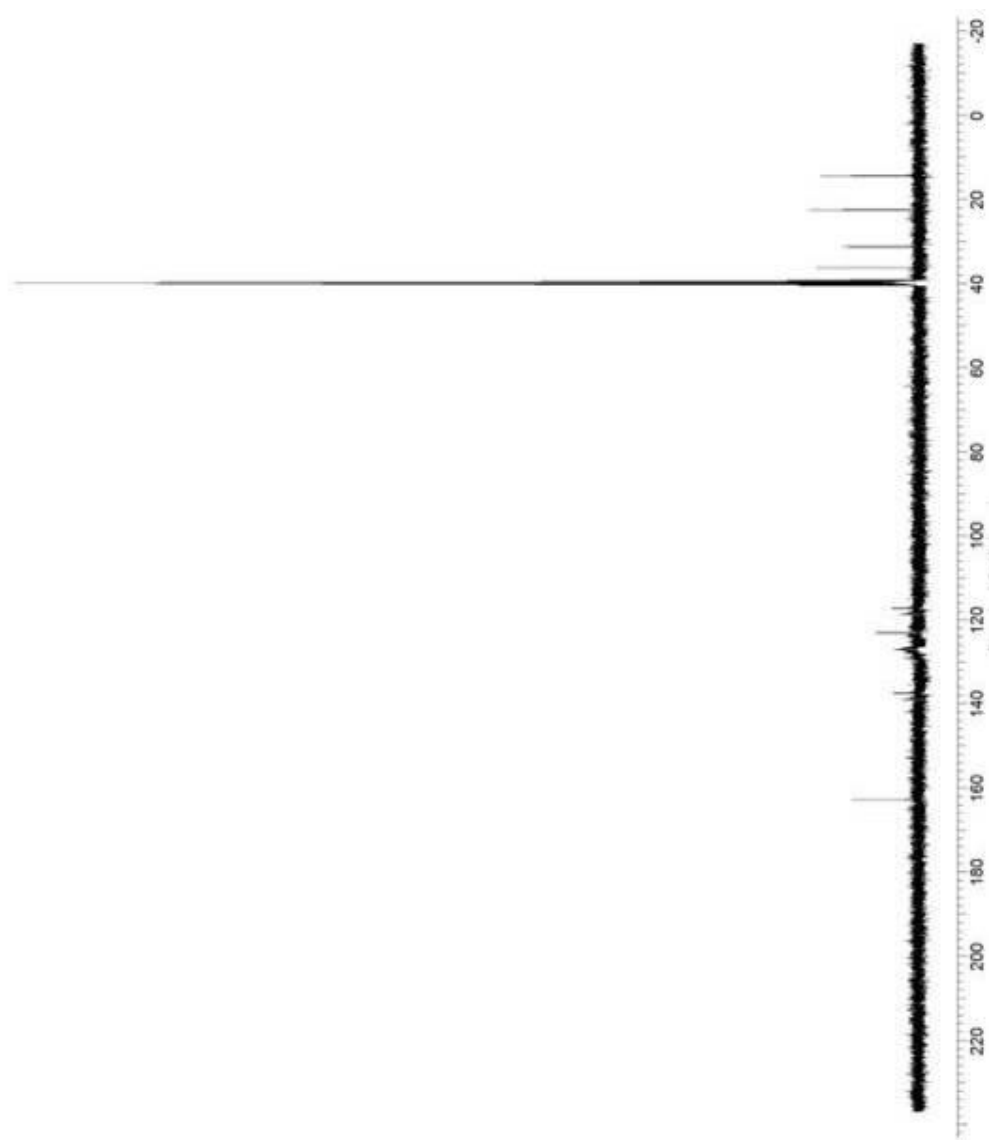


Figure A.46. ^{13}C NMR spectrum of $[\text{Mo}_2\text{O}_2(\mu_2\text{-O})\text{Cl}_4(\text{NH}_2\text{C}_6\text{H}_3\text{CINH})_2]$ (**22**)

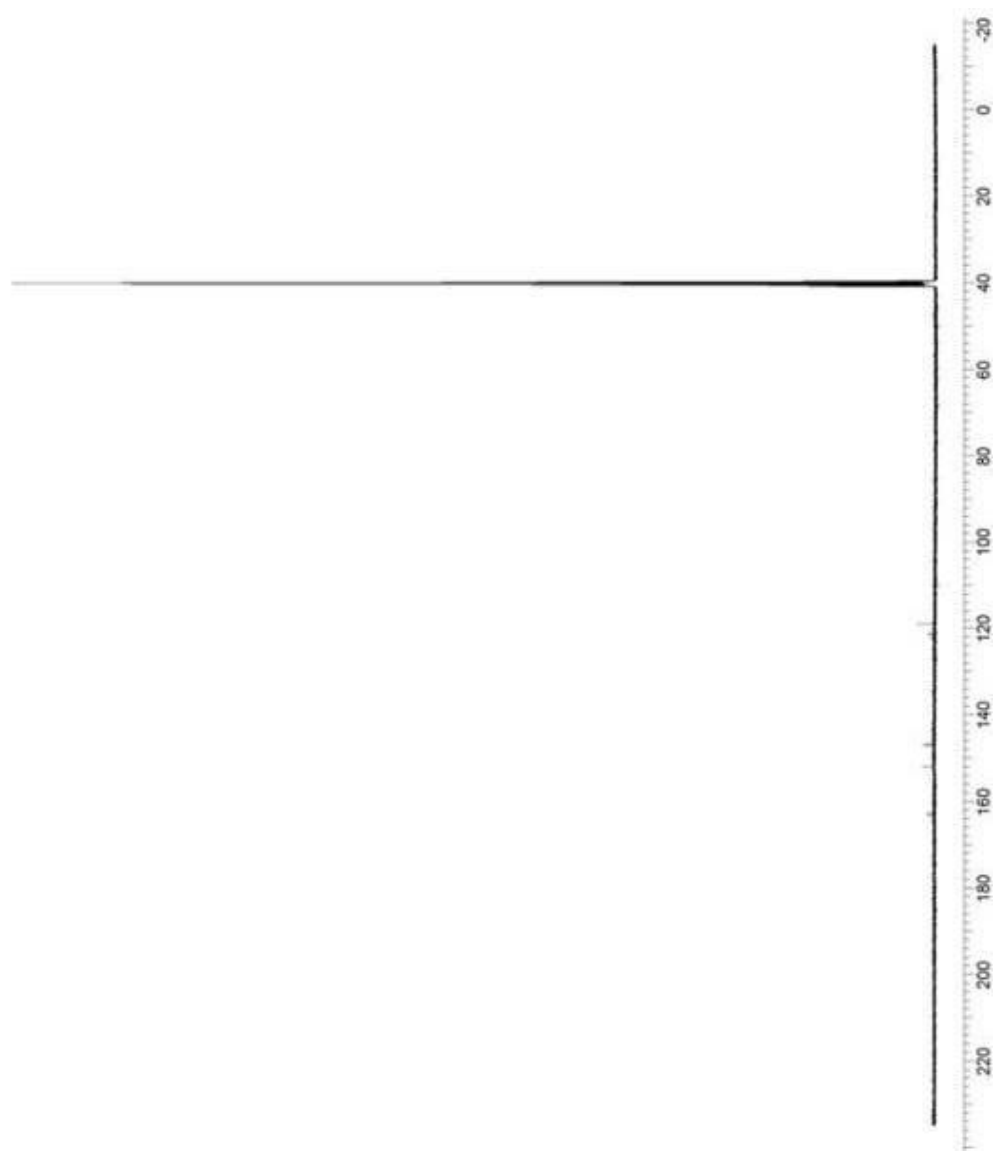


Figure A.47. ^{13}C NMR spectrum of $[\text{Mo}_2\text{O}_2(\mu_2\text{-O})\text{Cl}_4(\text{NHC}_6\text{H}_4\text{Cl}_2\text{NH})_2]$ (**23**)

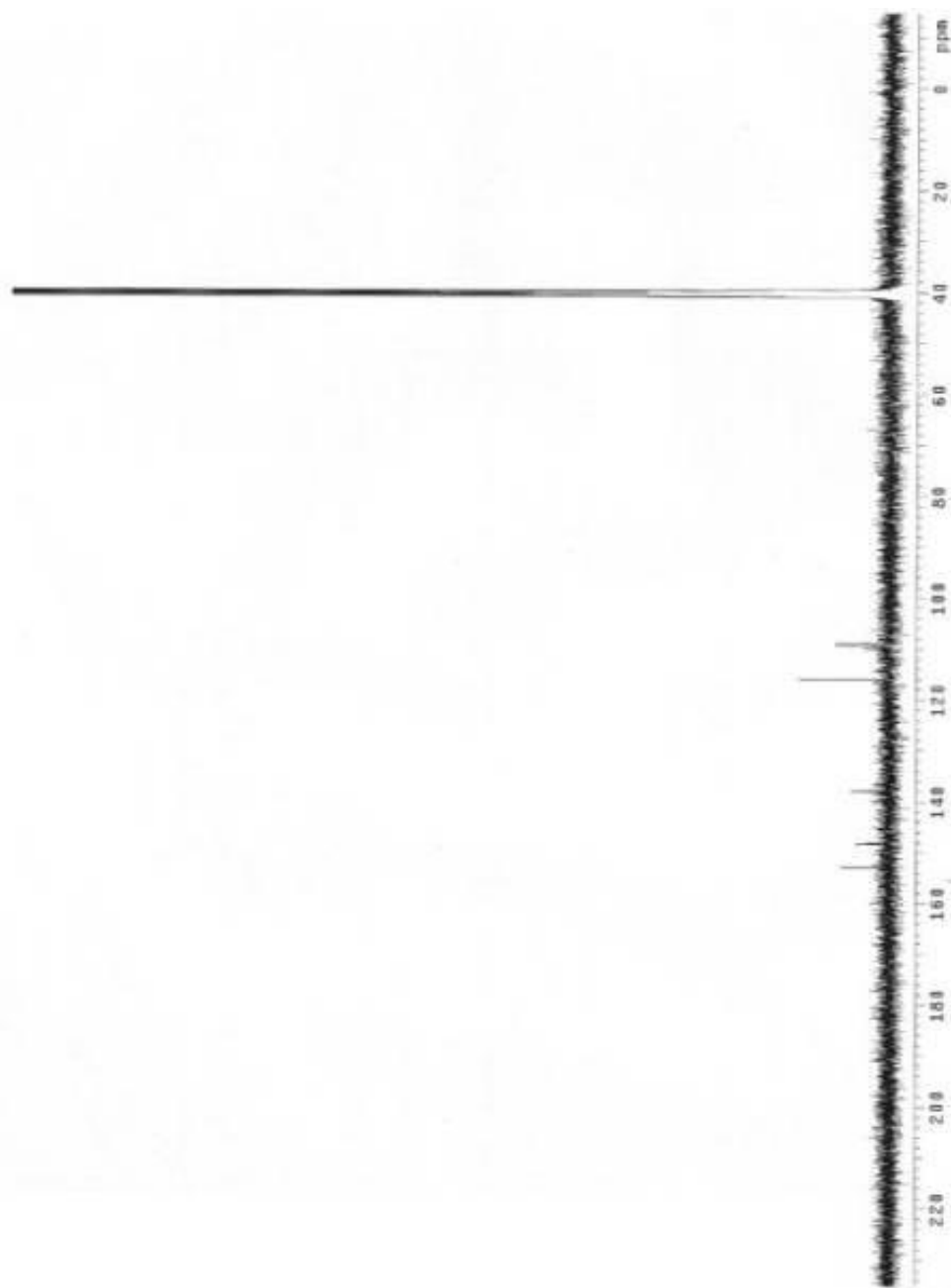


Figure A.48. ^{13}C NMR spectrum of $[\text{Mo}_2\text{O}_2(\mu_2\text{-O})\text{Cl}_4(\text{NH}_2\text{C}_6\text{H}_3\text{FN})_2]$ (**24**)

APPENDIX B

FT-IR SPECTRA OF THE PRODUCTS

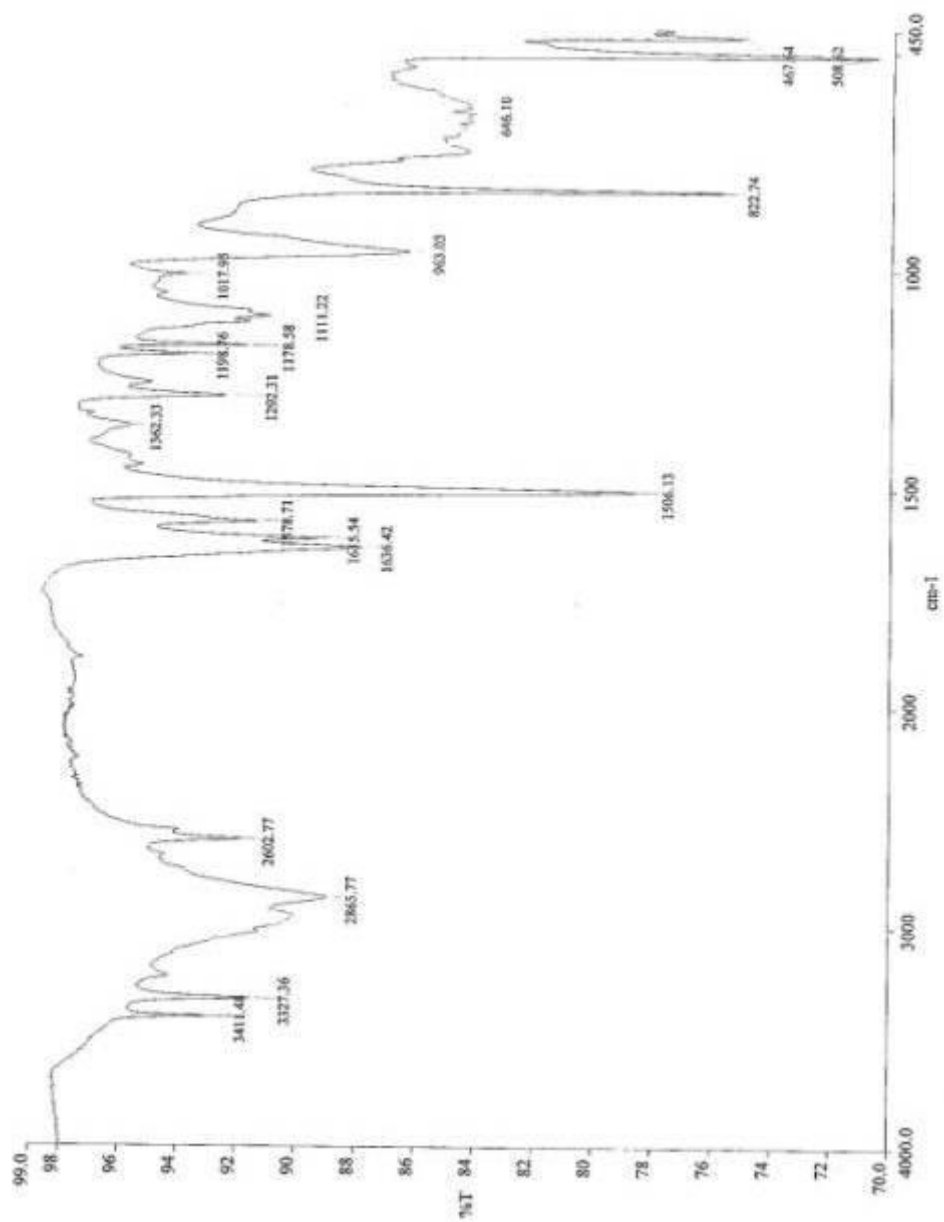


Figure B.1. FT-IR spectrum of $[\text{Mo}_2\text{O}_2(\mu_2\text{-O})\text{Cl}_4(\text{NH}_2\text{C}_6\text{H}_4\text{NH})_2]$ (1)

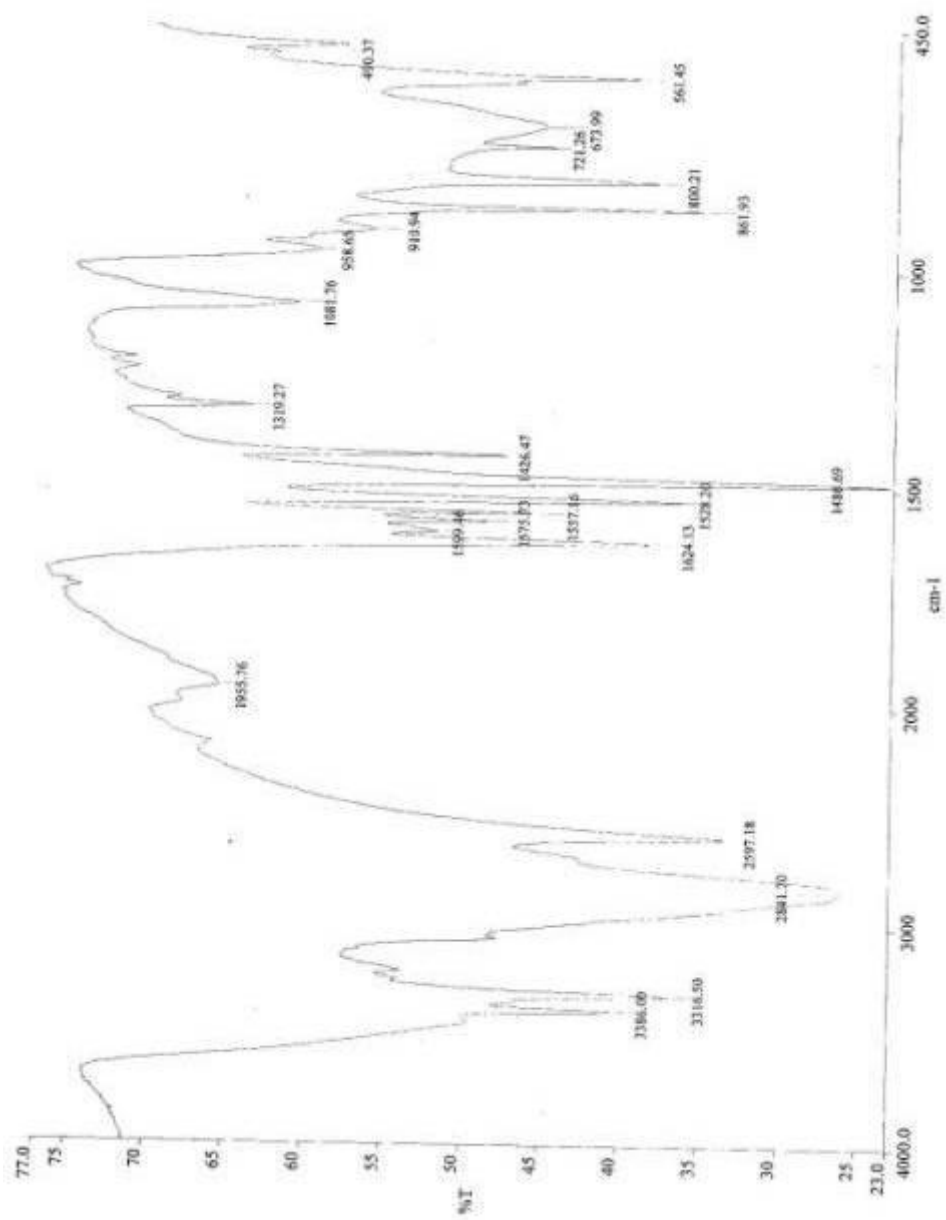


Figure B.2. FT-IR spectrum of $[\text{MoO}_2\text{Cl}_2(\text{NH}_2\text{C}_6\text{H}_4\text{Cl}_2\text{NH})]$ (2)

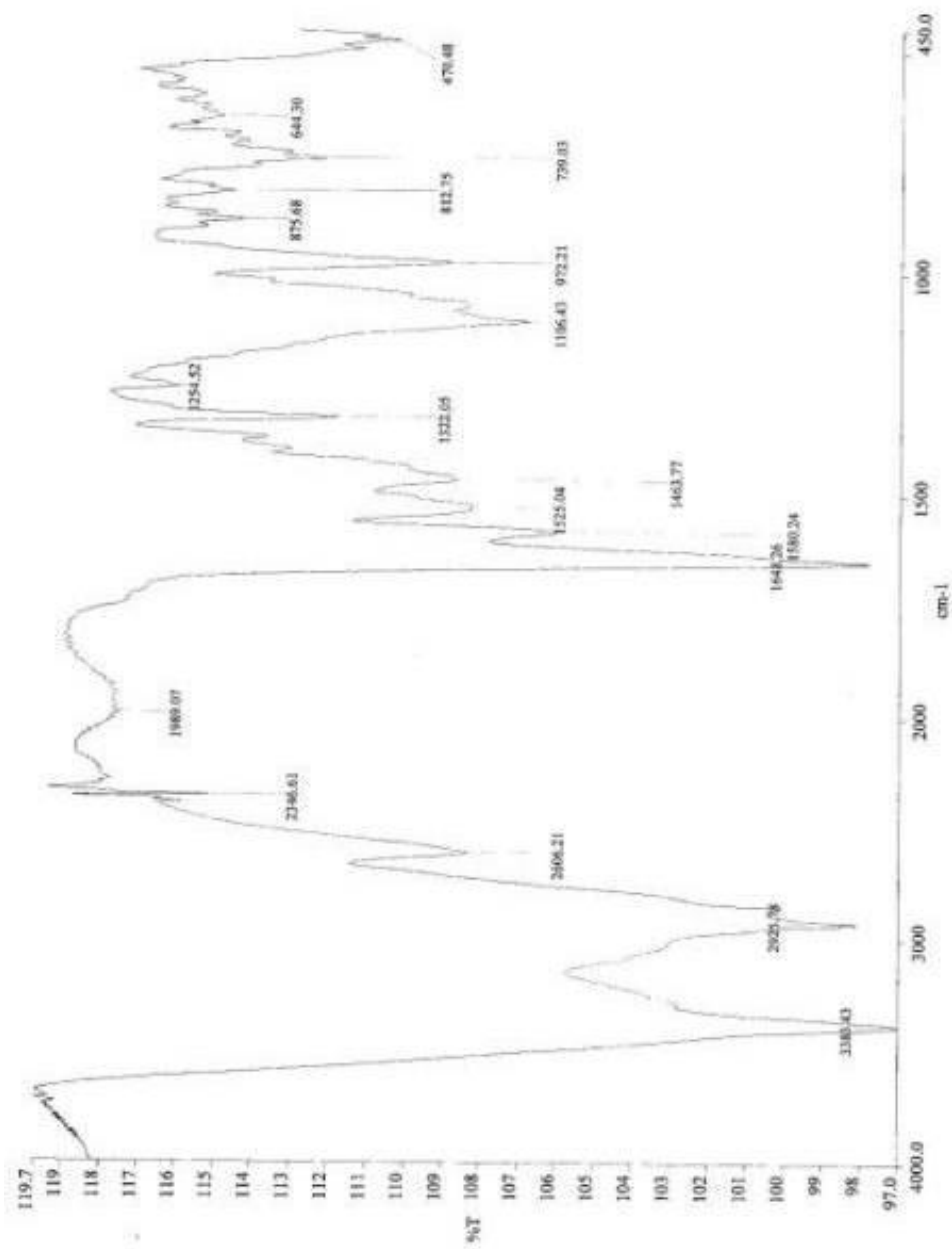


Figure B.3. FT-IR spectrum of $[\text{Mo}_2\text{O}_2(\mu_2\text{-O})\text{Cl}_4(\text{NH}_2\text{C}_6(\text{CH}_3)_4\text{NH}_2)_2]$ (3)

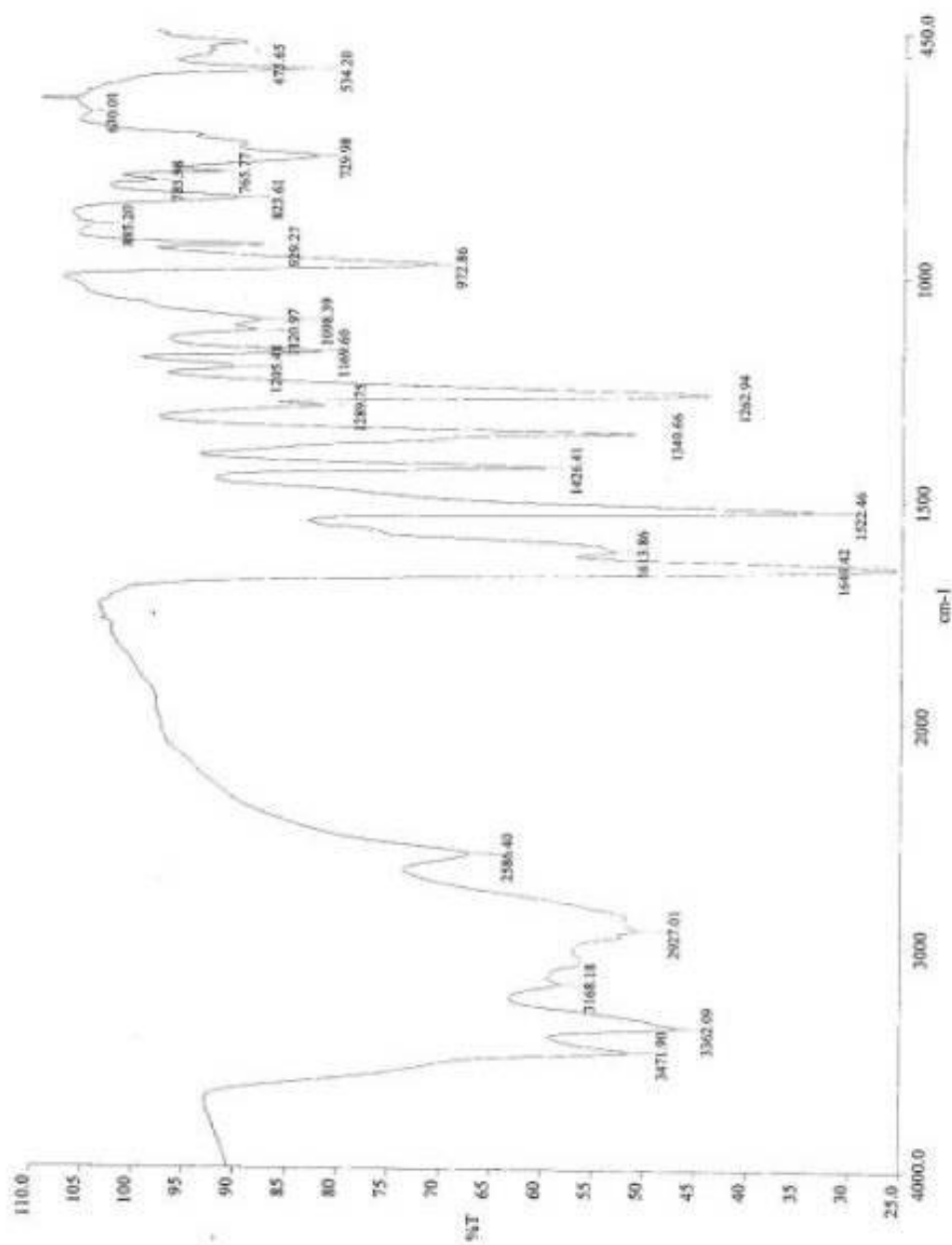


Figure B.4. FT-IR spectrum of $[\text{Mo}_2\text{O}_2(\mu_2\text{-O})\text{Cl}_4(\text{NH}_2\text{C}_6\text{H}_3\text{NO}_2\text{NH}_2)_2]$ (4)

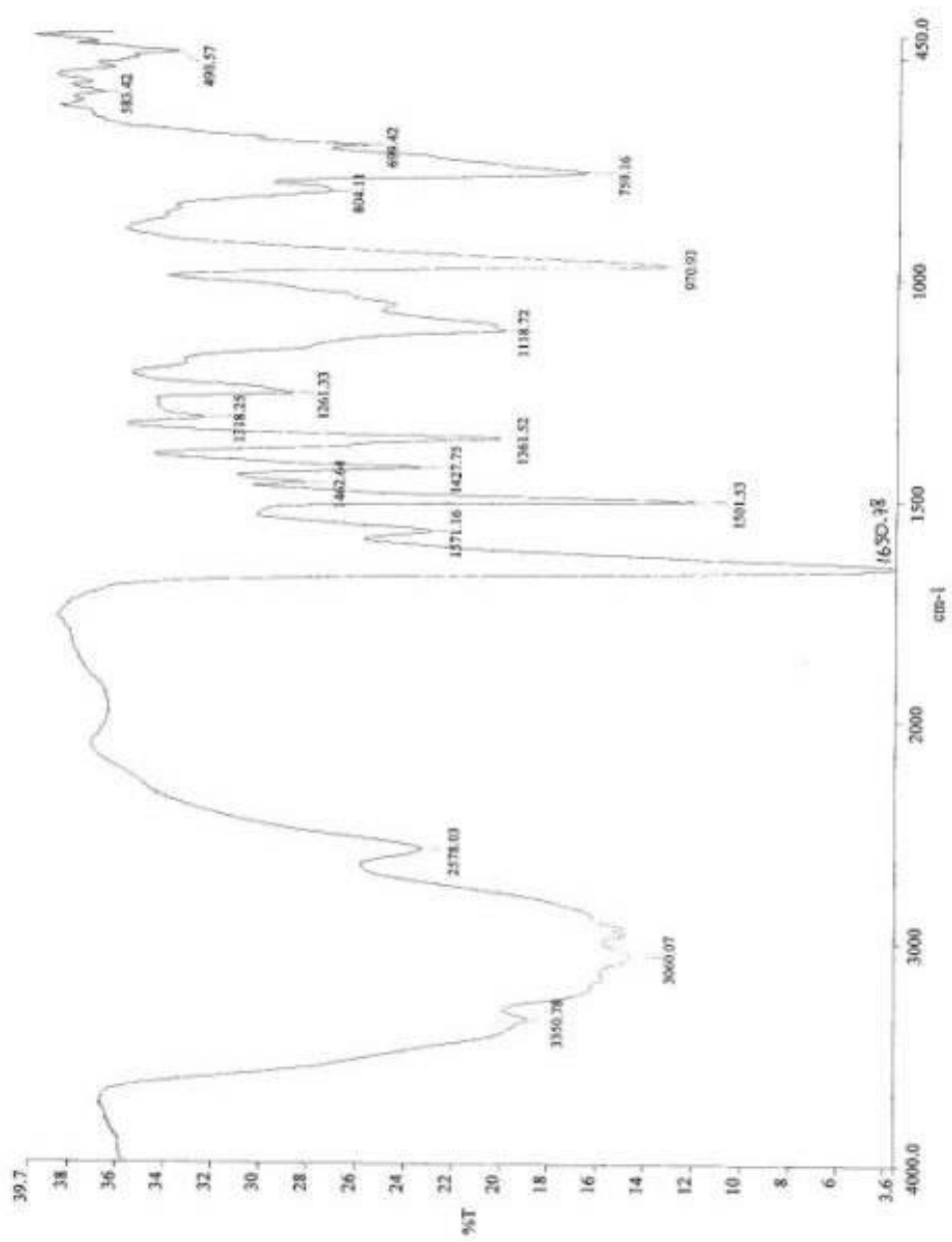


Figure B.5. FT-IR spectrum of $[\text{Mo}_2\text{O}_2(\mu_2\text{-O})\text{Cl}_4(\text{NH}_2\text{C}_6\text{H}_4\text{NH}_2)_2]$ (5)

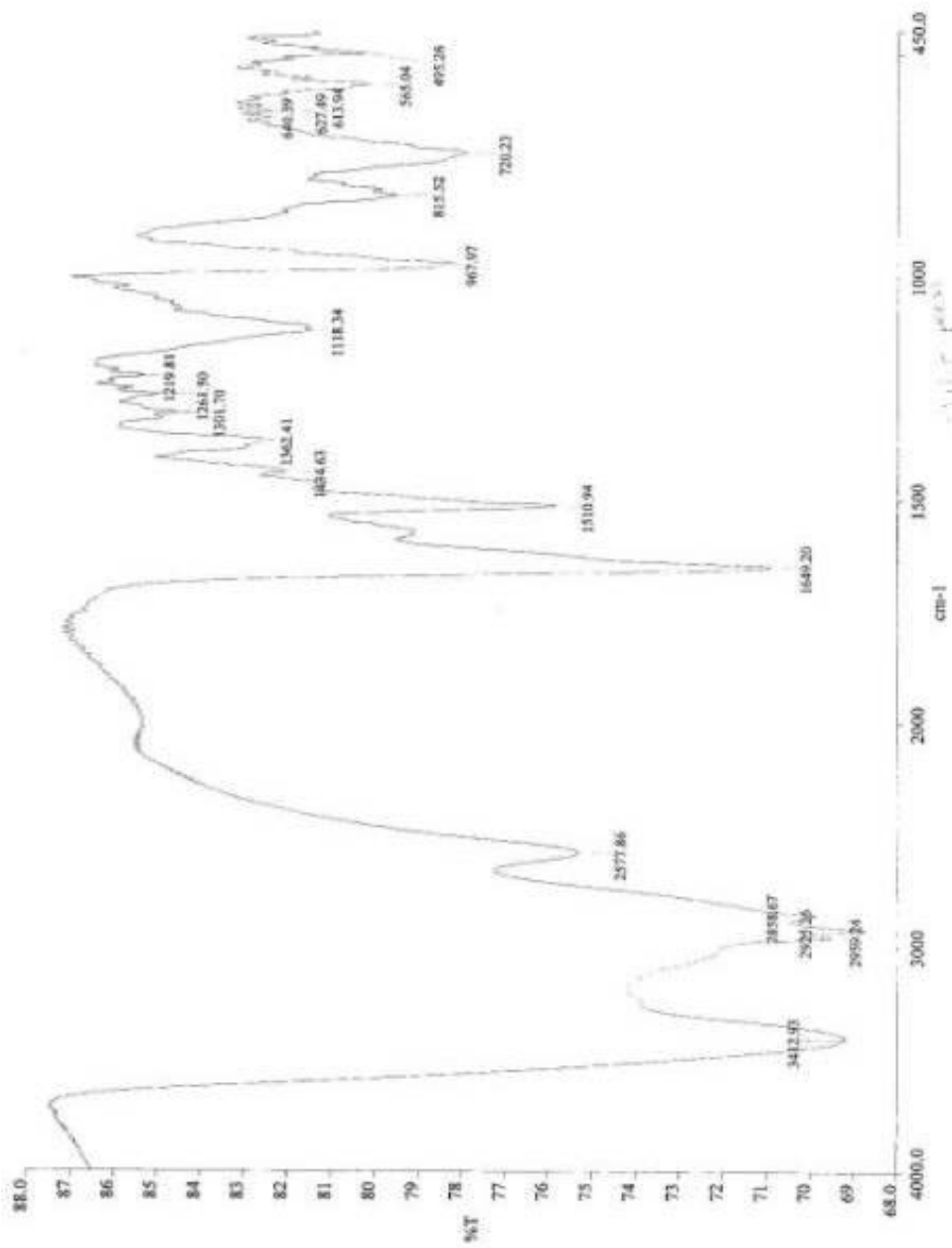


Figure B.6. FT-IR spectrum of [Mo₂O₂(μ₂-O)Cl₄(NH₂C₆H₃(CH₃)NH₂)] (6)

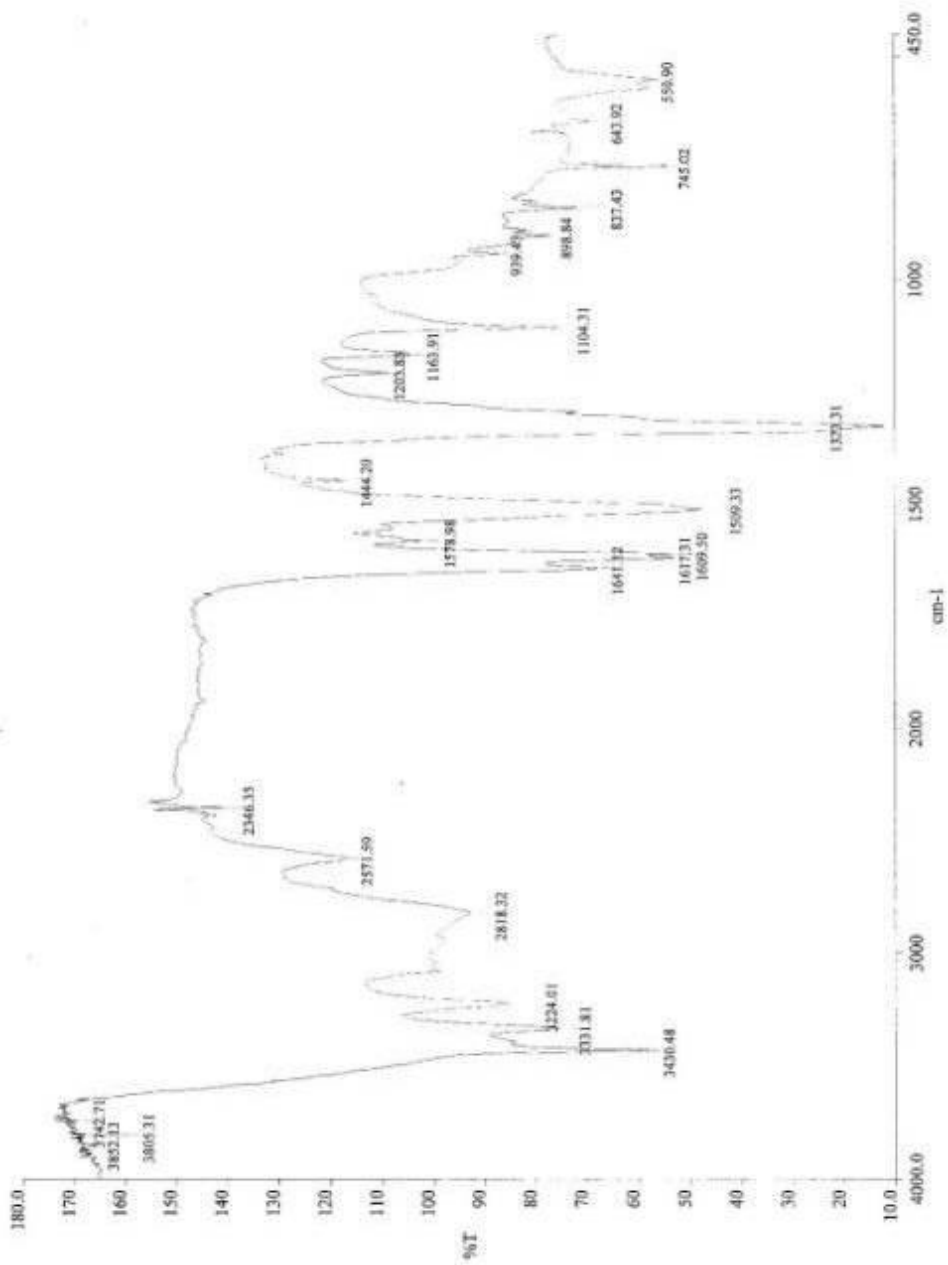


Figure B.7. FT-IR spectrum of $[\text{MoO}_2\text{Cl}_2(\text{NHC}_6\text{H}_3\text{NO}_2\text{NH})]$ (7)

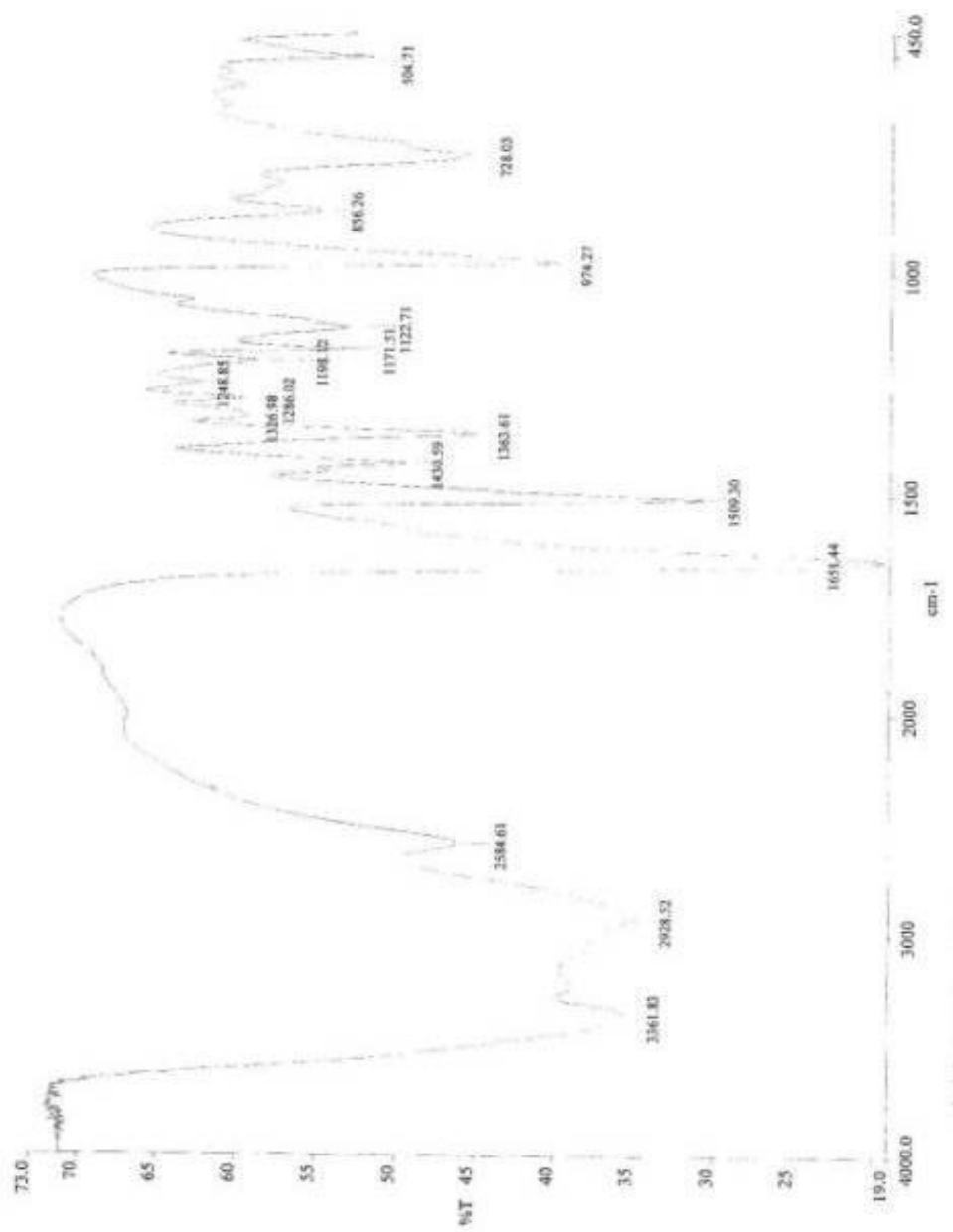


Figure B.8. FT-IR spectrum of $[\text{Mo}_2\text{O}_2(\mu_2\text{-O})\text{Cl}_4(\text{NH}_2\text{C}_6\text{H}_3\text{FNH}_2)_2]$ (**8**)

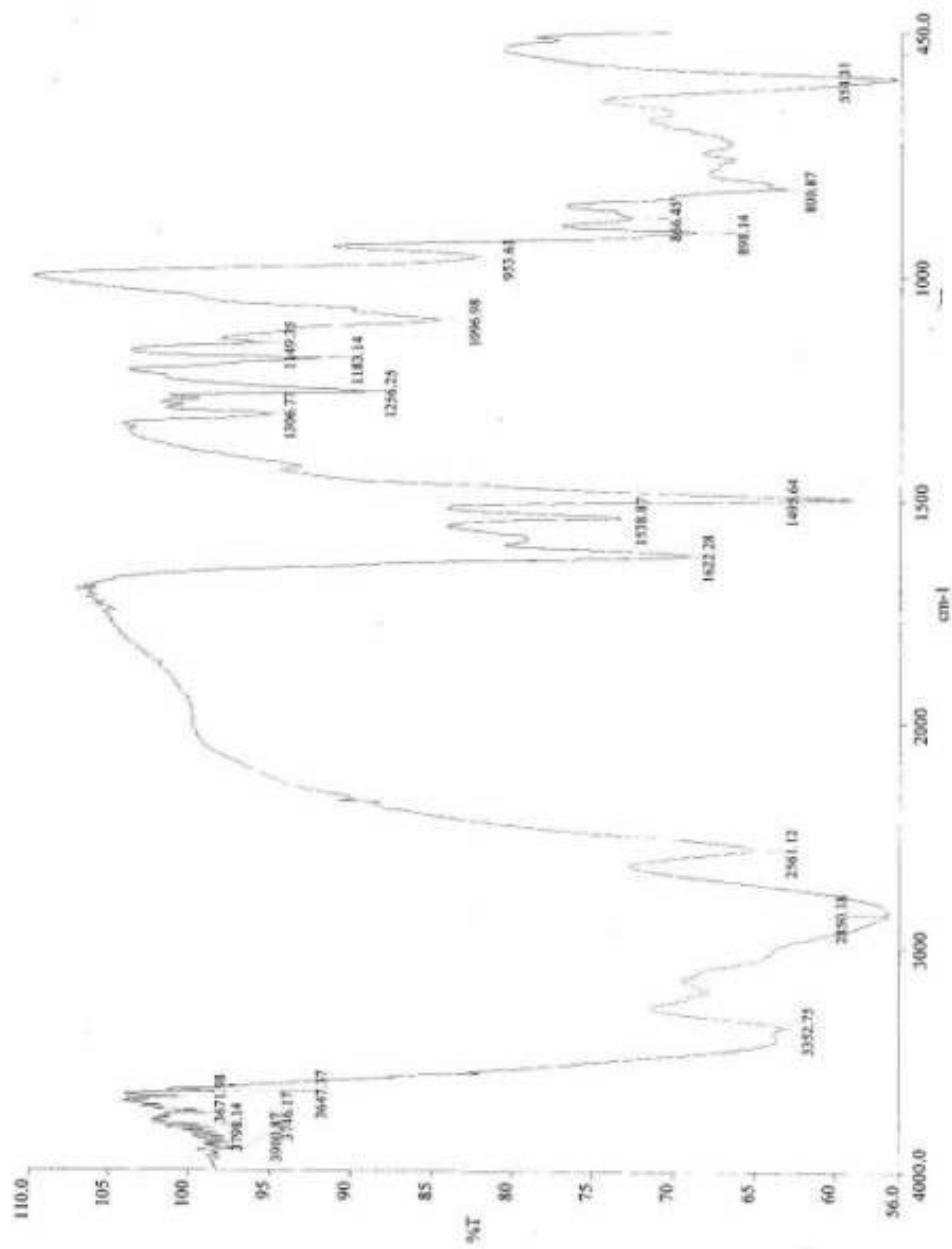


Figure B.9. FT-IR spectrum of $[\text{MoO}_2\text{Cl}_2(\text{NHC}_6\text{H}_3\text{CINH})]$ (9)

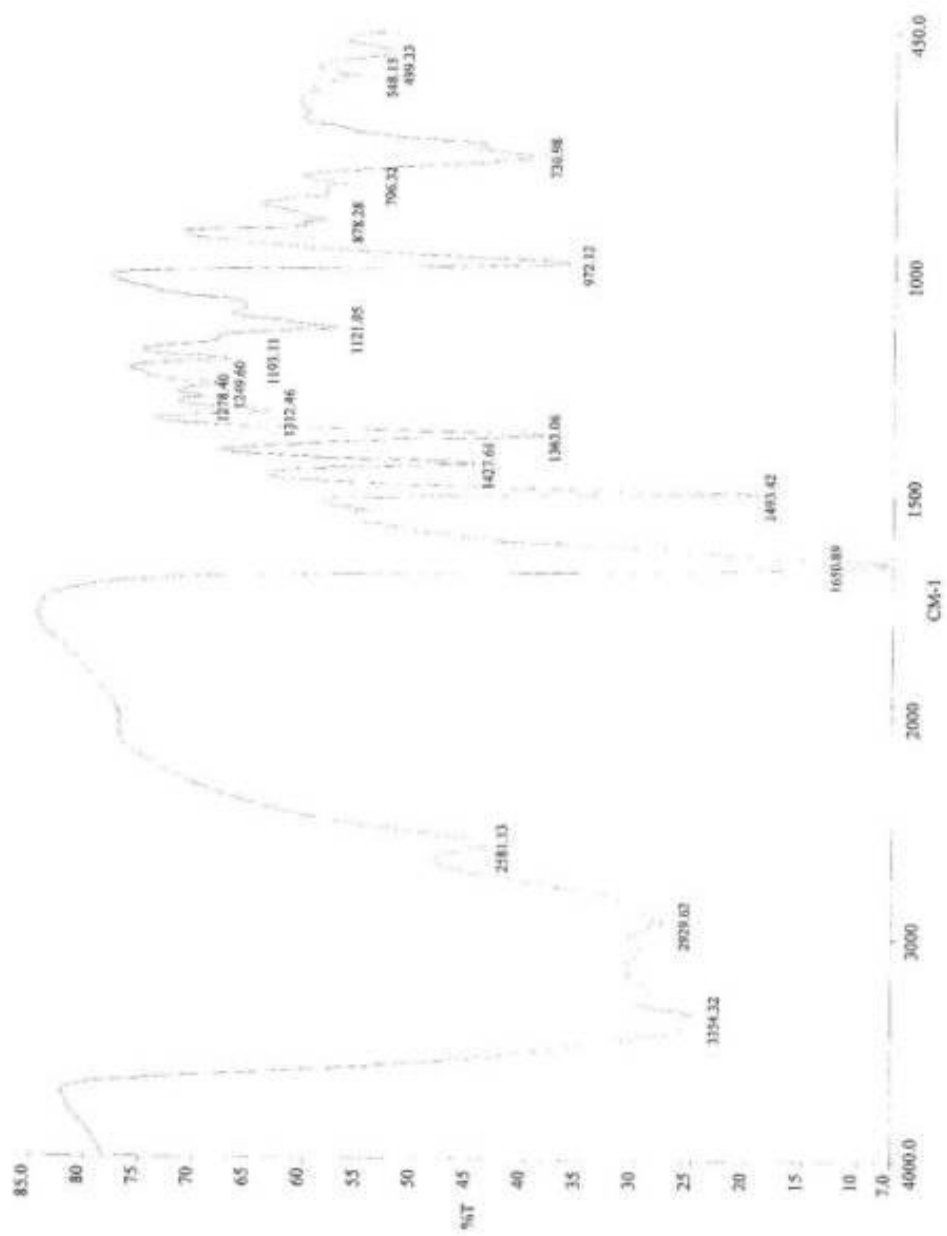


Figure B.10. FT-IR spectrum of $[\text{Mo}_2\text{O}_2(\mu_2\text{-O})\text{Cl}_4(\text{NH}_2\text{C}_6\text{H}_3\text{BrNH}_2)_2]$ (10)

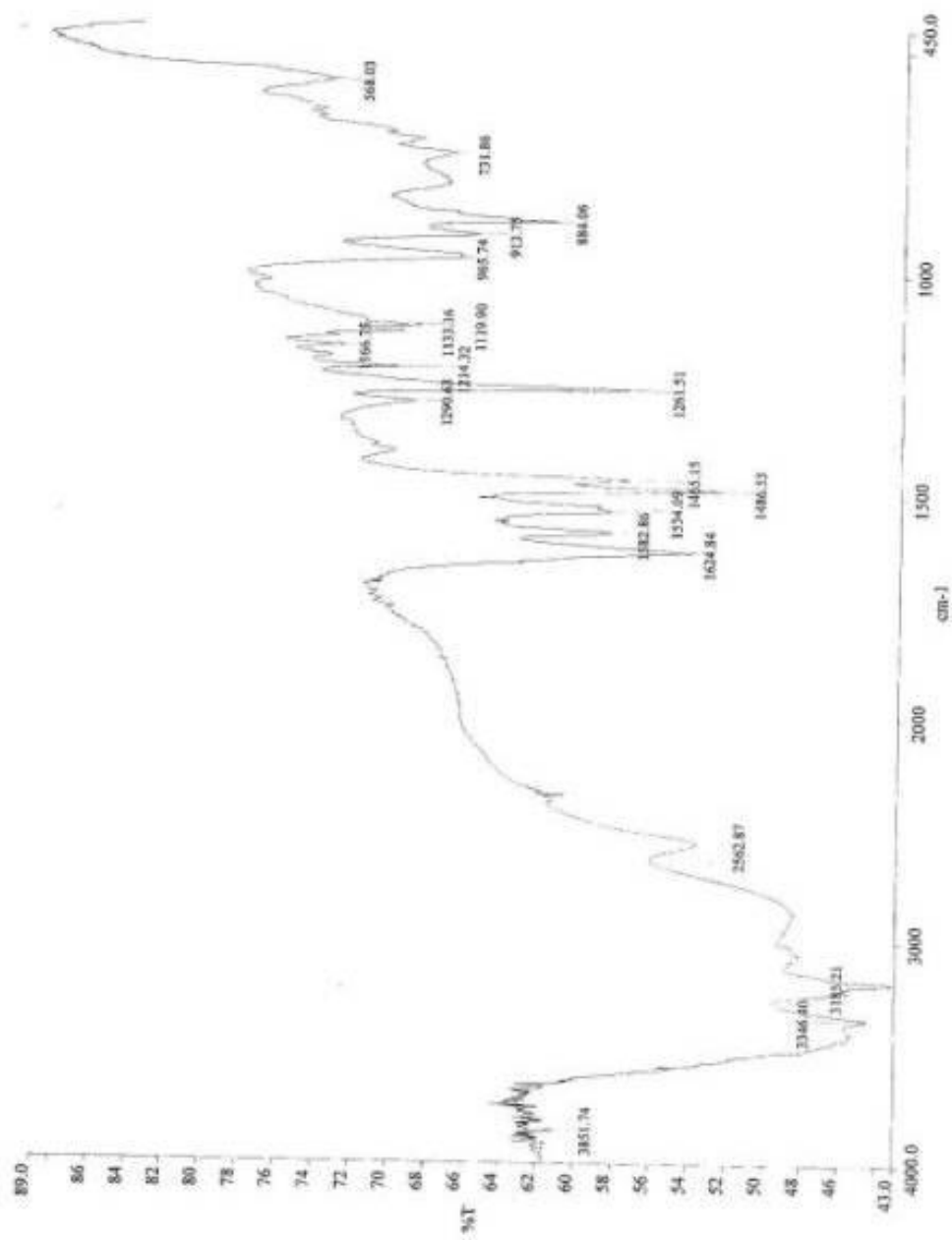


Figure B.11. FT-IR spectrum of $[\text{MoO}_2\text{Cl}_2(\text{NH}_2\text{C}_6\text{H}_4\text{Cl}_2\text{N})]$ (11)

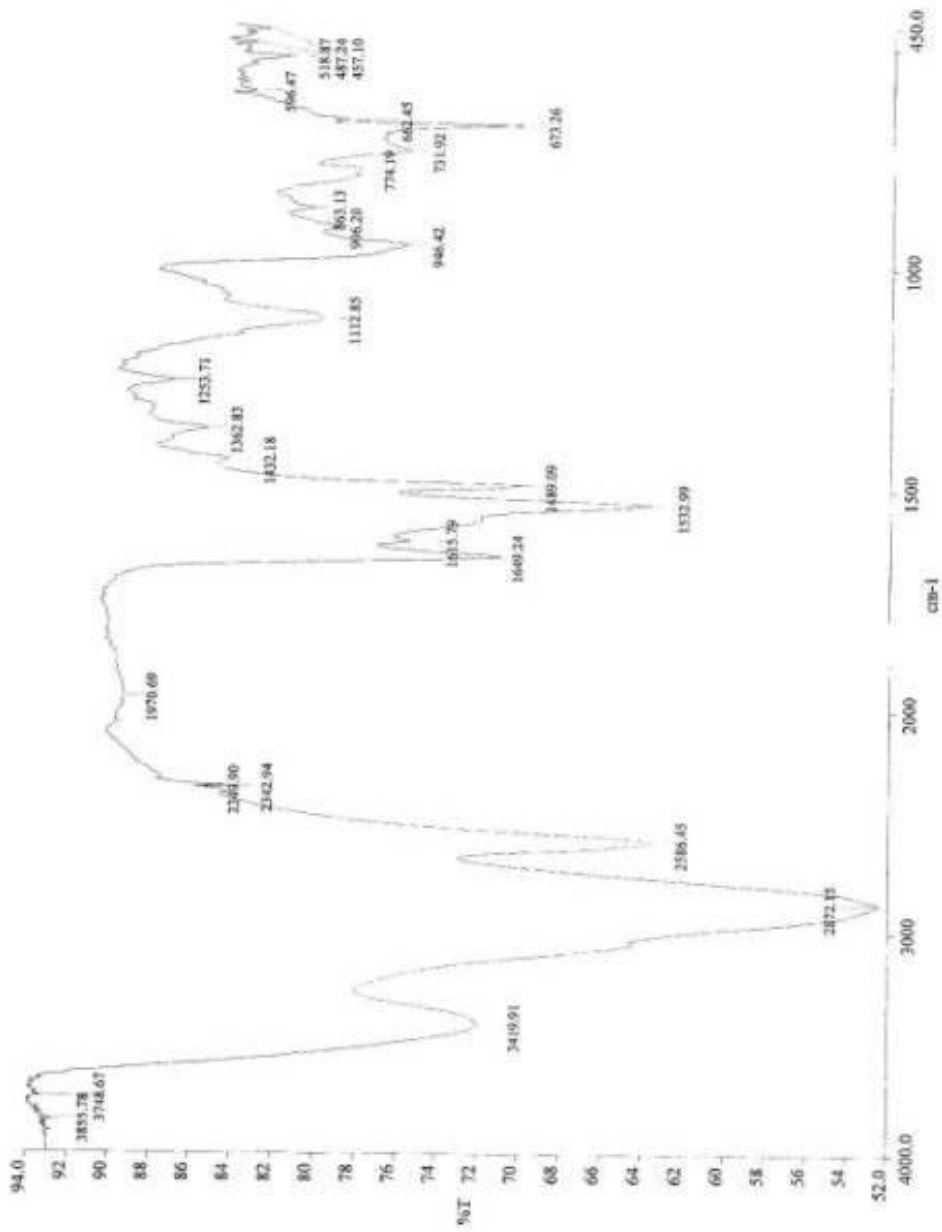


Figure B.12. FT-IR spectrum of $[\text{Mo}_2\text{O}_2(\mu_2\text{-O})\text{Cl}_4(\text{NH}_2\text{C}_6\text{H}_4\text{N})_2]$ (12)

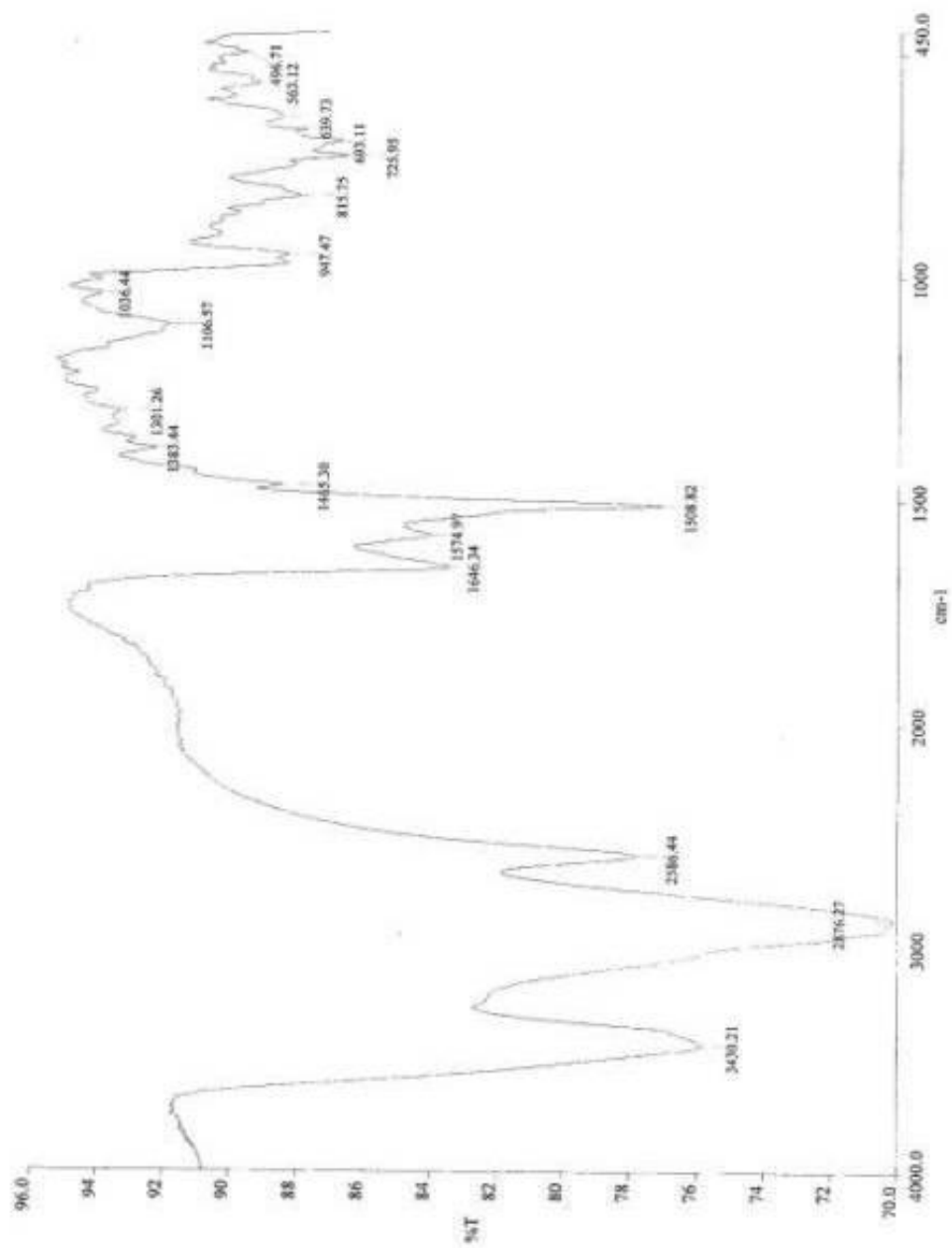


Figure B.13. FT-IR spectrum of $[\text{Mo}_2\text{O}_2(\mu_2\text{-O})\text{Cl}_4(\text{NH}_2\text{C}_6\text{H}_3(\text{CH}_3)\text{N})_2]$ (**13**)

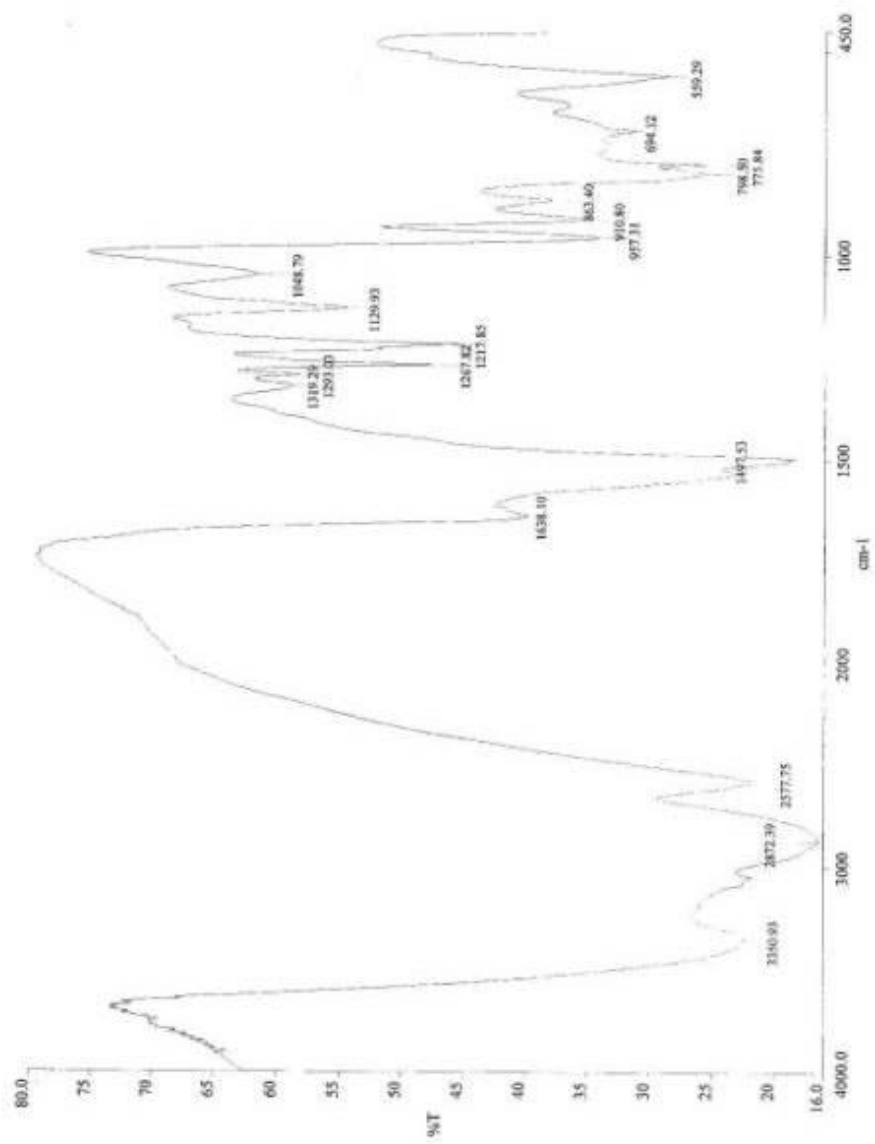


Figure B.14. FT-IR spectrum of $[\text{MoO}_2\text{Cl}_2(\text{NH}_2\text{C}_6\text{H}_3\text{FNH})]$ (14)

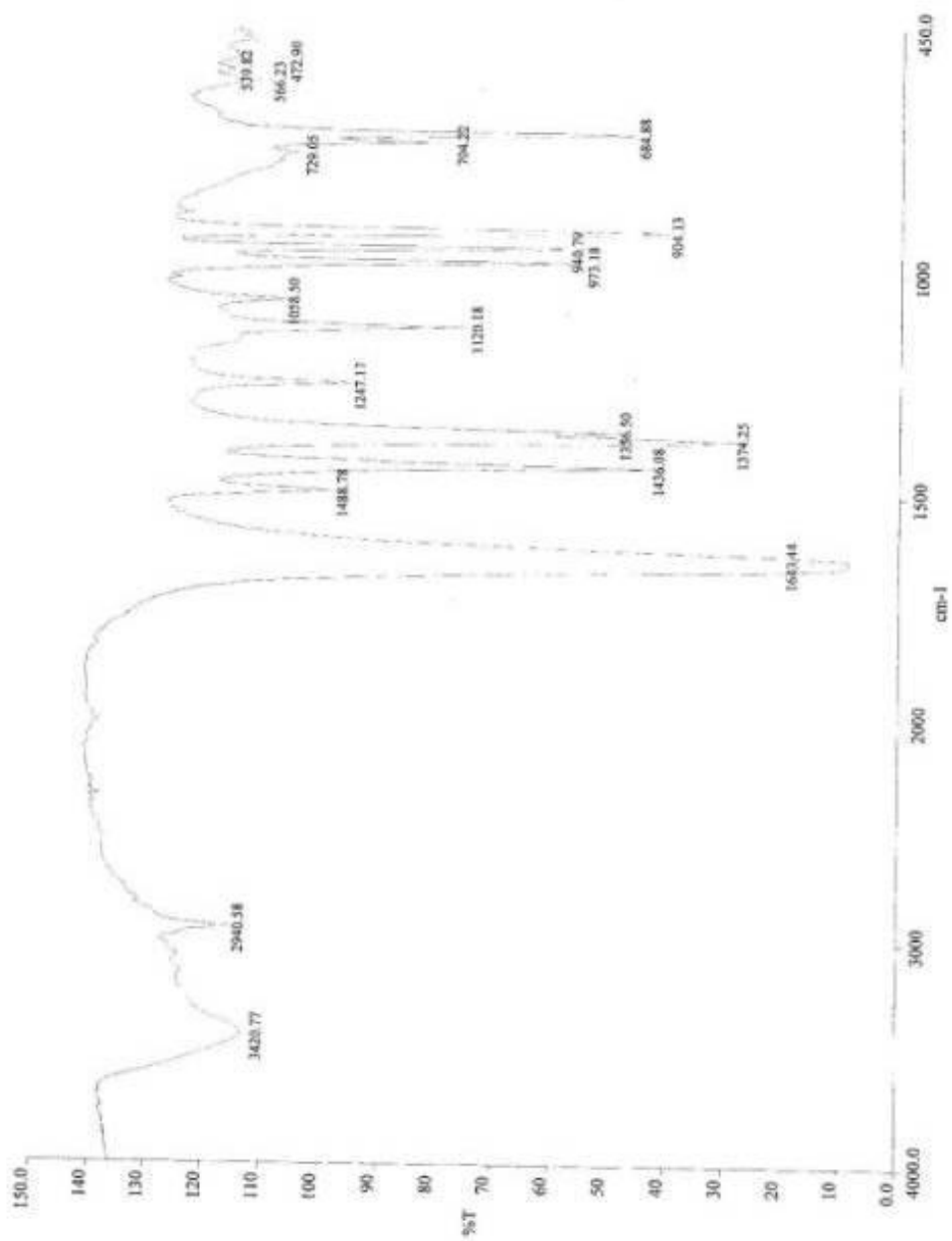


Figure B.15. FT-IR spectrum of $[\text{Mo}_2\text{O}_2(\mu_2\text{-O})\text{Cl}_4(\text{NH}_2\text{C}_6\text{H}_3\text{ClN})_2]$ (15)

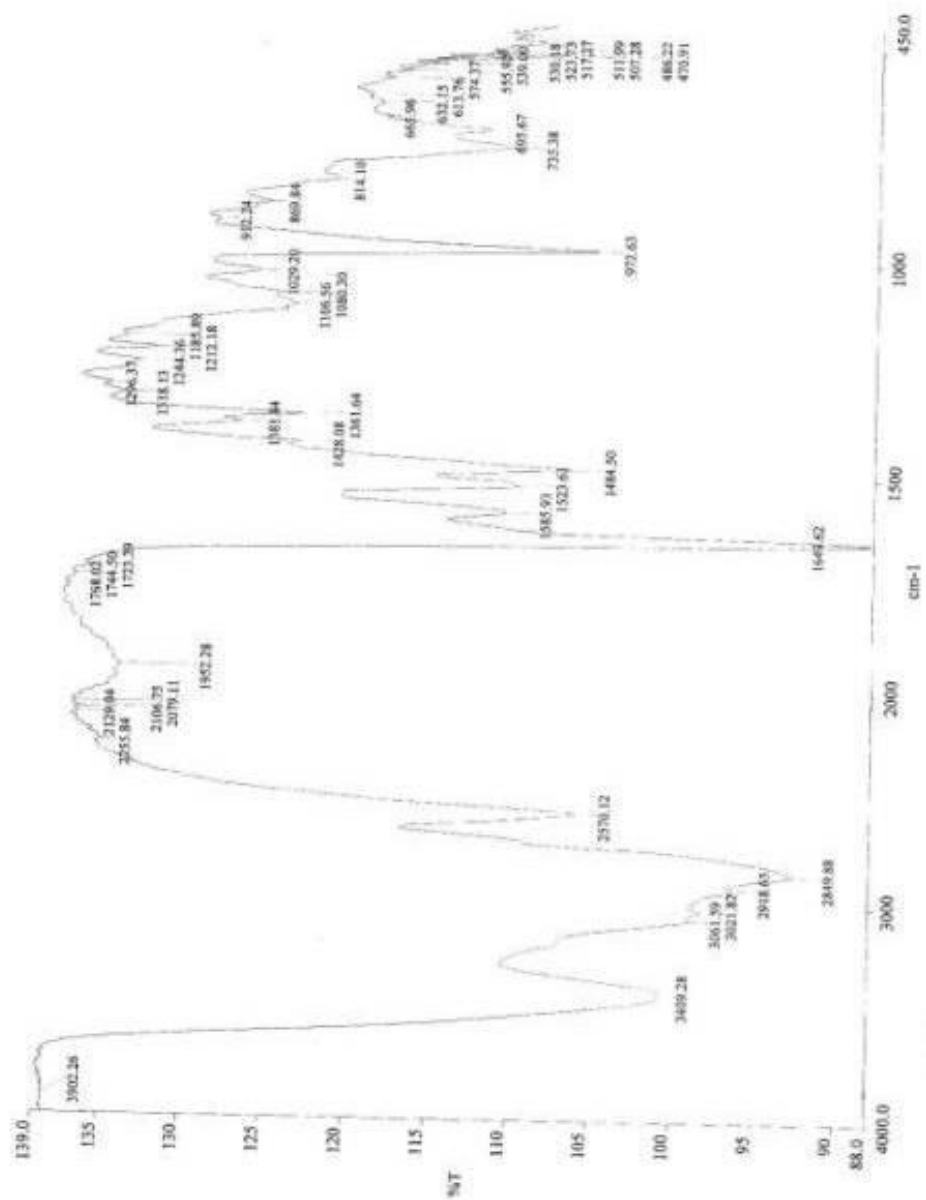


Figure B.16. FT-IR spectrum of $[\text{Mo}_2\text{O}_2(\mu_2\text{-O})\text{Cl}_4(\text{NH}_2\text{C}_6\text{H}(\text{CH}_3)_3\text{N})_2]$ (16)

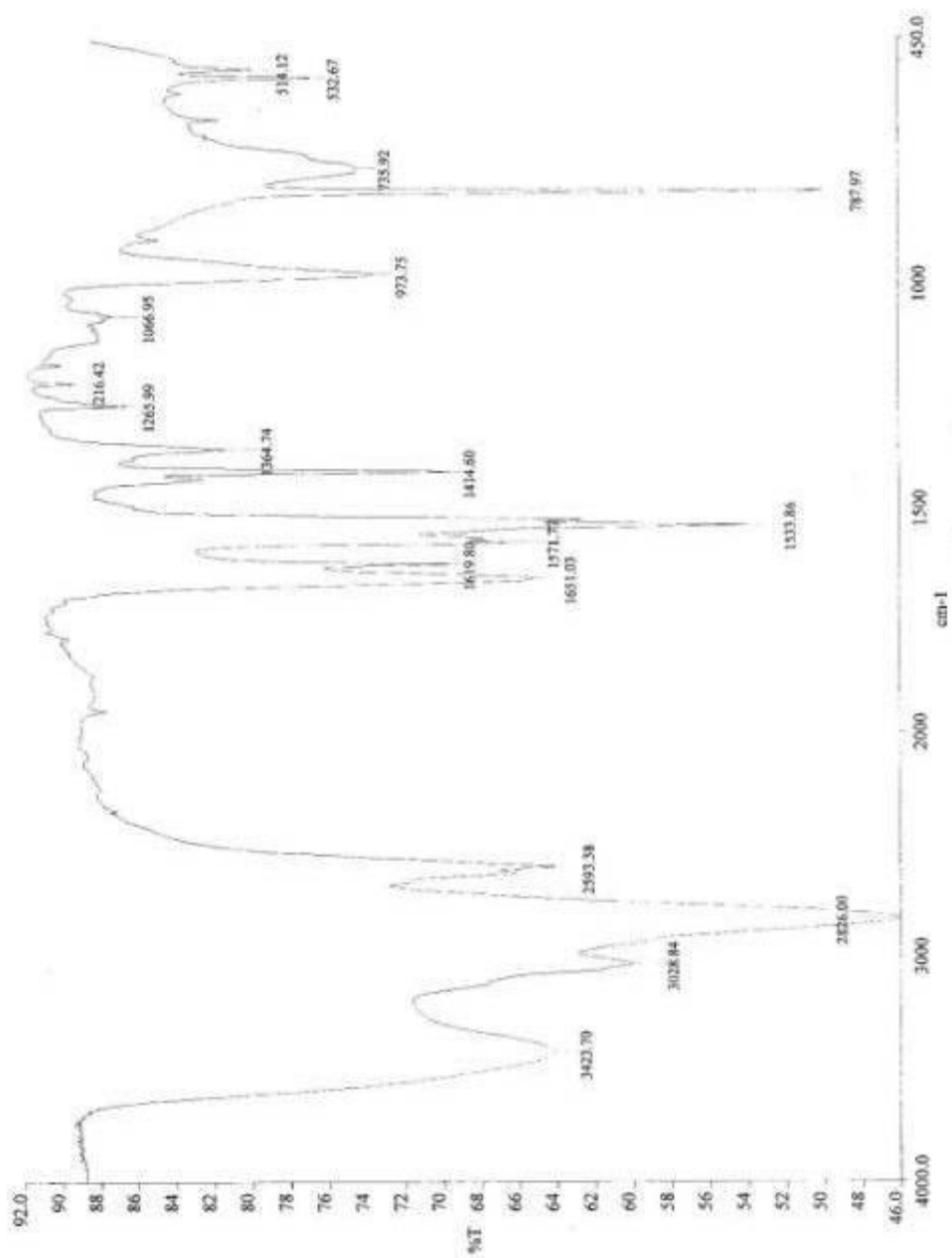


Figure B.17. FT-IR spectrum of $[\text{Mo}_2\text{O}_2(\mu_2\text{-O})\text{Cl}_4(\text{NH}_2\text{C}_{10}\text{H}_6\text{NH})_2]$ (17)

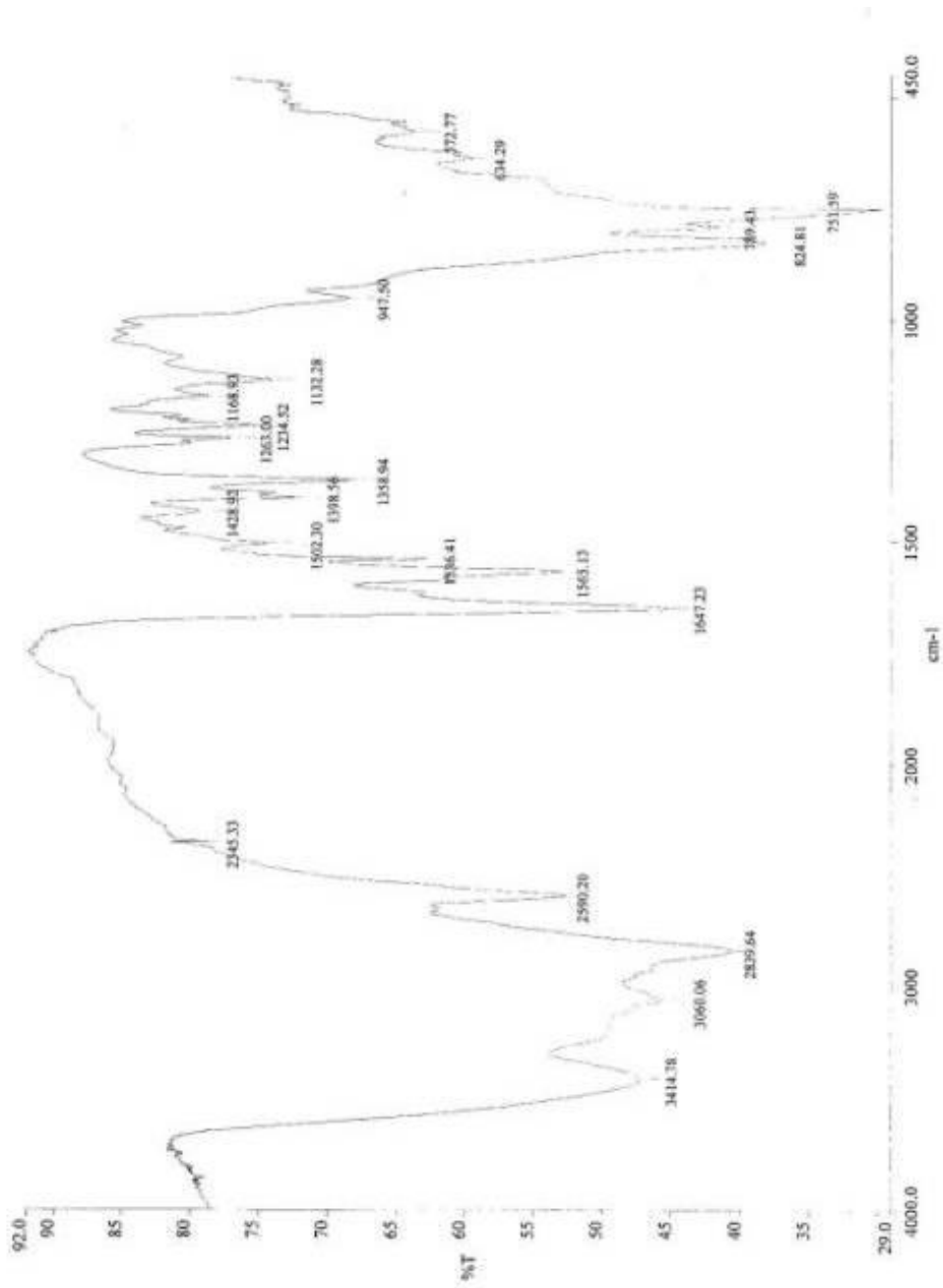


Figure B.18. FT-IR spectrum of $[\text{Mo}_2\text{O}_2(\mu_2\text{-O})\text{Cl}_4(\text{NH}_2\text{C}_{10}\text{H}_6\text{NH})_2]$ (**18**)

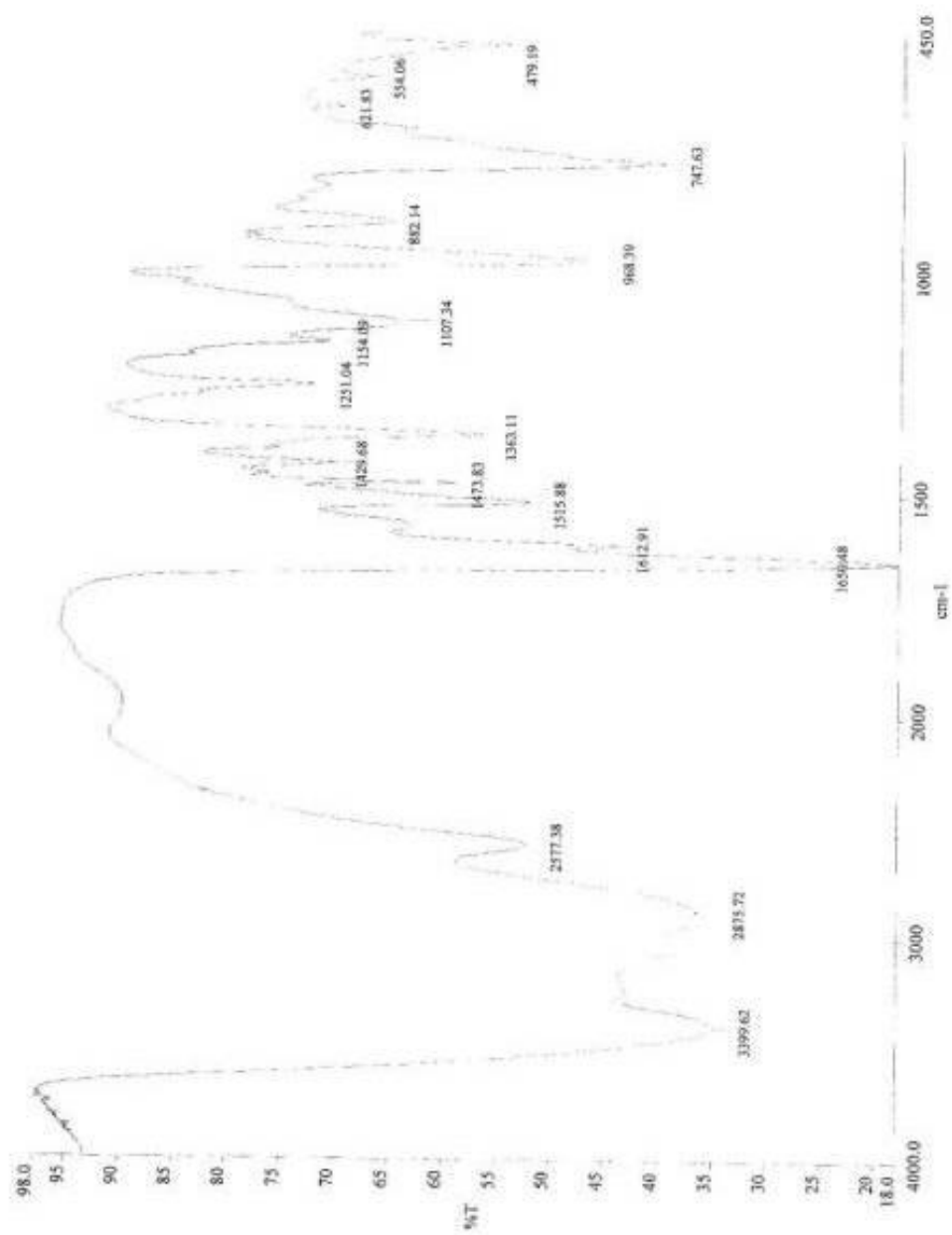


Figure B.19. FT-IR spectrum of $[\text{Mo}_2\text{O}_2(\mu_2\text{-O})\text{Cl}_4(\text{NH}_2\text{C}_{10}\text{H}_6\text{NH}_2)_2]$ (19)

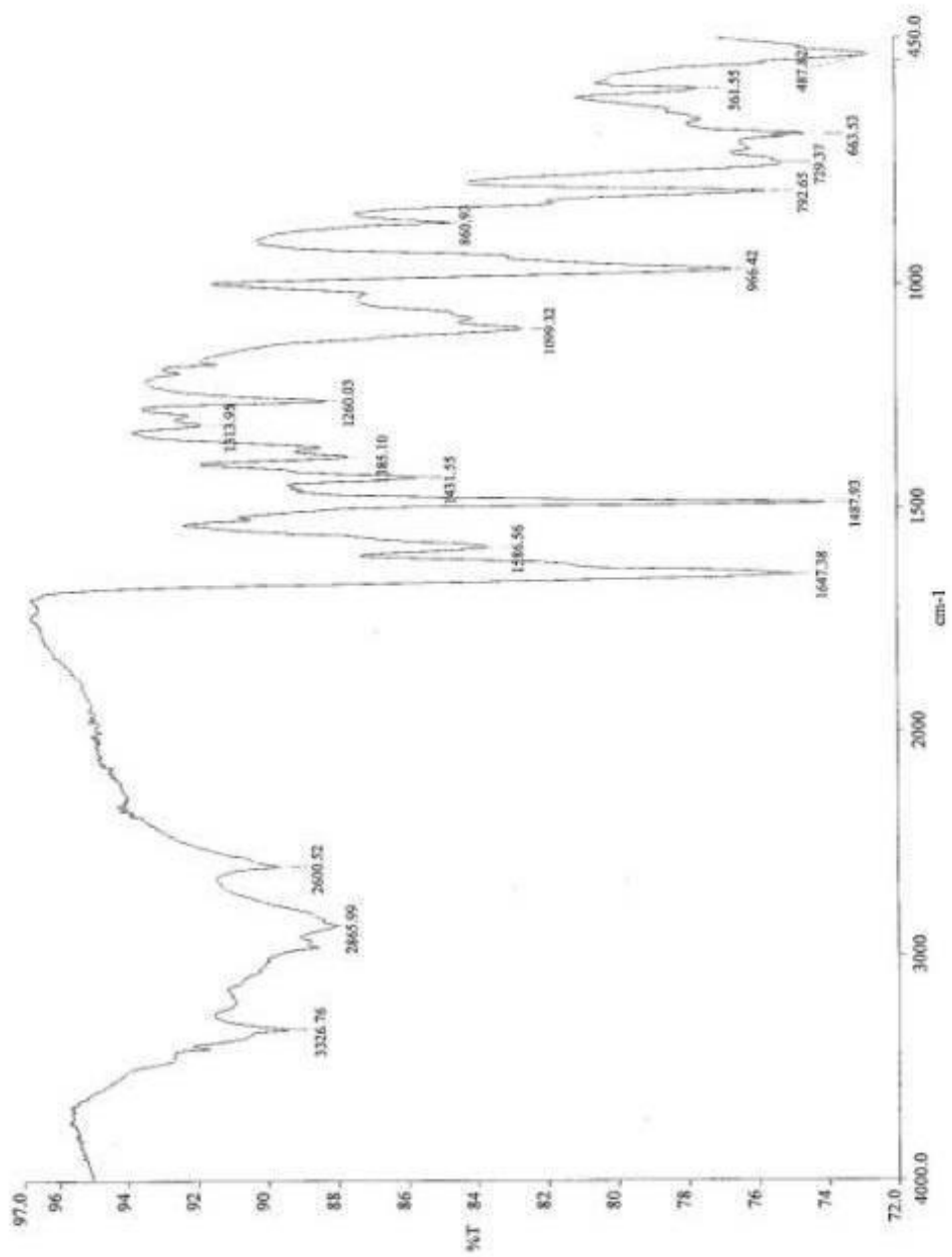


Figure B.20. FT-IR spectrum of $[\text{Mo}_2\text{O}_2(\mu_2\text{-O})\text{Cl}_4(\text{NH}_2\text{C}_6\text{H}_2\text{Cl}_2\text{NH})_2]$ (20)

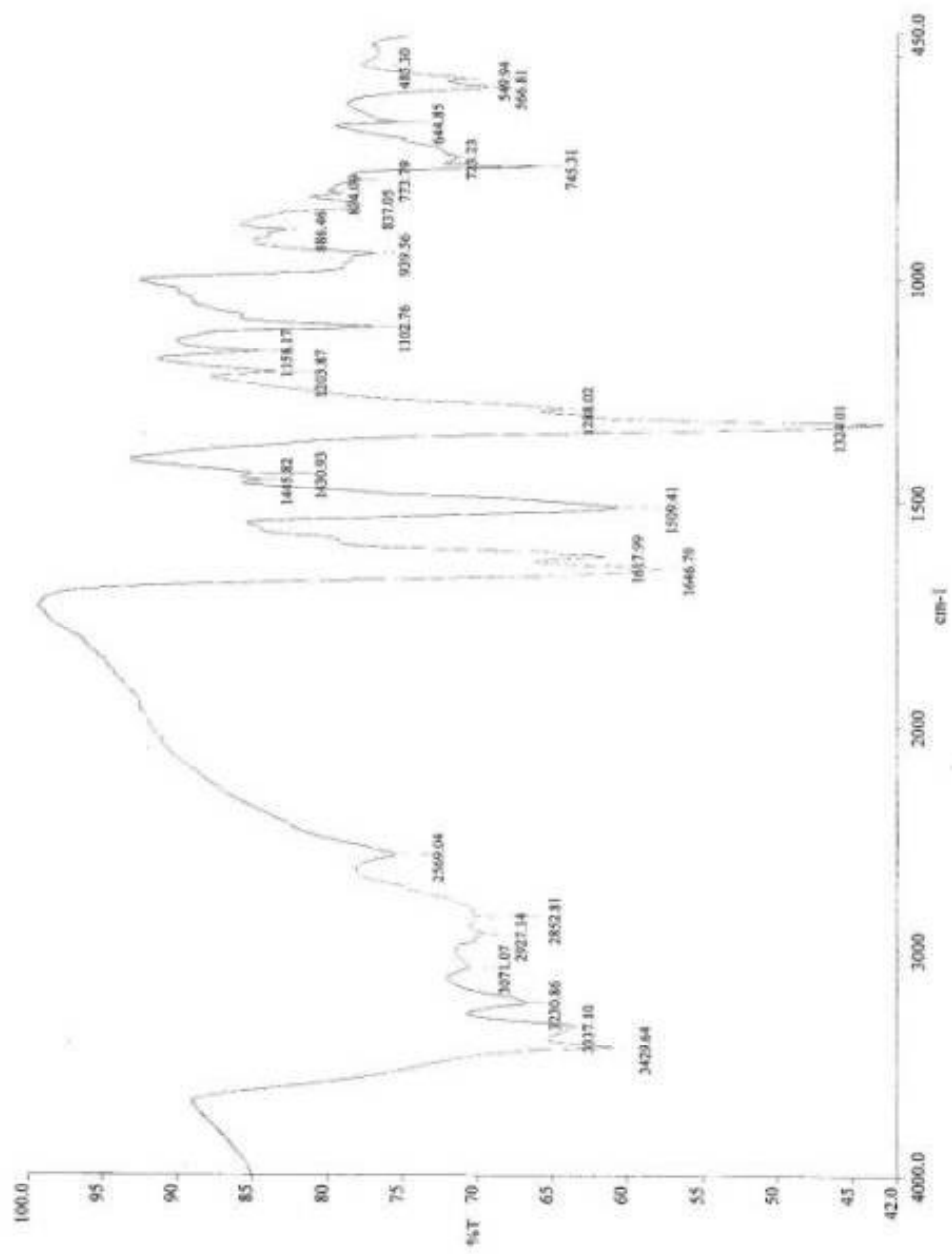


Figure B.21. FT-IR spectrum of $[\text{Mo}_2\text{O}_2(\mu_2\text{-O})\text{C}_4(\text{NH}_2\text{C}_6\text{H}_3\text{NO}_2\text{NH})_2]$ (21)

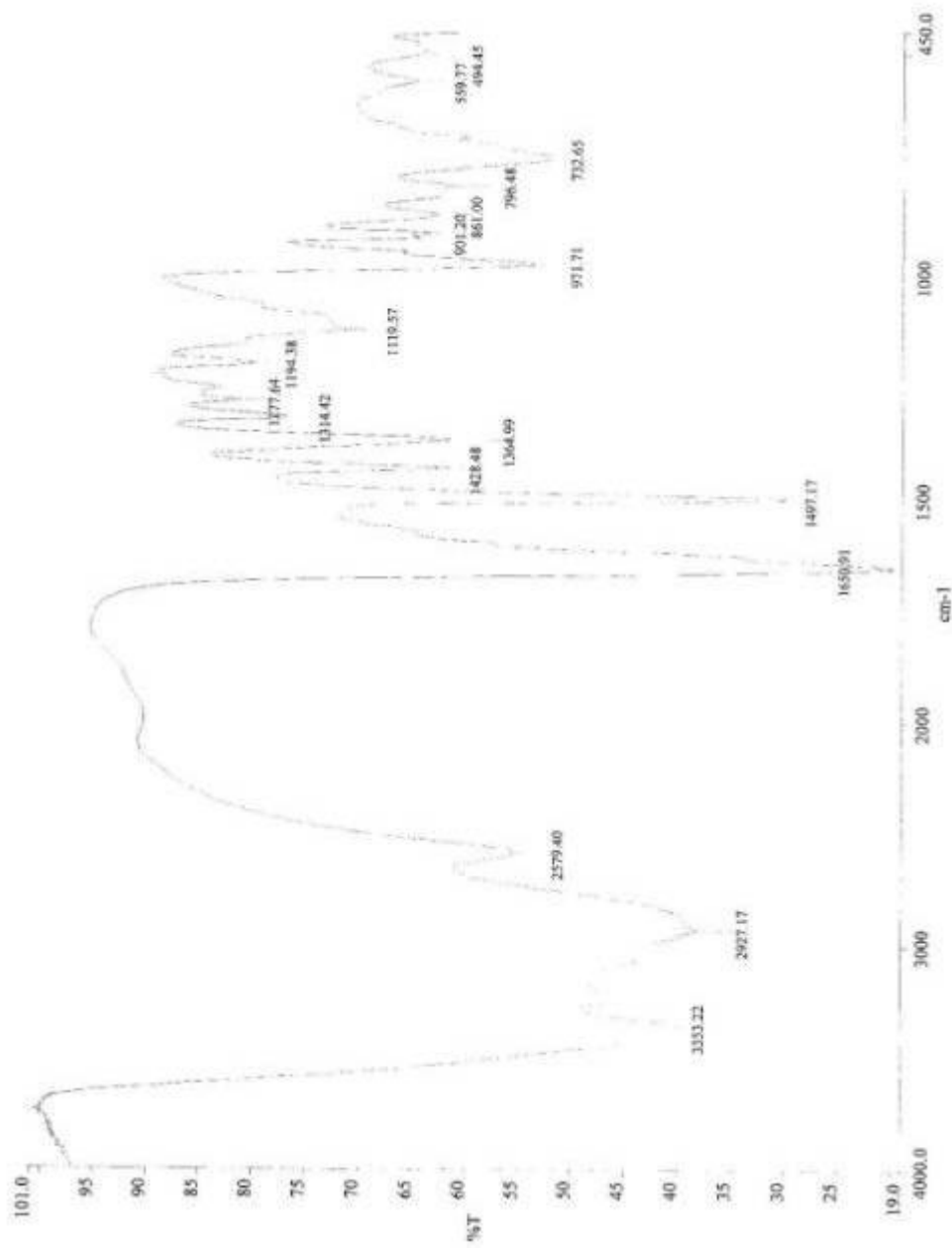


Figure B.22. FT-IR spectrum of $[\text{Mo}_2\text{O}_2(\mu_2\text{-O})\text{Cl}_4(\text{NH}_2\text{C}_6\text{H}_3\text{CINH})_2]$ (22)

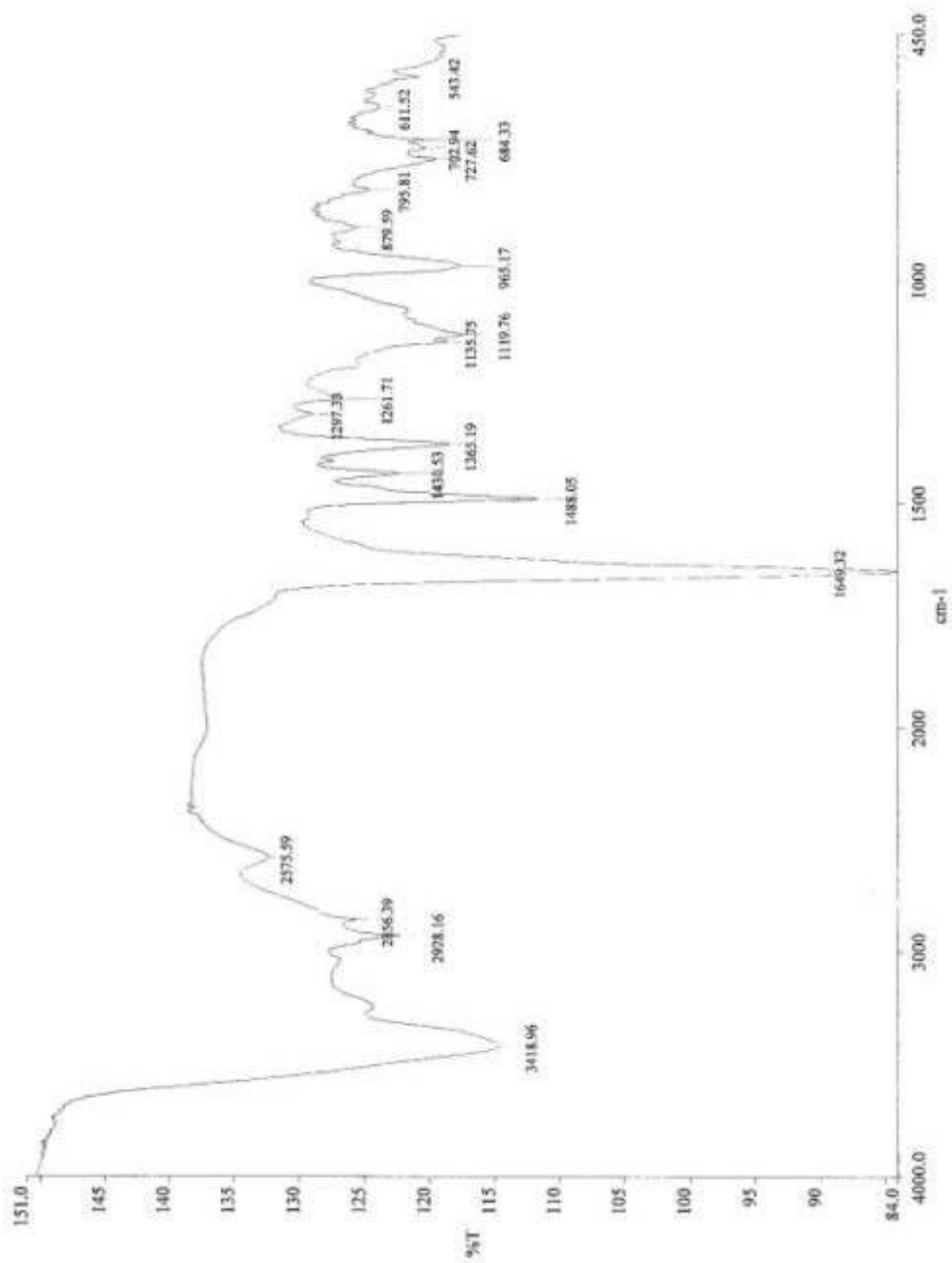


Figure .23. FT-IR spectrum of $[\text{Mo}_2\text{O}_2(\mu_2\text{-O})\text{Cl}_4(\text{NHC}_6\text{H}_2\text{Cl}_2\text{NH}_2)_2]$ (23)

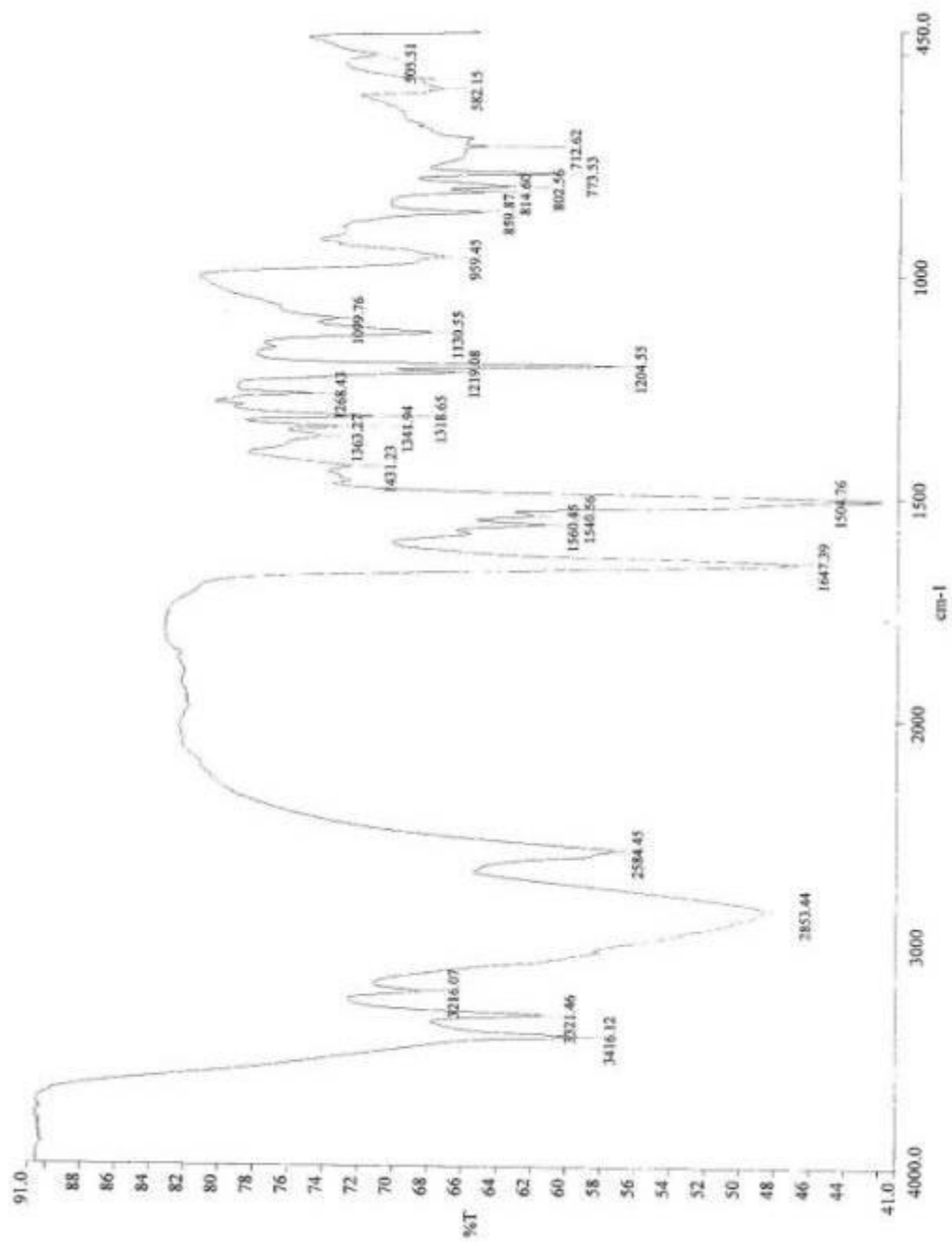


Figure B.24. FT-IR spectrum of $[\text{Mo}_2\text{O}_2(\mu_2\text{-O})\text{Cl}_4(\text{NH}_2\text{C}_6\text{H}_3\text{FN})_2]$ (24)

APPENDIX C

STRUCTURES AND CARTESIAN COORDINATES OF OPTIMIZED COMPLEXES

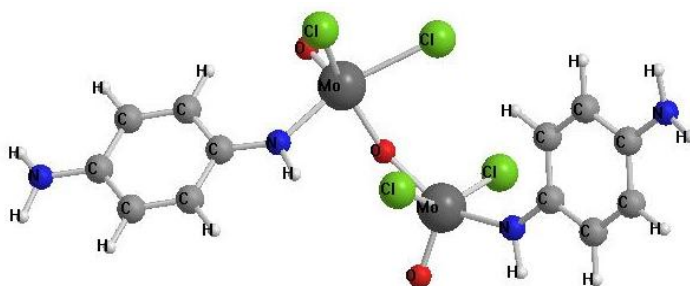


Figure C.1. DFT calculated complex $[\text{Mo}_2\text{O}_2(\mu_2\text{-O})\text{Cl}_4(p\text{-HNC}_6\text{H}_4\text{NH}_2)_2]$ (**1**)

Table C.1. Cartesian coordinates of $[\text{Mo}_2\text{O}_2(\mu_2\text{-O})\text{Cl}_4(p\text{-HNC}_6\text{H}_4\text{NH}_2)_2]$ (**1**)

ATOM	X	Y	Z	ATOM	X	Y	Z
Mo	1.12895172	-1.63904138	-0.3831069	Mo	-1.2270483	1.03995862	-0.7621069
O	0.63895172	-3.21804138	-0.0451069	O	-2.3210483	1.28695862	-2.0131069
Cl	0.57595172	-0.27204138	1.6368931	Cl	-1.3850483	3.02995862	0.5448931
Cl	1.98695172	-1.74704138	-2.5781069	Cl	0.8509517	1.96795862	-1.5881069
O	-0.35704828	-0.67604138	-1.0551069	N	-2.4530483	0.13795862	0.5218931
N	2.96595172	-1.63004138	0.3798931	C	-3.7950483	-0.06804138	0.6828931
C	3.93195172	-0.70604138	0.6628931	C	-6.5540483	-0.59304138	1.0448931
C	5.93295172	1.19495862	1.2618931	C	-4.2620483	-0.80504138	1.8028931
C	5.09095172	-1.07404138	1.3938931	C	-4.7550483	0.41295862	-0.2451069
C	3.80295172	0.63995862	0.2358931	C	-6.0960483	0.15495862	-0.0671069
C	4.77995172	1.56495862	0.5308931	C	-5.6040483	-1.06604138	1.9788931
C	6.07095172	-0.14904138	1.6838931	N	-7.8910483	-0.81904138	1.2298931
N	6.91195172	2.11195862	1.5278931	H	-1.9060483	-0.23804138	1.3008931
H	3.20195172	-2.55904138	0.7288931	H	-3.5420483	-1.18004138	2.5248931
H	5.20395172	-2.10204138	1.7288931	H	-4.4250483	0.98795862	-1.1021069
H	6.95395172	-0.44904138	2.2398931	H	-6.8170483	0.53295862	-0.7861069
H	7.62395172	1.89395862	2.2068931	H	-5.9380483	-1.63604138	2.8408931
H	6.71795172	3.09195862	1.3908931	H	-8.1860483	-1.50704138	1.9038931
H	4.66195172	2.59195862	0.1988931	H	-8.5290483	-0.64804138	0.4688931
H	2.92595172	0.95395862	-0.3221069				

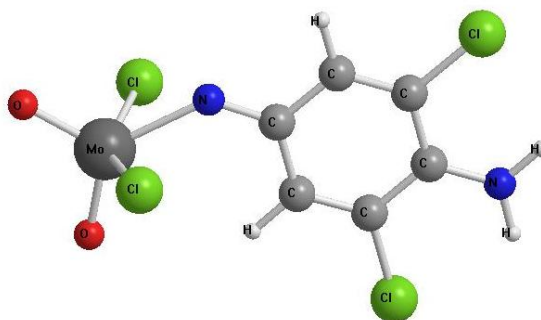


Figure C.2. DFT calculated complex $[\text{MoO}_2\text{Cl}_2(p\text{-NC}_6\text{H}_4\text{Cl}_2\text{NH}_2)]$ (**2**)

Table C.2. Cartesian coordinates of $[\text{MoO}_2\text{Cl}_2(p\text{-NC}_6\text{H}_4\text{Cl}_2\text{NH}_2)]$ (**2**)

ATOM	X	Y	Z
C	0.9180389	-0.8559333	0.0010889
C	3.2910389	-0.2729333	8.889E-05
C	0.5580389	0.5510667	0.0030889
C	2.2220389	-1.2399333	8.889E-05
C	2.9400389	1.1200667	0.0030889
C	1.6380389	1.5170667	0.0040889
Cl	-1.9109611	0.2730667	2.3120889
Cl	-1.9049611	0.2850667	-2.3109111
Cl	4.2450389	2.2920667	0.0030889
Cl	2.6630389	-2.9369333	-0.0029111
H	1.3640389	2.5650667	0.0060889
H	0.1250389	-1.5969333	8.889E-05
H	4.7910389	-1.6469333	-0.0039111
H	5.3050389	0.0220667	-0.0029111
Mo	-2.5309611	0.0240667	-0.0009111
N	-0.6659611	0.9970667	0.0030889
N	4.5620389	-0.6629333	-0.0029111
O	-2.8139611	-1.6649333	-0.0059111
O	-4.0019611	0.8980667	-0.0009111

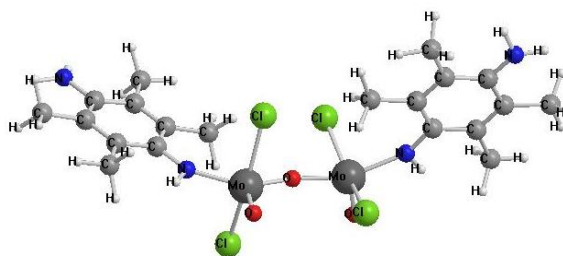


Figure C.3. DFT calculated complex $[\text{Mo}_2\text{O}_2(\mu_2\text{-O})\text{Cl}_4(p\text{-HNC}_6(\text{CH}_3)_4\text{NH}_2)_2]$ (**3**)

Table C.3. Cartesian coordinates of $[\text{Mo}_2\text{O}_2(\mu_2\text{-O})\text{Cl}_4(p\text{-HNC}_6(\text{CH}_3)_4\text{NH}_2)_2]$ (**3**)

ATOM	X	Y	Z	ATOM	X	Y	Z
C	8.25404802	0.82010734	-0.4830057	H	-2.633952	-0.83989266	-1.4720057
C	-8.01095198	1.70210734	0.69099435	H	-5.566952	1.09110734	-3.9090057
C	-4.91795198	1.66810734	-3.2360057	H	-8.822952	1.13610734	0.21399435
C	-2.79595198	0.23810734	-1.5790057	H	-5.778952	-0.79389266	2.55299435
C	6.18904802	-1.12589266	-1.6190057	H	3.959048	-1.32689266	-1.5260057
C	2.52804802	1.54810734	0.59799435	H	8.802048	0.75910734	0.46499435
C	-4.42095198	0.31910734	0.34099435	H	-6.903952	0.53010734	2.73699435
C	-6.37095198	1.56910734	-1.1980057	H	1.967048	1.43410734	-0.3350057
C	-5.68495198	0.64710734	0.93599435	H	2.139048	0.83310734	1.32999435
C	-4.13895198	0.63110734	-1.0280057	H	2.277048	2.54110734	0.96499435
C	-5.11495198	1.26710734	-1.7900057	H	5.229048	3.33510734	2.72499435
C	-6.65495198	1.28110734	0.16799435	H	3.577048	3.34410734	2.14599435
C	4.61304802	3.36910734	1.81799435	H	8.525048	-0.05989266	-1.0620057
C	4.95704802	2.22010734	0.89699435	H	8.641048	1.68910734	-1.0320057
C	6.76604802	0.93810734	-0.2410057	H	5.888048	-2.07389266	-1.1550057
C	5.82004802	0.05610734	-0.7490057	H	7.258048	-1.19589266	-1.8060057
C	4.00204802	1.35810734	0.36599435	H	5.706048	-1.06489266	-2.6020057
C	6.32704802	2.02210734	0.57599435	H	-1.982952	0.76910734	-1.0700057
C	4.43104802	0.25710734	-0.4410057	H	-2.679952	0.45510734	-2.6390057
C	-5.90395198	0.28310734	2.38799435	H	-5.149952	2.73010734	-3.3810057
Cl	2.19304802	-1.93789266	1.49099435	H	-3.896952	1.52010734	-3.5800057
Cl	0.93304802	0.29310734	-2.4960057	H	-8.189952	2.76510734	0.49199435
Cl	-0.90595198	1.40210734	1.41999435	Mo	1.636048	-1.26589266	-0.7660057
Cl	-2.32395198	-3.04089266	0.13199435	Mo	-1.605952	-0.94089266	1.12499435
H	-7.22295198	2.20910734	-2.9580057	N	-3.475952	-0.29589266	1.11299435
H	-8.27995198	2.21610734	-1.6270057	N	3.517048	-0.63489266	-0.9240057
H	-3.81595198	-0.46689266	2.05699435	N	-7.328952	2.19710734	-1.9570057
H	-8.11895198	1.56110734	1.76399435	N	7.262048	2.88110734	1.09499435
H	-5.19995198	0.80910734	3.04499435	O	-1.368952	-1.46389266	2.70799435
H	6.95904802	3.75010734	1.50099435	O	-0.141952	-1.06189266	-0.0780057
H	8.19604802	2.87910734	0.72099435	O	1.734048	-2.70189266	1.63700565
H	4.77904802	4.34510734	1.34099435				

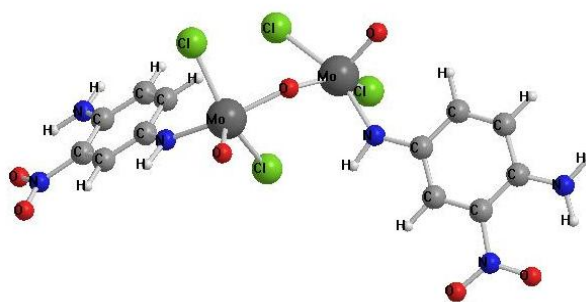


Figure C.4. DFT calculated complex $[\text{Mo}_2\text{O}_2(\mu_2\text{-O})\text{Cl}_4(p\text{-HNC}_6\text{H}_3\text{NO}_2\text{NH}_2)_2]$ (**4**)

Table C.4. Cartesian coordinates of $[\text{Mo}_2\text{O}_2(\mu_2\text{-O})\text{Cl}_4(p\text{-HNC}_6\text{H}_3\text{NO}_2\text{NH}_2)_2]$ (**4**)

ATOM	X	Y	Z	ATOM	X	Y	Z
C	5.82301796	-2.32876946	-0.25188024	H	-5.113982	-2.18688922	1.04411976
C	6.18901796	0.76211078	-0.30888024	H	2.056018	-0.81088922	-0.1598802
C	6.75001796	-0.54888922	-0.30688024	H	-3.156982	-1.44088922	2.02211976
C	-5.91098204	-1.26788922	-0.69588024	H	4.456018	1.99611078	-0.2758802
C	4.83701796	0.98211078	-0.26688024	H	6.869018	1.60711078	-0.3518802
C	4.45101796	-1.40888922	-0.20888024	H	-6.500982	0.62211078	-3.3998802
C	-3.83598204	-0.56888922	0.36111976	Mo	1.276018	1.58211078	-0.3598802
C	-5.77698204	-0.27088922	-1.71288024	Mo	-1.111982	0.03611078	1.77811976
C	-4.95798204	-1.40788922	0.30611976	N	8.086018	-0.70088922	-0.3568802
C	-3.69098204	0.43211078	-0.64188024	N	2.566018	0.07611078	-0.1638802
C	-4.62598204	0.56511078	-1.63288024	N	-7.039982	-2.18488922	-0.6598802
C	3.92301796	-0.10888922	-0.21488024	N	-6.662982	-0.09188922	-2.7088802
Cl	-0.45198204	-1.14388922	-0.31588024	N	-2.909982	-0.70588922	1.36011976
Cl	-2.05398204	1.96311078	2.72511976	N	6.263018	-3.02088922	-0.2418802
Cl	-0.82398204	2.69511078	-0.82288024	O	2.333018	2.85811078	-0.0608802
Cl	1.42101796	1.29911078	-2.71888024	O	-7.910982	-2.08988922	-1.5428802
H	-7.47098204	-0.69788922	-2.75588024	O	-7.087982	-3.01688922	0.24311976
H	-4.49498204	1.33211078	-2.39088024	O	0.420018	1.06011078	1.29411976
H	-2.83298204	1.09611078	-0.63088024	O	-0.692982	-0.93388922	3.08911976
H	8.68401796	0.10811078	-0.39988024	O	5.411018	-3.90288922	-0.1788802
H	3.80001796	-2.27488922	-0.16988024	O	7.483018	-3.25788922	-0.2978802
H	8.46701796	-1.63788922	-0.36488024				

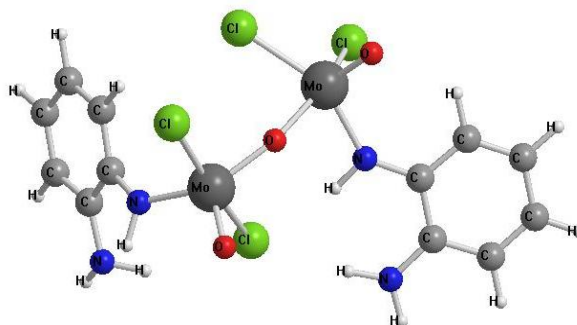


Figure C.5. DFT calculated complex $[\text{Mo}_2\text{O}_2(\mu_2\text{-O})\text{Cl}_4(o\text{-HNC}_6\text{H}_4\text{NH}_2)_2]$ (**5**)

Table C.5. Cartesian coordinates of $[\text{Mo}_2\text{O}_2(\mu_2\text{-O})\text{Cl}_4(o\text{-HNC}_6\text{H}_4\text{NH}_2)_2]$ (**5**)

ATOM	X	Y	Z	ATOM	X	Y	Z
C	6.23390345	-1.50905862	-0.48603103	H	6.75790345	0.54494138	-0.02003103
C	4.64490345	0.26994138	-0.14503103	H	-5.71409655	1.34894138	-3.26903103
C	3.86090345	-2.02005862	-0.65603103	H	7.26590345	-1.84605862	-0.53103103
C	-3.62909655	-0.47105862	-0.56503103	H	5.44790345	-3.45505862	-0.92503103
C	-4.10609655	-1.19805862	-1.69403103	H	-5.26409655	-1.07105862	-3.50203103
C	-3.84409655	0.91694138	-0.46803103	H	1.89590345	-2.76105862	-0.69103103
C	-4.59209655	1.56694138	-1.43903103	H	3.14190345	-3.89305862	-1.03503103
C	-5.12409655	0.83994138	-2.51303103	H	-3.27109655	-2.16405862	0.44396897
C	-4.88109655	-0.52505862	-2.64403103	H	-4.16709655	-3.02005862	-2.59103103
C	3.56690345	-0.62705862	-0.39203103	H	4.40990345	1.30794138	0.05596897
C	5.21890345	-2.41505862	-0.71403103	Mo	1.33690345	1.48894138	0.11596897
C	5.94990345	-0.15605862	-0.19103103	Mo	-1.31909655	-0.83705862	1.40296897
Cl	-0.35909655	-2.05605862	-0.79203103	N	2.88390345	-2.93705862	-0.84403103
Cl	1.94990345	2.44594138	-1.96203103	N	2.28190345	-0.18705862	-0.39303103
Cl	-0.65409655	2.78494138	-0.00003103	N	-3.79709655	-2.55605862	-1.77203103
Cl	-2.26109655	0.64494138	2.95596897	N	-2.98809655	-1.17905862	0.44096897
H	1.59190345	-0.86905862	-0.73403103	O	0.15590345	0.23794138	1.14096897
H	-4.77209655	2.63294138	-1.35703103	O	-1.03009655	-2.18505862	2.37896897
H	-3.45909655	1.45394138	0.39096897	O	2.40590345	2.22394138	1.18096897
H	-2.80809655	-2.75805862	-1.64903103				

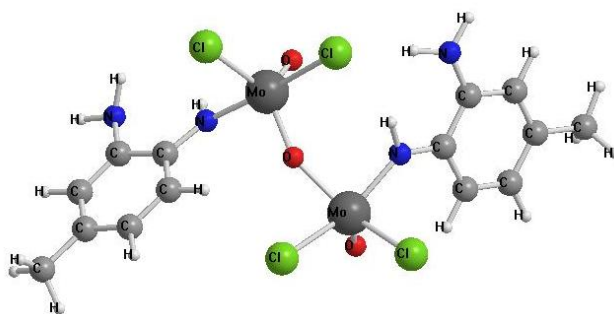


Figure C.6. DFT calculated complex $[\text{Mo}_2\text{O}_2(\mu_2\text{-O})\text{Cl}_4(o\text{-HNC}_6\text{H}_3(\text{CH}_3)\text{NH}_2)_2]$ (**6**)

Table C.6. Cartesian coordinates of $[\text{Mo}_2\text{O}_2(\mu_2\text{-O})\text{Cl}_4(o\text{-HNC}_6\text{H}_3(\text{CH}_3)\text{NH}_2)_2]$ (**6**)

ATOM	X	Y	Z	ATOM	X	Y	Z
Mo	-0.6715098	0.64618627	1.62613725	C	4.4504902	1.83918627	-2.78586275
O	-0.1625098	2.26118627	1.57613725	C	5.1274902	2.36818627	-0.52886275
Cl	1.4764902	-0.16581373	2.72013725	H	2.3704902	-0.25481373	0.54013725
Cl	-1.7055098	-0.14881373	3.59113725	H	2.8464902	0.45318627	-3.00586275
O	-0.2585098	-0.49881373	0.22613725	H	5.7624902	2.90818627	0.16913725
N	-2.4875098	1.10018627	0.93113725	H	-6.9335098	0.74518627	0.01513725
C	-3.5885098	0.35618627	0.60313725	N	3.9894902	1.41318627	1.34413725
C	-5.8305098	-1.06881373	-0.34286275	N	-4.9845098	2.31518627	0.96613725
C	-4.8725098	0.98418627	0.55913725	H	3.1824902	0.98918627	1.80113725
C	-3.4765098	-1.00981373	0.25113725	H	4.5884902	1.96518627	1.93713725
C	-4.5735098	-1.69781373	-0.22586275	H	-5.9185098	2.69618627	0.87913725
C	-5.9605098	0.26318627	0.06213725	H	-4.6015098	2.51618627	1.88313725
H	-2.6875098	2.09918627	0.92313725	H	-4.4595098	-2.73381373	-0.52786275
H	-2.5065098	-1.48981373	0.28813725	H	4.5884902	1.95818627	-3.85586275
Mo	0.8504902	-1.10881373	-1.32586275	C	-7.0195098	-1.83981373	-0.85186275
O	0.5854902	-0.18981373	-2.70786275	C	6.3704902	3.45018627	-2.43086275
Cl	2.4334902	-2.72481373	-2.01886275	H	-7.3545098	-2.57481373	-0.10986275
Cl	-0.7805098	-2.85781373	-1.36686275	H	-7.8645098	-1.18381373	-1.07686275
N	2.3284902	-0.06681373	-0.46886275	H	-6.7655098	-2.39681373	-1.75886275
C	3.2784902	0.79418627	-0.91786275	H	5.9314902	4.22918627	-3.06486275
C	5.3024902	2.54018627	-1.88886275	H	6.9354902	3.93818627	-1.63386275
C	4.1254902	1.52318627	0.00413725	H	7.0764902	2.89118627	-3.05686275
C	3.4744902	1.00018627	-2.31586275				

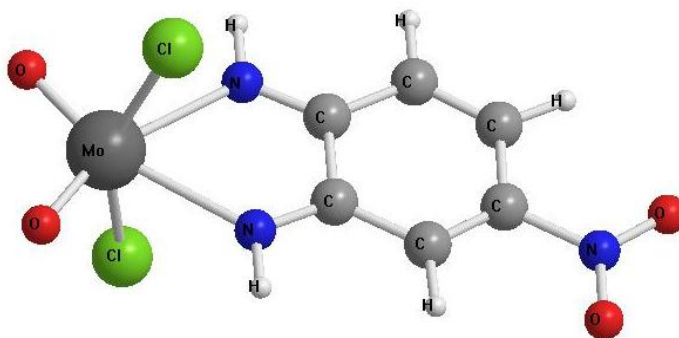


Figure C.7. DFT calculated complex $[\text{MoO}_2\text{Cl}_2(o\text{-HNC}_6\text{H}_3\text{NO}_2\text{NH})]$ (7)

Table C.7. Cartesian coordinates of $[\text{MoO}_2\text{Cl}_2(o\text{-HNC}_6\text{H}_3\text{NO}_2\text{NH})]$ (7)

ATOM	X	Y	Z
Mo	0.03012941	0.00000000	-2.22957059
Cl	0.07012941	-2.33000000	-1.64157059
Cl	0.07012941	2.33000000	-1.64157059
O	1.31112941	0.00000000	-3.35757059
O	-1.42287059	0.00000000	-3.12457059
N	-1.11087059	0.00000000	-0.10257059
C	-0.45687059	0.00000000	1.00542941
C	1.22212941	0.00000000	3.31442941
C	-1.04687059	0.00000000	2.33342941
C	1.04012941	0.00000000	0.88442941
C	1.82912941	0.00000000	2.10642941
C	-0.22487059	0.00000000	3.40342941
N	-0.82687059	0.00000000	4.75842941
O	-0.04987059	0.00000000	5.70942941
O	-2.05087059	0.00000000	4.83442941
H	2.91112941	0.00000000	2.02342941
H	-2.12387059	0.00000000	2.45942941
H	-2.12687059	0.00000000	-0.01457059
H	1.78312941	0.00000000	4.23942941
N	1.49712941	0.00000000	-0.31757059
H	2.51412941	0.00000000	-0.39957059

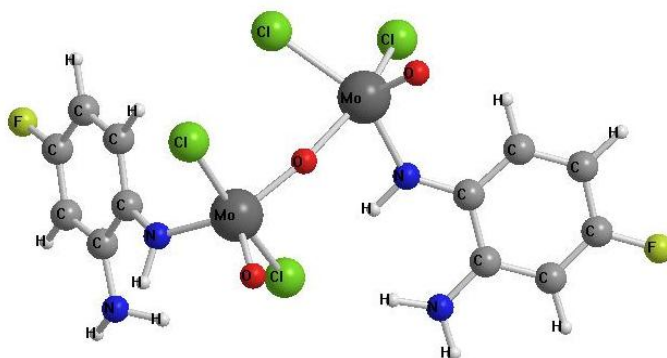


Figure C.8. DFT calculated complex $[\text{Mo}_2\text{O}_2(\mu_2\text{-O})\text{Cl}_4(o\text{-HNC}_6\text{H}_3\text{FNH}_2)_2]$ (**8**)

Table C.8. Cartesian coordinates of $[\text{Mo}_2\text{O}_2(\mu_2\text{-O})\text{Cl}_4(o\text{-HNC}_6\text{H}_3\text{FNH}_2)_2]$ (**8**)

ATOM	X	Y	Z	ATOM	X	Y	Z
Mo	-1.29791503	-0.79905556	1.59298366	C	6.11308497	-1.25705556	-0.79001634
O	-0.90491503	-2.00805556	2.70498366	C	3.78808497	-1.89005556	-0.67501634
Cl	-0.39091503	-2.22805556	-0.48801634	C	4.49808497	0.47994444	-0.53901634
Cl	-2.22791503	0.81694444	3.01398366	C	5.81708497	0.11194444	-0.65501634
O	0.08508497	0.31094444	1.09898366	C	5.14808497	-2.24005556	-0.80901634
N	-2.99391503	-1.29105556	0.75398366	H	1.45508497	-0.80405556	-0.69601634
C	-3.67691503	-0.71705556	-0.30501634	H	4.23108497	1.52594444	-0.47501634
C	-5.22591503	0.34694444	-2.32601634	H	5.44308497	-3.27905556	-0.89701634
C	-4.23091503	-1.58005556	-1.29801634	H	-5.48291503	-1.64805556	-3.06801634
C	-3.85191503	0.67794444	-0.40101634	N	2.84408497	-2.85505556	-0.64201634
C	-4.63191503	1.21794444	-1.41101634	N	-3.95791503	-2.94105556	-1.20201634
C	-5.03791503	-1.02905556	-2.29601634	H	1.86208497	-2.69105556	-0.43701634
H	-3.27991503	-2.26105556	0.91098366	H	3.12708497	-3.81905556	-0.72201634
H	-3.40991503	1.32194444	0.35198366	H	-4.38091503	-3.50705556	-1.92601634
Mo	1.29508497	1.60494444	0.17898366	H	-2.96891503	-3.15605556	-1.09501634
O	2.44308497	2.17794444	1.26098366	H	-4.79891503	2.28494444	-1.49401634
Cl	1.89008497	2.69994444	-1.83101634	H	6.61808497	0.83994444	-0.67301634
Cl	-0.63291503	2.98794444	0.26798366	F	-5.99491503	0.85894444	-3.30001634
N	2.15208497	-0.08705556	-0.46201634	F	7.39708497	-1.61705556	-0.90601634
C	3.44708497	-0.48205556	-0.55701634				

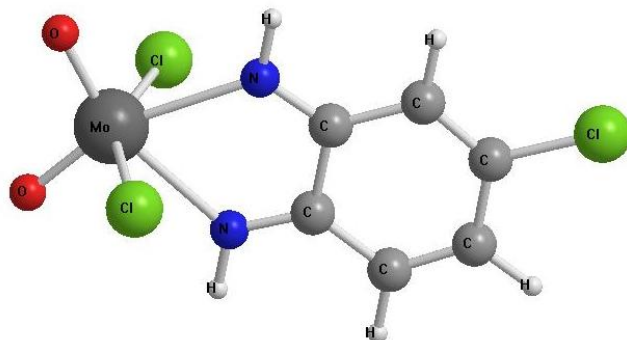


Figure C.9. DFT calculated complex $[\text{MoO}_2\text{Cl}_2(o\text{-HNC}_6\text{H}_3\text{ClNH})]$ (**9**)

Table C.9. Cartesian coordinates of $[\text{MoO}_2\text{Cl}_2(o\text{-HNC}_6\text{H}_3\text{ClNH})]$ (**9**)

ATOM	X	Y	Z
Mo	2.0220061	0.1140122	0.000000
Cl	1.4550061	0.0340122	-2.338000
Cl	1.4550061	0.0340122	2.338000
O	3.2060061	-1.1169878	0.000000
O	2.8510061	1.6070122	0.000000
N	-0.1429939	1.1440122	0.000000
C	-1.2249939	0.4460122	0.000000
C	-3.4469939	-1.3369878	0.000000
C	-2.5749939	0.9720122	0.000000
C	-1.0319939	-1.0439878	0.000000
C	-2.2149939	-1.8899878	0.000000
C	-3.6199939	0.1100122	0.000000
H	-2.0829939	-2.9669878	0.000000
H	-2.7259939	2.0460122	0.000000
H	-0.2719939	2.1550122	0.000000
H	-4.3379939	-1.9549878	0.000000
N	0.1890061	-1.4479878	0.000000
H	0.3160061	-2.4589878	0.000000
Cl	-5.2579939	0.7000122	0.000000

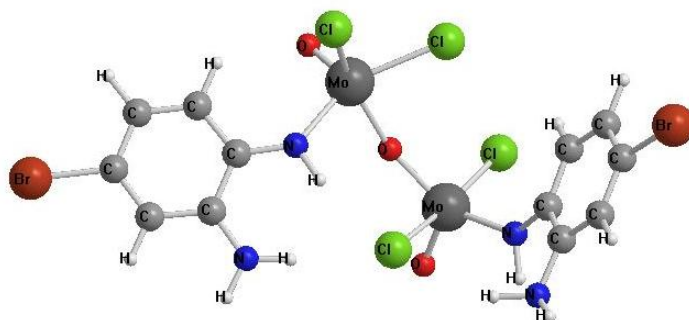


Figure C.10. DFT calculated complex $[\text{Mo}_2\text{O}_2(\mu_2\text{-O})\text{Cl}_4(o\text{-HNC}_6\text{H}_3\text{BrNH}_2)_2]$ (**10**)

Table C.10. Cartesian coordinates of $[\text{Mo}_2\text{O}_2(\mu_2\text{-O})\text{Cl}_4(o\text{-HNC}_6\text{H}_3\text{BrNH}_2)_2]$ (**10**)

ATOM	X	Y	Z	ATOM	X	Y	Z
Mo	1.06918156	-2.19797486	-0.4890838	C	-6.12881844	0.46502514	0.8609162
O	0.43318156	-3.72097486	-0.1350838	C	-3.90181844	-0.26597486	1.4819162
Cl	0.20318156	-1.16597486	1.8329162	C	-4.30181844	1.02802514	-0.5840838
Cl	2.03718156	-2.59797486	-2.5840838	C	-5.64881844	1.07602514	-0.3180838
O	-0.15681844	-1.00697486	-1.1790838	C	-5.28881844	-0.18697486	1.7419162
N	2.76718156	-2.05097486	0.4769162	H	-1.46081844	0.04202514	0.7929162
C	3.64918156	-0.99197486	0.6289162	H	-3.90781844	1.51202514	-1.4690838
C	5.58318156	0.96802514	0.9769162	H	-5.68481844	-0.66197486	2.6319162
C	4.13018156	-0.69997486	1.9379162	H	5.50918156	0.50102514	3.0789162
C	4.09918156	-0.23897486	-0.4720838	N	-3.09881844	-0.94197486	2.3339162
C	5.06918156	0.73802514	-0.3050838	N	3.60818156	-1.42597486	3.0049162
C	5.12318156	0.27102514	2.0919162	H	-2.12481844	-1.16197486	2.1469162
H	2.87318156	-2.73597486	1.2309162	H	-3.50681844	-1.38497486	3.1429162
H	3.71918156	-0.46697486	-1.4620838	H	3.99018156	-1.17797486	3.9079162
Mo	-0.93181844	0.79702514	-1.5680838	H	2.59118156	-1.45697486	3.0279162
O	-2.02681844	0.67302514	-2.8340838	H	5.43318156	1.30102514	-1.1550838
Cl	-1.01081844	3.09402514	-1.0270838	H	-6.32981844	1.58802514	-0.9860838
Cl	1.22918156	1.18502514	-2.4740838	Br	6.93618156	2.30202514	1.2179162
N	-2.05681844	0.37702514	0.0249162	Br	-7.99881844	0.54502514	1.2419162
C	-3.38581844	0.38302514	0.2939162				

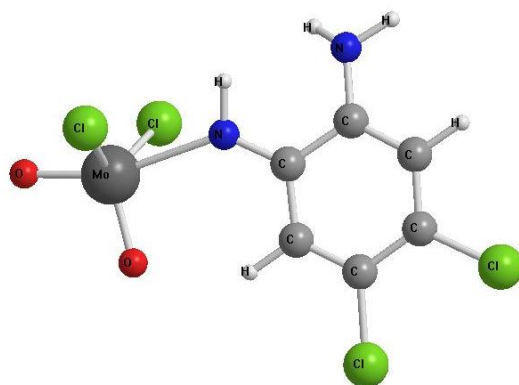


Figure C.11. DFT calculated complex $[\text{MoO}_2\text{Cl}_2(o\text{-HNC}_6\text{H}_2\text{Cl}_2\text{NH}_2)]$ (**11**)

Table C.11. Cartesian coordinates of $[\text{MoO}_2\text{Cl}_2(o\text{-HNC}_6\text{H}_2\text{Cl}_2\text{NH}_2)]$ (**11**)

ATOM	X	Y	Z
C	3.08209945	1.62500552	0.07890055
C	0.77609945	0.76800552	0.05290055
C	1.71009945	1.88200552	0.04390055
C	1.31409945	-0.55399448	-0.04709945
C	2.66909945	-0.77899448	-0.03509945
C	3.56809945	0.32100552	0.05090055
Cl	-2.62890055	0.39700552	2.17790055
Cl	3.26609945	-2.41399448	-0.11209945
Cl	-2.38290055	0.71600552	-2.10309945
Cl	5.28509945	0.07600552	0.08390055
H	0.37909945	3.34700552	-0.48909945
H	0.62209945	-1.38599448	-0.08109945
H	3.78809945	2.44800552	0.09490055
H	-0.76590055	1.92100552	0.41690055
H	1.89909945	3.91400552	-0.02509945
Mo	-2.47390055	-0.38899448	-0.02709945
N	-0.53690055	0.95700552	0.17890055
N	1.22209945	3.16700552	0.03890055
O	-4.11490055	-0.84299448	-0.15809945
O	-1.59790055	-1.84799448	-0.08709945

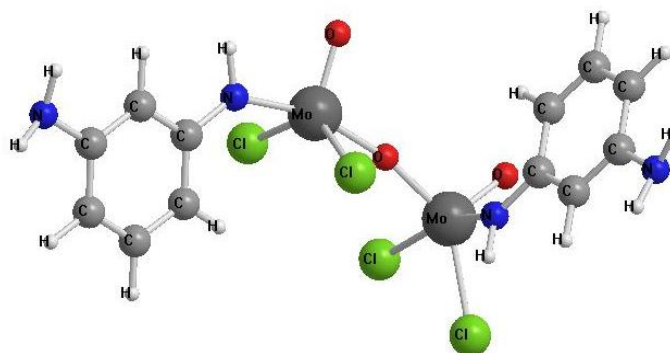


Figure C.12. DFT calculated complex $[\text{Mo}_2\text{O}_2(\mu_2\text{-O})\text{Cl}_4(m\text{-NC}_6\text{H}_4\text{NH}_2)_2]$ (**12**)

Table C.12. Cartesian coordinates of $[\text{Mo}_2\text{O}_2(\mu_2\text{-O})\text{Cl}_4(m\text{-NC}_6\text{H}_4\text{NH}_2)_2]$ (**12**)

ATOM	X	Y	Z	ATOM	X	Y	Z
Mo	-1.18912414	-0.00593103	-1.14298966	C	3.21687586	1.31106897	0.23701034
O	-0.89712414	0.70006897	-2.64198966	C	4.59387586	3.48106897	-0.86798966
Cl	-0.63712414	1.36806897	0.72801034	C	3.72487586	2.33406897	1.06901034
Cl	-2.10512414	-2.15593103	-1.33098966	C	3.39387586	1.39306897	-1.16398966
O	0.49187586	-0.87593103	-0.75198966	C	4.08487586	2.47706897	-1.68898966
N	-3.04612414	0.72906897	-0.96498966	C	4.41587586	3.42106897	0.53201034
C	-4.02812414	0.70506897	-0.00698966	H	2.38587586	0.40406897	1.81501034
C	-6.04312414	0.67706897	1.92901034	H	2.98487586	0.63106897	-1.81398966
C	-5.18912414	1.49306897	-0.17598966	H	4.22287586	2.55106897	-2.76298966
C	-3.88612414	-0.10093103	1.14701034	H	-6.82712414	0.65906897	2.68101034
C	-4.90012414	-0.10093103	2.09601034	H	5.13187586	4.32006897	-1.30098966
C	-6.20312414	1.49006897	0.78301034	H	-5.28712414	2.10906897	-1.06698966
H	-3.30012414	1.30906897	-1.76298966	H	3.58487586	2.25906897	2.14401034
H	-4.80312414	-0.71793103	2.98301034	N	-7.36812414	2.22106897	0.60201034
H	-3.00612414	-0.71793103	1.28101034	N	4.96987586	4.39306897	1.35301034
Mo	2.00087586	-1.55193103	0.14601034	H	-7.31312414	2.99806897	-0.03998966
O	3.19587586	-1.71893103	-1.03098966	H	-7.88912414	2.44206897	1.43801034
C	12.59587586	-2.09493103	2.43501034	H	5.15087586	5.28806897	0.92201034
Cl	1.04087586	-3.71293103	0.19601034	H	4.56687586	4.48006897	2.27501034
N	2.54287586	0.25906897	0.82001034				

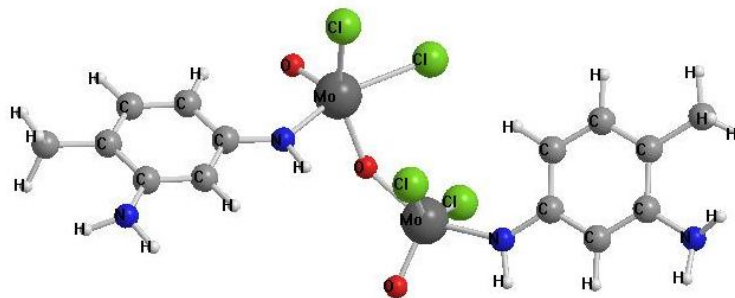


Figure C.13. DFT calculated complex $[\text{Mo}_2\text{O}_2(\mu_2\text{-O})\text{Cl}_4(m\text{-HNC}_6\text{H}_3(\text{CH}_3)\text{NH}_2)]$ (**13**)

Table C.13. Cartesian coordinates of $[\text{Mo}_2\text{O}_2(\mu_2\text{-O})\text{Cl}_4(m\text{-HNC}_6\text{H}_3(\text{CH}_3)\text{NH}_2)]$ (**13**)

ATOM	X	Y	Z	ATOM	X	Y	Z
Mo	1.13411765	-1.20504248	-1.14294118	C	-4.34888235	-1.32004248	1.13405882
O	0.66511765	-2.76204248	-1.58794118	C	-4.80888235	0.67595752	-0.19094118
Cl	0.48611765	-0.89904248	1.23905882	C	-6.16288235	0.40895752	-0.05594118
Cl	2.08911765	-0.26804248	-3.07194118	C	-5.71288235	-1.57404248	1.26705882
O	-0.36088235	-0.06004248	-1.37794118	H	-1.98788235	-0.70104248	0.83705882
N	2.93111765	-1.58204248	-0.39194118	H	-3.62788235	-1.99304248	1.59205882
C	3.91311765	-0.86304248	0.24605882	H	-4.46488235	1.54095752	-0.74294118
C	5.96511765	0.59995752	1.50505882	H	-6.88088235	1.08395752	-0.51294118
C	5.04011765	-1.52804248	0.77705882	N	7.20511765	-1.46804248	1.85505882
C	3.80811765	0.53895752	0.36205882	H	7.69411765	-1.03104248	2.62305882
C	4.83111765	1.23495752	0.98705882	H	7.11611765	-2.46704248	1.97805882
C	6.06411765	-0.81604248	1.39805882	N	-6.16488235	-2.64204248	2.03505882
H	3.14111765	-2.57904248	-0.43694118	H	-5.47688235	-3.35404248	2.23905882
H	5.11211765	-2.61004248	0.69105882	H	-7.05588235	-3.03504248	1.77005882
H	4.75411765	2.31495752	1.07505882	C	7.06911765	1.38795752	2.15405882
H	2.94511765	1.06795752	-0.02694118	C	-8.12388235	-0.93504248	0.81505882
Mo	-1.27588235	1.35895752	-0.41594118	H	-8.40888235	-0.98804248	1.87305882
O	-2.31288235	2.16095752	-1.46894118	H	-8.43288235	-1.88304248	0.35205882
Cl	-1.50988235	2.58295752	1.60405882	H	-8.70588235	-0.14004248	0.34505882
Cl	0.81811765	2.53495752	-0.66394118	H	7.17611765	1.14095752	3.22005882
N	-2.51988235	-0.00304248	0.30905882	H	6.87711765	2.45995752	2.08705882
C	-3.87988235	-0.20004248	0.41205882	H	8.03611765	1.18295752	1.67805882
C	-6.64788235	-0.69104248	0.66205882				

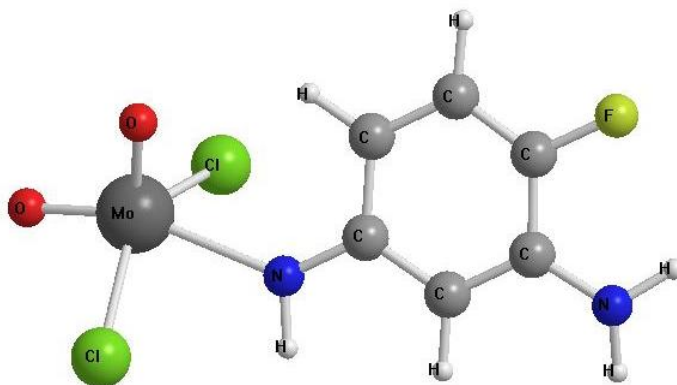


Figure C.14. DFT calculated complex $[\text{MoO}_2\text{Cl}_2(m\text{-HNC}_6\text{H}_3\text{FNH}_2)]$ (**14**)

Table C.14. Cartesian coordinates of $[\text{MoO}_2\text{Cl}_2(m\text{-HNC}_6\text{H}_3\text{FNH}_2)]$ (**14**)

ATOM	X	Y	Z
Mo	2.04607006	0.14494268	-0.13994268
Cl	1.35107006	1.68594268	1.49905732
Cl	2.34307006	-2.19905732	-0.31994268
O	3.71707006	0.45794268	0.04505732
O	1.61507006	0.78594268	-1.65594268
C	-1.30292994	-0.34305732	0.14605732
C	-3.89092994	0.48794268	-0.42294268
C	-2.42592994	-1.08905732	0.62605732
C	-1.53592994	0.84094268	-0.63594268
C	-2.82892994	1.24194268	-0.90894268
C	-3.72492994	-0.69505732	0.35305732
H	-3.04092994	2.12994268	-1.49394268
N	-4.84692994	-1.39205732	0.73705732
H	-5.72292994	-0.89205732	0.71405732
H	-4.75092994	-2.05405732	1.49105732
F	-5.15492994	0.87494268	-0.67194268
H	-0.68792994	1.39794268	-1.01194268
H	-2.24692994	-1.98505732	1.21405732
N	-0.04992994	-0.72905732	0.40305732
H	-0.01292994	-1.60105732	0.92905732

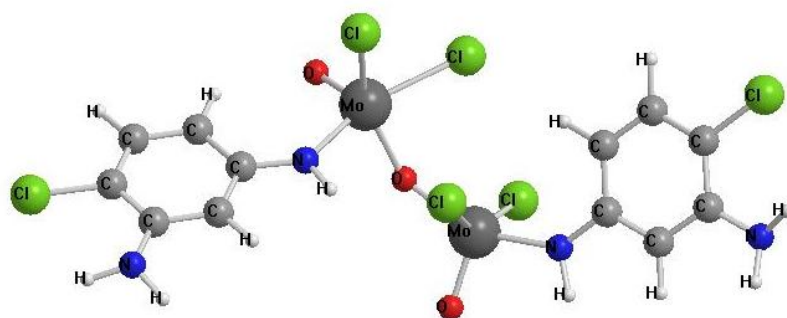


Figure C.15. DFT calculated complex $[\text{Mo}_2\text{O}_2(\mu_2\text{-O})\text{Cl}_4(m\text{-HNC}_6\text{H}_3\text{ClNH}_2)_2]$ (15)

Table C.15. Cartesian coordinates of $[\text{Mo}_2\text{O}_2(\mu_2\text{-O})\text{Cl}_4(m\text{-HNC}_6\text{H}_3\text{ClNH}_2)_2]$ (15)

ATOM	X	Y	Z	ATOM	X	Y	Z
Mo	1.10400621	-1.40598137	-1.11300311	N	-2.47399379	0.12101863	0.28699689
O	0.60300621	-2.99598137	-1.35400311	C	-3.83599379	-0.01698137	0.44399689
Cl	0.52000621	-0.78098137	1.22399689	C	-6.57099379	-0.38798137	0.80799689
Cl	2.03200621	-0.73798137	-3.15600311	C	-4.31299379	-0.97998137	1.35599689
O	-0.38199379	-0.27698137	-1.45300311	C	-4.75399379	0.77001863	-0.28800311
N	2.90500621	-1.73298137	-0.34500311	C	-6.11099379	0.57101863	-0.09600311
C	3.90600621	-0.97498137	0.21799689	C	-5.68099379	-1.18798137	1.56199689
C	5.95700621	0.53401863	1.32899689	H	-1.94899379	-0.49598137	0.91299689
C	5.00600621	-1.61198137	0.82699689	H	-3.59999379	-1.57798137	1.91799689
C	3.83800621	0.43501863	0.17499689	H	-4.40199379	1.51701863	-0.98800311
C	4.86900621	1.17201863	0.73499689	H	-6.83299379	1.16001863	-0.64900311
C	6.05500621	-0.87898137	1.38899689	N	7.15800621	-1.50198137	1.93299689
H	3.09200621	-2.73298137	-0.28600311	H	7.72300621	-0.95198137	2.56399689
H	5.04700621	-2.69798137	0.85499689	H	7.04100621	-2.46298137	2.21399689
H	4.83600621	2.25601863	0.71699689	N	-6.13599379	-2.09498137	2.49499689
H	2.99600621	0.94001863	-0.28300311	H	-5.49099379	-2.81798137	2.77599689
Mo	-1.20599379	1.30201863	-0.67700311	H	-7.09199379	-2.40398137	2.40099689
O	-2.24999379	1.98101863	-1.80500311	Cl	-8.29799379	-0.61198137	1.01099689
Cl	-1.30799379	2.81501863	1.14499689	Cl	7.23700621	1.50301863	2.02899689
Cl	0.92200621	2.32901863	-1.16000311				

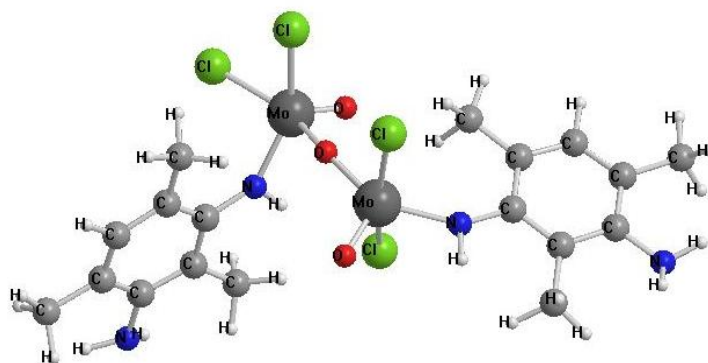


Figure C.16. DFT calculated complex $[\text{Mo}_2\text{O}_2(\mu_2\text{-O})\text{Cl}_4(m\text{-HNC}_6\text{H}(\text{CH}_3)_3\text{NH}_2)_2]$ (16)

Table C.16. Cartesian coordinates of $[\text{Mo}_2\text{O}_2(\mu_2\text{-O})\text{Cl}_4(m\text{-HNC}_6\text{H}(\text{CH}_3)_3\text{NH}_2)_2]$ (16)

ATOM	X	Y	Z	ATOM	X	Y	Z
C	-4.01201183	-1.73302959	-1.20190828	H	1.95998817	0.94997041	-1.15990828
C	2.83398817	1.43797041	-0.71390828	H	-5.60301183	-3.31602959	-2.56090828
C	-3.31001183	-2.19302959	-2.45790828	H	-6.71401183	-3.60902959	-1.35490828
C	-7.05801183	-2.70602959	0.89309172	H	-4.05101183	0.79597041	2.67409172
C	7.53298817	0.38997041	-2.16590828	H	-3.51901183	-3.24902959	-2.64590828
C	-3.53301183	0.78097041	1.71309172	H	-6.89601183	-3.78702959	0.98809172
C	4.01798817	-0.67502959	0.10309172	H	-7.89201183	-2.56302959	0.19209172
C	6.30998817	0.00597041	-1.37590828	H	-7.38401183	-2.32902959	1.86509172
C	5.14198817	-1.55302959	0.10309172	H	8.40798817	0.53697041	-1.51790828
C	4.01998817	0.51797041	-0.67090828	H	7.37098817	1.32397041	-2.70790828
C	5.17098817	0.81197041	-1.39290828	H	7.80098817	-0.38102959	-2.89990828
C	6.29498817	-1.18402959	-0.60590828	H	-3.61501183	-1.62402959	-3.34690828
C	-5.19801183	-2.36002959	-0.79890828	H	-3.65501183	1.77997041	1.27509172
C	-5.23801183	-0.99202959	1.20709172	H	7.57498817	-2.54202959	0.23609172
C	-4.10101183	-0.29202959	0.82509172	H	4.10998817	-3.30602959	0.87809172
C	5.11398817	-2.87402959	0.83509172	H	5.48898817	-2.80102959	1.86609172
C	-5.81201183	-2.00002959	0.42909172	H	5.72898817	-3.61102959	0.31009172
C	-3.49501183	-0.65702959	-0.41490828	H	3.04598817	2.31597041	-1.32790828
Cl	1.78398817	1.15897041	2.87709172	H	2.56398817	1.80997041	0.28309172
Cl	-1.01001183	3.63297041	0.72109172	Mo	-1.40401183	1.70397041	-0.57490828
Cl	-3.42301183	2.84097041	-1.27390828	Mo	1.05798817	-0.44002959	1.23309172
Cl	0.53098817	-1.54202959	-0.93790828	N	-5.75101183	-3.38902959	-1.56490828
H	-5.70901183	-0.73902959	2.15209172	N	7.41498817	-2.02202959	-0.61390828
H	5.18998817	1.72097041	-1.98790828	N	2.92898817	-0.98102959	0.88609172
H	3.09498817	-1.80802959	1.45709172	N	-2.40701183	0.02997041	-0.87590828
H	-4.0909497	-2.10393787	-1.69390828	O	0.48998817	-1.63502959	2.27709172
H	-2.22101183	-2.12502959	-2.37390828	O	-0.27201183	0.78297041	0.73109172
H	8.26598817	-1.59002959	-0.94290828	O	-0.43401183	1.78797041	-1.94190828
H	-2.47001183	0.62097041	1.92409172				

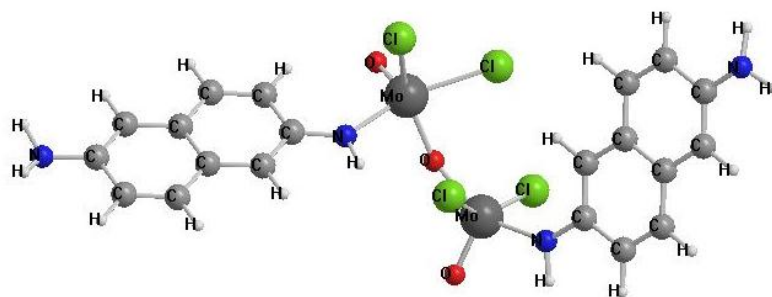


Figure C.17. DFT calculated complex $[\text{Mo}_2\text{O}_2(\mu_2\text{-O})\text{Cl}_4(1,5\text{-HNC}_{10}\text{H}_6\text{NH}_2)_2]$ (17)

Table C.17. Cartesian coordinates of $[\text{Mo}_2\text{O}_2(\mu_2\text{-O})\text{Cl}_4(1,5\text{-HNC}_{10}\text{H}_6\text{NH}_2)_2]$ (17)

ATOM	X	Y	Z	ATOM	X	Y	Z
Mo	1.09186842	-2.18199123	-0.1399152	H	-3.70313158	-0.15099123	2.0540848
O	0.40086842	-3.63799123	0.3530848	H	-3.95813158	0.86000877	-2.1349152
Cl	0.47686842	-0.45899123	1.5420848	C	3.85286842	-1.35799123	1.0570848
Cl	2.20286842	-2.70699123	-2.1549152	C	3.87886842	-0.11499123	0.4060848
O	-0.18213158	-1.20799123	-1.1709152	C	5.95586842	-0.83299123	2.1630848
N	2.82386842	-2.22799123	0.8460848	C	4.92586842	0.78800877	0.6240848
H	2.92586842	-3.09699123	1.3690848	C	4.92286842	-1.69999123	1.9490848
Mo	-0.84913158	0.58000877	-1.4379152	C	6.00086842	0.44200877	1.5150848
O	-1.73813158	0.63300877	-2.8659152	C	4.95886842	2.06100877	-0.0209152
Cl	-0.88213158	2.84100877	-0.6559152	C	5.98786842	2.93600877	0.1980848
Cl	1.42786842	1.08700877	-2.1069152	C	7.05986842	2.59300877	1.0780848
N	-2.29913158	0.19900877	-0.1279152	C	7.04786842	1.35300877	1.7210848
H	-1.87713158	-0.04699123	0.7720848	N	8.05986842	3.50700877	1.3070848
C	-3.65813158	0.33500877	-0.0449152	N	-9.87813158	0.56400877	1.6490848
C	-4.29913158	0.11400877	1.1840848	H	-10.39113158	1.03700877	0.9210848
C	-5.80813158	0.79800877	-1.0749152	H	-10.25613158	0.69200877	2.5750848
C	-5.69013158	0.22900877	1.3140848	H	-8.21213158	-0.03299123	3.6120848
C	-4.45113158	0.68500877	-1.1859152	H	3.08186842	0.16400877	-0.2759152
C	-6.48213158	0.57800877	0.1660848	H	4.90086842	-2.66299123	2.4520848
C	-6.35813158	0.01600877	2.5550848	H	6.76286842	-1.10399123	2.8380848
C	-7.71813158	0.13900877	2.6590848	H	7.85986842	1.08900877	2.3950848
C	-8.50713158	0.48900877	1.5220848	H	8.91186842	3.18900877	1.7440848
C	-7.87613158	0.70200877	0.2970848	H	8.16986842	4.27100877	0.6600848
H	-6.39913158	1.06600877	-1.9459152	H	5.99686842	3.90600877	-0.2919152
H	-8.46813158	0.96900877	-0.5749152	H	4.14486842	2.32600877	-0.6889152
H	-5.76813158	-0.24899123	3.4280848				

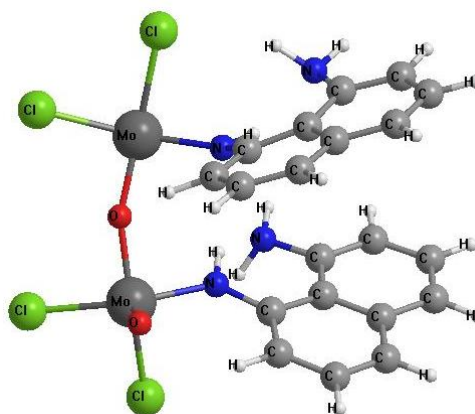


Figure C.18. DFT calculated complex $[\text{Mo}_2\text{O}_2(\mu_2\text{-O})\text{Cl}_4(I,8\text{-HNC}_{10}\text{H}_6\text{NH}_2)_2]$ (**18**)

Table C.18. Cartesian coordinates of $[\text{Mo}_2\text{O}_2(\mu_2\text{-O})\text{Cl}_4(I,8\text{-HNC}_{10}\text{H}_6\text{NH}_2)_2]$ (**18**)

ATOM	X	Y	Z	ATOM	X	Y	Z
Mo	1.44610526	1.94803801	0.7869386	C	-1.76989474	-2.45596199	0.9519386
O	1.44610526	1.62303801	2.4389386	C	-1.97989474	-3.75296199	-1.5750614
Cl	3.43910526	3.06703801	0.2519386	C	-2.98089474	-3.11796199	0.5539386
Cl	0.45010526	4.18503801	0.6789386	C	-1.71589474	-1.91296199	2.2749386
O	2.11610526	0.42003801	-0.1160614	C	-2.84889474	-1.91996199	3.0769386
N	-0.40889474	1.40503801	0.2709386	C	-4.05089474	-2.50596199	2.6449386
H	-1.04189474	1.39303801	1.0819386	C	-4.10689474	-3.12396199	1.4169386
Mo	2.22310526	-1.41496199	-0.6380614	N	-0.50289474	-1.35096199	2.7649386
O	1.91810526	-1.54796199	-2.2920614	N	-2.62589474	2.45203801	1.4439386
Cl	2.46610526	-3.71096199	-0.0200614	H	0.00310526	-3.00396199	-1.9520614
Cl	4.55910526	-1.22496199	-0.3460614	H	-2.03889474	-4.26796199	-2.5280614
N	0.40210526	-1.57496199	0.1979386	H	-3.97089474	-4.27896199	-0.9740614
H	0.31410526	-1.07696199	1.0949386	H	-5.01289474	-3.62296199	1.0859386
C	-0.41289474	1.33603801	-2.1200614	H	-4.91689474	-2.50096199	3.2989386
C	-1.10089474	1.51703801	-0.9090614	H	-2.78589474	-1.49396199	4.0749386
C	-2.47889474	1.37603801	-3.3580614	H	0.22310526	-2.05396199	2.8919386
C	-2.52989474	1.76003801	-0.9220614	H	-0.63289474	-0.86296199	3.6449386
C	-1.10089474	1.27503801	-3.3360614	H	-3.27989474	2.71503801	2.1739386
C	-3.21989474	1.61103801	-2.1700614	H	-1.92989474	3.19403801	1.3399386
C	-3.28589474	2.15503801	0.2259386	H	0.65910526	1.17503801	-2.0990614
C	-4.66989474	2.22903801	0.1399386	H	-0.54689474	1.11303801	-4.2540614
C	-5.34589474	1.98303801	-1.0690614	H	-3.01989474	1.28603801	-4.2960614
C	-4.63389474	1.71403801	-2.2150614	H	-5.13989474	1.58103801	-3.1670614
C	-0.81489474	-3.05296199	-1.2440614	H	-6.42889474	2.05403801	-1.0980614
C	-0.69489474	-2.36696199	-0.0240614	H	-5.23589474	2.51803801	1.0219386
C	-3.05189474	-3.76496199	-0.7070614				

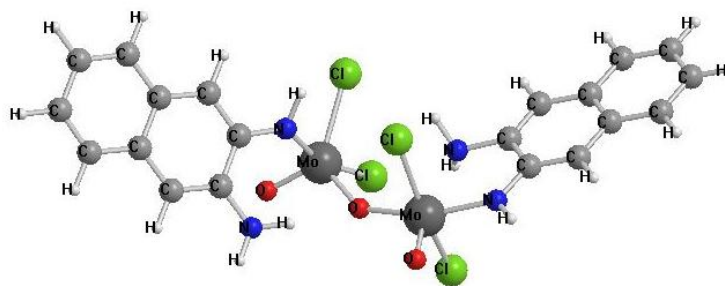


Figure C.19. DFT calculated complex $[\text{Mo}_2\text{O}_2(\mu_2\text{-O})\text{Cl}_4(2,3\text{-HNC}_{10}\text{H}_6\text{NH}_2)_2]$ (**19**)

Table C.19. Cartesian coordinates of $[\text{Mo}_2\text{O}_2(\mu_2\text{-O})\text{Cl}_4(2,3\text{-HNC}_{10}\text{H}_6\text{NH}_2)_2]$ (**19**)

ATOM	X	Y	Z	ATOM	X	Y	Z
Mo	1.18999415	-1.55101754	0.80594444	C	6.04499415	0.92298246	1.15194444
O	0.79799415	-2.68801754	1.99794444	C	3.55799415	0.45998246	-0.09805556
Cl	0.30199415	0.45898246	1.87794444	C	5.68499415	1.62598246	-0.04905556
Cl	2.13599415	-3.00301754	-0.84205556	C	7.30899415	1.18898246	1.74894444
O	-0.36200585	-1.37301754	-0.37905556	C	8.17299415	2.10198246	1.18794444
N	2.98499415	-1.14001754	1.56694444	C	7.81499415	2.79198246	0.00394444
H	3.25199415	-1.61001754	2.42894444	C	6.59799415	2.55798246	-0.59905556
Mo	-1.22900585	-0.18901754	-1.55505556	N	2.25099415	0.14498246	-0.62405556
O	-2.55300585	-0.93601754	-2.27305556	N	-3.35500585	-1.87301754	0.57194444
Cl	-0.53700585	2.13398246	-1.86305556	H	-2.35100585	-1.76901754	0.56294444
Cl	0.36299415	-0.57601754	-3.31605556	H	-3.70800585	-2.73901754	0.94594444
N	-2.34700585	0.72098246	-0.13505556	H	-5.92500585	-1.87701754	1.11794444
H	-1.99500585	1.64598246	0.10194444	H	-8.16700585	-0.88001754	1.48594444
C	-3.64800585	0.54098246	0.27694444	H	-9.60000585	1.11798246	1.66694444
C	-4.47800585	1.65898246	0.43694444	H	-8.66100585	3.39398246	1.29094444
C	-5.52100585	-0.89301754	0.89894444	H	-6.26800585	3.66798246	0.72094444
C	-5.83200585	1.54498246	0.77494444	H	-4.06000585	2.64298246	0.23794444
C	-4.17400585	-0.78101754	0.57594444	H	1.67799415	0.98798246	-0.70405556
C	-6.37200585	0.22598246	0.99194444	H	2.29999415	-0.26301754	-1.56105556
C	-6.68700585	2.67998246	0.89094444	H	4.14199415	1.89798246	-1.55605556
C	-8.01400585	2.52698246	1.20594444	H	6.32299415	3.08598246	-1.50805556
C	-8.54700585	1.22698246	1.42094444	H	8.50599415	3.50898246	-0.42805556
C	-7.75100585	0.10998246	1.31994444	H	9.13499415	2.29598246	1.65194444
C	3.90899415	-0.24701754	1.09594444	H	5.40599415	-0.53801754	2.61494444
C	5.13899415	-0.00701754	1.70494444	H	7.58099415	0.65898246	2.65694444
C	4.41999415	1.36698246	-0.65005556				

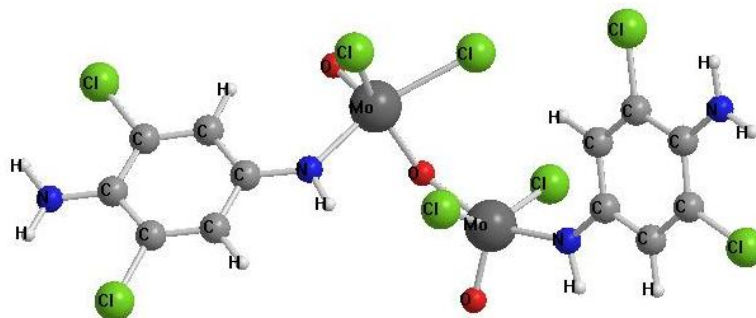


Figure C.20. DFT calculated complex $[\text{Mo}_2\text{O}_2(\mu_2\text{-O})\text{Cl}_4(p\text{-HNC}_6\text{H}_2\text{Cl}_2\text{NH}_2)_2]$ (**20**)

Table C.20. Cartesian coordinates of $[\text{Mo}_2\text{O}_2(\mu_2\text{-O})\text{Cl}_4(p\text{-HNC}_6\text{H}_2\text{Cl}_2\text{NH}_2)_2]$ (**20**)

ATOM	X	Y	Z	ATOM	X	Y	Z
Mo	1.17202825	-1.18305085	-1.54993503	N	-2.40197175	-0.15705085	0.24806497
O	0.71602825	-2.71505085	-2.08493503	C	-3.75297175	-0.30005085	0.42206497
Cl	0.63302825	-1.08005085	0.88806497	C	-6.56097175	-0.67405085	0.78006497
Cl	2.00602825	-0.10705085	-3.46193503	C	-4.25997175	-1.48305085	1.01406497
O	-0.35697175	-0.05905085	-1.60493503	C	-4.67097175	0.69994915	0.02006497
N	3.01102825	-1.57205085	-0.88493503	C	-6.02197175	0.50394915	0.19506497
C	3.97602825	-0.95005085	-0.13993503	C	-5.61597175	-1.65505085	1.18106497
C	6.00302825	0.32594915	1.40306497	N	-7.89297175	-0.85105085	0.93806497
C	5.10302825	-1.67505085	0.31406497	H	-1.87697175	-0.94505085	0.63506497
C	3.87002825	0.42194915	0.18906497	H	-8.23997175	-1.66105085	1.42706497
C	4.85702825	1.02694915	0.93406497	H	-8.52797175	-0.10705085	0.70206497
C	6.07902825	-1.05005085	1.05706497	H	3.01502825	1.00594915	-0.13493503
N	6.96602825	0.93794915	2.12606497	H	5.20502825	-2.73005085	0.08006497
H	3.23802825	-2.54905085	-1.06993503	H	-3.57797175	-2.26405085	1.33406497
H	7.74302825	0.40894915	2.48606497	H	-4.31097175	1.61894915	-0.42393503
H	6.85702825	1.90394915	2.38806497	Cl	4.71502825	2.72694915	1.33606497
Mo	-1.13197175	1.24594915	-0.38993503	Cl	7.47102825	-1.97105085	1.60706497
O	-2.25297175	2.20294915	-1.19793503	Cl	-6.21297175	-3.13305085	1.92106497
Cl	-1.12397175	2.18194915	1.79306497	Cl	-7.14297175	1.76194915	-0.30493503
Cl	0.95702825	2.41994915	-0.72293503				

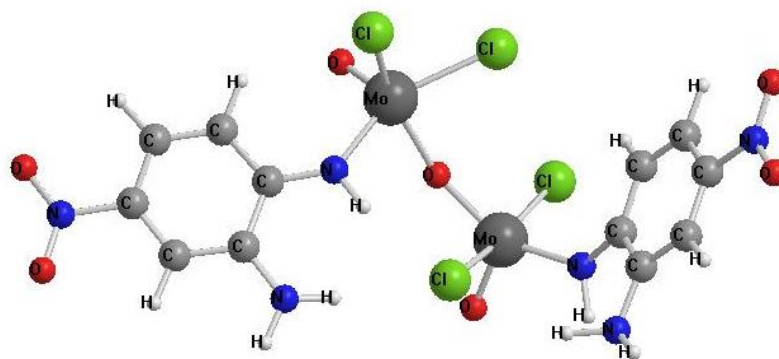


Figure C.21. DFT calculated complex $[\text{Mo}_2\text{O}_2(\mu_2\text{-O})\text{Cl}_4(o\text{-HNC}_6\text{H}_3\text{NO}_2\text{NH}_2)_2]$ (**21**)

Table C.21. Cartesian coordinates of $[\text{Mo}_2\text{O}_2(\mu_2\text{-O})\text{Cl}_4(o\text{-HNC}_6\text{H}_3\text{NO}_2\text{NH}_2)_2]$ (**21**)

ATOM	X	Y	Z	ATOM	X	Y	Z
Mo	1.10503892	-1.37896707	-1.53297904	C	-4.40096108	1.04303293	0.21802096
O	0.50403892	-2.82496707	-2.15897904	C	-5.74496108	0.86103293	0.44002096
Cl	0.26103892	-1.91096707	0.93802096	C	-5.29496108	-1.37996707	1.31802096
Cl	2.06703892	-0.41796707	-3.42997904	H	-1.49796108	-0.44596707	0.77602096
O	-0.16496108	-0.04996707	-1.39797904	H	-4.03996108	1.98103293	-0.18297904
N	2.81303892	-1.80496707	-0.66897904	H	-5.68596108	-2.30096707	1.73102096
C	3.66503892	-1.02696707	0.09802096	H	5.56003892	-1.25896707	2.94302096
C	5.53803892	0.37403293	1.55802096	N	-3.06796108	-2.24596707	1.35802096
C	4.16703892	-1.58196707	1.31302096	N	3.68503892	-2.82396707	1.71202096
C	4.05903892	0.26103293	-0.31597904	H	-2.08596108	-2.25896707	1.10202096
C	5.00303892	0.96703293	0.41302096	H	-3.44196108	-3.09996707	1.74102096
C	5.13703892	-0.87296707	2.02302096	H	4.09303892	-3.17896707	2.56802096
H	2.94803892	-2.80296707	-0.47997904	H	2.67103892	-2.89196707	1.72702096
H	3.65603892	0.67103293	-1.23497904	H	5.34303892	1.94703293	0.10502096
Mo	-1.04296108	1.59203293	-0.66097904	H	-6.47296108	1.62903293	0.21802096
O	-2.13196108	2.18603293	-1.78997904	N	6.55503892	1.10903293	2.33102096
Cl	-1.26196108	3.12003293	1.11202096	N	-7.60396108	-0.56496707	1.25302096
Cl	1.08403892	2.53803293	-1.10097904	O	6.87703892	2.22603293	1.93002096
N	-2.11996108	0.25003293	0.34402096	O	7.02003892	0.55803293	3.32902096
C	-3.44796108	0.03503293	0.53902096	O	-7.94596108	-1.63496707	1.75502096
C	-6.16396108	-0.35996707	0.99702096	O	-8.36596108	0.34803293	0.94602096
C	-3.91196108	-1.22496707	1.08202096				

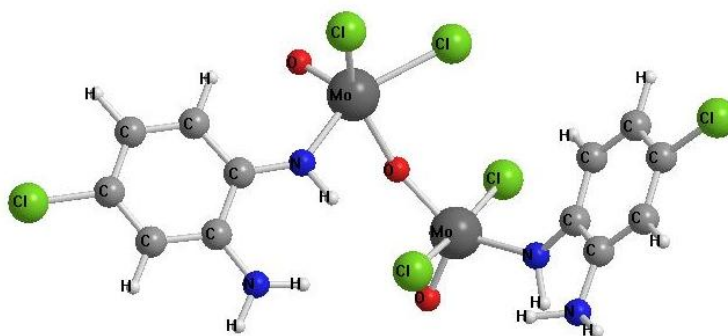


Figure C.22. DFT calculated complex $[\text{Mo}_2\text{O}_2(\mu_2\text{-O})\text{Cl}_4(o\text{-HNC}_6\text{H}_3\text{ClNH}_2)_2]$ (**22**)

Table C.22. Cartesian coordinates of $[\text{Mo}_2\text{O}_2(\mu_2\text{-O})\text{Cl}_4(o\text{-HNC}_6\text{H}_3\text{ClNH}_2)_2]$ (**22**)

ATOM	X	Y	Z	ATOM	X	Y	Z
Mo	1.1700559	-1.36210559	-1.46603727	C	-6.1839441	-0.47910559	1.02796273
O	0.6280559	-2.81410559	-2.13703727	C	-3.9109441	-1.31710559	1.08996273
C	10.23705590	-2.00310559	0.97096273	C	-4.4259441	0.94489441	0.23796273
Cl	2.1730559	-0.35910559	-3.32903727	C	-5.7659441	0.74989441	0.46996273
O	-0.1079441	-0.04210559	-1.32903727	C	-5.2909441	-1.48510559	1.33496273
N	2.8500559	-1.72710559	-0.53203727	H	-1.5029441	-0.52110559	0.74396273
C	3.6280559	-0.90810559	0.27096273	H	-4.0819441	1.88789441	-0.16503727
C	5.3780559	0.59489441	1.81096273	H	-5.6469441	-2.42310559	1.74796273
C	4.1210559	-1.43910559	1.49796273	H	5.4240559	-1.06710559	3.17896273
C	3.9600559	0.40389441	-0.11603727	N	-3.0569441	-2.33010559	1.35596273
C	4.8380559	1.15789441	0.64796273	N	3.6990559	-2.71010559	1.87596273
C	5.0260559	-0.68010559	2.24696273	H	-2.0699441	-2.32610559	1.11696273
H	3.0270559	-2.71810559	-0.34803727	H	-3.4179441	-3.18610559	1.74796273
H	3.5630559	0.80389441	-1.04303727	H	4.0880559	-3.04010559	2.74996273
Mo	-1.0789441	1.56589441	-0.64103727	H	2.6900559	-2.83610559	1.84696273
O	-2.2119441	2.13889441	-1.73803727	H	5.1150559	2.15889441	0.34496273
Cl	-1.2989441	3.03289441	1.19096273	H	-6.4909441	1.52389441	0.25096273
Cl	0.9750559	2.64989441	-1.15403727	Cl	6.5050559	1.53089441	2.76796273
N	-2.1369441	0.17889441	0.33596273	Cl	-7.8839441	-0.72810559	1.33596273
C	-3.4569441	-0.05210559	0.54696273				

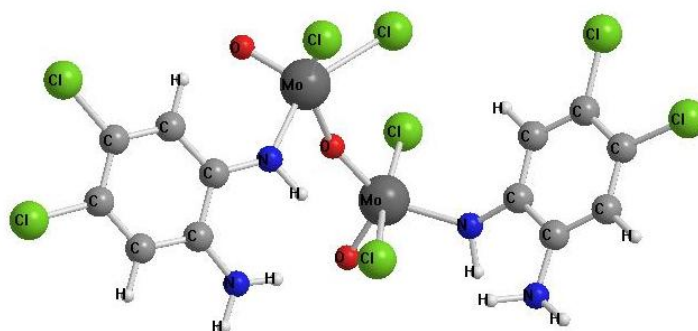


Figure C.23. DFT calculated complex $[\text{Mo}_2\text{O}_2(\mu_2\text{-O})\text{Cl}_4(o\text{-HNC}_6\text{H}_2\text{Cl}_2\text{NH})_2]$ (**23**)

Table C.23. Cartesian coordinates of $[\text{Mo}_2\text{O}_2(\mu_2\text{-O})\text{Cl}_4(o\text{-HNC}_6\text{H}_2\text{Cl}_2\text{NH})_2]$ (**23**)

ATOM	X	Y	Z	ATOM	X	Y	Z
Mo	1.22691243	-1.58294915	-1.44987288	C	-6.14908757	-0.65794915	0.99412712
O	0.68491243	-3.04394915	-2.09887288	C	-3.86508757	-1.50594915	1.08012712
Cl	0.29591243	-2.19494915	0.99712712	C	-4.35308757	0.75905085	0.23312712
Cl	2.22291243	-0.59794915	-3.32087288	C	-5.69808757	0.57305085	0.44712712
O	-0.06908757	-0.28194915	-1.33187288	C	-5.24908757	-1.66194915	1.30112712
N	2.90991243	-1.95394915	-0.51587288	H	-1.44708757	-0.71494915	0.77712712
C	3.70991243	-1.13594915	0.26812712	H	-4.00308757	1.70505085	-0.15787288
C	5.49991243	0.37005085	1.78812712	H	-5.62008757	-2.59694915	1.70412712
C	4.14591243	-1.62594915	1.53212712	H	5.41591243	-1.21894915	3.22412712
C	4.11791243	0.13305085	-0.17787288	N	-3.02008757	-2.52494915	1.35512712
C	5.01291243	0.88505085	0.57112712	N	3.66191243	-2.85794915	1.95912712
C	5.06091243	-0.86594915	2.26212712	H	-2.03108757	-2.52494915	1.12112712
H	3.05791243	-2.94294915	-0.29687288	H	-3.38908757	-3.38194915	1.73612712
H	3.77791243	0.50205085	-1.13787288	H	4.00491243	-3.15594915	2.86412712
Mo	-1.01208757	1.34805085	-0.64287288	H	2.65091243	-2.94894915	1.89612712
O	-2.11208757	1.90705085	-1.78087288	Cl	5.53091243	2.43305085	-0.03587288
Cl	-1.28908757	2.87105085	1.13312712	Cl	6.63691243	1.26605085	2.75512712
Cl	1.08591243	2.35505085	-1.08087288	Cl	-7.83608757	-0.93794915	1.29212712
N	-2.07408757	-0.01994915	0.35212712	Cl	-6.81308757	1.85605085	0.06712712
C	-3.39908757	-0.24394915	0.54812712				

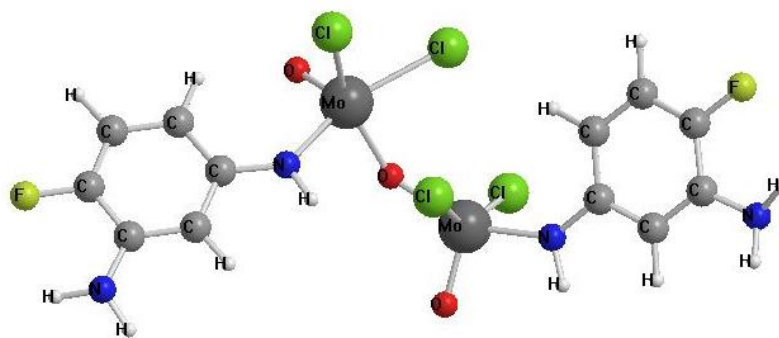


Figure C.24. DFT calculated complex $[\text{Mo}_2\text{O}_2(\mu_2\text{-O})\text{Cl}_4(m\text{-HNC}_6\text{H}_3\text{FNH}_2)_2]$ (**24**)

Table C.24. Cartesian coordinates of $[\text{Mo}_2\text{O}_2(\mu_2\text{-O})\text{Cl}_4(m\text{-HNC}_6\text{H}_3\text{FNH}_2)_2]$ (**24**)

ATOM	X	Y	Z	ATOM	X	Y	Z
Mo	1.15495098	-1.31904575	-0.97896078	N	-2.52904902	-0.04604575	0.31703922
O	0.73295098	-2.93804575	-1.18696078	C	-3.89104902	-0.17204575	0.47003922
Cl	0.53695098	-0.71604575	1.34903922	C	-6.61704902	-0.50504575	0.77503922
Cl	2.02895098	-0.62004575	-3.03996078	C	-4.40204902	-1.34304575	1.08103922
O	-0.39004902	-0.27104575	-1.32496078	C	-4.77504902	0.83995425	0.03103922
N	2.97695098	-1.55004575	-0.22796078	C	-6.14304902	0.65795425	0.18803922
C	3.95995098	-0.75904575	0.31803922	C	-5.77304902	-1.53504575	1.23903922
C	5.95795098	0.80995425	1.39303922	H	-2.00504902	-0.76704575	0.81803922
C	5.08795098	-1.36404575	0.92203922	H	-3.71304902	-2.11004575	1.42203922
C	3.84995098	0.64795425	0.26403922	H	-4.38704902	1.74795425	-0.40796078
C	4.86195098	1.42595425	0.81303922	H	-6.85404902	1.40995425	-0.13296078
C	6.11095098	-0.59204575	1.46703922	N	7.26395098	-1.12204575	2.01303922
H	3.19695098	-2.54304575	-0.15696078	H	7.78995098	-0.49704575	2.60503922
H	5.16295098	-2.44804575	0.95503922	H	7.20395098	-2.06604575	2.36503922
H	4.80995098	2.50895425	0.79903922	N	-6.32404902	-2.63704575	1.86603922
H	2.98895098	1.12195425	-0.19096078	H	-5.76904902	-3.48004575	1.86503922
Mo	-1.29404902	1.25695425	-0.53096078	H	-7.30404902	-2.79304575	1.68103922
O	-2.34204902	1.92895425	-1.66196078	F	-7.94704902	-0.69304575	0.91803922
Cl	-1.56504902	2.70295425	1.32003922	F	6.94195098	1.55795425	1.93603922
Cl	0.80395098	2.38595425	-0.92596078				